Tissue Engineering

- Creating Living Cardiovascular Grafts -

ISBN: 978-90-393-6519-9
Cover Design and Layout by Dimitri EP Muylaert
Printed by Gildeprint Drukkerijen

Tissue Engineering: Creating Living Cardiovascular Grafts

Tissue Engineering: Het Creëren van Levende Cardiovasculaire Implantaten

(Met een samenvatting in het Nederlands)

Proefschrift

ter verkrijging van de graad van doctor aan de Universiteit Utrecht op gezag van de rector magnificus, prof.dr. G.J. van der Zwaan, ingevolge het besluit van het college voor promoties in het openbaar te verdedigen op donderdag 7 april 2016 des middags te 4.15 uur

door

Dimitri Elke Paul Muylaert

geboren op 22 januari 1986

te Amsterdam

Promotor: Prof. dr. M.C. Verhaar

Copromotor: Dr. J.O.Fledderus

Het onderzoek in dit proefschrift werd uitgevoerd als onderdeel van het Project P1.01 iValve van het onderzoeksprogramma van het BioMedical Materials instituut, (mede) mogelijk gemaakt met financiële steun van het Ministerie van Economische Zaken, Landbouw en Innovatie.

Financial support by the Dutch Heart Foundation for the publication of this thesis is gratefully acknowledged. The research described in this thesis was supported by a grant of the Dutch Heart Foundation (DHF-2008T089).

Voor mijn vader en moeder
en voor mijn grootouders, Mamie en Papie

Contents

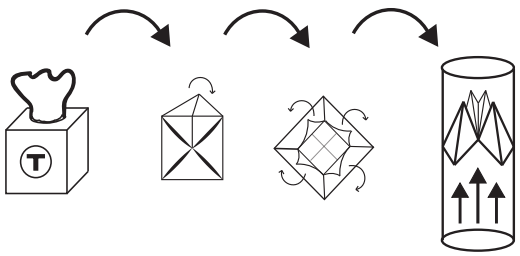

I

Introduction

Introduction

Science fiction is rapidly becoming science reality. One of the most intriguing concepts that is now becoming real is that of taking an inert material and changing it into living tissue for the replacement of human organs.

Replacing a damaged cardiovascular tissue such as a damaged heart valve or an occluded blood vessel is an invasive approach and the graft material will inevitably come into extensive contact with blood, resulting in an immunologic response. An argument could be made to view blood as a liquid organ itself. Blood cleanses, it nourishes, it heals, it attacks, it defends, and perhaps most strikingly; it rebuilds. Blood and the cardiovascular system are not entirely separate entities. During embryonic development the first definitive hematopoietic cells appear in the aortic arch[1], and eventually migrate to the bone marrow where they find a niche to produce blood cells for an entire lifetime. These very same cells then repair and contribute to new or damaged vascular structures in later life. This capacity of circulating cells to contribute to tissue regeneration may be employed for engineering new blood vessels and heart valves.

I. Planting Vessels and Squeezing Heart Valves

This dissertation focusses on two cardiovascular structures, for which the approach to developing graft material overlaps; heart valves and small-diameter blood vessels. The development of surgical approaches to both of these structures has developed strongly in the past half century. In 1950, dr. Arthur Vineberg implanted the left mammary artery directly into the myocardium of patients with myocardial ischemia, but did not connect the artery directly to a coronary vessel[2]. Due to the lack of a connection to the vascular system this approach was of limited success. The first aortocoronary graft was performed over a decade later, in 1964, by dr. Mason Sones using the vena saphena magna[3]. This vein continues to be used as replacement graft for coronary bypasses to this day but requires an invasive procedure to harvest and represents a limited supply. Essentially, restoring blood flow to the coronary system depends on the implantation of small diameter tubes. Ideally, during the implantation procedure, these grafts could simply be taken out of a package rather than the body of the patient.

While manipulation of coronary vessels takes place outside of the heart, approaching the heart valves necessarily involves access to the inner lumen of the heart. In the early-20th century this presented an almost impossible challenge. In 1952 the first prosthetic aortic valve replacement was implanted into the descending aorta of a patient by Hufnagel and Harvey at Georgetown University[4]. Importantly, the cardio-pulmonary bypass machine would not be developed by dr. John Heysham Gibbon until 1954, two years later[5]. The prosthetic was based on a ball-and-cage system. Patients (or their spouses) would sometimes complain they could hear the valve clicking like a grandfather clock. Surgical treatment of stenotic heart valves was largely

limited to commisurotomies and debridement of calcified leaflets, sometimes achieved by simply squeezing the thickened valve between thumb and forefinger. Post-surgical complications such as bacterial endocarditis were common and often detrimental. In the early 60's surgeons began to replace heart valves with prostheses under direct vision. In 1969, the recently deceased dr. Ross revolutionized the treatment of aortic stenosis by performing the first pulmonary autograft procedure, which later would become known as the 'Ross procedure'[6]. At the time very little was known about the long-term effects of implanting a foreign body directly into the bloodstream. Valve prostheses based on porcine valves treated with formaldehyde were already being used, but they deteriorated quickly. Alternative treatment methods using gluteraldehyde improved the longevity of these grafts, and by the 80's the ball-cage system was largely replaced. Regardless of the type of prosthetic, the surgical procedure of heart valve replacement is spectacularly invasive, greatly increasing the risk of complications. In 2002, Cribier et al performed a transcatheter aortic heart valve replacement in Rouen, France[7]. This approach reduces the invasiveness of the procedure considerably, however it also imposes different requirements on the graft itself. The material needs to be foldable without losing strength or shape, and ideally will minimize adverse immunological and hemodynamic responses.

None of these non-viable grafts are capable of growing or adapting their structure as needed by a growing, living patient. Particularly for pediatric patients, prosteses that can grow along as the heart increases in size will be extremely advantageous. In addition, small diameter tubes that can be applied off-the-shelf will remove the need to harvest vessels for autografting. As our understanding of the regenerative capabilities of the body grows, and as our ability to manipulate materials on a molecular level develops, new possibilities for the creation of graft materials to replace heart valves or implant small-diameter blood vessels keep arising.

II. iValve

The requirements of a functional cardiovascular structure, be it a valve or vessel, can be roughly brought down to two qualities; being strong enough to withstand blood flow and blood pressure, avoiding occlusion or stenosis. The former can be achieved by the production and maintenance of extracellular matrix (ECM) by specialized cells. The latter can be achieved by a monolayer of endothelial cells. This dissertation is focussed on how the interplay of synthetic materials, hemodynamics, biologically active factors and cells can lead to the in-situ development of a cardiovascular tissue that offers these qualities. The research presented here was performed within the iValve project, a part of the national BioMedical Materials program (BMM) which was founded in 2007 to promote innovation in life sciences and health. The approach we took can be divided up into two parts: Firstly, studying how candidate cells can be stimulated towards tissue formation and how they respond to biochemical and mechanical stimuli, and secondly, creating synthetic materials capable of biologically interacting with and stimulating circulating cells after in-vivo implantation.

Chapter II discusses how the environment of a cardiovascular graft, particularly the mechanical and biochemical stimuli found there, will influence the cellular development of the graft. Endothelial cells constitute an ideal luminal surface for blood contact in cardiovascular structures. The cells are capable of transdifferentiation into an ECM producing cell type through a process called endothelial to mesenchymal transition (EndMT). This process is a driving force in the embryonic development of heart valves and leads to two different cell populations that closely communicate to maintain a mechanically sufficient tissue. It is of great interest to tissue engineering approaches, as endothelialized grafts could be triggered to undergo EndMT and produce and maintain ECM. However, following implantation the graft will experience a myriad of stimuli such as mechanical strain, hemodynamic shear stress and biochemical and cellular responses of the immune system. These are all capable of influencing EndMT, either stimulating or inhibiting it. The growth factor TGFb is particularly important in this process, functioning as a major regulator on which many of the environmental stimuli converge. In the design of grafts that rely on EndMT it is important to know which elements of the environment are helpful and which should be compensated for.

Cells isolated out of circulation can be cultured to yield large monolayers of endothelium. The origin of these progenitor cells, named endothelial colony forming cells (ECFCs), is the subject of some debate. Nevertheless it is clear that these cells are found in circulation and capable of constituting functional endothelium. Chapter III investigates the response of ECFCs to cyclic strain with a focus on the production and remodeling of extracellular matrix (ECM). By exposing the cells to biochemical stimuli prior to mechanical stimuli we were able to manipulate the cells response. In this model, the cells were exposed to both biochemical and mechanical strain but did not experience fluid flow. In chapter IV we report preliminary results of pilot experiments in which ECFCs were exposed to fluid shear stress. Fluid shear stress is capable of triggering TGFb signaling, and TGFb in turn is capable of downregulating the expression of microRNAs. MicroRNAs are short RNA molecules capable of repressing their target mRNA leading to the reduced translation of specific proteins. Since miRNAs can target multiple mRNAs and an mRNA molecule may be targeted by multiple miRNAs they can regulate elaborate cellular programs. The chapter investigates how hemodynamic shear stress, through TGFb signaling, influences mirRNAs capable of regulating ECM protein expression. Of the proteins within the ECM, elastin is of particular importance to cardiovascular structures because of its compliant mechanical properties, and we investigated the role of hemodynamic shear and miRNAs on its expression in ECFCs.

Zooming out from from a molecular level to a cellular and tissue level, chapter V explores how physiological processes such as damage repair in ischemic tissues can be used to inspire tissue engineering approaches. Based on the concept that the human body is capable of rebuilding damaged tissues by attracting and stimulating cells out of circulation we explore how repair processes can point to candidates for bioactive molecules to incorporate in graft materials. Using novel synthetic techniques we can create materials that offer a microenvironment capable of

mimicking repair processes on a molecular level and guide the development of new tissue. For instance, through the process of electrospinning a microfiber mesh material can be produced that resembles the ECM and allows cells to pervade and bind throughout the graft. The versatility of this approach is, in part, due to the possible chemical modifications to the electrospun material. The chapter highlights chemokines such as monocyte chemoattractive protein 1 (MCP1) and stromal cell derived factor 1a (SDF1a) as candidates to guide the response of immune cells. This approach, in which cells perceive a synthetic graft as a wounded tissue that is to be healed, effectively turns the body of the recipient of into a bioreactor that actively helps to develop the graft.

To investigate the initial systemic response to material containing a chemokine and to study the effect on tissue development, chapter VI reports the implantation of electrospun tubes soaked in a fibrin gel containing MCP1 into the abdominal aorta of rats. To ensure that the cells invading the graft were primarily attracted out of circulation and not out of lateral ingrowth along the anastomoses, we used gore-tex tubes set on either side of the graft to bridge contact between the synthetic material and the native aorta. The initial burst release of MCP1 led to an increased early influx of cells, and after 9 months of implantation there was a significant impact on the attraction of progenitor cells and tissue development. In this approach the chemokine was not directly bound to the graft material but instead incorporated into a gel. However, following tissue damage, chemokines adhere to the ECM in the direct vicinity of the tissue in addition to expelling chemokines into circulation. These molecules present a molecular domain to circulating cells and provide a homing signal to guide cellular adhesion and migration. This dynamic can be imitated in synthetic materials. Looking at the molecular structure of the chemokine SDF1a, several domains can be distinguished, each with specific functions: A domain responsible for binding to ECM, a hinge domain, and a receptor activating domain, which is held in place by the former domains and presented to cells. Functionally speaking, cell surface receptors only need to ‘see’ the receptor activating domain, regardless of what molecular structure is presenting it to them. In chapter VII we report the development of a molecule based on the receptor-activating domain of the chemokine SDF1a, as well as the direct incorporation of this molecule into the graft material through supramolecular coupling. The production method, based on UPy groups that enable easy mixing of materials and further processing through electrospinning, is completely synthetic and does not rely on full-length proteins, which improves reproducibility and scalability . The SDF1a-derived peptide molecules are firmly attached to the fibers of the graft, allowing cells to home to and disperse throughout the material. We used human-derived circulating mononuclear cells in a bioreactor capable of producing a pulsatile flow of culture medium along a surface of the graft material. In order to investigate an in vivo systemic response to the material we implanted tubular grafts in the rat model described in chapter VI, including the gore-tex anastomoses but without the use of any gels. Chapter VII combines ideas from the preceding chapters in a fully synthetic approach to tissue engineering and represents a step forward towards the ultimate goal of turning synthetic materials in to living tissues.

References

1. J.-C. Boisset, W. van Cappellen, C. Andrieu-Soler, N. Galjart, E. Dzierzak, C. Robin, In vivo imaging of haematopoietic cells emerging from the mouse aortic endothelium, Nature. 464 (2010) 116–120. doi:10.1038/nature08764.
2. A.M. VINEBERG, P.H. NILOFF, The value of surgical treatment of coronary artery occlusion by implantation of the internal mammary artery into the ventricular myocardium; an experimental study, Surg Gynecol Obstet. 91 (1950) 551–561.
3. D.B. EFFLER, L.K. GROVES, F.M. SONES, E.K. SHIREY, ENDARTERECTOMY IN THE TREATMENT OF CORONARY ARTERY DISEASE, The Journal of Thoracic and Cardiovascular Surgery. 47 (1964) 98–108.
4. C.A. HUFNAGEL, W.P. HARVEY, The surgical correction of aortic regurgitation preliminary report, Bull Georgetown Univ Med Cent. 6 (1953) 60–61.
5. J.H. GIBBON, Application of a mechanical heart and lung apparatus to cardiac surgery, Minn Med. 37 (1954) 171–85– passim.
6. D.N. Ross, R. Radley-Smith, J. Somerville, Pulmonary autograft replacement for severe aortic valve disease, Br Heart J. 31 (1969) 797–798.
7. A. Cribier, H. Eltchaninoff, A. Bash, N. Borenstein, C. Tron, F. Bauer, et al., Percutaneous transcatheter implantation of an aortic valve prosthesis for calcific aortic stenosis: first human case description, Circulation. 106 (2002) 3006–3008.

Part One

II

Environmental Influences on Endothelial to Mesenchymal Transition in Developing Implanted Cardiovascular Tissue-Engineered Grafts

(published in Tissue Engineering part B)

Dimitri E.P. Muylaert

Olivier G. de Jong

Gisela G.G. Slaats

Frederieke E. Nieuweboer

Joost O. Fledderus

Marie-Jose Goumans

Beerend P. Hierck

and Marianne C. Verhaar

Abstract

Tissue engineered grafts for cardiovascular structures experience biochemical stimuli and mechanical forces that influence tissue development after implantation such as the immunological response, oxidative stress, hemodynamic shear stress and mechanical strain. Endothelial cells are a cell source of major interest in vascular tissue engineering because of their ability to form a luminal antithrombotic monolayer. In addition, through their ability to undergo endothelial to mesenchymal transition (EndMT), endothelial cells may yield a cell type capable of increased production and remodeling of the extracellular matrix (ECM). ECM is of major importance to the mechanical function of all cardiovascular structures. Tissue engineering approaches may employ EndMT to recapitulate, in part, the embryonic development of cardiovascular structures. Improved understanding of how the environment of an implanted graft could influence EndMT in endothelial cells may lead to novel tissue engineering strategies. This review presents an overview of biochemical and mechanical stimuli capable of influencing EndMT, discusses the influence of these stimuli as found in the direct environment of cardiovascular grafts, and discusses approaches to employ EndMT in tissue-engineered constructs.

Introduction

To replace damaged or malfunctioning cardiovascular structures such as heart valves or blood vessels, grafts may be implanted that are capable of stimulating the development of neo-tissue. Such implanted replacement grafts experience a multitude of stimuli in situ that influence cellular influx and development. These stimuli include mechanical strain, fluid shear stress, and biochemical stimuli due to the immune response to non-native material. Understanding how these stimuli will impede or aid tissue formation is important for the development of tissue engineering strategies. The main requirements of tissue engineered vascular replacement structures such as heart valves and blood vessels are an anti-thrombotic surface lining provided by endothelial cells and sufficient mechanical integrity, provided by the extracellular matrix (ECM). Endothelial cells are of major interest to cardiovascular tissue engineering because of their ability to form a luminal antithrombotic monolayer as well as their ability to yield a cell type capable of increased production and remodeling of extracellular matrix (ECM) through endothelial to mesenchymal transition (EndMT).

EndMT plays an important role in embryonic development and remodeling of adult heart valves[1]. During embryonic development semilunar valves emerge from endocardial cushions that bulge into the cardiac outflow tract. This happens in response to a tightly regulated combination of growth factors, microRNAs, matrix proteins, and mechanical stimuli [2] that will be discussed further in this review. As they undergo EndMT, endothelial cells lining the cushions migrate inward from the endothelial monolayer into the cardiac jelly, becoming a matrix-producing and matrix-remodeling cell type with myofibroblast-like characteristics [2]. These cells, which are responsible for producing and maintaining the interstitial cardiovascular tissue, will continue to populate the adult heart valve and are responsible for life-long remodeling and mechanical functioning of the valve leaflets [3].

In addition, EndMT plays a role in the response of the adult vasculature to hypoxia or injury. In addition to hypoxia-inducible factor 1 alpha (HIF1α) induced proliferation, migration and adhesion of endothelial cells[4,5], EndMT enables the remodeling and expansion of the existing vessel network through transdifferentiation of the endothelial cells into smooth muscle cells and pericytes in the newly sprouted vessels [2,5]. In this process, EndMT is triggered by growth factors, microRNAs, matrix proteins, and mechanical stimuli, and involves signaling factors that are highly similar to developing heart valves. These factors, which will be discussed further in this review, may be applied in a stepwise approach to vascular tissue engineering for both heart valve replacement grafts and vascular replacement grafts (Figure 1). While replacement heart valves and blood vessels are distinct structures that will require separate approaches, both are dependent on an endothelial monolayer and a population of ECM producing cells. EndMT, therefore, is of great interest to tissue engineering strategies for both heart valve replacement grafts and vascular replacement grafts.

Heart valve or vascular graft scaffold material may be pre-seeded with endothelial cells or cell-free material may be designed to self-endothelialize with host-derived cells after implantation [2,6]. Following implantation, endothelial cells can be stimulated to undergo EndMT to give rise to an autologous cell-population that produces and maintains sufficient ECM to achieve functional tissue. It should also be taken into account that accumulation of ECM and in particular collagens may be associated with fibrosis in vivo [3,7]. Fibrosis can potentially lead to stenosis and subsequent graft failure. The stiffness of fibrotic material differs from that of healthy tissue and can impair tissue function[8]. Mechanically sturdy tissue, however, is required for mechanically loaded replacement grafts. A balance, therefore, between EndMT induction and inhibition, is necessary to harness EndMT for tissue engineering.

Understanding how the environment regulates EndMT in endothelial cells is crucial and studies should focus on appropriate cell sources. Endothelial cells from a wide variety of sources have been investigated in this context, such as human umbilical arterial endothelial cells (HUAECs), human umbilical vein endothelial cells (HUVECs) and endothelial colony forming cells (ECFCs) (see supplementary table 1). In particular ECFCs represent an easily accessible candidate cell source for pre-seeded tissue engineered constructs as they can be cultured out of the peripheral blood and can produce large colonies of monolayered endothelial cells[9]. In addition, ECFCs are considered a model cell type for circulating endothelial progenitor cells[10]. Moreover, ECFC have been shown to be capable of undergoing EndMT[11].
This review aims to present an overview of the influence of biochemical stimuli and mechanical forces in the direct environment of vascular and valvular grafts on EndMT, and discuss approaches to employ EndMT in tissue-engineered constructs for cardiovascular application.

Mechanisms of EndMT

The capacity of endothelial cells to undergo transition into a mesenchymal cell type resembles that of epithelial cells, which can undergo epithelial to mesenchymal transition (EMT). EMT plays a role in embryonic development and wound healing but also organ fibrosis, and its pathways are well studied[12]. EMT and EndMT have many regulatory pathways in common, and both yield a cell type capable of producing and remodeling ECM. EndMT in cardiovascular development comprises migration and the production and remodeling of ECM. Endothelial cells that originally form a monolayer reduce their adhesion to the surrounding cells and develop the ability to migrate [13-15]. As cells begin to migrate away from a monolayer their cortical cytoskeleton is rearranged to enable cell motility by developing actin-rich projections in sheet-shaped lamellopodia or spike-shaped filopodia[16-19]. Loss of endothelial markers (vascular endothelial cadherin; VE-Cadherin, platelet endothelial cell adhesion molecule; PECAM-1 or CD31) corresponds to loss of cell-cell adhesion, migration, and marks endothelial cell dedifferentiation. As cells move away from the monolayer and deeper into the ECM-rich environment they develop the ability to increase production and remodeling of ECM [2,20]. In-

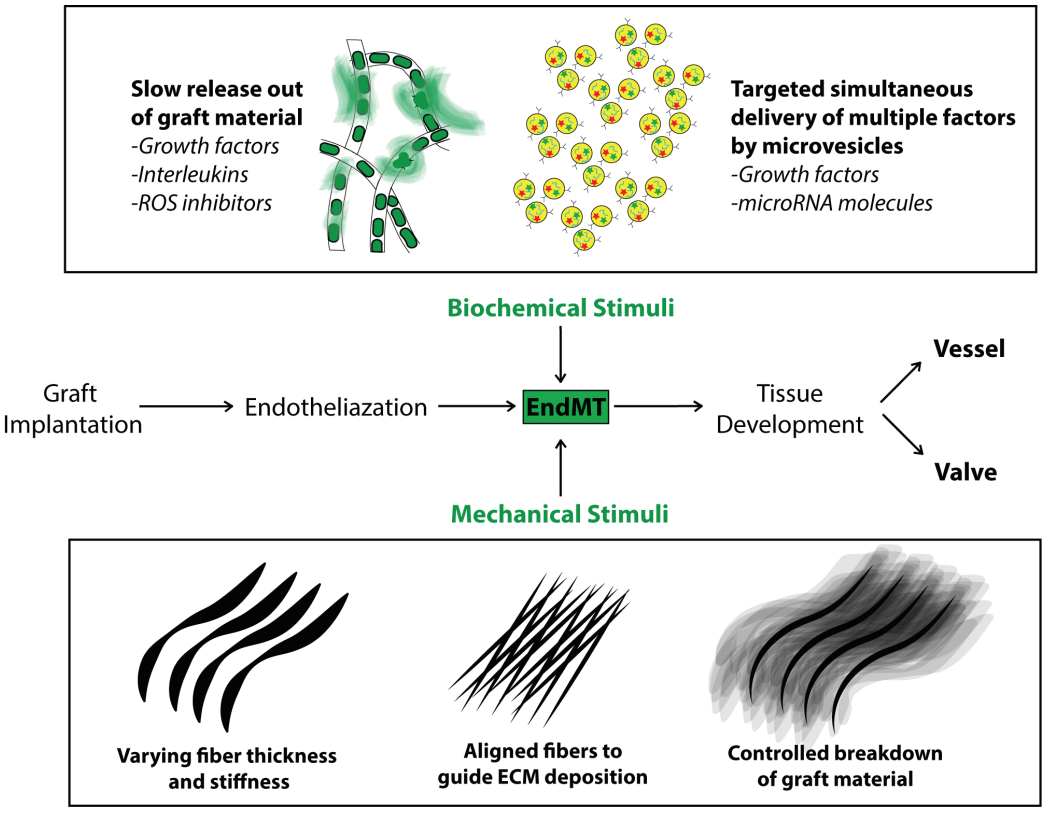

Figure 1. Endothelialized cardiovascular tissue engineered grafts experience environmental stimuli influencing tissue development. To influence this environment, local delivery of biochemical stimuli such as growth factors, interleukins or ROS inhibitors by slow-release mechanisms, or simultaneous delivery of biochemical factors and microRNA molecules by microvesicles can help guide tissue formation. Additionally, the mechanical properties of the graft material itself can help guide cellular development by locally varying material stiffness, fiber alignment and the controlled breakdown of fibers allowing the newly formed tissue to take over the mechanical load.

creased expression of collagens and elastin but also ECM degrading enzymes such as MMP2 and MMP9 are important and functional indicators of EndMT. The gain of myofibroblasts markers (Fibroblast specific protein 1; FSP1, alpha smooth muscle actin; α-SMA, Collagen type 1) corresponds to a newly acquired ability to produce and remodel ECM. Intracellular signaling proteins such as Snail, Twist, Slug and zinc-finger E-box binding homeobox 1 (ZEB1) [4,21] are important regulators of EndMT and are commonly used as markers in EndMT research. The pathways that induce EndMT converge on several signaling proteins including Snail, which downregulates the expression of proteins involved in maintaining cell-cell adhesion such as integrins and focal adhesion kinases and upregulates proteins involved in migration and ECM production and remodeling such as collagen type 1, elastin and matrix metalloproteinases (MMPs) [5,22-24]. Besides Snail, EndMT also requires a downregulation of GSK3β to decrease Snail degradation, which can be achieved by transforming growth factor β2 (TGFβ2) induced PI3K signaling[14]. This is different from EMT where Snail alone is sufficient for induction [25]. Factors such as TGFβ2, therefore, are of major interest to tissue engineering approaches focused on EndMT.

Biochemical factors regulating EndMT

I. TGFβ is a Major Regulator of EndMT

The major inducers of EndMT are members of the transforming growth factorβ (TGFβ) super family, which, among others, contains bone morphogenic proteins (BMPs), growth and differentiation factors and three mammalian types of TGFβ: TGFβ1, TGFβ2, and TGFβ3 [26]. The crucial role of TGFβs in cardiovascular development is apparent from knockdown experiments. Loss of TGFβ1[15] and 2[20] results in severe malformation of vasculature and absence of cellular migration into the cushions of the developing heart valves[17-19] due to inhibition of EndMT, underlining its role in valvular development. TGFβ3, rather than inducing EndMT in cardiac development, appears to play a role in EndMT-related processes in lung tissue[27]. Endothelium-specific knockdown of TGFβ receptors has been shown to specifically inhibit the migration of mesenchymal cells into the cardiac cushions[28]. Another clinical example demonstrating the importance of TGFβ-signaling is Loeys-Dietz syndrome[29], which is caused by autosomal dominant mutations in Sma and Mad 3 protein (SMAD3) and TGFβ receptor encoding genes. Dysfunctional TGFβ receptors prevent EndMT leading to reduced structural integrity of connective tissue and a higher chance of developing aortic aneurysms[30,31]. There are two types of TGFβ receptors; TGFβR type I (activin receptor-like kinase 5 (ALK5) and ALK1) and TGFβR type II, which upon ligand binding, combine to form a heterotetrameric receptor complex, and phosphorylate receptor-regulated SMAD proteins (R-SMADs). In addition, binding to co-receptors endoglin and beta-glycan can further modulate the response to TGFβ. Downstream of TGFβ signaling, phosphorylated R-Smads will form a complex with the co-Smad SMAD4 and move into the nucleus where they bind DNA and regulate the transcription of many of the TGFβ target genes[32]. The signaling between TGFβ receptors and SMAD proteins is elaborate and enables a fine-tuning of the cellular response[33]. This indicates that TGFβ sig-

naling is regulated by multiple pathways that may be targeted in order to control EndMT. For example, a high level of TGFβ will mainly regulate transcription by signaling through ALK5, while low levels of TGFβ will bind to a complex of two type I receptors, ALK5 and ALK1. Therefore, high levels of TGFβ will lead to the phosphorylation of Smad2 and Smad3 by ALK5 which will induce EndMT[5]. Low levels of TGFβ, however, will activate Smad1, Smad5 and/or Smad8 through ALK1. Within the heterotetrameric complex, the ALK1 kinase will inhibit ALK5 signaling and therefore inhibit EndMT[5]. Combined, this indicates that including the timed release of either high or low doses of TGFβ in scaffold materials may allow for increased control over EndMT. Synthetic materials for vascular grafts that are capable of controlled local release of factors have been described and would allow a single material to release both high and low doses of TGFβ with control over the timing of release[34]. This material has previously been used to enhance the development of tissue engineered small-diameter vessels by timed release of vascular endothelial growth factor (VEGF) and platelet derived growth factor (PDGF) [35]. An alternative method to deliver multiple factors simultaneously may be found in extracellular vesicles. Extracellular vesicles are lipid membrane vesicles that are involved in intercellular communication[36] including TGFβ signaling[37]. The formation of extracellular vesicles occurs in the endocytotic pathway when intraluminal vesicles are formed in the late endosome, thereby forming the multivesicular body (MVB) [36,38,39]. Importantly, this means that the contents of extracellular vesicles are dependent on the cytosolic contents of the cell. The physiological role of extracellular vesicles is intercellular communication either by direct interaction with cell surface receptors, by fusing with the target cell membrane, or by endocytosis by target cells. Extracellular vesicles have been shown to be able to present TGFβ on their surface and effectively deliver it to fibroblast to trigger differentiation into myofibroblasts[37,40]. The contents of extracellular vesicles can be manipulated[41,42]. To optimize extracellular vesicles for tissue engineering approaches they could be harvested from cells cultured under specific conditions such as hypoxia, which increases the content of ECM-remodeling proteins in extracellular vesicles[41].

II. MicroRNAs Can Modulate EndMT by Targeting ECM Expression

MicroRNAs (mirs) are small non-coding RNA molecules that strongly bind to the 3' UTR of mRNA and inhibit their translation. Many mirs have been reported to be involved in the induction or inhibition of EndMT. Mir23, for example, inhibits TGFβ induced EndMT in the embryonic heart and restricts cardiac cushion formation[43]. Overexpression of Mir155 inhibits EndMT by targeting Ras homolog gene family, member a (RhoA) [44]. In contrast, mir21 overexpression induces EndMT[45]. Multiple cellular programs that play a role in EndMT are regulated by mirs. For instance, mir29a, mir29b and mir29c target the expression of collagen type 1 and elastin and are lowered by TGFβ signaling[46]. Mir29b (along with mir195) plays a role in the development of aortic aneurysms through regulation of ECM expression[47]. Importantly, TGFβ1 only appears to lower the expression of mir29b, and thus will not lead to a complete silencing of these mirs[48]. TGFβ2, however, has been shown to lower all three of these mirs and lead to an increased expression of collagen type 1 and elastin even in haploinsufficient fi-

broblasts[49]. This means that TGFβ2 may be more effective in the targeting of mirs in order to manipulate ECM production. The ability of mirs to fine-tune ECM expression may be of value in developing implanted grafts (Figure 1). Determining which mirs guide the ECM reconstitution of native vascular structures will point out novel candidates. Either mirs (for example mir21) or mir inhibitors (for example against mir29) may be incorporated in delivery vehicles and released as the graft cells undergo EndMT, and guide the development of the ECM to avoid a predominantly fibrotic development and instead lead to a mixed ECM composition that includes elastin and resembles native vasculature. Here, too, extracellular vesicles are a potential delivery vehicle, capable of delivering mirs in addition to growth factors. Extracellular vesicles from a variety of cell sources were shown to contain mir-29, mir-192, and Let-7 miRNAs, which are all implicated in EMT-mediated metastasis[50-53]. Let-7 also plays a major role in fibroblast growth factor (FGF) induced EndMT. Disruption FGF reduces Let-7 expression and leads to an increase of TGFβ ligands and receptors, ultimately resulting in EndMT[54]. Therefore, extracellular vesicles containing microRNAs such as Let-7 may target multiple mechanisms driving EndMT. Control over the microRNAs within extracellular vesicles can be achieved by using overexpression vectors applied to the cells producing the vesicles [55,56]. In addition to enriching extracellular vesicles it is possible to reduce the presence of specific miRNAs by transfecting cells with antisense single RNA molecules[57]. The possibility to tailor the contents of extracellular vesicles makes them a versatile tool for cardiovascular tissue engineering.

III. Inflammatory Signaling and Oxidative Stress Promote EndMT

Implantation of a replacement vascular graft will induce an immunological response[58]. The resulting inflammatory environment will contain a myriad of signaling proteins such as tumor necrosis factor α (TNFα), interferon gamma (IFNγ), TGFβ, interleukins (ILs) and reactive oxygen species (ROS)[6]. The factors released into this environment have individual effects on EndMT and the combination of factors will dictate the net outcome. In order to avoid adverse effects of the inflammatory environment on EndMT, grafts may be designed to minimize the impact of inflammation. For example, oxidative stress increases the expression and secretion of TGFβ1 and TGFβ2[59], which could induce EndMT in the implanted graft (Figure 2). Montorfano et al demonstrated that H_2O_2 can induce the conversion of endothelial cells into myofibroblasts, shown by decreased expression of the endothelial markers VE-cadherin and CD31, and increased levels of fibrotic (FSP1) and ECM proteins (fibronectin)[59]. Graft material may incorporate factors to reduce ROS, thereby limiting EndMT in a timely manner. ROS inhibitors such as astaxanthin were shown to reduce fibrotic development through SMAD/TGFβ signaling[60]. The intended vascular structure may also be designed with regard for the expected oxygen tension in situ. Hypoxia has been shown to induce Snail expression through hypoxia inducible factor 1 alpha (HIF1α) in mice[61]. With regard to the design of heart valve replacement grafts the influence of oxygen tension may be highly relevant, considering that in vivo a pulmonary valve experiences a different oxygen tension than an aortic valve[62].

The implantation of graft material will likely trigger a foreign body response mediated largely through interleukins. Mahler et al have shown that an inflammatory signaling environment induces EndMT through IL-6 and TNFα via TGFβ signaling[63]. Further supporting the influence of immune signaling in EndMT, in the context of chronic inflammatory bowel disease, TGFβ, IL1 and TNFα were shown to induce EndMT in microvessels contributing to intestinal fibrosis[64]. Maleszewska et al. showed that co-stimulation of human umbilical vein endothelial cells (HUVECs) with IL-1 and TGFβ2 induces EndMT, further indicating that inflammatory signaling can induce EndMT[65]. Interestingly, IFN-α and IFN-γ can either downregulate or respectively upregulate EndMT related genes in human dermal microvascular endothelial cells (HDMVECs), indicating that some modulation of EndMT is possible depending on which IFN types are present[66]. Based on the studies described above, the inflammatory environment provoked by implantation of tissue engineered vascular grafts is likely to induce EndMT (figure 2). Therefore, incorporating a slow release of immunomodulating factors such as interleukins or growth factors directly in the scaffold material is a potential approach to guiding inflammatory signaling and mediate EndMT.

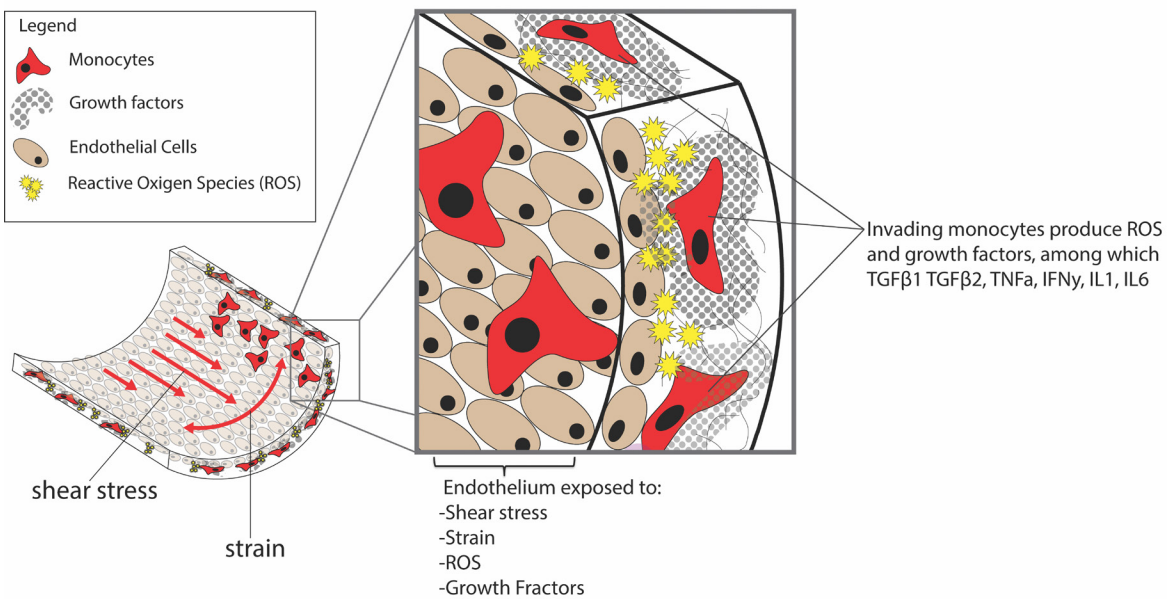

Figure 2. Overview of stimuli influencing EndMT in implanted cardiovascular grafts. Shear stress and strain may enhance EndMT depending on the local composition of growth factors that the endothelium is exposed to. This composition, in turn, is dependent on the invasion of inflammatory cells, ROS and inflammatory signaling. The sum of the inhibitory and stimulatory effects will determine if EndMT will proceed.

The mechanical in-situ environment of a vascular graft can modulate EndMT

I. Hemodynamic Shear Patterns Can Inhibit or Stimulate EndMT

Endothelium experiences shear stress as blood flows by. Shear stress (τ) relates to the viscosity of the blood (μ), the fluid flow (Q) and the radius of the blood vessel (r) in the following equation[33,67]: **$\tau=4\mu Q/\pi r3$.** The shear stress found along the endothelium of the human aorta ranges between 10-20 dynes/cm^2[68]. Along the surface of the aortic heart valve, however, shear stress ranges between 30 and 1500 dynes/cm^2[69]. The patterns of blood flow vary enormously depending on the location within the circulatory system, and endothelial cells are capable of responding to different patterns of flow in a number of ways. Endothelial cells are capable of sensing fluid flow via adhesion molecules[70], cytoskeletal deformation[71], nuclear displacement[72] and cilia; small organelles on the cell membranes capable of translating mechanical stimulation to intracellular signaling[68,73-75]. The ciliary state of the endothelium responds to the differing fluid patterns, where a laminar flow with high shear stress results in loss of cilia and a disturbed flow with low shear stresses, such as found in bifurcations and around valves, correlates to ciliated endothelium[76]. The endothelial response to shear stress has been associated with development of atherosclerosis, and a growing body of evidence suggests that EndMT plays a role in this pathological development. Adult endothelium responds with programs of signaling and development that differ from embryonic endothelium. Egovora et al. have shown that embryonic endothelium is capable of responding to shear patterns with EndMT through TGFβ/ALK5 signaling, suggesting that fluid flow may have a major influence on the developing implanted vascular grafts (Figure 2). The response of ECFCs to shear stress appears to be similar to that of adult endothelium[77], however it is not fully known what the effect of other mechanical forces, such as strain, will be on EndMT, ECM production and remodeling in these candidate cells for tissue engineering. In addition, manipulating the ciliary state of ECFCs may influence their tendency to undergo EndMT, where a lack of cilia primes endothelial cells for shear-induced EndMT through TGFβ/ALK5 signaling[78], but also for calcification through BMP signaling[79]. This is of particular relevance to heart valve replacements, where the entire graft needs to develop homogenously while the ventricular face of the valve leaflet will experience a pulsatile and laminar flow pattern every systole, and the aortic face of the valve leaflets will experience a turbulent pattern of fluid flow[80]. Due to the differences in flow patterns the ventricular face therefore may lack cilia and be more prone to undergoing EndMT compared to the aortic face. Incorporating chemical factors on the aortic face of the graft to chemically induce the loss of cilia[81] may be used to correct for this discrepancy.

II. Mechanical Strain Influences Mechanical Integrity Through ECM Production and Alignment

Statically cultured ECFCs have been reported to arrange ECM fibers along the fiber axis of electrospun materials while mature endothelial cells (HUVECs) arrange their fibers perpendic-

ularly, suggesting that ECFCs do not fully behave like mature endothelium[82]. Understanding these effects is particularly important in the context of heart valves and heart valve replacement grafts, since in addition to fluid flow vascular structures experience considerable strain. For blood vessels this strain is perpendicular to the blood flow and dependent on blood pressure and the mechanical properties of the vessel wall (Figure 2). For heart valves the strain is distributed along a specific pattern in each valve leaflet[83], and the ECM of the valve is adapted to the pattern allowing for ideal mechanical support[84]. Underlining how different levels of shear can induce different mechanisms, sheep valve endothelial cells exposed to high and low cyclic mechanical strain have been shown to undergo EndMT through Wnt/β-catenin or TGFβ signaling respectively[85]. Mechanical strain also has a strong influence on the ECM remodeling behavior of myofibroblasts[86]. Strain, therefore, could both induce endothelial cells to transition to myofibroblasts-like cells, and guide their ECM production and remodeling. While it has been previously shown that strain may inhibit EndMT in ECFCs, pre-treating the cells with TGFβ1 enables ECFCs to respond to a mechanical environment with increased matrix production[11,84]. Synthetic scaffolds may be designed to distribute mechanical stresses along thicker fibers and in such a way that the tissue development is maximally stimulated, for instance by both guiding the alignment of ECM produced by cells and relieving areas of the graft of maximal strain to avoid inhibition of EndMT.

Bioreactors Combine Biochemical and Mechanical Stimuli to Investigate EndMT

To achieve control over EndMT for vascular tissue engineering it is crucial to consider the combined effects of mechanical stresses, biochemical factors and the immune response. Importantly, in addition to inducing EndMT, it is also likely that some inhibition of EndMT is required in regions of implanted vascular grafts prone to fibrosis or calcification. To achieve a well-timed induction or inhibition of EndMT, in-depth knowledge is required of the combinations of stimuli found in situ. In vitro tools such as bioreactors can allow simultaneous study of mechanical and biochemical stimuli. Mahler et al. developed a bioreactor with the capacity to test 3-dimensional cultures including co-cultures of multiple cell types[69]. Using a single cell type they have reported the development of a migratory phenotype out of an endothelial monolayer up to a depth of 60μm deep in response to fluid shear, along with an increased expression of α-SMA and Snail, indicating EndMT. Matrix production or remodeling was not measured. Bioreactors such as these may allow the testing of bioactive materials as well as hemodynamic variables. However, in this analysis the endothelial cells were exposed to a constant single shear pattern for 48h, whereas in-vivo the hemodynamic patterns change along with pulsations. Pulsatile flow patterns can be included in bioreactor designs such as described by Smits et al. [87]. Egorova et al. used a bioreactor to study the response of ECFCs, HUVECs and human umbilical arterial endothelial cells (HUAECs) to shear stress. All cell types were subjected to low and high shear stress for 5 hours using a parallel plate flow chamber, and a similar transcriptional response was found between the cell types pointing to a response of ECFCs to shear similar to adult endothelium[77]. The adhesion of cells to peptide-linked polymers in shear flow can

be studied using a radial flow chamber, where the shear rate varies linearly with radial position, allowing for the study of the effect of a range of shear rates[88].

Exposing cell-seeded grafts to appropriate shear and strain stresses may help to develop a mechanically capable vascular graft with not only the proper cell populations, but also with an appropriate ECM fiber orientation level[84]. Emphasizing the importance of the orientation of mechanical force, Balachandran et al. used a bioreactor to apply strain regimes on a VEC monolayer to induce EndMT, and found that when cyclic strain was applied orthogonal, instead of parallel, to the tissue alignment, EndMT increased and the cell microarchitecture was disrupted [85]. The bioreactors described above were mostly used to study mechanical stimulation. Ideally, relevant mechanical and biochemical stimuli would be included in a single bioreactor, allowing for a combined approach. Liang et al. reported on synergistic effects of mechanical strain and TGFβ stimulation on vascular wall function in a bioreactor applying cyclic strain[89]. Such bioreactors would allow for the investigation of EndMT in an environment approaching the intended environment of cardiovascular graft. In addition, bioreactors capable of combining mechanical and biochemical stimuli may be used to guide the development of cellularized grafts in vitro, prior to implantation in vivo.

Conclusions

A tissue engineered vascular structure can be designed to exploit the in situ stimuli and guide tissue formation by regulating EndMT. Advanced molecular design of biomaterials and production methods will dictate the possibilities of including these factors. Novel biomaterials can incorporate the timed release of multiple EndMT inducing or limiting factors in controlled concentrations. Provided that a graft contains endothelial cells these factors may boost cell migration and ECM production to achieve a mechanically sufficient interstitium. Considering that the inflammatory and mechanical environment may combine to push EndMT towards a fibrotic development, inhibitory factors should also be considered. ROS inhibitors such as astaxanthin, for instance, could be administered to halt EndMT after tissue formation is sufficient. In addition, the fine-tuning of the ECM can be aided by regulation by mirs, potentially delivered through microvesicles. The content of these vesicles can be controlled, for instance by the transfection of expression vectors into the cells producing the extracellular microvesicles (56). Furthermore, since ECM deposition and remodeling is highly dependent on both the alignment of cells adhering to materials and hemodynamic flow patterns, the structural design of cardiovascular grafts in itself provides options to manipulate EndMT. Additional research, for instance using bioreactors capable of applying simultaneous mechanical and biochemical stimulation, is needed to accurately predict how candidate cell sources will respond to the complex environment of an implanted vascular replacement graft. This approach may lead to an improved clinical transition of functionalized implanted scaffolds, carefully designed to develop into living, functional cardiovascular replacements.

Acknowledgements

This research forms part of the Project P1.01 iValve of the research program of the BioMedical Materials institute, co-funded by the Dutch Ministry of Economic Affairs. The financial contribution of the Nederlandse Hartstichting is gratefully acknowledged. We acknowledge the support for PHAEDRA (CVON-2012-08) and for 1Valve (CVON-2012-01) from the Netherlands CardioVascular Research Initiative: the Dutch Heart Foundation, Dutch Federation of University Medical Centers, the Netherlands Organisation for Health Research and Development, and the Royal Netherlands Academy of Sciences.

References

1. J. Wylie-Sears, R.A. Levine, J. Bischoff, Losartan inhibits endothelial-to-mesenchymal transformation in mitral valve endothelial cells by blocking transforming growth factor-β-induced phosphorylation of ERK, Biochemical and Biophysical Research Communications. 446 (2014) 870–875. doi:10.1016/j.bbrc.2014.03.014.
2. P.W. Riem Vis, J. Kluin, J.P.G. Sluijter, L.A. van Herwerden, C.V.C. Bouten, Environmental regulation of valvulogenesis: implications for tissue engineering, Eur J Cardiothorac Surg. 39 (2011) 8–17. doi:10.1016/j.ejcts.2010.05.032.
3. R. Hinton Jr, J. Lincoln, G. Deutsch, H. Osinska, P. Manning, D. Benson, et al., Extracellular matrix remodeling and organization in developing and diseased aortic valves, Circ Res. 98 (2006) 1431.
4. K.M. Welch-Reardon, N. Wu, C.C.W. Hughes, A Role for Partial Endothelial-Mesenchymal Transitions in Angiogenesis? Arteriosclerosis, Thrombosis, and Vascular Biology. 35 (2015) 303–308. doi:10.1161/ATVBAHA.114.303220.
5. M.-J. Goumans, F. Lebrin, G. Valdimarsdottir, Controlling the angiogenic switch: a balance between two distinct TGF-b receptor signaling pathways, Trends in Cardiovascular Medicine. 13 (2003) 301–307.
6. D.E.P. Muylaert, J.O. Fledderus, C.V.C. Bouten, P.Y.W. Dankers, M.C. Verhaar, Combining tissue repair and tissue engineering; bioactivating implantable cell-free vascular scaffolds, Heart. 100 (2014) 1825–1830. doi:10.1136/heartjnl-2014-306092.
7. L.A. van Meeteren, P. ten Dijke, Regulation of endothelial cell plasticity by TGF-β, Cell Tissue Res. 347 (2012) 177–186. doi:10.1007/s00441-011-1222-6.
8. B. Hinz, The extracellular matrix and transforming growth factor-β1: Tale of a strained relationship, Matrix Biol. (2015). doi:10.1016/j.matbio.2015.05.006.
9. D.A. Ingram, L.E. Mead, H. Tanaka, V. Meade, A. Fenoglio, K. Mortell, et al., Identification of a novel hierarchy of endothelial progenitor cells using human peripheral and umbilical cord blood, …. (2004).
10. M.C. Yoder, L.E. Mead, D. Prater, T.R. Krier, K.N. Mroueh, F. Li, et al., Redefining

endothelial progenitor cells via clonal analysis and hematopoietic stem/progenitor cell principals, Blood. 109 (2007) 1801–1809. doi:10.1182/blood-2006-08-043471.
11. N. de Jonge, D.E.P. Muylaert, E.S. Fioretta, F.P.T. Baaijens, J.O. Fledderus, M.C. Verhaar, et al., Matrix production and organization by endothelial colony forming cells in mechanically strained engineered tissue constructs, PLoS ONE. 8 (2013) e73161. doi:10.1371/journal.pone.0073161.
12. J.P. Thiery, H. Acloque, R.Y.J. Huang, M.A. Nieto, Epithelial-mesenchymal transitions in development and disease, Cell. 139 (2009) 871–890. doi:10.1016/j.cell.2009.11.007.
13. R. Kalluri, R.A. Weinberg, The basics of epithelial-mesenchymal transition, J. Clin. Invest. 119 (2009) 1420–1428. doi:10.1172/JCI39104.
14. D. Medici, S. Potenta, R. Kalluri, Transforming growth factor-β2 promotes Snail-mediated endothelial–mesenchymal transition through convergence of Smad-dependent and Smad-independent signalling, Biochem. J. 437 (2011) 515–520. doi:10.1038/onc.2010.181.
15. M.C. Dickson, J.S. Martin, F.M. Cousins, A.B. Kulkarni, S. Karlsson, R.J. Akhurst, Defective haematopoiesis and vasculogenesis in transforming growth factor-beta 1 knock out mice, Development. 121 (1995) 1845–1854.
16. S. Lamouille, J. Xu, R. Derynck, Molecular mechanisms of epithelial-mesenchymal transition, Nat. Rev. Mol. Cell Biol. 15 (2014) 178–196. doi:10.1038/nrm3758.
17. R.B. Runyan, R.R. Markwald, Invasion of mesenchyme into three-dimensional collagen gels: a regional and temporal analysis of interaction in embryonic heart tissue, Developmental Biology. 95 (1983) 108–114.
18. R.R. Markwald, J.M. Krook, G.T. Kitten, R.B. Runyan, Endocardial cushion tissue development: structural analyses on the attachment of extracellular matrix to migrating mesenchymal cell surfaces, Scan Electron Microsc. (1981) 261–274.
19. E.L. Krug, R.B. Runyan, R.R. Markwald, Protein extracts from early embryonic hearts initiate cardiac endothelial cytodifferentiation, Developmental Biology. 112 (1985) 414–426.
20. M. Azhar, K. Brown, C. Gard, H. Chen, S. Rajan, D.A. Elliott, et al., Transforming growth factor Beta2 is required for valve remodeling during heart development, Dev. Dyn. 240 (2011) 2127–2141. doi:10.1002/dvdy.22702.
21. P. Zhang, Y. Wei, L. Wang, B.G. Debeb, Y. Yuan, J. Zhang, et al., ATM-mediated stabilization of ZEB1 promotes DNA damage response and radioresistance through CHK1, Nat Cell Biol. 16 (2014) 864–875. doi:10.1038/ncb3013.
22. M. Klüppel, J.L. Wrana, Turning it up a Notch: cross-talk between TGFβ and Notch signaling, Bioessays. 27 (2005) 115–118.
23. A. Cano, M.A. Pérez-Moreno, I. Rodrigo, A. Locascio, M.J. Blanco, M.G. del Barrio, et al., The transcription factor snail controls epithelial-mesenchymal transitions by repressing E-cadherin expression, Nat Cell Biol. 2 (2000) 76–83. doi:10.1038/35000025.
24. J. Yoshino, T. Monkawa, M. Tsuji, M. Inukai, H. Itoh, M. Hayashi, Snail1 is involved in the renal epithelial-mesenchymal transition, Biochemical and Biophysical Research Communications. 362 (2007) 63–68. doi:10.1016/j.bbrc.2007.07.146.
25. A. Boutet, C.A. De Frutos, P.H. Maxwell, M.J. Mayol, J. Romero, M.A. Nieto, Snail

activation disrupts tissue homeostasis and induces fibrosis in the adult kidney, Embo J. 25 (2006) 5603–5613. doi:10.1038/sj.emboj.7601421.
26. E. Pardali, M.-J. Goumans, P. ten Dijke, Signaling by members of the TGF-beta family in vascular morphogenesis and disease, Trends Cell Biol. 20 (2010) 556–567. doi:10.1016/j.tcb.2010.06.006.
27. V. Kaartinen, J.W. Voncken, C. Shuler, D. Warburton, D. Bu, N. Heisterkamp, et al., Abnormal lung development and cleft palate in mice lacking TGF-beta 3 indicates defects of epithelial-mesenchymal interaction, Nat Genet. 11 (1995) 415–421. doi:10.1038/ng1295-415.
28. S. Sridurongrit, J. Larsson, R. Schwartz, P. Ruiz-Lozano, V. Kaartinen, Signaling via the Tgf-beta type I receptor Alk5 in heart development, Developmental Biology. 322 (2008) 208–218. doi:10.1016/j.ydbio.2008.07.038.
29. L. Van Laer, H. Dietz, B. Loeys, Loeys-Dietz syndrome, Adv. Exp. Med. Biol. 802 (2014) 95–105. doi:10.1007/978-94-007-7893-1_7.
30. K. Felgentreff, M. Siepe, S. Kotthoff, Y. von Kodolitsch, K. Schachtrup, L.D. Notarangelo, et al., Severe eczema and Hyper-IgE in Loeys-Dietz-syndrome - contribution to new findings of immune dysregulation in connective tissue disorders, Clin. Immunol. 150 (2014) 43–50. doi:10.1016/j.clim.2013.11.008.
31. B.L. Loeys, J. Chen, E.R. Neptune, D.P. Judge, M. Podowski, T. Holm, et al., A syndrome of altered cardiovascular, craniofacial, neurocognitive and skeletal development caused by mutations in TGFBR1 or TGFBR2, Nat Genet. 37 (2005) 275–281. doi:10.1038/ng1511.
32. V.C. Garside, A.C. Chang, A. Karsan, P.A. Hoodless, Co-ordinating Notch, BMP, and TGF-β signaling during heart valve development, Cell. Mol. Life Sci. 70 (2013) 2899–2917. doi:10.1007/s00018-012-1197-9.
33. P.T. Dijke, C.S. Hill, New insights into TGF-β–Smad signalling, Trends in Biochemical Sciences. 29 (2004) 265–273. doi:10.1016/j.tibs.2004.03.008.
34. H. Zhang, X. Jia, F. Han, J. Zhao, Y. Zhao, Y. Fan, et al., Dual-delivery of VEGF and PDGF by double-layered electrospun membranes for blood vessel regeneration, Biomaterials. 34 (2013) 2202–2212. doi:10.1016/j.biomaterials.2012.12.005.
35. F. Han, X. Jia, D. Dai, X. Yang, J. Zhao, Y. Zhao, et al., Performance of a multilayered small-diameter vascular scaffold dual-loaded with VEGF and PDGF, Biomaterials. 34 (2013) 7302–7313. doi:10.1016/j.biomaterials.2013.06.006.
36. C. Théry, L. Zitvogel, S. Amigorena, Exosomes: composition, biogenesis and function, Nature Reviews Immunology. 2 (2002) 569–579. doi:10.1038/nri855.
37. F.T. Borges, S.A. Melo, B.C. Özdemir, N. Kato, I. Revuelta, C.A. Miller, et al., TGF-β1-containing exosomes from injured epithelial cells activate fibroblasts to initiate tissue regenerative responses and fibrosis, Journal of the American Society of Nephrology. 24 (2013) 385–392. doi:10.1681/ASN.2012101031.
38. W. Stoorvogel, M.J. Kleijmeer, H.J. Geuze, G. Raposo, The biogenesis and functions of exosomes, Traffic. 3 (2002) 321–330.
39. P. Vader, X.O. Breakefield, M.J.A. Wood, Extracellular vesicles: emerging targets for cancer therapy, Trends Mol Med. 20 (2014) 385–393. doi:10.1016/j.molmed.2014.03.002.

40. J. Webber, R. Steadman, M.D. Mason, Z. Tabi, A. Clayton, Cancer exosomes trigger fibroblast to myofibroblast differentiation, Cancer Research. 70 (2010) 9621–9630. doi:10.1158/0008-5472.CAN-10-1722.
41. O.G. de Jong, M.C. Verhaar, Y. Chen, P. Vader, H. Gremmels, G. Posthuma, et al., Cellular stress conditions are reflected in the protein and RNA content of endothelial cell-derived exosomes, J Extracell Vesicles. 1 (2012) 569. doi:10.3402/jev.v1i0.18396.
42. O.G. de Jong, B.W.M. van Balkom, R.M. Schiffelers, C.V.C. Bouten, M.C. Verhaar, Extracellular Vesicles: Potential Roles in Regenerative Medicine, Front. Immunol. 5 (2014). doi:10.3389/fimmu.2014.00608.
43. A.K. Lagendijk, M.-J. Goumans, S.B. Burkhard, J. Bakkers, MicroRNA-23 restricts cardiac valve formation by inhibiting Has2 and extracellular hyaluronic acid production, Circ Res. 109 (2011) 649–657. doi:10.1161/CIRCRESAHA.111.247635.
44. R. Bijkerk, R.G. de Bruin, C. van Solingen, J.M.G.J. Duijs, K. Kobayashi, E.P. van der Veer, et al., MicroRNA-155 Functions as a Negative Regulator of RhoA Signaling in TGF-β-induced Endothelial to Mesenchymal Transition, Microrna. 1 (2012) 2–10.
45. R. Kumarswamy, I. Volkmann, V. Jazbutyte, S. Dangwal, D.-H. Park, T. Thum, Transforming growth factor-β-induced endothelial-to-mesenchymal transition is partly mediated by microRNA-21, Arteriosclerosis, Thrombosis, and Vascular Biology. 32 (2012) 361–369. doi:10.1161/ATVBAHA.111.234286.
46. E. van Rooij, L.B. Sutherland, J.E. Thatcher, J.M. DiMaio, R.H. Naseem, W.S. Marshall, et al., Dysregulation of microRNAs after myocardial infarction reveals a role of miR-29 in cardiac fibrosis, Proceedings of the National Academy of Sciences. 105 (2008) 13027–13032. doi:10.1073/pnas.0805038105.
47. A. Zampetaki, R.Q. Attia, U. Mayr, R.S. Gomes, A. Phinikaridou, X. Yin, et al., Role of miR-195 in Aortic Aneurysmal Disease, Circ Res. 115 (2014) 857–866. doi:10.1161/CIRCRESAHA.115.304361.
48. C. Luna, G. Li, J. Qiu, D.L. Epstein, P. Gonzalez, Cross-talk between miR-29 and Transforming Growth Factor-Betas in Trabecular Meshwork Cells, Invest. Ophthalmol. Vis. Sci. 52 (2011) 3567–3572. doi:10.1167/iovs.10-6448.
49. P. Zhang, A. Huang, J. Ferruzzi, R.P. Mecham, B.C. Starcher, G. Tellides, et al., Inhibition of MicroRNA-29 Enhances Elastin Levels in Cells Haploinsufficient for Elastin and in Bioengineered Vessels, Arteriosclerosis, Thrombosis, and Vascular Biology. 32 (2011) 756–759. doi:10.1161/ATVBAHA.111.238113.
50. M. Hulsmans, P. Holvoet, MicroRNA-containing microvesicles regulating inflammation in association with atherosclerotic disease, Cardiovascular Research. 100 (2013) 7–18. doi:10.1093/cvr/cvt161.
51. K. Valencia, D. Luis-Ravelo, N. Bovy, I. Antón, S. Martínez-Canarias, C. Zandueta, et al., miRNA cargo within exosome-like vesicle transfer influences metastatic bone colonization, Mol Oncol. 8 (2014) 689–703. doi:10.1016/j.molonc.2014.01.012.
52. K. Ohshima, K. Inoue, A. Fujiwara, K. Hatakeyama, K. Kanto, Y. Watanabe, et al., Let-7 microRNA family is selectively secreted into the extracellular environment via exosomes

in a metastatic gastric cancer cell line, PLoS ONE. 5 (2010) e13247. doi:10.1371/journal.pone.0013247.
53. A. Díaz-López, G. Moreno-Bueno, A. Cano, Role of microRNA in epithelial to mesenchymal transition and metastasis and clinical perspectives, Cancer Manag Res. 6 (2014) 205–216. doi:10.2147/CMAR.S38156.
54. P.-Y. Chen, L. Qin, C. Barnes, K. Charisse, T. Yi, X. Zhang, et al., FGF regulates TGF-β signaling and endothelial-to-mesenchymal transition via control of let-7 miRNA expression, Cell Rep. 2 (2012) 1684–1696. doi:10.1016/j.celrep.2012.10.021.
55. K. Shimbo, S. Miyaki, H. Ishitobi, Y. Kato, T. Kubo, S. Shimose, et al., Exosome-formed synthetic microRNA-143 is transferred to osteosarcoma cells and inhibits their migration, Biochemical and Biophysical Research Communications. 445 (2014) 381–387. doi:10.1016/j.bbrc.2014.02.007.
56. R. Singh, R. Pochampally, K. Watabe, Z. Lu, Y.-Y. Mo, Exosome-mediated transfer of miR-10b promotes cell invasion in breast cancer, Mol. Cancer. 13 (2014) 256. doi:10.1186/1476-4598-13-256.
57. B.W.M. van Balkom, O.G. de Jong, M. Smits, J. Brummelman, K. den Ouden, P.M. de Bree, et al., Endothelial cells require miR-214 to secrete exosomes that suppress senescence and induce angiogenesis in human and mouse endothelial cells, Blood. 121 (2013) 3997–4006–S1–15. doi:10.1182/blood-2013-02-478925.
58. A. Mikos, L. McIntire, J. Anderson, J. Babensee, Host response to tissue engineered devices, Advanced Drug Delivery Reviews. 33 (1998) 111–139.
59. I. Montorfano, A. Becerra, R. Cerro, C. Echeverría, E. Sáez, M.G. Morales, et al., Oxidative stress mediates the conversion of endothelial cells into myofibroblasts via a TGF-β1 and TGF-β2-dependent pathway, Lab. Invest. 94 (2014) 1068–1082. doi:10.1038/labinvest.2014.100.
60. Y. Yang, B. Kim, Y.-K. Park, S.I. Koo, J.-Y. Lee, Astaxanthin prevents TGFβ1-induced pro-fibrogenic gene expression by inhibiting Smad3 activation in hepatic stellate cells, Biochim. Biophys. Acta. 1850 (2015) 178–185. doi:10.1016/j.bbagen.2014.10.014.
61. D. Luo, J. Wang, J. Li, M. Post, Mouse snail is a target gene for HIF, Mol. Cancer Res. 9 (2011) 234–245. doi:10.1158/1541-7786.MCR-10-0214.
62. P.M. Angel, D. Nusinow, C.B. Brown, K. Violette, J.V. Barnett, B. Zhang, et al., Networked-based characterization of extracellular matrix proteins from adult mouse pulmonary and aortic valves, J. Proteome Res. 10 (2011) 812–823. doi:10.1021/pr1009806.
63. G.J. Mahler, E.J. Farrar, J.T. Butcher, Inflammatory cytokines promote mesenchymal transformation in embryonic and adult valve endothelial cells, Arteriosclerosis, Thrombosis, and Vascular Biology. 33 (2013) 121–130. doi:10.1161/ATVBAHA.112.300504.
64. F. Rieder, S.P. Kessler, G.A. West, S. Bhilocha, C. de la Motte, T.M. Sadler, et al., Inflammation-induced endothelial-to-mesenchymal transition: a novel mechanism of intestinal fibrosis, Am J Pathol. 179 (2011) 2660–2673. doi:10.1016/j.ajpath.2011.07.042.
65. M. Maleszewska, J.-R.A.J. Moonen, N. Huijkman, B. van de Sluis, G. Krenning, M.C. Harmsen, IL-1β and TGFβ2 synergistically induce endothelial to mesenchymal transition in an NFκB-dependent manner, Immunobiology. 218 (2013) 443–454. doi:10.1016/j.im-

bio.2012.05.026.
66. I. Chrobak, S. Lenna, L. Stawski, M. Trojanowska, Interferon-γ promotes vascular remodeling in human microvascular endothelial cells by upregulating endothelin (ET)-1 and transforming growth factor (TGF) β2, J Cell Physiol. 228 (2013) 1774–1783. doi:10.1002/jcp.24337.
67. J.D. Humphrey, S.L. Delange, An Introduction to Biomechanics: Solids and Fluids, Analysis and Design - Jay D. Humphrey, Sherry L. Delange - Google Books, (2004).
68. J. Ando, K. Yamamoto, Flow detection and calcium signalling in vascular endothelial cells, Cardiovascular Research. 99 (2013) 260–268. doi:10.1093/cvr/cvt084.
69. G.J. Mahler, C.M. Frendl, Q. Cao, J.T. Butcher, Effects of shear stress pattern and magnitude on mesenchymal transformation and invasion of aortic valve endothelial cells, Biotechnol. Bioeng. 111 (2014) 2326–2337. doi:10.1002/bit.25291.
70. J.Y.-J. Shyy, S. Chien, Role of integrins in endothelial mechanosensing of shear stress, Circ Res. 91 (2002) 769–775.
71. D.E. Ingber, Tensegrity: the architectural basis of cellular mechanotransduction, Annu. Rev. Physiol. 59 (1997) 575–599. doi:10.1146/annurev.physiol.59.1.575.
72. E. Tkachenko, E. Gutierrez, S.K. Saikin, P. Fogelstrand, C. Kim, A. Groisman, et al., The nucleus of endothelial cell as a sensor of blood flow direction, Biol Open. 2 (2013) 1007–1012. doi:10.1242/bio.20134622.
73. A.D. Egorova, K. Van der Heiden, R.E. Poelmann, B.P. Hierck, Primary cilia as biomechanical sensors in regulating endothelial function, Differentiation. 83 (2012) S56–S61. doi:10.1016/j.diff.2011.11.007.
74. P. ten Dijke, A.D. Egorova, M.-J.T.H. Goumans, R.E. Poelmann, B.P. Hierck, TGF-β signaling in endothelial-to-mesenchymal transition: the role of shear stress and primary cilia, Science Signaling. 5 (2012) pt2–pt2. doi:10.1126/scisignal.2002722.
75. S. Kallakuri, J.A. Yu, J. Li, Y. Li, B.M. Weinstein, S. Nicoli, et al., Endothelial Cilia Are Essential for Developmental Vascular Integrity in Zebrafish, Journal of the American Society of Nephrology. 26 (2014) 864–875. doi:10.1681/ASN.2013121314.
76. K. Van der Heiden, B.P. Hierck, R. Krams, R. de Crom, C. Cheng, M. Baiker, et al., Endothelial primary cilia in areas of disturbed flow are at the base of atherosclerosis, Atherosclerosis. 196 (2008) 542–550. doi:10.1016/j.atherosclerosis.2007.05.030.
77. A.D. Egorova, M.C. Deruiter, H.C. de Boer, S. Van de Pas, A.C. Gittenberger-de Groot, A.J. van Zonneveld, et al., Endothelial colony-forming cells show a mature transcriptional response to shear stress, In Vitro Cellular & Developmental Biology-Animal. 48 (2012) 21–29. doi:10.1007/s11626-011-9470-z.
78. A.D. Egorova, P.P.S.J. Khedoe, M.-J.T.H. Goumans, B.K. Yoder, S.M. Nauli, P. ten Dijke, et al., Lack of primary cilia primes shear-induced endothelial-to-mesenchymal transition, Circ Res. 108 (2011) 1093–1101. doi:10.1161/CIRCRESAHA.110.231860.
79. G. Sánchez-Duffhues, A.G. de Vinuesa, J.H. Lindeman, A. Mulder-Stapel, M.C. Deruiter, C. Van Munsteren, et al., SLUG Is Expressed in Endothelial Cells Lacking Primary Cilia to Promote Cellular Calcification, Arteriosclerosis, Thrombosis, and Vascular Biology. 35 (2015) 616–627. doi:10.1161/ATVBAHA.115.305268.

80. H. Bahraseman, K. Hassani, A. Khosravi, M. Navidbakhsh, D. Espino, N. Fatouraee, et al., Combining numerical and clinical methods to assess aortic valve hemodynamics during exercise, Perfusion. 29 (2014) 340–350. doi:10.1177/0267659114521103.
81. B.P. Hierck, K. Van der Heiden, F.E. Alkemade, S. Van de Pas, J.V. Van Thienen, B.C.W. Groenendijk, et al., Primary cilia sensitize endothelial cells for fluid shear stress, Dev. Dyn. 237 (2008) 725–735. doi:10.1002/dvdy.21472.
82. E.S. Fioretta, M. Simonet, A.I.P.M. Smits, F.P.T. Baaijens, C.V.C. Bouten, Differential response of endothelial and endothelial colony forming cells on electrospun scaffolds with distinct microfiber diameters, Biomacromolecules. 15 (2014) 821–829. doi:10.1021/bm4016418.
83. N.J.B. Driessen, A. Mol, C.V.C. Bouten, F.P.T. Baaijens, Modeling the mechanics of tissue-engineered human heart valve leaflets, J Biomech. 40 (2007) 325–334. doi:10.1016/j.jbiomech.2006.01.009.
84. M.A.J. Cox, J. Kortsmit, N. Driessen, C.V.C. Bouten, F.P.T. Baaijens, Tissue-engineered heart valves develop native-like collagen fiber architecture, Tissue Eng Part A. 16 (2010) 1527–1537. doi:10.1089/ten.TEA.2009.0263.
85. K. Balachandran, P.W. Alford, J. Wylie-Sears, J.A. Goss, A. Grosberg, J. Bischoff, et al., Cyclic strain induces dual-mode endothelial-mesenchymal transformation of the cardiac valve, Proceedings of the National Academy of Sciences. 108 (2011) 19943–19948. doi:10.1073/pnas.1106954108.
86. A. Mol, M.I. van Lieshout, C.G. Dam-de Veen, S. Neuenschwander, S.P. Hoerstrup, F.P.T. Baaijens, et al., Fibrin as a cell carrier in cardiovascular tissue engineering applications, Biomaterials. 26 (2005) 3113–3121. doi:10.1016/j.biomaterials.2004.08.007.
87. A.I.P.M. Smits, A. Driessen-Mol, C.V.C. Bouten, F.P.T. Baaijens, A Mesofluidics-Based Test Platform for Systematic Development of Scaffolds for In Situ Cardiovascular Tissue Engineering, Tissue Engineering Part C: Methods. 18 (2012) 475–485. doi:10.1089/ten.TEC.2011.0458.
88. X. Wang, S. Cooper, Adhesion of endothelial cells and endothelial progenitor cells on peptide-linked polymers in shear flow, Tissue Eng Part A. 19 (2013) 1113–1121. doi:10.1089/ten.TEA.2011.0653.
89. M.-S. Liang, M. Koobatian, P. Lei, D.D. Swartz, S.T. Andreadis, Differential and synergistic effects of mechanical stimulation and growth factor presentation on vascular wall function, Biomaterials. 34 (2013) 7281–7291. doi:10.1016/j.biomaterials.2013.05.073.

Supplementary Table S1. Overview of Endothelial Cell Types and Sources Used in EndMT Research

Species	Cell Type	References
Human	Endothelial Colony Forming Cells (ECFC)	(1-4)
	Glomerular Endothelial Cells (GEC)	(5,6)
	Human Aortic Endothelial Cells (HAEC)	(1,7-11)
	Human Cutaenous Microvascular Endothelial Cells (HCMEC)	(2,12)
	Human Dermal Microvascular Endothelial Cells (HDMVEC)	(5,13,14)
	Human Esophageal Microvascular Endothelial Cells (HEMEC)	(15,16)
	Human Intestinal Microvascular Endothelial Cells (HIMEC)	(17-21)
	Human Microvascular Endothelial Cells (HMEC-1)	(12,22,23)
	Human Microvascular Endothelial Cells (HMVEC)	(24,25)
	Human Umbilical Vein Endothelial Cells (HUVEC)	(15,26-31)
	Lymphatic Endothelial Cells (LEC)	(19,32,33)
Mouse	Lymphatic Endothelial Cells (LEC)	(32,34,35)
	Mouse Embryonic Endothelial Cells (MEEC)	(36,37)
	Mouse Embryonic Stem Cell Derived Endothelial Cells (MESEC)	(5,38,39)
	Mouse Pancreatic Microvascular Endothelial Cells (MS-1)	(1,8,40,41)
	Mouse Pulmonary Endothelial Cells	(2,42-44)
Porcine	Porcine Aortic Valve Endothelial Cells (PAVEC)	(5,14,39,41,45,46)
Rat	Endothelial Progenitor Cells (EPC)	(27)
Sheep	Valvular Endothelial Cells (VEC)	(47)

References

1. Riem Vis PW, Kluin J, Sluijter JPG, van Herwerden LA, Bouten CVC. Environmental regulation of valvulogenesis: implications for tissue engineering. Eur J Cardiothorac Surg. 39(1), 8, 2011.
2. de Jonge N, Muylaert DEP, Fioretta ES, Baaijens FPT, Fledderus JO, Verhaar MC, et al. Matrix production and organization by endothelial colony forming cells in mechanically strained engineered tissue constructs. Kumar S, editor. PLoS ONE [Internet]. 8(9), e73161, 2013. Available from: http://eutils.ncbi.nlm.nih.gov/entrez/eutils/elink.fcgi?dbfrom=pubmed&id=24023827&retmode=ref&cmd=prlinks
3. Moonen J, Krenning G, Brinker M, Koerts J, van Luyn M, Harmsen M. Endothelial progenitor cells give rise to pro-angiogenic smooth muscle-like progeny. Cardiovascular research. 2010.
4. Wylie-Sears J, Levine RA, Bischoff J. Losartan inhibits endothelial-to-mesenchymal transformation in mitral valve endothelial cells by blocking transforming growth factor-β-induced phosphorylation of ERK. Biochemical and Biophysical Research Communications. 446(4), 870, 2014.

5. Hinton R Jr, Lincoln J, Deutsch G, Osinska H, Manning P, Benson D, et al. Extracellular matrix remodeling and organization in developing and diseased aortic valves. Circ Res. 98(11), 1431, 2006.
6. Wu M, Tang R-N, Liu H, Ma K-L, Lv L-L, Liu B-C. Nuclear Translocation of β-Catenin Mediates the Parathyroid Hormone-Induced Endothelial-to-Mesenchymal Transition in Human Renal Glomerular Endothelial Cells. Journal of cellular biochemistry. 115(10), 1692, 2014.
7. Tang R, Li Q, Lv L, Dai H, Zheng M, Ma K, et al. Angiotensin II mediates the high-glucose-induced endothelial-to-mesenchymal transition in human aortic endothelial cells. Cardiovasc Diabetol. 9(1), 31, 2010.
8. Goumans M-J, Lebrin F, Valdimarsdottir G. Controlling the angiogenic switch: a balance between two distinct TGF-b receptor signaling pathways. Trends in Cardiovascular Medicine. 13(7), 301, 2003.
9. Tang R, Gao M, Wu M, Liu H, Zhang X, Liu B. High glucose mediates endothelial-to-chondrocyte transition in human aortic endothelial cells. Cardiovasc Diabetol. 11(1), 113, 2012.
10. Kim M, Choi S-H, Jin YB, Lee H-J, Ji YH, Kim J, et al. The effect of oxidized low-density lipoprotein (ox-LDL) on radiation-induced endothelial-to-mesenchymal transition. Int. J. Radiat. Biol. 89(5), 356, 2013.
11. Zeng L, Wang G, Ummarino D, Margariti A, Xu Q, Xiao Q, et al. Histone deacetylase 3 unconventional splicing mediates endothelial-to-mesenchymal transition through transforming growth factor β2. Journal of Biological Chemistry. 288(44), 31853, 2013.
12. Fu Y, Chang ACY, Fournier M, Chang L, Niessen K, Karsan A. RUNX3 maintains the mesenchymal phenotype after termination of the Notch signal. Journal of Biological Chemistry. 286(13), 11803, 2011.
13. Chrobak I, Lenna S, Stawski L, Trojanowska M. Interferon-γ promotes vascular remodeling in human microvascular endothelial cells by upregulating endothelin (ET)-1 and transforming growth factor (TGF) β2. J Cell Physiol. 228(8), 1774, 2013.
14. Kalluri R, Weinberg RA. The basics of epithelial-mesenchymal transition. J. Clin. Invest. 119(6), 1420, 2009.
15. Lamouille S, Xu J, Derynck R. Molecular mechanisms of epithelial-mesenchymal transition. Nat. Rev. Mol. Cell Biol. 15(3), 178, 2014.
16. Nie L, Lyros O, Medda R, Jovanovic N, Schmidt JL, Otterson MF, et al. Endothelial -Mesenchymal Transition in Normal Human Esophageal Endothelial Cells Co-cultured with Esophageal Adenocarcinoma cells: Role of IL-1β and TGF-β2. Am. J. Physiol., Cell Physiol. 307(9), C859, 2014.
17. Klüppel M, Wrana JL. Turning it up a Notch: cross-talk between TGFβ and Notch signaling. Bioessays. Wiley Online Library; 27(2), 115, 2005.
18. Rieder F, Kessler SP, West GA, Bhilocha S, la Motte de C, Sadler TM, et al. Inflammation-induced endothelial-to-mesenchymal transition: a novel mechanism of intestinal fibrosis. Am J Pathol. 179(5), 2660, 2011.

19. Cano A, Pérez-Moreno MA, Rodrigo I, Locascio A, Blanco MJ, del Barrio MG, et al. The transcription factor snail controls epithelial-mesenchymal transitions by repressing E-cadherin expression. Nat Cell Biol. 2(2), 76, 2000.
20. Sadler T, Scarpa M, Rieder F, West G, Stylianou E. Cytokine-induced chromatin modifications of the type I collagen alpha 2 gene during intestinal endothelial-to-mesenchymal transition. Inflamm. Bowel Dis. 19(7), 1354, 2013.
21. Yoshino J, Monkawa T, Tsuji M, Inukai M, Itoh H, Hayashi M. Snail1 is involved in the renal epithelial-mesenchymal transition. Biochemical and Biophysical Research Communications. 362(1), 63, 2007.
22. Boutet A, De Frutos CA, Maxwell PH, Mayol MJ, Romero J, Nieto MA. Snail activation disrupts tissue homeostasis and induces fibrosis in the adult kidney. EMBO J. 25(23), 5603, 2006.
23. Fu Y, Chang A, Chang L, Niessen K, Eapen S, Setiadi A, et al. Differential regulation of transforming growth factor beta signaling pathways by Notch in human endothelial cells. J. Biol. Chem. 284(29), 19452, 2009.
24. Medici D, Potenta S, Kalluri R. Transforming growth factor-β2 promotes Snail-mediated endothelial–mesenchymal transition through convergence of Smad-dependent and Smad-independent signalling. Biochem. J. 437(3), 515, 2011.
25. Garcia J, Sandi MJ, Cordelier P, Binétruy B, Pouysségur J, Iovanna JL, et al. Tie1 deficiency induces endothelial-mesenchymal transition. EMBO Rep. 13(5), 431, 2012.
26. Rodríguez MI, Peralta-Leal A, O'Valle F, Rodriguez-Vargas JM, Gonzalez-Flores A, Majuelos-Melguizo J, et al. PARP-1 regulates metastatic melanoma through modulation of vimentin-induced malignant transformation. Clurman BE, editor. PLoS Genet. 9(6), e1003531, 2013.
27. Zhang W, Chen G, Ren J-G, Zhao Y-F. Bleomycin induces endothelial mesenchymal transition through activation of mTOR pathway: a possible mechanism contributing to the sclerotherapy of venous malformations. Br. J. Pharmacol. 170(6), 1210, 2013.
28. Kumarswamy R, Volkmann I, Jazbutyte V, Dangwal S, Park D-H, Thum T. Transforming growth factor-β-induced endothelial-to-mesenchymal transition is partly mediated by microRNA-21. Arteriosclerosis, Thrombosis, and Vascular Biology. 32(2), 361, 2012.
29. Maleszewska M, Moonen J-RAJ, Huijkman N, van de Sluis B, Krenning G, Harmsen MC. IL-1β and TGFβ2 synergistically induce endothelial to mesenchymal transition in an NFκB-dependent manner. Immunobiology. 218(4), 443, 2013.
30. Welch-Reardon KM, Ehsan SM, Wang K, Wu N, Newman AC, Romero-Lopez M, et al. Angiogenic sprouting is regulated by endothelial cell expression of Slug. Journal of Cell Science. 127(Pt 9), 2017, 2014.
31. Zhu K, Pan Q, Jia L-Q, Dai Z, Ke A-W, Zeng H-Y, et al. MiR-302c inhibits tumor growth of hepatocellular carcinoma by suppressing the endothelial-mesenchymal transition of endothelial cells. Sci Rep. 4, 5524, 2014.
32. Ichise T, Yoshida N, Ichise H. FGF2-induced Ras-MAPK signalling maintains lymphatic endothelial cell identity by upregulating endothelial-cell-specific gene expression and sup-

pressing TGFβ signalling through Smad2. Journal of Cell Science. 127(Pt 4), 845, 2014.
33. Naber HPH, Drabsch Y, Snaar-Jagalska BE, Dijke ten P, van Laar T. Snail and Slug, key regulators of TGF-β-induced EMT, are sufficient for the induction of single-cell invasion. Biochemical and Biophysical Research Communications. 435(1), 58, 2013.
34. Ivanova L, Butt MJ, Matsell DG. Mesenchymal transition in kidney collecting duct epithelial cells. Am. J. Physiol. Renal Physiol. 294(5), F1238, 2008.
35. LeBleu VS, Taduri G, O'Connell J, Teng Y, Cooke VG, Woda C, et al. Origin and function of myofibroblasts in kidney fibrosis. Nature medicine. 19(8), 1047, 2013.
36. Thiery JP, Acloque H, Huang RYJ, Nieto MA. Epithelial-mesenchymal transitions in development and disease. Cell. 139(5), 871, 2009.
37. Bijkerk R, de Bruin RG, van Solingen C, Duijs JMGJ, Kobayashi K, van der Veer EP, et al. MicroRNA-155 Functions as a Negative Regulator of RhoA Signaling in TGF-β-induced Endothelial to Mesenchymal Transition. Microrna. 1(1), 2, 2012.
38. Kokudo T, Suzuki Y, Yoshimatsu Y, Yamazaki T, Watabe T, Miyazono K. Snail is required for TGFbeta-induced endothelial-mesenchymal transition of embryonic stem cell-derived endothelial cells. Journal of Cell Science. 121(Pt 20), 3317, 2008.
39. Martin-Ramirez J, Hofman M, van den Biggelaar M, Hebbel RP, Voorberg J. Establishment of outgrowth endothelial cells from peripheral blood. Nat Protoc. 7(9), 1709, 2012.
40. Mihira H, Suzuki HI, Akatsu Y, Yoshimatsu Y, Igarashi T, Miyazono K, et al. TGF-β-induced mesenchymal transition of MS-1 endothelial cells requires Smad-dependent cooperative activation of Rho signals and MRTF-A. J. Biochem. 151(2), 145, 2012.
41. Ingram DA, Mead LE, Tanaka H, Meade V, Fenoglio A, Mortell K, et al. Identification of a novel hierarchy of endothelial progenitor cells using human peripheral and umbilical cord blood. …. 2004.
42. Li Z, Wermuth PJ, Benn BS, Lisanti MP, Jimenez SA. Caveolin-1 deficiency induces spontaneous endothelial-to-mesenchymal transition in murine pulmonary endothelial cells in vitro. Am J Pathol. 182(2), 325, 2013.
43. Yoder MC. Is Endothelium the Origin of Endothelial Progenitor Cells? Arteriosclerosis, Thrombosis, and Vascular Biology. 30(6), 1094, 2010.
44. Lee PSS, Poh KK. Endothelial progenitor cells in cardiovascular diseases. World J Stem Cells. 6(3), 355, 2014.
45. Mahler GJ, Farrar EJ, Butcher JT. Inflammatory Cytokines Promote Mesenchymal Transformation in Embryonic and Adult Valve Endothelial Cells. atvb.ahajournals.org.
46. Mahler GJ, Frendl CM, Cao Q, Butcher JT. Effects of shear stress pattern and magnitude on mesenchymal transformation and invasion of aortic valve endothelial cells. Biotechnol. Bioeng. 111(11), 2326, 2014.
47. Balachandran K, Alford PW, Wylie-Sears J, Goss JA, Grosberg A, Bischoff J, et al. Cyclic strain induces dual-mode endothelial-mesenchymal transformation of the cardiac valve. Proceedings of the National Academy of Sciences. 108(50), 19943, 2011.

III

Matrix Production and Organization by Endothelial Colony Forming Cells in Mechanically Strained Engineered Tissue Constructs

(Published in PlosOne)

Dimitri E. P. Muylaert *

Nicky de Jonge *

Emanuela S. Fioretta

Frank P. T. Baaijens

Joost O. Fledderus

Marianne C. Verhaar *

and Carlijn V. C. Bouten *

* these authors contributed equally

Abstract

Aims: Tissue engineering is an innovative method to restore cardiovascular tissue function by implanting either an in vitro cultured tissue or a degradable, mechanically functional scaffold that gradually transforms into a living neo-tissue by recruiting tissue forming cells at the site of implantation. Circulating endothelial colony forming cells (ECFCs) are capable of differentiating into endothelial cells as well as a mesenchymal ECM-producing phenotype, undergoing Endothelial-to-Mesenchymal-transition (EndoMT). We investigated the potential of ECFCs to produce and organize ECM under the influence of static and cyclic mechanical strain, as well as stimulation with transforming growth factor β1 (TGFβ1). Methods and results: A fibrin-based 3D tissue model was used to simulate neo-tissue formation. Extracellular matrix organization was monitored using confocal laser-scanning microscopy. ECFCs produced collagen and also elastin, but did not form an organized matrix, except when cultured with TGFβ1 under static strain. Here, collagen was aligned more parallel to the strain direction, similar to Human Vena Saphena Cell-seeded controls. Priming ECFC with TGFβ1 before exposing them to strain led to more homogenous matrix production. Conclusions: Biochemical and mechanical cues can induce extracellular matrix formation by ECFCs in tissue models that mimic early tissue formation. Our findings suggest that priming with bioactives may be required to optimize neo-tissue development with ECFCs and has important consequences for the timing of stimuli applied to scaffold designs for both in vitro and in situ cardiovascular tissue engineering. The results obtained with ECFCs differ from those obtained with other cell sources, such as vena saphena-derived myofibroblasts, underlining the need for experimental models like ours to test novel cell sources for cardiovascular tissue engineering.

Introduction

Cardiovascular diseases are a growing concern worldwide [1]. Surgical replacement of vascular structures such as heart valves and blood vessels is a commonly used therapy. While current cardiovascular replacements are effective [2,3], they often rely on autologous tissues in the case of vascular replacement therapy or have significant shortcomings, including lack of remodeling and growth potential and the need for lifelong anticoagulation therapy. These concerns apply to pediatric patients in particular, necessitating reoperations throughout life as they outgrow their prostheses [4]. Tissue engineering (TE) has been proposed as a potential alternative to overcome these limitations. A tissue engineered cardiovascular construct can be produced in vitro by seeding human-derived autologous cells [5,6] onto a biodegradable polymeric scaffold [7], followed by the application of biochemical and mechanical stimuli in bioreactors [8]. The final product is a living tissue [9], able to integrate, grow, and remodel with the patient upon scaffold degradation [7]. By using a pre-shaped scaffold, a tissue engineered construct can be obtained by seeding and conditioning human vena saphena cells (HVSCs) [8,10]. HVSCs are often used for this approach because of their capacity to produce a strong extracellular matrix (ECM) network with distinct collagen fiber orientation [11], which is particularly critical when producing a mechanically functional substitute for the frequently affected load-bearing cardiovascular tissues. An important aim of functional TE is to gain control over the collagen orientation in a tissue, to create tissue substitutes that can remain mechanically functional and endure ongoing straining while in circulation.

The production of in vitro tissue engineered constructs, while promising, is time consuming and has limited scalability. In situ tissue engineering has been proposed as an innovative approach to obtain off-the-shelf available cardiovascular substitutes. Cardiovascular tissue function could be restored by the implantation of a mechanically functional but degradable scaffold that gradually transforms into a living tissue at the site of implantation by recruiting and stimulating circulating cells to form neo-tissue [12,13]. For both in vitro and in situ cardiovascular tissue engineering approaches, major challenges are the selection of an appropriate cell source and to provide the right stimuli to guide the formation of an organized ECM to achieve and maintain tissue integrity and mechanical functioning.

Adult peripheral blood contains a rare population of circulating cells with endothelial colony forming capacity [14], high proliferative potential, and in vivo vasculogenic potential: Endothelial Colony Forming Cells (ECFCs). ECFCs have been proposed as a potential cell source for in situ cardiovascular TE [15,16,17] because they express haematopoietic markers as well as endothelial markers [18]. Laminar shear stress on ECFCs in 2D has been thoroughly investigated: it differentiates ECFCs towards the endothelial phenotype, as assessed by the anti-thrombogenic potential of ECFCs [19,20] and the achievement of mature endothelial

Figure 1

Top view	2D	2D 3D static	2D 3D cyclic	2D 3D static 3D cyclic
	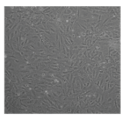	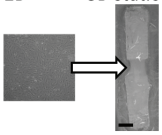	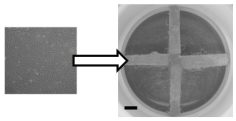	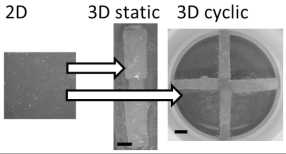
Side view			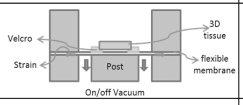	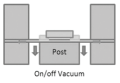
Medium groups	-Full medium -Full medium +TGFβ1 -Bare medium -Bare medium +TGFβ1	2D: Full medium 3D: -Full medium -Full medium +TGFβ1 -Bare medium -Bare medium +TGFβ1	2D: Full medium 3D: -Full medium -Full medium +TGFβ1 -Bare medium -Bare medium +TGFβ1	2D: Bare medium +TGFβ1 3D static: Bare medium +TGFβ1 3D cyclic: Bare medium +TGFβ1
Analysis	qPCR, immuno-fluorescence, phase contrast images, FACS, at 14 days	qPCR, histology, confocal images, after 19 days in 3D	qPCR, histology, confocal images, after 19 days in 3D	qPCR, confocal images, after 19 days in 3D

Figure 1. Schematic overview of the experimental set up. Top view shows 2D cell layer and 3D constructs on Bioflex plates with 2 (static strain protocol) or 4 (cyclic strain protocol) rectangular Velcro strips glued to the flexible membrane. Scale bar indicates 3 mm. Velcro strips leave space for cell-populated fibrin gels. Side views show schematic cross-section of the Flexcell setup used for cyclic strain application. When vacuum is applied, the flexible membrane is deformed over a rectangular loading post resulting in a uniaxial strain of the membrane and, thus, of the tissue. ECFCs were cultured in full medium, full medium+TGFb1, bare medium and bare medium+TGFb1. The bottom row shows analyses performed on the samples.

cell markers [21] with an arterial-like phenotype [22]. Moreover, ECFCs can change their differentiation pathway towards a mesenchymal phenotype, undergoing Endothelial-to-Mesenchymal-transition (EndoMT); this same process occurs during embryonic valvulogenesis and is of great interest for matrix production for TE, the focus of this paper.

A major stimulus that is present in cardiovascular tissues is cyclic strain. With in situ TE, for example, right after implantation of the scaffold, cells recruited to the scaffold in vivo will be under immediate and continuous cyclic strain, while producing the ECM that eventually should take over mechanical functionality from the scaffold. In adults, cyclic strain has been shown to induce EndoMT in valvular endothelial cells [23,24,25]. This process is characterized by a down-regulation of Tyrosine kinase with immunoglobulin-like domains (TIE2) [26] and an up-regulation of alpha smooth muscle actin (αSMA) [27]. An easily accessible circulating cell source capable of differentiating into endothelial cells as well as an ECM-producing cell type, such as ECFCs, would be of great potential for cardiovascular TE.

ECFCs can be isolated from adult peripheral blood, though their presence in umbilical cord blood is 15-fold higher [28], and they are a useful tool for in vitro experiments. In addition, in the context of in vitro TE, the high proliferative potential, ability to constitute an endothelial monolayer, and easily accessible source make these cells an interesting alternative to HVSCs, which have to be harvested invasively. Sheep ECFCs have been shown to respond to TGFβ1

with αSMA upregulation and tissue formation in pre-seeded in vitro cultured heart valves [15,29,30]. There is evidence of colony forming cells expressing both hematopoetic and endothelial markers homing to cell-free constructs in vivo in response to chemokines such as stromal cell derived factor 1α (SDF1α) [31]. However, little is known about the response of human ECFCs to mechanical strain with regard to their ability to create an oriented collagen matrix for load-bearing cardiovascular regeneration and TE.

Here we investigated the influence of static and cyclic mechanical strain on the production of an organized ECM by human ECFCs, by using a previously developed fibrin-based 3D tissue model to simulate neo-tissue formation [32]. As a control, HVSCs were used, since the response of HVSCs to mechanical strain has previously been well characterized [33,34,35,36]. While native (cardiovascular) cells would be a good reference for an end-point comparison, we focused on the matrix organization in response to growth factors and mechanical strain.
Firstly, ECFC matrix production was assessed in the presence or absence of TGFβ1 and endothelial growth factors (eGFs), and in response to static or cyclic strain. We found that ECFCs were able to produce collagen and elastin. To test the hypothesis that transdifferentiated ECFCs can respond differently to strain (i.e.: by producing an oriented collagen matrix), cells were primed with TGFβ1, in medium without eGFs, prior to the application of static or cyclic strain. The ECM composition (collagen I, III, IV and elastin) was determined by mRNA expression analysis, flow cytometry, colorimetric elastin assay and histology, whereas ECM architecture was monitored using confocal laser scanning microscopy (CLSM) combined with live imaging. Furthermore, cell phenotype, or a change thereof, was assessed from endothelial (Von Willebrand factor (VWF) and TIE2) and mesenchymal (αSMA) markers.

Materials and methods

I. Cell Culture and Experimental Design

Cell isolation and culture

ECFCs were isolated from human umbilical cord blood as previously described [37]. Approval was granted by a local ethics review board for the use of umbilical cord blood for stem cell research (01/230K, Medisch Ethisch Toetsings Commissie (METC), University Medical Center Utrecht). Written informed consent was given prior to collection of material. This consent procedure was approved by the METC. The study conforms with the principles outlined in the Declaration of Helsinki [38]. Three donors were used for the 2D studies; one donor was used for the 3D studies in triplo. Briefly, the mononuclear cell (MNC) fraction was isolated from whole blood using Ficoll-paque density gradient centrifugation (400 g. for 30 minutes). MNCs were plated on rat-tail collagen type I (BD Biosciences, Bedford, MA) coated six-well culture plates (Costar; Corning Incorporated, Corning, NY) in a final concentration of $2x10^7$ cells per well in endothelial growth medium (Medium A), consisting of endothelial basal medium (EBM-2) (Lonza) supplemented with 10% fetal bovine serum

(FBS; Greiner Bio-One, Monroe, NC), 1% GlutaMax (Gibco, Carlsbad, CA), 1% penicillin streptomyocin (PenStrep; Lonza, Belgium) and Single Quots (EGM-2 BulletKit (CC-3162) containing hEGF, Hydrocortisone, GA-1000 (Gentamicin, Amphotericin-B), VEGF, hFGF-B, R3-IGF-1, Ascorbic Acid, Heparin), hereafter referred to as full medium. Medium was refreshed daily for the first 4 days. On day 7 the cells were trypsinized and plated on fresh collagen type I coated wells until colonies appeared. ECFC colonies were isolated and passaged at 90% confluency. ECFCs were used at passage 7-9.

ECFCs were expanded in full endothelial growth medium (Figure 1). These cells were then cultured in 2D in different medium groups, referred to as; 1) full medium (as described before), 2) full medium +TGFβ1, 3) bare medium, and 4) bare medium +TGFβ1 (Figure 1). 5 ng/ml TGFβ1 is used for medium +TGFβ1. Bare medium consist of EBM-2, supplemented with 2% FBS for 2D culture and 5% FBS for 3D culture, 1% GlutaMax, 1% PenStrep and from Single Quots only Hydrocortisone, GA-1000, Ascorbic Acid and Heparin. 2% FBS was used in bare medium in 2D to slow down proliferation and allow transdifferentiation. 5% FBS was used in bare medium in 3D fibrin gels to avoid cell starvation. The effects of eGF depletion and TGFβ1 addition during exposure to static or cyclic strain were analyzed. To study the effect of sequential exposure to TGFβ1 and strain, primed ECFCs, defined as those cells obtained by 15 days of 2D culture of ECFCs in bare medium +TGFβ1, were subsequently cultured in 3D fibrin gels subjected to static or cyclic strain, cultured in bare medium +TGFβ1 as well.

Vascular-derived cells, for 2D and 3D culture of control groups, were acquired from one donor in accordance to Dutch guidelines for secondary use material. HVSCs were isolated from a human vena saphena magna following established protocols [39]. Culture medium consisted of advanced Dulbecco's modified Eagle's medium (a-DMEM; Gibco, Carlsbad, CA), supplemented with 10% FBS, 1% GlutaMax and 1% PenStrep and was refreshed every three days. The cells were passaged at 100% confluency. HVSCs were used at passage 7.

II. Tissue Culture and Strain Application

Tissue culture

To investigate strain-induced matrix formation and organization by the cells, a previously developed system was used to host and strain 3D tissue constructs[32]. In brief, Velcro strips (8x3 mm) were glued to the flexible membranes of untreated 6-well Bioflex culture plates (Flexcell, McKeesport, PA) by using Silastic MDX4-4210 (Dow Corning, Midland, MI). For static culture, two Velcro strips per membrane were placed in opposite position to leave a rectangular space (4x5 mm) for a cell-populated fibrin gel of 80 µl (Figure 1). For cyclic culture, four rectangular Velcro strips were glued per membrane to form a cross shape and leaving a square space (5x5 mm) for a cell-populated fibrin gel of 120 µl (Figure 1). This procedure was chosen because uniaxial static culture induces collagen orientation [32,40], while cyclic straining of biaxially constrained tissues induces strain avoidance with concomitant collagen orientation in myofibroblast-seeded tissues[40,41]. Hence this set-up allows to study the mechano-response of cells and collagen organization in 3D constructs. The Bioflex plates were placed on a Flexcell

FX-40001 system (Flexcell Int.) located in an incubator for prolonged strain application. The fibrin gels were used as temporary matrix to create 3D cell-populated constructs with sufficient tissue integrity for strain application [32]. In brief, bovine fibrinogen and bovine thrombin were combined to produce final construct concentrations of 10 mg/ml fibrinogen, 10 IU/ml thrombin and $15x10^6$ cells/ml, based on methods used for TE heart valves [11]. ECFCs, primed ECFCs, and HVSCs (for control tissues) were mixed with the fibrin gel forming solution and plated immediately between the Velcro strips. The gels did not adhere to the flexible membrane (Figure 1). The constructs were incubated for 30 min at 37°C in a humidified 95/5% air/CO_2 incubator to allow gelation before culture medium was added. For the first seven days of culture 1 mg/ml ε-Amino Caproic Acid (εACA; Sigma-Aldrich, St Louis, MO) was added to prevent fibrin degradation. Medium was replaced three times a week, and constructs were cultured up to 19 days in medium groups A-D. All medium groups for ECFCs contained EBM-2 with 1% GlutaMax and 1% Penstrep.

Straining protocols

The Flexcell system applies a strain to the Bioflex plates by applying a vacuum to the membrane, pulling the membrane over a loading post (Figure 1). Rectangular posts were used underneath the membranes, resulting in uniaxial strain applied to the tissues. Constructs in all experimental groups were first cultured statically for 5 days to achieve initial tissue integrity. Static strain constructs were then cultured for another 14 days while the tissue compacted between the Velcro constraints. Cyclic constructs were subjected to cyclic strain for the next 14 days, using a previously established intermittent uniaxial straining protocol[32]. This protocol consisted of an intermittent strain of a sine wave between 0% and 5%, at a frequency of 1 Hz for periods of 3 hours, alternated with 3 hours resting periods. Previous studies with HVSC-seeded constructs indicated that this protocol rapidly (< 3 days) results in aligned collagen formation in 3D tissues[32,42].

III. Tissue Analysis

qPCR

Total RNA was isolated from the tissues using Trizol isolation according to the manufacturer's protocol (Trizol, cat#10296-010, Invitrogen, Life Technologies Europe BV, Bleiswijk, the Netherlands). Samples were dissolved in Trizol and homogenized in a Precellys 24 tissue homogenizer (Precellys, Bertin Technologies, Aix-en Provence, France). cDNA was synthesized using iScript according to the manufacturer's protocol (iScript, Cat#170-8891, Bio-Rad, Hercules, California, United States). qPCR was performed using the primers listed in Table 1 and data was analyzed using the delta-delta CT method, normalized to GAPDH expression.

Immunohistochemistry and histology

Immunohistochemistry was performed on cells cultured in monolayers on coverglasses. Cells were fixed with 10% formalin (Sigma-Aldrich) for 15 minutes and permeabilized with 0.1%

Triton-X-100 (Merck, Germany) in PBS (Sigma-Aldrich) for 10 minutes. To block non-specific binding, cells were incubated for 1h in 2% w/v solution of bovine serum albumin (BSA, Roche) in PBS, followed by 2 hours incubation with the primary antibody solution in 0.5% BSA. After washing, the cells were incubated with the secondary antibody solutions and, subsequently, with DAPI. Samples were mounted onto rectangular microscope slides using Mowiol mounting medium and analyzed by fluorescent microscopy (Axiovert 200, Carl Zeiss). All used antibodies are listed in Table 2. Histology was performed on 3D tissue constructs. The constructs were first washed in phosphate-buffered saline (PBS), embedded in Tissue-Tek (Sakura, the Netherlands) and then frozen in isopentane at -800C. Transverse cross-sections of 10 μm were cut and stained with Verhoeff van Gieson (VvG) for detection of collagen and elastic fibers and visualized by light microscopy.

Live confocal microscopy

To visualize the organization of cells and collagen fibers in the engineered constructs, confocal microscopy was performed as described previously [43]. In short, samples were labeled by Cell Tracker Orange (CTO; Invitrogen Molecular Probes) and CNA35-OG488 (CNA) [44], to fluorescently stain cell cytoplasm and collagen respectively. CTO and CNA are excitable at 466 nm and 520 nm. Scans were made using an inverted Zeiss Axiovert 200 microscope (Carl Zeiss, Oberkochen, Germany) coupled to an LSM 510 Meta (Carl Zeiss) laser scanning microscope.

Flow Cytometry

Cells cultured in 2D with medium A and D were trypsinized and allowed to recover for 10 minutes at room temperature in EBM-2 medium with 2% serum. After washing with PBS the cells were fixated, permeabilized and stained with LeukoPerm (cat# YSRTBUF09, Gentaur Belgium BV, Kampenhout, Belgium) according to the manufacturers protocol. Briefly: cells were washed in PBS and stained for the extracellular marker CD31, washed and fixated for 15 minutes in fixation buffer. Following washing steps in PBS the cells were permeabilized and stained for the intracellular marker αSMA for 30 minutes. After final washing steps the cells were analyzed on a FACS CANTO II flow cytometer and data was analyzed using FACSDIVA software.

Elastin quantification

The Fastin Elastin Assay (Biocolor, UK) was used to quantify elastin content of tissue samples, after qPCR was performed. To extract proteins from tissue samples in Trizol, protein isolation was performed using 2-propanol (Merck) and proteins were washed using guanidine hydrochlorine (0.3 M, Sigma), according to manufacturer's protocol. To extract insoluble α-elastin from tissue samples, several extraction steps were used, incubating tissue samples with oxalic acid anhydrous (0.25 M, Fluka Chemie, St. Louis, MO) for 1 hour at 1000C. The extract is treated as described in the manufacturer's protocol, and dye intensity is measured at 513 nm. For three tissue samples per experimental condition, elastin content was calculated in μg per tissue sample.

Table 1: EndoMT markers and ECM genes and corresponding primer sequences used for qPCR.

Gene	Type	Function	Forward primer	Backward primer
VWF	Endothelial	Clotting factor	CCGATGCAG-CCTTTTCGGA	TCTGGAAGTC-CCCAATAATCGAG
TIE2	Endothelial	Angiopoietin receptor	TCCGCTGGAAGT-TACTCAAGA	GAACTCG-CCCTTCA-CAGAAATAA
αSMA	Mesenchymal	Cell contractility, structure	CAGGGCTGTTTTC-CCATCCAT	GCCATGTTCTATC-GGGTACTTC
Elastin	Extracellular matrix	Elastic part	CGCCCAGTTTGG-GTTAGTTC	CACCTTGGCAGC-GGATTTTG
Collagen type I	Extracellular matrix	Load bearing part	GTCGAGGGC-CAAGACGAAG	CAGATCACGT-CATCGCACAAC
Collagen type III	Extracellular matrix	Fibrillar collagen	TTGAAGGAGGAT-GTTCCCATCT	ACAGACA-CATATTTGGCAT-GGTT
Collagen type IV	Extracellular matrix	Basal lamina	AGATAAGGGTC-CAACTGGTGT	ACCTTTAACGG-CACCTAAAATGA

Table 2: Antibodies and corresponding secondary antibodies used for immunofluorescence.

Marker	Primary antibody	Secondary antibody
CD31	Mouse anti-human IgG1 (Dako)	Alexa fluor 555 goat anti-mouse IgG1 (Invitrogen)
	1:200 v/v	1:300 v/v
Collagen type 1	Rabbit anti-human IgG (Abcam)	Alexa fluor 555 goat anti-rabbit IgG(H+L) (Invitrogen)
	1:300 v/v	1:300 v/v
Collagen type III	Rabbit anti-human IgG (Abcam)	Alexa fluor 555 donkey anti-rabbit IgG(H+L) (Invitrogen)
	1:200 v/v	1:300 v/v
Collagen type IV	Mouse anti-human IgG1 (Abcam)	
	1:200 v/v	1:300 v/v
αSMA	Mouse anti-human IgG2a (Sigma)	Alexa Fluor 488 goat anti-mouse IgG2a (Invitrogen)
	1:500 v/v	1:300 v/v

IV. Statistical Analysis

Data is shown as means +/- standard deviation. Statistical analysis was performed using GraphPad Prism 5.0 (GraphPad Software, San Diego, California, USA) and p values <0.05 were considered significant. T-test was used to analyze flow cytometry data and one-way ANOVA with post-hoc Tukey analyses were used to analyze qPCR and Elastin Fastin data.

Results

Culturing ECFCs in 3D under static strain resulted in an upregulation of gene expression for collagen I and III relative to ECFCs in 2D (Figure 3). In addition, histology showed that ECFCs had produced collagen as well as elastin throughout the tissue constructs (Figure 2A). No clear elastin structures were found in HVSC tissue constructs, though the elastin quantification (Figure 2B) showed that α-elastin monomers was produced in amounts similar to ECFCs. The strained ECFCs showed no differences in elastin content for the different conditions (Figure 2B). The expression of collagen I and III in cyclically strained constructs was significantly reduced relative to the static controls (Figure 3A), indicating an inhibitory effect of cyclic strain. These results were consistent for all medium groups, indicating collagen I and III gene expression was mostly related to the type of strain applied, rather than to growth factors in the culture medium. The confocal images showed that, contrary to HVSCs, ECFCs deposited collagen in tubular structures, except when cultured in the presence of TGFβ1 and the absence of eGFs under static strain (Figure 4A). Here, collagen was aligned to strain direction, similar to HVSC-seeded controls (Figure 4C). Tubular structures extend through the construct, as shown in a 3D reconstruction of confocal images (Supplemental Movie 1, corresponding to the 2D image in Figure 4D).

We tested whether priming ECFCs by TGFβ1 addition and eGF depletion could initiate transdifferentiation into an ECM-expressing cell type that is strain-responsive. To confirm endothelial phenotype, ECFCs were analyzed by flow cytometry (Supplemental Figure 1): ECFCs were positive for endothelial markers CD105, CD31 and KDR, while being negative for leukocyte markers CD14 and CD45, indicating a mature endothelial phenotype [28]. After two weeks of 2D culture in bare medium +TGFβ1, the mRNA levels of endothelial markers (VWF and TIE-2) were downregulated, while the expression of αSMA was significantly upregulated compared to full medium (Figure 5A). The expression of the ECM genes collagen I, III and elastin was upregulated significantly in bare medium, with or without TGFβ1 (Figure 5B), while a downregulation in collagen type IV expression was found. Immunohistochemistry showed that, while αSMA stress fibers were present, CD31 also remained detectable (Figure 6). However, in the presence of TGFβ1 the localization of the CD31 protein shifted from the cell membrane

Figure 2

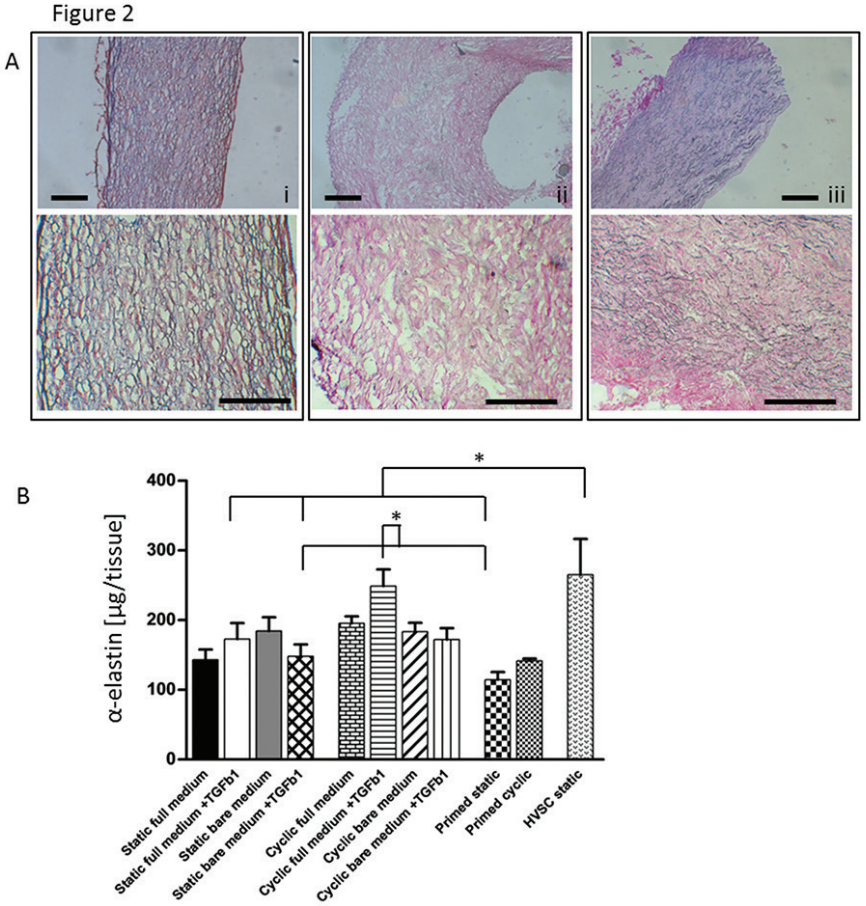

Figure 2. Elasin and collagen staining on slices of 3D constructs (A) and quantification of elastin (B). Representative images are shown for the Verhoeff van Gieson staining (A), with elastin in blue-black and collagen in red. On this global scale results for all ECFC groups (all medium groups, static or cyclic strain) were similar. (i) ECFCs showed both collagen and elastin, (ii) HVSCs showed only collagen. (iii) Native human tissue was used as a positive control for collagen and elastin. Scale bar 200 mm. Elastin quantification by Fastin Elastin assay (B) showed significant differences, where cyclic full medium+TGFb1 is significantly higher than primed static and static bare medium+TGFb1, and HVSC static is significantly higher than primed static, static bare medium +TGFb1 and static full medium +TGFb1; * indicates p,0.05, N = 3.

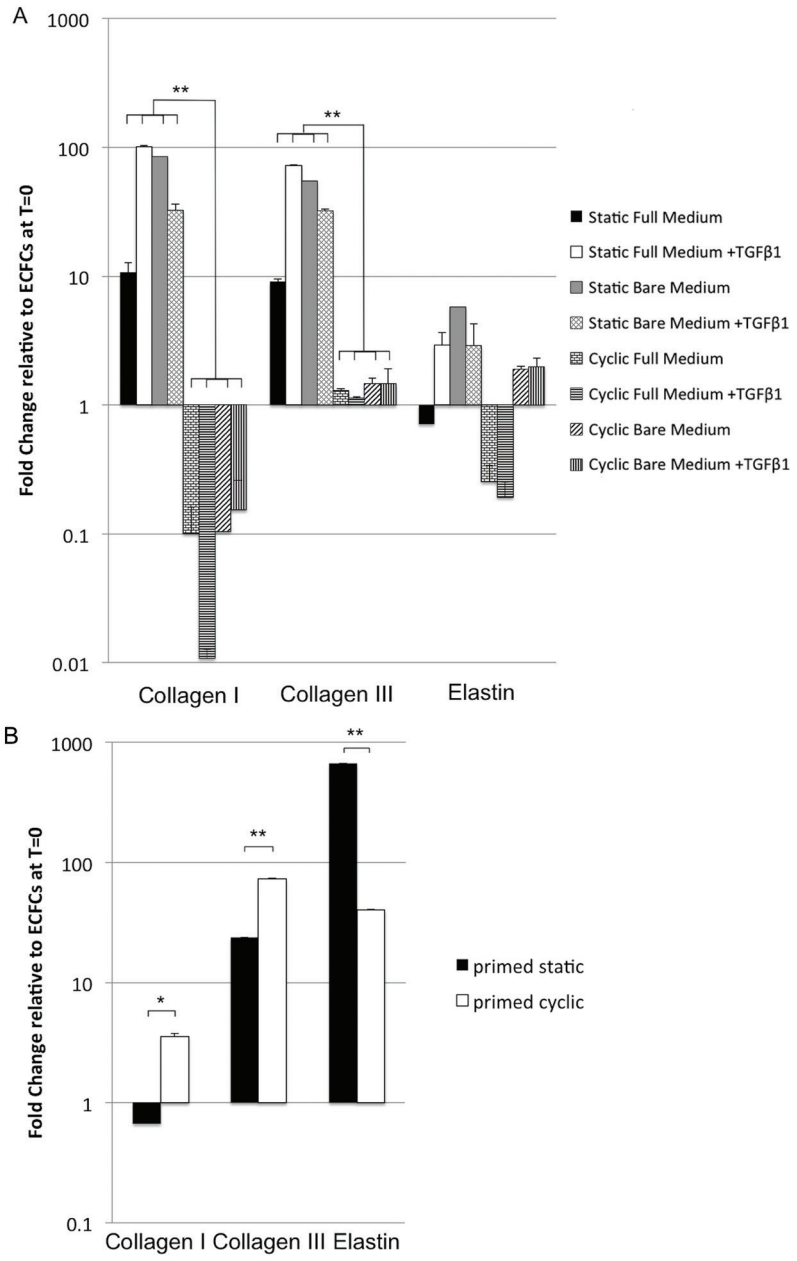

Figure 3. qPCR of ECFCs and primed ECFCs under static and cyclic strain in 3D. Expression of ECM genes is shown relative to primed ECFCs before seeding into the 3D gels. (A) Cyclic strain significantly decreased expression of collagen type I and III in ECFCs for all medium groups. The expression of collagen IV was not detected. (B) Cyclic strain significantly upregulated expression of collagen type I and III in ECFCs primed with TGFb1. Elastin expression was reduced in these cells in response to cyclic strain. * = p,0.05, ** = p,0.01, N = 3.

to a more cytosolic distribution (Figure 6), indicating a loss of intercellular adhesion. Culturing ECFCs in a 3D environment in these culture media under static or cyclic strain resulted in no reduction of endothelial markers or increase in αSMA for any medium condition (Supplemental Figure 2).

To assess the response to sequential exposure to TGFβ1, in bare medium, in 2D followed by mechanical strain in 3D, the cells were cultured for two weeks in bare medium + TGFβ1. 20% of the cells were positive for αSMA and 100% for CD31 as measured by flow cytometry, confirming qPCR (Supplemental Figure 3) and immunohistochemistry results (Figure 6). The primed ECFCs were then all cultured under static or cyclic strain conditions in 3D, in bare medium +TGFβ1. These cells distributed more homogenously throughout the fibrin tissue (Figure 4B, Supplemental Movie 2), similar to HVSCs (Figure 4C), and deposited collagen in a more homogenous pattern (Figure 4B). Collagen I and III expression was significantly increased and elastin was decreased in response to cyclic strain as compared to static strain (Figure 3B). No Collagen IV expression was observed. Although lowered by cyclic strain, the elastin gene expression in static constructs remained higher in primed ECFCs in 3D compared to primed ECFCs in 2D. There was, however, no alignment of the produced collagen fibers in response to strain directionality (Figure 4B). In contrast, HVSCs, frequently used in pre-seeded tissue TE, showed a higher gene expression for collagen I (Supplemental Figure 4) and a clear alignment of matrix in response to strain direction (Figure 4C).

Discussion

Cardiovascular tissue engineered constructs have to function under continuous hemodynamic loads. Here, we analyzed the response of a potential new cell source for cardiovascular tissue engineering, ECFCs, to combined and sequential stimulation with cyclic mechanical strain and growth factors. Although sequential stimulation of cells has been studied for the production of ECM for in vitro cardiovascular tissue engineering applications [5,29,42,45,46], the production and orientation of matrix by circulating progenitor cells in response to cyclic strains has received little attention. Our results showed that EFCFs in 3D constructs produced organized collagen and elastin, albeit in a different fashion than the control HVSCs. At the gene expression level cyclic straining of the ECFC constructs – even in the presence of TGFβ1 – was shown to inhibit ECM expression as compared to static strain conditions after 19 days of culture. Interestingly, priming ECFCs with TGFβ1 prior to exposure to strain was shown to upregulate the expression of ECM genes in a mechanically active environment. The observation that priming with TGFβ1 is beneficial to obtain proper neo-tissue development (under cyclic strain) is consistent with results in heart valve TE [47] and other tissue engineering fields such as myocardial and vascular regeneration [45,48].

One of the main drawbacks of HVSCs as a cell source for vascular structures is their lack of elastin network formation. Histology showed that in spite of elastin production

Figure 4

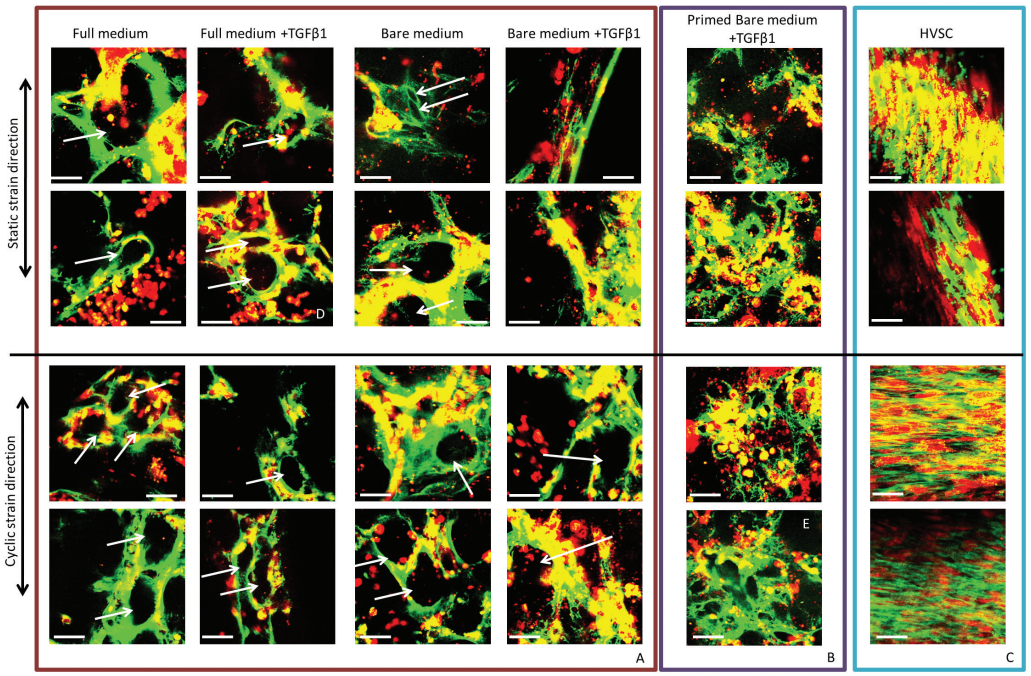

Figure 4. Confocal images of details (duplo) of ECFC- and HVSC-seeded constructs. Constructs were cultured for 19 days in all medium groups and under static or cyclic strain. Cells are shown in red, collagen in green. (A) ECFCs formed cell colonies and produced tubular collagen structures (indicated by white arrows) independent of medium type or strain, except when cultured in bare medium +TGFβ1 under static strain, when a slightly more alinged matrix was observed. (B) Primed ECFCs distributed more homogenously throughout the tissue and deposite collagen more homogenously throughout the tissue. (C) HVSCs showed distinct collagen alignment and strain responsiveness: collagen aligned parallel to the uniaxial strain direction in case of static straining and orthogonal to the strain direction in the cyclically loaded, biaxially constrained tissues. Scale bar indicates 50 mm. The difference in tubular structure for ECFCs and more homogeneous collagen distribution for primed ECFCs is shown in Movies for image (D) and (E).

(immunohistochemistry), HVSCs were not able to polymerize and form an elastin network at the tissue level, whereas ECFCs did produce elastin in a more organized manner, visualized by histology (Figure 2A). There was no significant influence on the amount of elastin protein produced by ECFCs regardless of culture medium or straining. This contrasts with the downregulation of elastin mRNA found in response to cyclic strain in all conditions. This may be explained by deposition of elastin proteins prior to downregulation of the elastin gene. A similar effect was seen by Seliktar et al., who studied elastin production by smooth muscle cells and myofibroblasts in collagen gels: On mRNA level, elastin upregulation by these cells was detected up to 8 days, but upregulation was less in strained gels compared to unstrained gels [49].

In 2D static ECFC culture, removal of eGFs and addition of TGFβ1 induced a change of phenotype towards a tissue producing phenotype on a gene expression level. Interestingly, in

3D fibrin gels under static strain conditions ECFCs showed an upregulation of ECM genes, regardless of TGFβ1 or eGF depletion, indicating that placement in the 3D fibrin environment by itself promotes ECM gene expression. However, this upregulation was not seen when the ECFCs in their 3D environment were cyclically strained, indicating that cyclic strain, such as found in the cardiovascular system, may not be beneficial for matrix production by ECFCs. This response contrasts with the behavior of HVSCs, which align themselves and their produced matrix in response to strain, underlining the relevance of mechanic 3D in-vitro model systems to test potential cell sources for TE.

In contrast to untreated ECFCs, TGFβ1-primed ECFCs gave a more homogeneous distribution of cells and collagen throughout the 3D constructs and an upregulation of ECM gene expression for collagen I and III in cyclic compared to static strain. These results underline the importance of the 3D in vitro environment and an appropriate sequence of exposure to biochemical and mechanical stimuli for matrix production, relevant for the engineering of load-bearing cardiovascular tissues. Compared to the tubular structures that developed with non-primed ECFC cultures (Supplemental Movie 1), the ECM structure formed by TGFβ1-primed ECFCs may result in better load-bearing tissues. These cells produced a more homogeneous distributed matrix, and even though 2D images seem to show tubular structures with smaller diameters (Figure 4B), in the 3D reconstruction (Supplemental Movie 2) it can be appreciated that these structures do not extend throughout the construct. This may provide improved mechanical properties to the tissue, though the collagen structure does not resemble the load-bearing, anisotropic collagen network comparable to the aligned collagen fibers formed by HVSCs (Figure 4C).

Our data suggest that optimizing the timing between attracting circulating cells to the scaffold and exposing them to biochemical cues may be of critical importance for cardiovascular TE. The timing could potentially be influenced in an in situ TE context by incorporating TGFβ1 directly into the scaffold material with tunable slow release systems [50,51]. The idea of combining the effects of bioactive stimuli to induce EndoMT with scaffolds with load-bearing mechanical properties was explored by Sewell-Loftin et al.[52]. In addition, it was previously reported that after seeding sheep ECFCs into a 3D scaffold, expression of αSMA and ECM genes was increased [29,30]; though no mechanical straining was applied in these studies. Consistent with our results, these cells were reported to express both αSMA and CD31 after TGFβ1 stimulation. In our study only a limited number of cells primed with TGFβ1 responded with αSMA gene upregulation. A non-uniform transdifferentiation of ECFCs into tissue producing cells may be due to a variation in differentiation potential [53], and could also explain why the TGFβ1-primed ECFCs were not strain responsive and unable to align themselves and the deposited collagen fibers. A limitation to our experiments is that we only studied neo-tissue formation at one time point in its early phase. How the tissue develops and matures over longer periods of time should be carefully examined in in vivo studies.

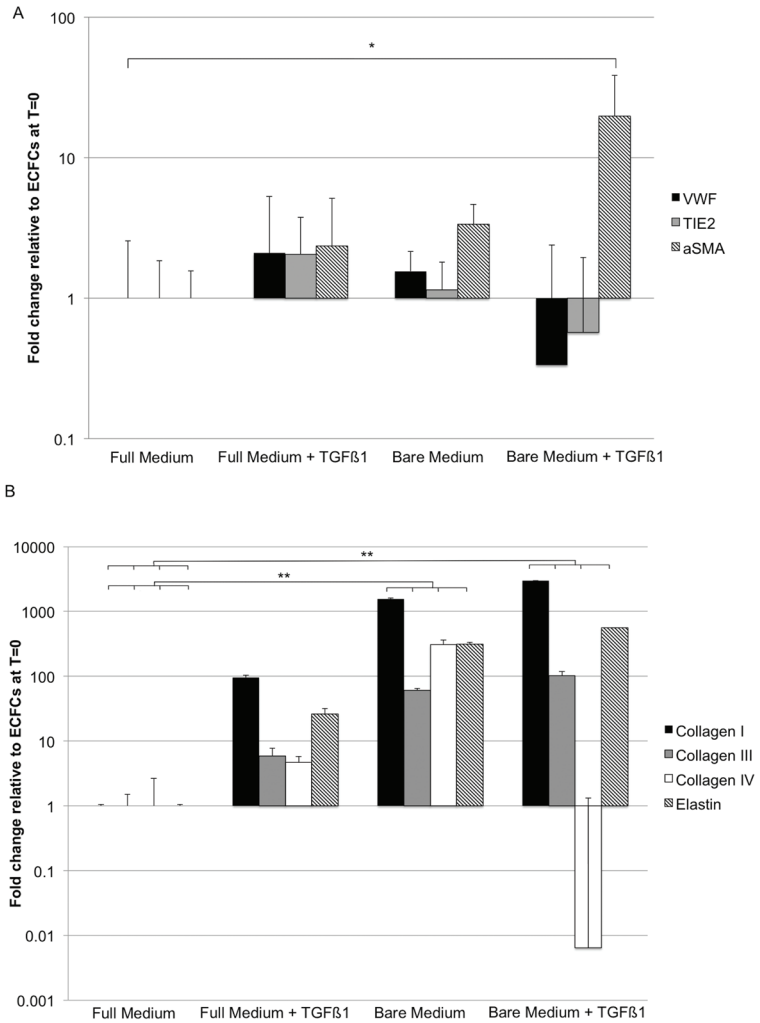

Figure 5. qPCR of ECFCs cultured in 2D for 14 days on collagen type I coating. (A) Full medium +TGFβ1 and bare medium showed an increased aSMA expression compared to ECFCs of full medium. Bare medium +TGFβ1 showed a light downregulation of endothelial markers VWF and TIE2, while the expression of aSMA was significantly upregulated. (B) With full medium +TGFβ1 and bare medium with or withour TGFβ1 a significant increase in collagen type I, III and elastin was detected. A decrease in collagen IV expession was found for collagen type IV. * = p,0.05, ** = p,0.01, N = 3.

Figure 6

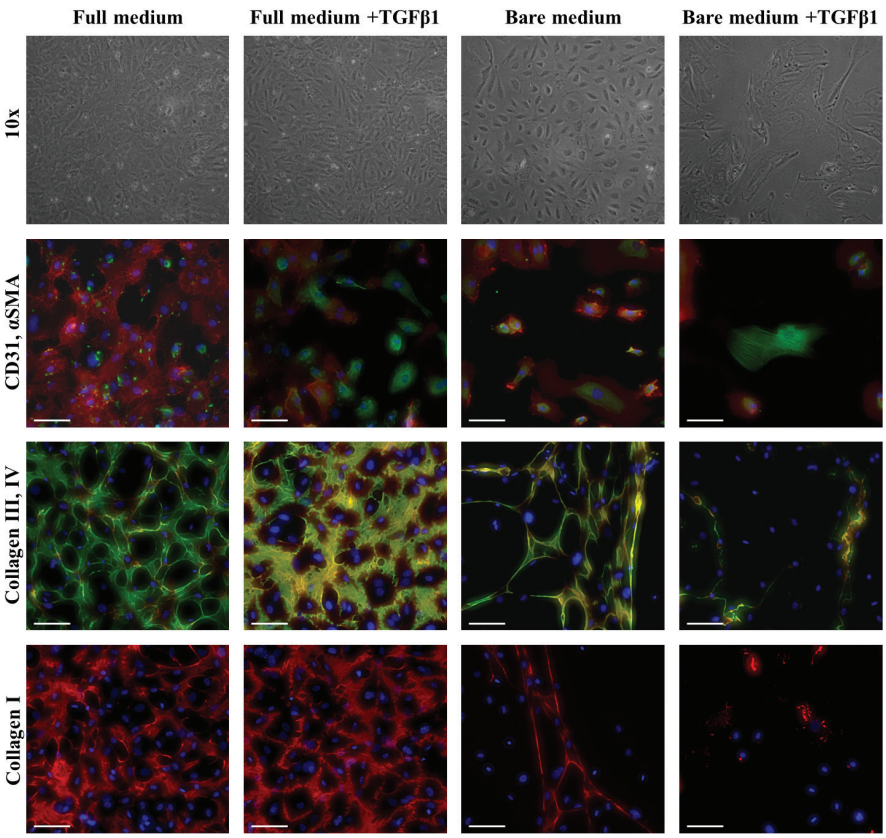

Figure 6. Phase contrast and immunofluorescent images of ECFCs on coverglasses in different media. Phase contrast pictures, after 14 days of culture, at 106magnification show the complete change in ECFC morphology in bare medium +TGFβ1, where cells are elongated and they have lost the cobblestone morphology, still retained by ECFCs cultured in the other media. Immunostaining for CD31 (red), aSMA (green) and DAPI (blue), confirmed the differences observed by optical imaging, with loss of CD31 in part of the cells cultured in full medium +TGFβ1 and bare medium +TGFβ1, and aSMA stress fibers only detected in bare medium +TGFβ1. Immunostaining for collagen type III (green), IV (red) and DAPI (blue) showed a decrease in matrix production in bare medium with or without TGFβ1. This result was also confirmed for collagen type I (red). The scalebar represents 100 mm.

A clear advantage of ECFCs compared to HVCS is their circulating nature, making them a more easily accessible cell source for both in situ and in vitro tissue engineering strategies. In addition ECFCs are capable of constituting a mature endothelial lining after culture [19,20,21,22] and stem from a circulating progenitor precursor. Though ECFCs and primed ECFCs are the result of extensive in vitro treatments, they also represent a model system for circulating progenitor cells capable of populating single-step in situ vascular grafts and heart valves [16,54,55]. The lower circulating progenitor cell number in peripheral blood and specific attraction of ECFCs into such grafts remain challenging and important hurdles [56,57]. Potential strategies could draw inspiration from studies showing increased mobilization in response to factors released following ischemic damage [58]. It has been shown that with use of VEGF the number of circulating endothelial progenitor cells (EPCs) can be increased [57]. It is likely that any cell-free graft will attract a mixed population of cells, and strategies are actively being explored to preferentially attract progenitor cells [56,57]. Attraction of a selective cell population has been extensively reviewed by de Mel et al. [57], where they discuss a strategy where endothelium derived macromolecules are used to assist in specific EPC adhesion.

In conclusion, ECFCs are an interesting potential cell source for cardiovascular tissue engineering since they can both form an endothelial lining on the surface of an engineered tissue and have the potential to produce ECM. We showed that ECFCs can produce ECM in a 3D construct, but not in response to cyclic strain to create an oriented, load-bearing collagen organization, needed for cardiovascular functioning. This implies that cyclic mechanical strain, such as found in the cardiovascular system may inhibit ECM formation by ECFCs. TGFβ1-priming of ECFCs before exposure to strain, however, enhanced matrix production and matrix organization, suggesting that sequential exposure to these soluble and mechanical factors is paramount to achieve the desired cellular response and tissue formation. Additional knowledge on how to control and time these factors may assist in the development of scaffold materials that guide the development of functional cardiovascular tissue. It should be noted, however, that the observed responses may be highly cell-type specific. Our results indicate that the well-studied response to mechanical strain of HVSCs in terms of matrix production and remodeling cannot be extrapolated to ECFCs. 3D in-vitro model system, such as presented here, offer the possibility to systematically investigate cell responses and tissue formation in dependency of cell source and environmental stimuli.

References

1. Rippel RA, Ghanbari H, Seifalian AM (2012) Tissue-engineered heart valve: future of cardiac surgery. World J Surg 36: 1581-1591.

2. Holmes DR, Jr., Mack MJ, Kaul S, Agnihotri A, Alexander KP, et al. (2012) 2012 ACCF/AATS/SCAI/STS expert consensus document on transcatheter aortic valve replacement: Developed in collabration with the American Heart Association, American Society of Echocardiography, European Association for Cardio-Thoracic Surgery, Heart Failure

Society of America, Mended Hearts, Society of Cardiovascular Anesthesiologists, Society of Cardiovascular Computed Tomography, and Society for Cardiovascular Magnetic Resonance. J Thorac Cardiovasc Surg 144: e29-84.

3. Reardon MJ (2012) Cost-Effectiveness Analysis of TAVR. Methodist Debakey Cardiovasc J 8: 26-28.

4. Rosengart TK, Feldman T, Borger MA, Vassiliades TA, Jr., Gillinov AM, et al. (2008) Percutaneous and minimally invasive valve procedures: a scientific statement from the American Heart Association Council on Cardiovascular Surgery and Anesthesia, Council on Clinical Cardiology, Functional Genomics and Translational Biology Interdisciplinary Working Group, and Quality of Care and Outcomes Research Interdisciplinary Working Group. Circulation 117: 1750-1767.

5. van Geemen D, Riem Vis PW, Soekhradj-Soechit S, Sluijter JP, de Liefde-van Beest M, et al. (2011) Decreased mechanical properties of heart valve tissue constructs cultured in platelet lysate as compared to fetal bovine serum. Tissue Eng Part C Methods 17: 607-617.

6. Shin'oka T, Matsumura G, Hibino N, Naito Y, Watanabe M, et al. (2005) Midterm clinical result of tissue-engineered vascular autografts seeded with autologous bone marrow cells. J Thorac Cardiovasc Surg 129: 1330-1338.

7. Mol A, Smits AI, Bouten CV, Baaijens FP (2009) Tissue engineering of heart valves: advances and current challenges. Expert Rev Med Devices 6: 259-275.

8. Thomas LV, Lekshmi V, Nair PD (2012) Tissue engineered vascular grafts - Preclinical aspects. Int J Cardiol.

9. Hinz B, Gabbiani G (2003) Mechanisms of force generation and transmission by myofibroblasts. Curr Opin Biotechnol 14: 538-546.

10. Mol A, Driessen NJ, Rutten MC, Hoerstrup SP, Bouten CV, et al. (2005) Tissue engineering of human heart valve leaflets: a novel bioreactor for a strain-based conditioning approach. Ann Biomed Eng 33: 1778-1788.

11. Mol A, van Lieshout MI, Dam-de Veen CG, Neuenschwander S, Hoerstrup SP, et al. (2005) Fibrin as a cell carrier in cardiovascular tissue engineering applications. Biomaterials 26: 3113-3121.

12. De Visscher G, Vranken I, Lebacq A, Van Kerrebroeck C, Ganame J, et al. (2007) In vivo cellularization of a cross-linked matrix by intraperitoneal implantation: a new tool in heart valve tissue engineering. Eur Heart J 28: 1389-1396.

13. Roh JD, Sawh-Martinez R, Brennan MP, Jay SM, Devine L, et al. (2010) Tissue-engineered vascular grafts transform into mature blood vessels via an inflammation-mediated process of vascular remodeling. Proc Natl Acad Sci U S A 107: 4669-4674.

14. Vranken I, De Visscher G, Lebacq A, Verbeken E, Flameng W (2008) The recruitment of primitive Lin(-) Sca-1(+), CD34(+), c-kit(+) and CD271(+) cells during the early intraperitoneal foreign body reaction. Biomaterials 29: 797-808.

15. Sales VL, Mettler BA, Engelmayr GC, Jr., Aikawa E, Bischoff J, et al. (2010) Endothelial progenitor cells as a sole source for ex vivo seeding of tissue-engineered heart valves. Tissue Eng Part A 16: 257-267.

16. Mazzolai L, Bouzourene K, Hayoz D, Dignat-George F, Liu JW, et al. (2011) Characterization of human late outgrowth endothelial progenitor-derived cells under various flow conditions. J Vasc Res 48: 443-451.
17. Fioretta ES, Fledderus JO, Burakowska-Meise EA, Baaijens FP, Verhaar MC, et al. (2012) Polymer-based scaffold designs for in situ vascular tissue engineering: controlling recruitment and differentiation behavior of endothelial colony forming cells. Macromol Biosci 12: 577-590.
18. Mund JA, Estes ML, Yoder MC, Ingram DA, Jr., Case J (2012) Flow cytometric identification and functional characterization of immature and mature circulating endothelial cells. Arterioscler Thromb Vasc Biol 32: 1045-1053.
19. Yang Z, Tao J, Wang JM, Tu C, Xu MG, et al. (2006) Shear stress contributes to t-PA mRNA expression in human endothelial progenitor cells and nonthrombogenic potential of small diameter artificial vessels. Biochem Biophys Res Commun 342: 577-584.
20. Yang Z, Wang JM, Wang LC, Chen L, Tu C, et al. (2007) In vitro shear stress modulates antithrombogenic potentials of human endothelial progenitor cells. J Thromb Thrombolysis 23: 121-127.
21. Yamamoto K, Takahashi T, Asahara T, Ohura N, Sokabe T, et al. (2003) Proliferation, differentiation, and tube formation by endothelial progenitor cells in response to shear stress. J Appl Physiol 95: 2081-2088.
22. Obi S, Yamamoto K, Shimizu N, Kumagaya S, Masumura T, et al. (2009) Fluid shear stress induces arterial differentiation of endothelial progenitor cells. J Appl Physiol 106: 203-211.
23. Balachandran K, Alford PW, Wylie-Sears J, Goss JA, Grosberg A, et al. (2011) Cyclic strain induces dual-mode endothelial-mesenchymal transformation of the cardiac valve. Proc Natl Acad Sci U S A 108: 19943-19948.
24. Ghazanfari S, Tafazzoli-Shadpour M, Shokrgozar MA (2009) Effects of cyclic stretch on proliferation of mesenchymal stem cells and their differentiation to smooth muscle cells. Biochem Biophys Res Commun 388: 601-605.
25. Michalopoulos E, Knight RL, Korossis S, Kearney JN, Fisher J, et al. (2011) Development of methods for studying the differentiation of human mesenchymal stem cells under cyclic compressive strain. Tissue Eng Part C Methods 18: 252-262.
26. Medici D, Kalluri R (2012) Endothelial-mesenchymal transition and its contribution to the emergence of stem cell phenotype. Semin Cancer Biol.
27. Krenning G, Moonen JR, van Luyn MJ, Harmsen MC (2008) Vascular smooth muscle cells for use in vascular tissue engineering obtained by endothelial-to-mesenchymal transdifferentiation (EnMT) on collagen matrices. Biomaterials 29: 3703-3711.
28. Ingram DA, Mead LE, Tanaka H, Meade V, Fenoglio A, et al. (2004) Identification of a novel hierarchy of endothelial progenitor cells using human peripheral and umbilical cord blood. Blood 104: 2752-2760.
29. Sales VL, Engelmayr GC, Jr., Mettler BA, Johnson JA, Jr., Sacks MS, et al. (2006) Transforming growth factor-beta1 modulates extracellular matrix production, proliferation, and

apoptosis of endothelial progenitor cells in tissue-engineering scaffolds. Circulation 114: I193-199.
30. Dvorin EL, Wylie-Sears J, Kaushal S, Martin DP, Bischoff J (2003) Quantitative evaluation of endothelial progenitors and cardiac valve endothelial cells: proliferation and differentiation on poly-glycolic acid/poly-4-hydroxybutyrate scaffold in response to vascular endothelial growth factor and transforming growth factor beta1. Tissue Eng 9: 487-493.
31. Segers VF, Tokunou T, Higgins LJ, MacGillivray C, Gannon J, et al. (2007) Local delivery of protease-resistant stromal cell derived factor-1 for stem cell recruitment after myocardial infarction. Circulation 116: 1683-1692.
32. de Jonge N, Kanters FM, Baaijens FP, Bouten CV (2012) Strain-induced Collagen Organization at the Micro-level in Fibrin-based Engineered Tissue Constructs. Ann Biomed Eng.
33. Ingber DE (2009) From cellular mechanotransduction to biologically inspired engineering: 2009 Pritzker Award Lecture, BMES Annual Meeting October 10, 2009. Ann Biomed Eng 38: 1148-1161.
34. Hinz B (2007) Formation and function of the myofibroblast during tissue repair. J Invest Dermatol 127: 526-537.
35. Huang H, Kamm RD, Lee RT (2004) Cell mechanics and mechanotransduction: pathways, probes, and physiology. Am J Physiol Cell Physiol 287: C1-11.
36. Wang JH, Grood ES (2000) The strain magnitude and contact guidance determine orientation response of fibroblasts to cyclic substrate strains. Connect Tissue Res 41: 29-36.
37. Broxmeyer HE, Srour E, Orschell C, Ingram DA, Cooper S, et al. (2006) Cord blood stem and progenitor cells. Methods Enzymol 419: 439-473.
38. (1997) World Medical Association Declaration of Helsinki. Recommendations guiding physicians in biomedical research involving human subjects. Cardiovasc Res 35: 2-3.
39. Schnell AM, Hoerstrup SP, Zund G, Kolb S, Sodian R, et al. (2001) Optimal cell source for cardiovascular tissue engineering: venous vs. aortic human myofibroblasts. Thorac Cardiovasc Surg 49: 221-225.
40. Weidenhamer NK, Tranquillo RT (2013) Influence of Cyclic Mechanical Stretch and Tissue Constraints on Cellular and Collagen Alignment in Fibroblast-Derived Cell Sheets. Tissue Eng Part C Methods.
41. Foolen J, Deshpande VS, Kanters FMW, Baaijens FPT (2012) The influence of matrix integrity on stress-fiber remodeling in 3D. Biomaterials 33: 7508-7518.
42. Rubbens MP, Mol A, Boerboom RA, Bank RA, Baaijens FPT, et al. (2009) Intermittent straining accelerates the development of tissue properties in engineered heart valve tissue. Tissue Engineering Part A 15: 999-1008.
43. Boerboom RA, Krahn KN, Megens RT, van Zandvoort MA, Merkx M, et al. (2007) High resolution imaging of collagen organisation and synthesis using a versatile collagen specific probe. J Struct Biol 159: 392-399.
44. Krahn KN, Bouten CV, van Tuijl S, van Zandvoort MA, Merkx M (2006) Fluorescently labeled collagen binding proteins allow specific visualization of collagen in tissues and live cell culture. Anal Biochem 350: 177-185.

45. Mann BK, Schmedlen RH, West JL (2001) Tethered-TGF-beta increases extracellular matrix production of vascular smooth muscle cells. Biomaterials 22: 439-444.
46. Syedain ZH, Tranquillo RT (2011) TGF-beta1 diminishes collagen production during long-term cyclic stretching of engineered connective tissue: implication of decreased ERK signaling. J Biomech 44: 848-855.
47. De Visscher G, Lebacq A, Mesure L, Blockx H, Vranken I, et al. (2010) The remodeling of cardiovascular bioprostheses under influence of stem cell homing signal pathways. Biomaterials 31: 20-28.
48. Bax NA, van Marion MH, Shah B, Goumans MJ, Bouten CV, et al. (2012) Matrix production and remodeling capacity of cardiomyocyte progenitor cells during in vitro differentiation. J Mol Cell Cardiol 53: 497-508.
49. Seliktar D, Nerem RM, Galis ZS (2003) Mechanical strain-stimulated remodeling of tissue-engineered blood vessel constructs. Tissue Eng 9: 657-666.
50. Pham QP, Sharma U, Mikos AG (2006) Electrospinning of polymeric nanofibers for tissue engineering applications: a review. Tissue Eng 12: 1197-1211.
51. Sengupta D, Heilshorn SC (2010) Protein-engineered biomaterials: highly tunable tissue engineering scaffolds. Tissue Eng Part B Rev 16: 285-293.
52. Sewell-Loftin MK, Chun YW, Khademhosseini A, Merryman WD (2011) EMT-inducing biomaterials for heart valve engineering: taking cues from developmental biology. J Cardiovasc Transl Res 4: 658-671.
53. Paruchuri S, Yang JH, Aikawa E, Melero-Martin JM, Khan ZA, et al. (2006) Human pulmonary valve progenitor cells exhibit endothelial/mesenchymal plasticity in response to vascular endothelial growth factor-A and transforming growth factor-beta2. Circ Res 99: 861-869.
54. Jordan JE, Williams JK, Lee SJ, Raghavan D, Atala A, et al. (2012) Bioengineered self-seeding heart valves. J Thorac Cardiovasc Surg 143: 201-208.
55. Andukuri A, Sohn YD, Anakwenze C, Lim DJ, Brott B, et al. (2012) Enhanced human endothelial progenitor cell adhesion and differentiation by a bioinspired multifunctional nanomatrix. Tissue Eng Part C Methods.
56. Timmermans F, Plum J, Yoder MC, Ingram DA, Vandekerckhove B, et al. (2009) Endothelial progenitor cells: identity defined? J Cell Mol Med 13: 87-102.
57. de Mel A, Jell G, Stevens MM, Seifalian AM (2008) Biofunctionalization of biomaterials for accelerated in situ endothelialization: a review. Biomacromolecules 9: 2969-2979.
58. Massa M, Rosti V, Ferrario M, Campanelli R, Ramajoli I, et al. (2005) Increased circulating hematopoietic and endothelial progenitor cells in the early phase of acute myocardial infarction. Blood 105: 199-206.

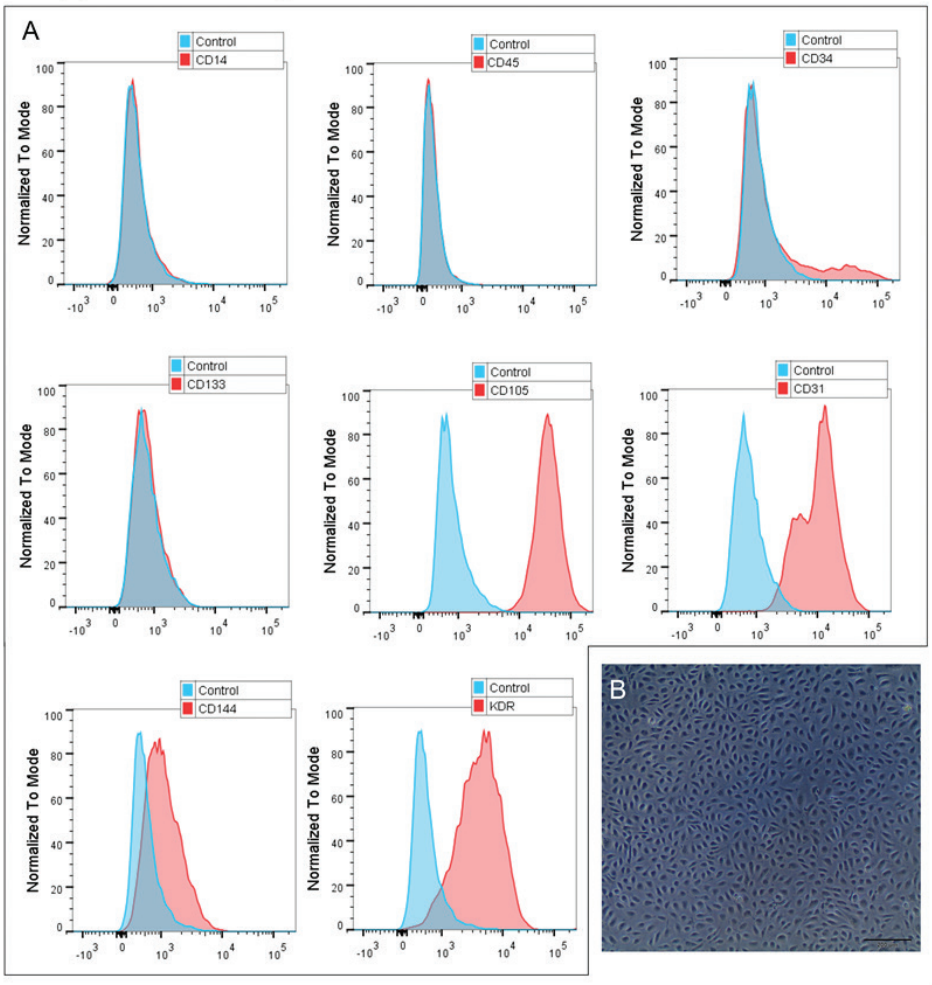

Supplemental Figure 1. Characterization of ECFCs by (A) flow cytometry of cell type markers and microscopy (B). ECFCs do not express the leukocyte markers CD14 or CD45, retain some CD34 expression but not CD133, and express the endothelial markers CD105 (Endoglin), CD31 (PECAM), CD144 (VE-Cadherin) and KDR (VEGFR-2). A monolayer of ECFCs shows a typical cobblestone pattern in vitro (magnification 4x).

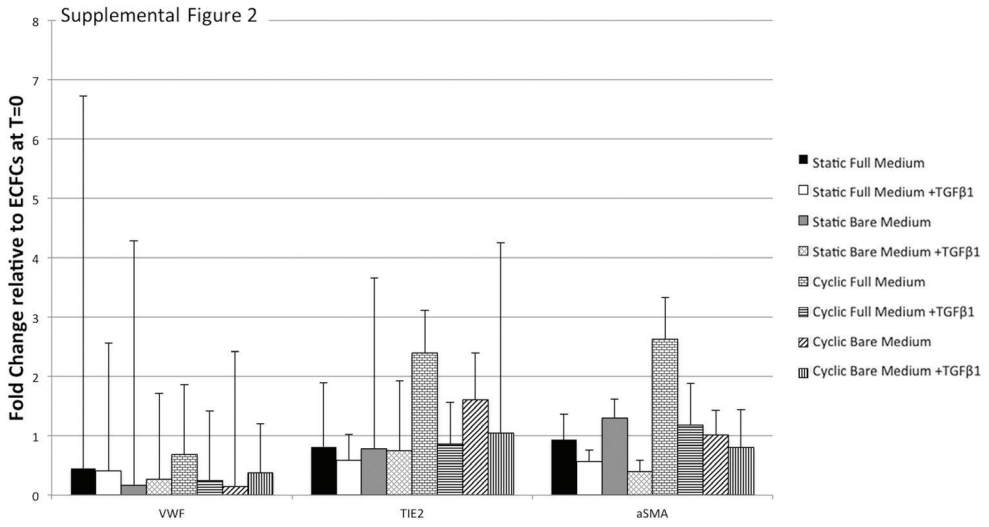

Supplemental Figure 2. qPCR of ECFCs cultured in 3D in all medium groups under static or cyclic strain. Expression of EndoMT genes is shown relative to ECFCs before seeding into the 3D gels. Medium groups and static or cyclic strain did not result in any significant altering of the gene expression of VWF, TIE2 and αSMA. N=3

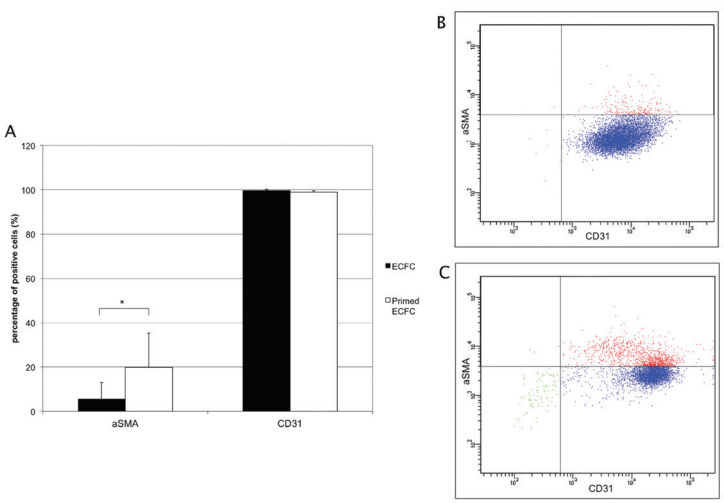

Supplemental Figure 3. Flow cytometry of ECFCs before and after priming with TGFβ1 and depletion of eGFS for 15 days. (A) The percentage of cells positive for αSMA increased to 20%. The percentage of cells positive for CD31 remained 100%. (B) Representative scatterplots of ECFCs before priming with TGFβ1 and (C) after priming with TGFβ1.

Supplemental Figure 4

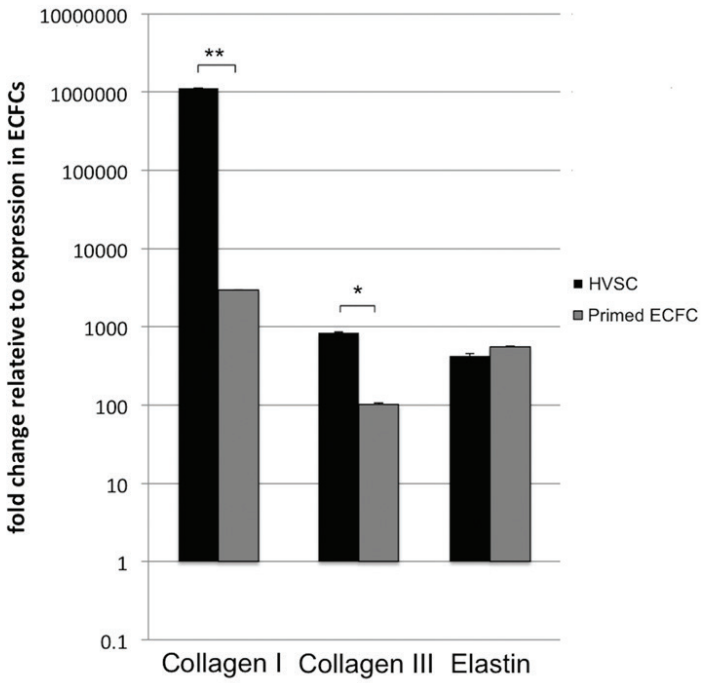

Supplemental Figure 4. qPCR of HVSCs and pre-treated ECFCs cultured in 2D. Expression of ECM genes is shown relative to ECFCs, cultured in 2D with full medium. Pre-treated ECFCs show an up-regulation of collagen I compared to ECFCs. HVSCs on the other hand, express collagen type I significantly more than pre-treated ECFCs do. No significant differences were found comparing HVSCs with pre-treated ECFCs for collagen III, IV and elastin. ** = $p < 0.01$, N=3.

Supplemental Movie 1. (Online only) A 3D reconstruction of tubular structures formed by ECFCs in 3D fibrin gels. Confocal scans are converted to a 3D reconstruction showing a typical example. The tubular structures extend through the construct. Cells are shown in red, collagen in green. Scale bar indicates 50 μm.

Supplemental Movie 2. (Online only) A 3D reconstruction of more homogeneous collagen distribution by primed ECFCs in 3D fibrin gels. Confocal scans are converted to a 3D reconstruction showing a typical example. No tubular structures can be observed. Cells are shown in red, collagen in green. Scale bar indicates 50 μm.

IV

Shear stress on endothelial colony forming cells modulates the microRNA29 family through TGFβ2 signaling: preliminary data

Dimitri E.P. Muylaert

Merle M. Krebber

Christian G.M. van Dijk

Caroline K.L. Cheng

Joost O. Fledderus

and Marianne C. Verhaar

Abstract

Since implanted cardiovascular grafts have to function in a mechanically active environment, understanding how hemodynamic shear stress on endothelium regulates ECM production is highly relevant to tissue engineering strategies. ECM production can be regulated by microRNAs such as the mir29 family, which can inhibit the expression of elastin and collagen type 1. The expression of the mir29 family is in part regulated by members of the transforming growth factor β (TGFβ) family. It is currently not known if shear stress influences ECM production through mir29 expression via TGFβ signaling. In a set of pilot experiments, we investigated the effect of mir29 knockdown in endothelial colony forming cells (ECFCs). We exposed ECFCs to fluid flow shear stress and analyzed the influence of mir29 expression through TGFβ2 signaling on ECM gene expression. We found that knockdown of mir29 in ECFCs led to an upregulation of elastin expression. Furthermore, we found indications that shear stress may result in a downregulation of TGFβ2 and subsequent upregulation of mir29, as well as an upregulation of the endothelium-specific mechanosensing complex PECAM1/VE Cadherin/VEGFR2. These preliminary observations are in line with a protective effect of laminar shear stress on the endothelial phenotype of ECFCs in comparison to static culture conditions.

Introduction

Tissue engineered cardiovascular grafts experience a mechanically active environment consisting of cyclic strain and fluid shear stress immediately after implantation. Shear stress influences endothelial development by regulating extracellular matrix (ECM) production and maintenance. ECM capable of withstanding considerable mechanical forces is crucial to the function of a vascular structure. Blood pressure exerts mechanical strain in a circumferential direction while blood flow causes shear stress along the implanted graft. Mechanical forces directly influence the production and remodeling of the ECM in vasculature, allowing it to adapt to the changing needs of a mature vascular system(1). Shear stresses upward of 1Pa (10 dyn/cm2) are typical of physiological arterial flow(1). Weaker stresses are associated with pathological conditions such as atherosclerosis(2) or aneurysmata(3), underlining the importance of hemodynamic flow to endothelium homeostasis. Endothelial cells may contribute to a cell population capable of producing and remodeling ECM through a process called endothelial to mesenchymal transition (EndMT)(4). This process is induced and regulated by both biochemical factors such as transforming growth factor β1 (TGFβ1) and TGFβ2(5,6) and mechanical forces such as strain(7) and shear stress(8). These mechanical stimuli converge on TGFβ signaling (4). Members of the TGFβ family are capable of downregulating the expression of microRNAs that are involved in ECM production. Mir-29a, 29b and 29c can inhibit the expression of collagen type 1and elastin post-transcriptionally(9). TGFβ1 specifically targets mir29b and allows the continued expression of mir29a and mir29c(10). Considering the similarity between the three types of the mir29 family it is likely that there is redundant activity of mir29a and mir29c when mir29b alone is lowered, and that simultaneous repression of the entire mir29 family will lead to further reduced repression of target mRNA. Interestingly, TGFβ2 has been implicated in the regulation of all three members of mir29(10). Experimental knockdown of the entire mir-29 family in human dermal fibroblasts led to a reduction in mir29a, mir29b and mir29c, resulting in a net increase in ECM and elastin production(11). It is currently not known if mir29 plays a role in regulating ECM expression in endothelial colony forming cells (ECFCs) through TGFβ signaling.

We hypothesized that shear stress can regulate the expression of mir-29a, 29b and 29c through increased TGFβ2 signaling in endothelial cells. ECFCs are an accessible primary cell source that represents in vivo endothelium and, in addition, may be a promising cell source to seed vascular tissue engineering constructs(7). They are capable of constituting an endothelial monolayer(12) as well as transdifferentiation into an extracellular matrix producing cell type through EndMT(6). In a series of pilot experiments, we used ECFCs cultured under flow conditions to investigate the effects of shear stress on TGFβ signaling, the expression of the mir29 family and ECM gene expression. In addition, the effects of exogenous mir29 knockdown was studied.

Materials and Methods

I. Cell Isolation and Culture

ECFCs were isolated from human umbilical cord blood as previously described(13). Approval was granted by a local ethics review board for the use of umbilical cord blood for stem cell research (01/230K, Medisch Ethisch Toetsings Commissie (METC), University Medical Center Utrecht). Written informed consent was given prior to collection of material. This consent procedure was approved by the METC. The study conforms to the principles outlined in the Declaration of Helsinki. Briefly, the mononuclear cell fraction was isolated using Ficoll-paque density gradient centrifugation. Cells were plated on rat-tail collagen type I (BD Biosciences, Bedford, MA) coated six-well culture plates (Costar; Corning Incorporated, Corning, NY) in a final concentration of 2x107 cells per well in endothelial basal medium (EBM-2) (Lonza) supplemented with 10% fetal bovine serum (FBS; Greiner Bio-One, Monroe, NC), 1% GlutaMax (Gibco, Carlsbad, CA), 1% penicillin streptomyocin (PenStrep; Lonza, Belgium) and Single Quots (EGM-2 BulletKit (CC-3162) containing hEGF, Hydrocortisone, GA-1000 (Gentamicin, Amphotericin-B), VEGF, hFGF-B, R3-IGF-1, Ascorbic Acid, Heparin), hereafter referred to as EGM2 (Endothelial Growth Medium). 5ng/ml TGFβ2 was added to EGM2 in stimulation experiments.

II. Transfection

Locked nucleic acid (LNA) molecules can specifically bind to microRNA molecules through Watson-Crick base paring, inhibiting their function. LNAs targeting mir29a, mir29b and mir29c (LNA-29 family power inhibitor, #460039, Exiqon, Vedbaek, Denmark) or a scrambled control (#199020-00, Negative control A LNA inhibitor, Exiqon, Vedbaek, Denmark) were transfected into ECFCs using Lipofectamine RNAiMAX (RNAiMax transfection reagent, #13778-075, Life Technologies, Carlsbad, California, USA). Briefly, LNA or control and Lipofectamine were diluted in serum-free optimem (Optimem transfection medium, #31985-062, Life Technologies, Carlsbad, California, USA) separately and then mixed and incubated for 20 minutes at room temperature. Cells were then rinsed with PBS twice and incubated with the transfection medium for 4 hours at 37 degrees Celsius before being rinsed and further cultured in EGM2 culture medium. Cells were collected for analysis after 48 hours.

III. Flow Experiments

ECFCs from 4 different donors were cultured in EGM-2 medium on collagen coated flasks in 5% CO2 at 37°C to a maximum passage number of 7. For flow experiments 1.5 x 105 cells were cultured on IBIDI µ-slides (µ-slide I 0.4 luer Collagen IV, cat# 80172, IBIDI GmbH, Germany). After 8 hours of incubation to allow cell adhesion, ECFCs were exposed to 5 or 15 dyn/cm2

Table 1. Used primers.

Target	Forward Sequence	Reverse Sequence
VE Cadherin	TTGGAACCAGATGCACATTGAT	TCTTGCGACTCACGCTTGAC
PECAM1	AACAGTGTTGACATGAAGAGCC	TGTAAAACAGCACGTCATCCTT
VEGFR2	TCTCTGCCTACCTCACCTGT	GCTCTTTCGCTTACTGTTCTGC
aSMA	CAGGGCTGTTTTCCCATCCAT	GCCATGTTCTATCGGGTACTTC
Col1	GTCGAGGGCCAAGACGAAG	CAGATCACGTCATCGCACAAC
Col4	AGATAAGGGTCCAACTGGTGT	ACCTTTAACGGCACCTAAAATGA
elastin	CGCCCAGTTTGGGTTAGTTC	CACCTTGGCAGCGGATTTTG
FSP1	GATGAGCAACTTGGACAGCAA	CTGGGCTGCTTATCTGGGAAG
TGFβ2	TTGACGTCTCAGCAATGGAG	TTCGCCTTCTGCTCTTGTTT
β Glycan	CCAAGATGAATGGCACACAC	ATTTCAGGTCGGGTGAACAG
Endoglin	CACTAGCCAGGTCTCGAAGG	CTGAGGACCAGAAGCACCTC
SNAIL	TCGGAAGCCTAACTACAGCGA	AGATGAGCATTGGCAGCGAG

shear stress applied by an IBIDI pump (IBIDI GmbH, Germany) for 24 hours according to the manufacturers protocol. ECFCs cultured for 8 (T=0) and 24 hours (Static) in µ-slides which were not connected to the IBIDI pump were used as static controls. RNA was isolated using Trizol for all conditions.

IV. qPCR

Total RNA was isolated from the cells using Trizol isolation according to the manufacturer's protocol (Trizol, cat#10296-010, Invitrogen, Life Technologies Europe BV, Bleiswijk, the Netherlands). For SYBRgreen qPCR, cDNA was synthesized using iScript according to the manufacturer's protocol (iScript, Cat#170-8891, Bio-Rad, Hercules, California, United States). For Taqman miRNA qPCR specific cDNA was synthesized per target miRNA (mir29a, mir29b, mir19c, RNU19) prior to qPCR. qPCR was performed using the primers listed in Table 1 and data was analyzed using the delta-delta CT method, normalized to p0 expression and T=0 for SYBRgreen-qPCR and RNU19 for taqman miRNA-qPCR.

V. Statistical Analysis

Data is shown as mean +/- standard deviation. Statistical significance was tested with one-way ANOVA with post-hoc Tukey or student t-test where appropriate, using GraphPad Prism 5.0 (GraphPad Software, San Diego, California, USA) and p values <0.05 were considered significant.

Results

Shear stress maintains expression of endothelial markers and does not induce EndMT

SNAIL, a marker for endothelial to mesenchymal transition (EndMT), fibroblast specific protein 1 (FSP1) as well as TGFβ2 receptors β glycan and endoglin showed indications for increase in expression in high shear conditions relative to static conditions in ECFCs after 24h of exposure to shear stress (Figure 1). EndMT is marked by a loss of expression of endothelial proteins. In the investigated shear conditions, however, the expression of endothelial markers VE cadherin, PECAM1 and VEGFR2 were not reduced, and their expression was most pronounced in high-shear flow (Figure 2). The myofibroblasts marker aSMA remained unchanged across conditions, further indicating that EndMT was not triggered in these conditions (Figure 2). The expression of collagen type 1 appeared lower in static controls compared to shear conditions, however expression levels were highly variable (Figure 3). The expression of collagen type 4, associated with the basal lamina produced by endothelial cells in vivo, appeared to be highest in high flow conditions. Expression of elastin was lowered in static controls but not significantly increased in flow conditions (Figure 3). Combined, these results may indicate a pro-endothelial expression pattern under laminar shear with evidence of matrix production typical for endothelium.

The influence of shear stress on TGFβ2 and mir29 expression

Following 24 hours of exposure to laminar flow of low (5dyn/cm2) or high (15dyn/cm2) laminar shear the mir29 family showed higher expression in both shear conditions and particularly the high shear condition, however all measured expression levels showed considerable variation between ECFC donors (Figure 4a). The expression of TGFβ2 appeared to be lower in shear conditions compared to static controls, however no statistical significance was found in these pilot data (Figure 3). ECFC alignment along the direction of flow was detected at 42hour and 48hour time points indicating a response to flow conditions (Figure 5).

Knockdown of mir29abc increased the expression of elastin but not collagen type 1 in human ECFCs

Treatment with LNAs that specifically target mir29a, mir29b and mir29c significantly lowered the levels in ECFCs (Figure 6a). This corresponded to an approximately 4-fold increase in the expression of elastin ($p=0.04$) (Figure 6b). There were no differences in the expression of collagen type 1 between specific LNA and a scrambled control. 24hour and 48hour culture of ECFCs in the presence of TGFβ2 did not affect the expression levels of mir29ab or c in static culture conditions. Mir29a was strikingly more abundant compared to expression levels of mir29b and mir29c in ECFCs regardless of presence of TGFβ2 (Figure 7).

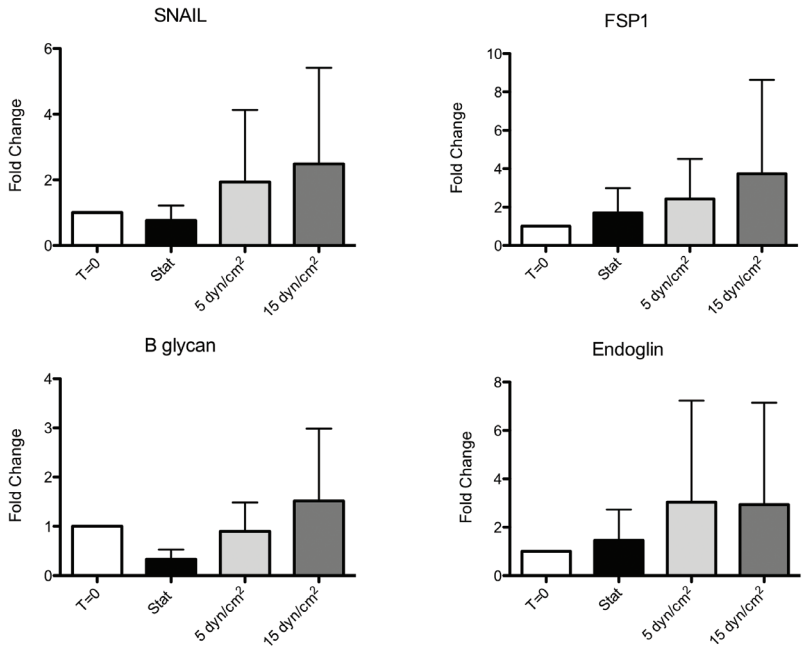

Figure 1. Expression of SNAIL, FSP1, β Glycan and Endoglin, and EndMT marker SNAIL (respectively p=0.6, p=0.5, p=0.6, p=0.7) following 24 hours of exposure of ECFCs to shear stress.

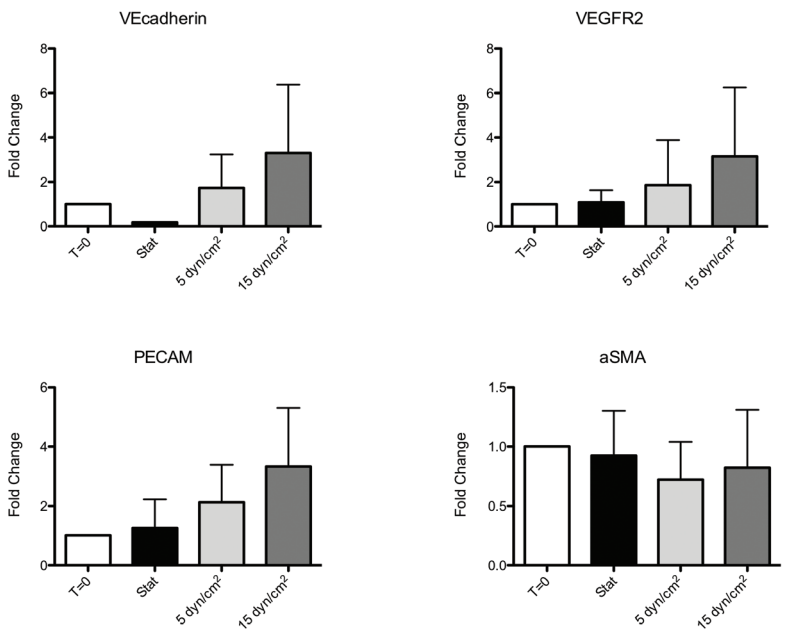

Figure 2. Expression of Endothelial mechanosensory complex VE Cadherin, PECAM1 and VEGFR2 following 24 hours of exposure of ECFCs to shear stress (respectively p=0.4, p=0.2, p=0.5). Expression of myofibroblasts marker aSMA(p=0.7).

Discussion

We report preliminary findings on the response of ECFCs to fluid flow shear stress. We have previously shown that ECFCs reduce the expression of matrix proteins in response to mechanical strain, and that this inhibition may be overcome by pre-treating the cells with TGFβ1 to induce transdifferentiation before applying strain(7). Our preliminary results indicate that shear stress on ECFCs may influence the expression of mir29 through TGFβ2 signaling, thereby regulating ECM expression. We found that the knockdown of mir29a, mir29b and mir29c resulted in an increased expression of elastin, indicating that mirs play a role in the regulation of matrix protein expression in ECFCs. Shear stress on ECFCs appeared to lower the expression of TGFβ2 and increased the expression of mir29a, in keeping with mir29 regulation by the TGFβ family. The expression of endothelial adhesion molecules PECAM1 and VE cadherin appread to be increased, as well as endothelial marker VEGFR2. These three proteins form an essential endothelium-specific mechanosensing complex required to respond to fluid flow. It has previously been reported that mechanical stimulation of PECAM1 triggers VE cadherin dependent activation of VEGFR2 within 15 seconds of onset of flow(14). An increase in expression of these proteins could point to shear-dependent mechanosensing in ECFCs and would indicate a protective effect of shear stress on endothelial phenotype.

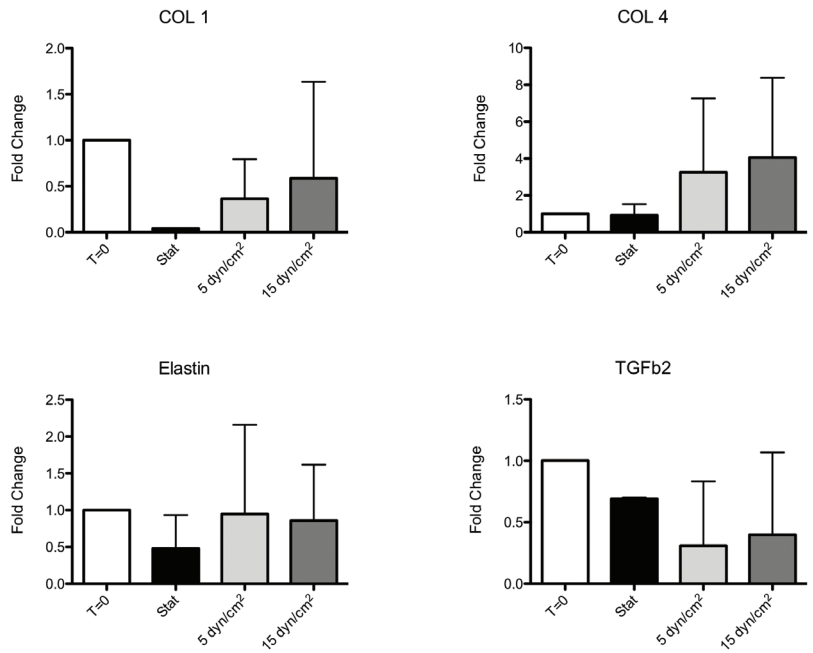

Figure 3. Expression of ECM proteins collagen type 1, collagen type 4 and Elastin following 24 hours of exposure of ECFCs to shear stress (respectively p=0.4, p=0.5, p=0.8). Expression of TGFb2 (P=0.3).

The high shear stress condition we investigated translates to a physiological stress in vivo. Our static controls consistently showed lower expression of endothelial markers and a trend towards lower collagen type 4 expression. Static culture of ECFCs with TGFβ2 for up to 48 hours did not lead to any change in expression of mir29a mir29b or mir29c. We observed that static culture conditions appeared to lower the expression of TGFβ2 receptors compared to shear stressed conditions, suggesting that static conditions do not favor responsiveness to TGFβ2. This would indicate that, in tissue engineering approaches, merely exposing endothelium to TGFβ2 in static in vitro conditions may not be sufficient to induce ECM production. Furthermore, static conditions are likely less than ideal for the maintenance of ECFCs in vitro and, where possible, experiments with these cells should aim to include fluid flow during culture. A limitation to the preliminary data presented here is that they did not achieve statistical significance, most likely due to a low number of replicates and the documented variability in endothelial cell response to shear

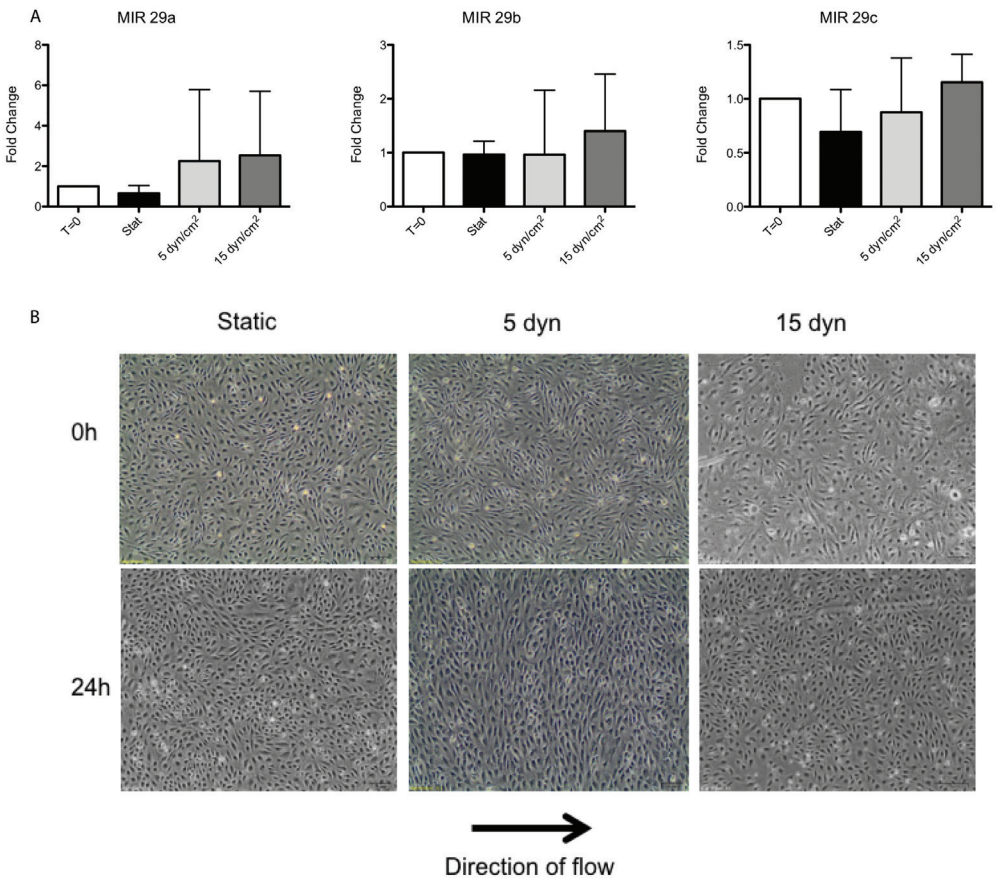

Figure 4. A; Expression of mir29 after exposure to shear stress. Mir29a mir29b and mir29c may show higher expression while static conditions appear to lower the expression (respectively p=0.7, p=0.8, p=0.3). N=5. B; ECFCs after 24 hours of exposure to shear stress. No clear alignment was found.

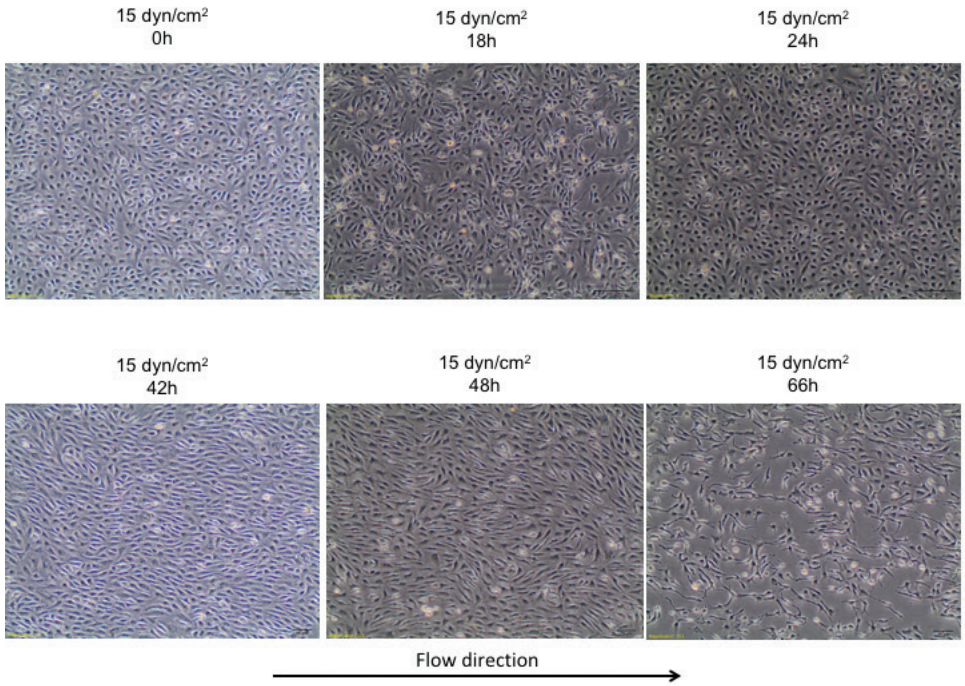

Figure 5. ECFC alignment along the direction of fluid flow. After 42h cellular alignment becomes apparent. At 66 hours confluency is lower, likely due to loss of cells.

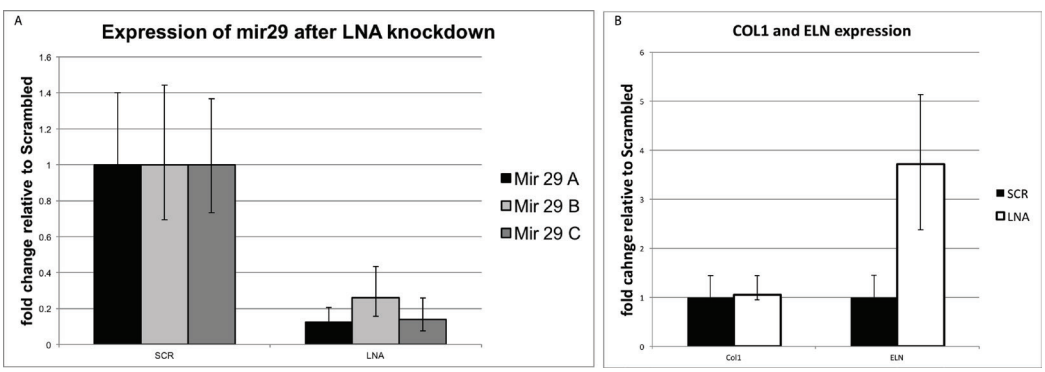

Figure 6. A; mir29 expression following knockdown with LNA29. There was a significant reduction in expression of mir29a, mir29b, mir29c (respectively p=0.002, p=0.006, P=0.009). B; collagen type 1 and elastin expression after knockdown of mir29. Collagen type 1 expression was unchanged compared to scrambled control (p=0.9). Elastin was increased 4-fold (p=0.04). N=3.

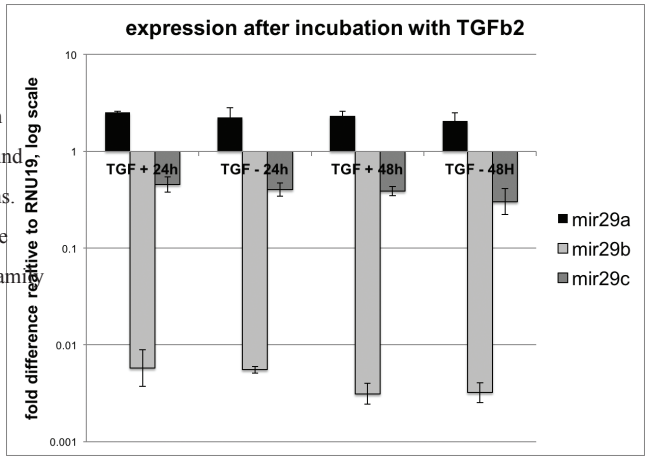

Figure 7. Expression of mir29 after incubation of ECFCs with TGFβ2. No difference was found on expression of mir29 between any conditions. Compared to mir29b and mir29c, mir29a is the most highly expressed member of the mir29 family in ECFCs. N=3.

stress(1). The culture medium used in these experiments contained growth factors such as VEGF, which is a potent regulator of the endothelial phenotype and may influence the outcome of the experiments. Experiments with culture medium containing less growth factors combined with additional ECFC donors and conditions with higher levels of shear stress will help to further investigate how ECFCs behave under fluid flow that is representative of in vivo conditions. The variation in our results highlight important considerations with regard to the ideal conditions to investigate the response of ECFCs to flow. For instance, the design of the flow chamber, in addition to offering limited space for cell culture, only allowed us to investigate laminar flow across a wider, flat surface while actual blood vessels and implanted grafts will have a tubular and most likely curved conformation. Potentially the flow conditions found in-vivo may be approached by a 3-D tissue printing approach including ECFCs to build models of vasculature based on in-vivo conformations.

In vivo vascular endothelium maintains a synergy between flow sensing and force generation by relaying changes in shear stress to underlying myofibroblasts via cross-talk(1,15). We investigated endothelial cells in an isolated manner. Co-culture systems including myofibroblasts, therefore, could be of additional benefit.

Our preliminary results indicate that the effect of a mechanically active environment on ECFCs in vitro warrants further research into which conditions most closely reflect the in vivo environment of tissue engineered cardiovascular grafts.

References

1. Perrault CM, Brugues A, Bazellieres E, Ricco P, Lacroix D, Trepat X. Traction Forces of Endothelial Cells under Slow Shear Flow. Biophys. J. 109(8), 1533, 2015.
2. Malek AM, Alper SL, Izumo S. Hemodynamic shear stress and its role in atherosclerosis. JAMA. 282(21), 2035, 1999.
3. Meng H, Tutino VM, Xiang J, Siddiqui A. High WSS or low WSS? Complex interactions of hemodynamics with intracranial aneurysm initiation, growth, and rupture: toward a unifying hypothesis. AJNR Am J Neuroradiol. American Society of Neuroradiology; 35(7), 1254, 2014.
4. Muylaert DEP, de Jong OG, Slaats GGG, Nieuweboer FE, Fledderus JO, Goumans M-J, et al. Environmental Influences on Endothelial to Mesenchymal Transition in Developing Implanted Cardiovascular Tissue-Engineered Grafts. ten.teb.2015.0167, 2015. Available from: http://online.liebertpub.com/doi/10.1089/ten.teb.2015.0167
5. Azhar M, Brown K, Gard C, Chen H, Rajan S, Elliott DA, et al. Transforming growth factor Beta2 is required for valve remodeling during heart development. Dev. Dyn. 240(9), 2127, 2011.
6. Moonen J, Krenning G, Brinker M, Koerts J, van Luyn M, Harmsen M. Endothelial progenitor cells give rise to pro-angiogenic smooth muscle-like progeny. 2010.
7. de Jonge N, Muylaert DEP, Fioretta ES, Baaijens FPT, Fledderus JO, Verhaar MC, et al. Matrix production and organization by endothelial colony forming cells in mechanically strained engineered tissue constructs. Kumar S, editor. PLoS ONE [Internet]. 8(9), e73161, 2013. Available from: http://eutils.ncbi.nlm.nih.gov/entrez/eutils/elink.fcgi?dbfrom=pubmed&id=24023827&retmode=ref&cmd=prlinks
8. Egorova AD, Khedoe PPSJ, Goumans M-JTH, Yoder BK, Nauli SM, Dijke ten P, et al. Lack of primary cilia primes shear-induced endothelial-to-mesenchymal transition. Circ Res. 108(9), 1093, 2011.
9. van Rooij E, Sutherland LB, Thatcher JE, DiMaio JM, Naseem RH, Marshall WS, et al. Dysregulation of microRNAs after myocardial infarction reveals a role of miR-29 in cardiac fibrosis. Proceedings of the National Academy of Sciences. 105(35), 13027, 2008.
10. Luna C, Li G, Qiu J, Epstein DL, Gonzalez P. Cross-talk between miR-29 and Transforming Growth Factor-Betas in Trabecular Meshwork Cells. Invest. Ophthalmol. Vis. Sci. 52(6), 3567, 2011.
11. Zhang P, Huang A, Ferruzzi J, Mecham RP, Starcher BC, Tellides G, et al. Inhibition of MicroRNA-29 Enhances Elastin Levels in Cells Haploinsufficient for Elastin and in Bioengineered Vessels. Arteriosclerosis, Thrombosis, and Vascular Biology. 32(3), 756, 2011.
12. Yoder MC, Mead LE, Prater D, Krier TR, Mroueh KN, Li F, et al. Redefining endothelial progenitor cells via clonal analysis and hematopoietic stem/progenitor cell principals. Blood. 109(5), 1801, 2007.
13. Broxmeyer HE, Srour E, Orschell C, Ingram DA, Cooper S, Plett PA, et al. Methods in

Enzymology. Elsevier; p. 439–73, 2006.
14. Tzima E, Irani-Tehrani M, Kiosses WB, Dejana E, Schultz DA, Engelhardt B, et al. A mechanosensory complex that mediates the endothelial cell response to fluid shear stress. Nature. 437(7057), 426, 2005.
15. Coen M, Gabbiani G, Bochaton-Piallat M-L. Myofibroblast-mediated adventitial remodeling: an underestimated player in arterial pathology. Arteriosclerosis, Thrombosis, and Vascular Biology. Lippincott Williams & Wilkins; 31(11), 2391, 2011.

Part Two

V

Combining tissue repair and tissue engineering; bioactivating implantable cell-free vascular scaffolds

(Published in Heart)

Dimitri E.P. Muylaert

Joost O. Fledderus

Carlijn V.C. Bouten

Patricia Y.W. Dankers

and Marianne C. Verhaar

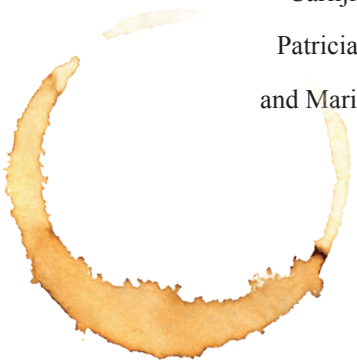

Abstract

Synthetic replacement grafts for heart valves and small-diameter blood vessels such as coronary arteries have the potential to circumvent many of the limitations of currently available autologous grafting materials. Cell-free material incorporating biologically active compounds may guide the formation of fully autologous new tissue in situ derived from host cells after implantation. Inspiration for such bioactive compounds and their dynamics can be found in in vivo repair processes. Molecules such as stromal cell-derived factor 1α (SDF1α) that can attract progenitor cells from the bloodstream and modulate immune responses may be able to improve neo-tissue development in cell-free vascular and valvular grafts. Advances in the development of fully synthetic molecules and scaffold materials allow the spatial and temporal control of biologically active factors, enabling tissue engineers to mimic complex cellular signaling. This review focuses on combining knowledge of the molecular dynamics of factors involved in in vivo damage repair with the possibilities offered by newly developed synthetic materials. This approach has lead to encouraging results in the field of in situ vascular tissue engineering, and can ultimately lead to the development of off-the-shelf available vascular and valvular replacement grafts.

Introduction

There is a growing clinical need for replacement of vascular structures such as coronary arteries and heart valves. Tissue engineered structures are emerging as a future alternative to grafting autologous tissues. Ideally, tissue engineered vascular tissues would be achieved by an off-the-shelf available implant capable of recruiting host cells and stimulating tissue development. In this in situ tissue engineering approach, a cell-free scaffold is implanted into the patient using the body as a bioreactor. After tissue formation the material breaks down and the remaining structure consists of the patient's own cells and is able to grow and remodel, which is especially relevant to pediatric patients. To function properly, native vascular structures such as heart valves and coronary arteries require a multi-layered distribution of an anti-thrombotic endothelial lining, matrix-producing cells and, in case of arteries, smooth muscle cells. These requirements indicate that, while the in situ approach is attractive, it also presents formidable challenges such as how to achieve a scaffold material that is immediately functional upon implantation, how to attract and guide cells to build a layered tissue, how to avoid adverse developments such as hyperplasia, how to modulate the foreign body response, and how to maintain functionality throughout the patient's lifespan. We propose that cell-free material with specific bioactivity can address these issues, and that much can be learned from in vivo tissue regeneration mechanisms, where cells capable of aiding the production and remodeling of new tissue play an important role. In vivo, the recruitment of cells into damaged tissue is mediated through chemokine signaling[1-7], providing clues to factors and dynamics that could be incorporated into a bio-inspired material.

This review will discuss endogenous regenerative mechanisms that may be exploited to develop cell-free tissue engineering constructs by mimicking the timing and presentation of chemokines using novel molecular approaches. There is great overlap in tissue engineering approaches to developing material for valvular and coronary-artery replacement grafts. We will focus on advances in both scaffolds for vascular and valvular replacement grafts, with special emphasis on use of stromal cell-derived factor 1α (SDF1α). The introduction of bioactivity and in vivo analysis of pre-existing decellularized extracellular matrix (ECM) structures as well as fully synthetic, implantable scaffolds will be discussed.

Signaling in Tissue Repair and Relevance to Tissue Engineering

Tissue damage creates a complex inflammatory environment, particularly in response to hypoxia. The hypoxic environment stimulates the expression of hypoxia-inducible factor 1α (HIF1α), which in turn induces downstream factors such as vascular endothelial growth factor (VEGF), SDF1α, platelet derived growth factor b (PDGFb)[8-12] and macrophage chemotactic protein 1 (MCP1)[1,13,14]. Cytokines stimulate the expression of cellular adhesion molecules such as integrins, and are capable of adhering to the ECM and endothelium adjacent

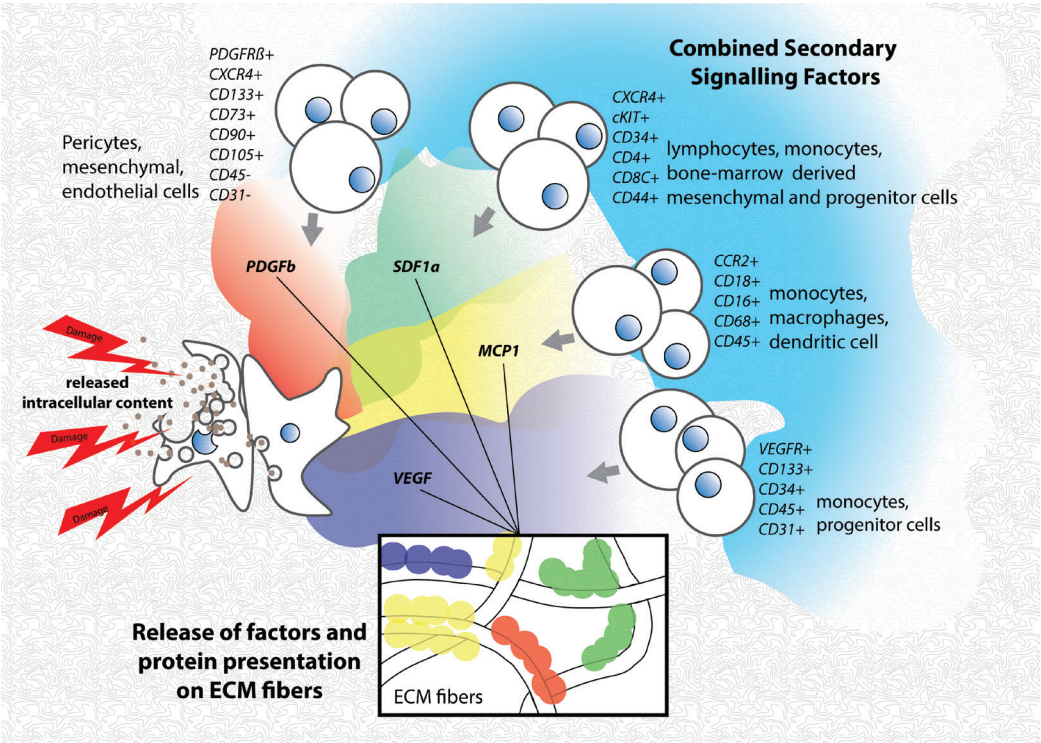

Figure 1. Cellular attraction towards damaged tissue. Damaged cells locally release intracellular content and chemokines that constitute a gradient of signalling factors, bound to and presented on the extracellular matrix (ECM). Cells are attracted along this gradient towards the highest concentration in the vicinity of the damaged area. In response to their environment, the attracted cells produce a complex secondary signalling environment of interleukins and chemokines that further influences the inflammatory and regenerative process. The dynamics of the initial release and subsequent binding and presentation of proteins on the ECM directly modulate this secondary cellular influx and regenerative processes. This initial step may serve as a good starting point for tissue-engineered materials mimicking these dynamics.

to the damaged area[1-7,9,15-18]. This distribution allows circulating cells to home to these molecules and invade the damaged area to aid repair and initiate neovascularization. Cells deprived of oxygen for prolonged periods of time undergo lysis by autodigestive enzymes and release intracellular material into their direct surroundings, activating the immune system by priming resident macrophages, as well as complement and coagulation systems[8-12,14,19,20]. Free radicals and cytokines are released into this environment, stimulating adjacent endothelial cells and fibroblasts but also mast cells, neutrophils and monocytes, which participate in an inflammatory response[1,2,5-7,13,14]. This milieu, in combination with release of matrix-degrading enzymes such as matrix-metalloproteinases (MMPs), is primarily detrimental to the structural environment[8,9,11,12,15]. In response to environmental cues such as interleukins, damaged cells and cross-talk between macrophages and T-helper cells[1,13,19], a shift in subtypes of macrophages, primarily from the classically activated M1 type (inflammatory) to the alternatively activated M2 type (anti-inflammatory) can occur[1,2,4,6,7,21,22]. M2 macrophages are associated with tissue repair[8,9,11,16-18,23]. In addition to macrophages, cell types such as pericytes[1,14,24] and mesenchymal stem cells (MSCs)[1-7] are involved in vascular tissue repair. The attraction of these cells is mediated through a spreading pattern of released chemokines[8-12] with the highest concentration in the vicinity of the damaged area, creating a concentration gradient much like a path of breadcrumbs for the cells to follow. The attracted cells produce a secondary signaling environment, which further modulates the inflammatory and repair processes[1,13,14]. The initial signaling environment, therefore, plays a crucial role in determining the character of the cellular response (see Figure 1).

The factors that are capable of mobilizing and attracting cells involved in tissue regeneration may provide clues as to which signaling proteins might be used to trigger a beneficial cellular response in implanted vascular or valvular grafts. VEGF, PDGFb, MCP1 and SDF1α are major signaling proteins in tissue repair[1,5,9,15-18] (Figure 1). These factors are candidates to biofunctionalize vascular tissue engineered constructs. In this review we chose to focus on SDF1α to highlight the potential of chemokines in the development of cell-free graft material. SDF1α is highly expressed in damaged and naturally hypoxic environments such as the bone marrow, where it is instrumental in homing and mobilization of progenitor cells in the stroma[9,12,14,19,20]. Stem cells expressing the SDF1α receptor CXCR4 in the bone marrow respond to increased serum levels of SDF1α resulting in mobilization into circulation[1,2,5-7,13]. The cells then home to the site of injury and participate in repair mechanisms that lead to improved tissue function[8,9,11,12,15]. SDF1α is highly conserved across species[1,13,19] and is expressed in a variety of tissues such as brain, kidney, lung, heart and vasculature[1,2,4,6,7,21,22]. In all of these tissues it plays a role in the attraction of progenitor cells and repair of damaged tissue[8,9,11,16-18,23]. SDF1α is a strong attractant of lymphocytes, and is capable of influencing the polarization of T-helper cells towards an anti-inflammatory subtype[1,14,24]. In addition to its role in cell attraction, SDF1α stimulation of macrophages can induce the expression of factors associated with an M2 pro-tissue formation macrophage subtype such as VEGF and interleukin-10[25]. As such, SDF1α plays a central role in tissue re-

pair, remodeling and regeneration. Of note, SDF1α is also implicated in neo-intima hyperplasia formation[26], indicating a role for SDF1α in pathological vascular lesions. This underlines the potential of cells attracted to SDF1α to participate in neo-tissue formation, but also highlights important future clinical considerations such as how to avoid a pathological development of neo-tissues. A potential strategy to achieve a balanced neo-tissue formation and to ensure safety and efficacy of vascular replacement grafts is through intelligent delivery systems of bioactive factors.

Introducing Bioactivity Into Scaffold Materials

Cell-free biological grafts suitable for heart halves have already found their way into clinical practice[27]. Usually, these grafts consist of decellularized extracellular matrix, often derived from animal pericardium[28], which has been treated to remove immunogenic epitopes. Biologically active components can be added to decellularized grafts. Application of VEGF to the adventitial side of a decellularized vessel in a murine model showed reduced neointimal hyperplasia and increased endotheliasation in vivo [29-32]. Decellularized porcine aortic heart valves treated with a heparin-VEGF film coating reduce the adhesion of platelets and enhance endotheliasation in vitro[33,34] though this concept was not tested in vivo. The results obtained from bio activated scaffolds for vascular and valvular grafts in vivo (Table 1) underline the potential of bioactivation to influence cellular development, but also reveal that there is still much to learn about the timing and presentation of bioactive molecules. Nevertheless, the implantations of valves treated with SDF1a and fibronectin performed by de Visscher et al and Flameng et al show these strategies are feasible for valvular grafts (Table 1). Considering that the molecular structure of SDF1α contains an ECM-binding domain, it is likely that the proper presentation of the protein on fibronectin can facilitate cell binding by forming a solid phase concentration gradient, as chemokines are known to do in damaged tissues to facilitate repair[35,36].

Importantly, materials based on pre-existing extracellular matrix have shown limited re-cellularization, are prone to degenerative processes and calcification[27,42] and have limited scalability. In clinical practice, biological vascular graft failure induced by incomplete decellularization, structural degradation and adverse remodeling poses a dangerous threat, illustrated by the failure of incompletely decellularized porcine valves resulting in the deaths of three children[44,45]. Synthetic scaffolds, designed to avoid a degenerative foreign body response and to resemble a three-dimensional ECM structure could circumvent these dangers. The different types of polymers used to achieve the appropriate mechanical properties are reviewed elsewhere[46]. Methods such as electrospinning result in a three-dimensional environment based on fibers spun on a micrometer scale (microfibers), which allow for cellular penetration and mechanical tuning, as well as chemical modification of the fibers themselves[29,31,32]. Importantly, cells alter their behavior in response to cues from their three-dimensional surroundings such as mechanical stimuli[33]. Cell differentiation, proliferation, and matrix production can be influenced by mechanical stiffness, composition and architecture of the microenvironment. Several approaches to

bioactivate implantable materials can be identified.

I. Non-covalent and Covalent Binding

In a non-covalent modification strategy bioactive molecules are mixed directly into a delivery system and function by passive release, for instance through injectable gels[39,47] or alginate microspheres. Timed release from microspheres can mimic the release of factors by cells in distress and create a gradient of chemokines capable of attracting cells at a distance of hundreds of microns [48]. These materials influence local cellular processes by slow release. Mixing the bioactive factors in with the materials is simple, but they are not suitable for load-bearing grafts. In covalent modification bioactive molecules can be anchored directly on the surface of scaffold

Table 1 In vivo results of bioactivated vascular and valvular grafts

Vascular	Reference	Approach	Results	Impact
	Assmann et al PMID 23683757	Decellularized aortic conduits including valve coated with fibronectin, implanted in a rat abdomina aorta bypass model	accelerated luminal endotheliazation and neointima formation	Fibronectin surface coating of decellularized vascular material is feasible and enhances cellular repopulation
	Visscher et al PMID 21964214	synthetic knitted polyester coated with FN and SDFa used as carotic interposition graft in sheep	higher number of CD34+ and CD117+ cells adhered, increased endotheliasation and reduced neointimal hyperplasia	combining fibronectin and SDF1a leads to improved presentation of the molecule and influences cellular adhesion to graft material
	Thevenot et al PMID 20185171	Subcutaneous implants in Balb/C mice of PLGA scaffolds incorporating SDF1a through adsorption or osmotic pumps inserted directly into the scaffold core	reduced numbers of mast cells and a reduction in inflammatory signaling, enhanced MSC recruitment	Timed release of SDF1a modulated the foreign body response and enhanced MSC recruitment
	Zhang et al PMID 23290468 and Han et al PMID 23830580	development and implantation of an electrospun graft incorporating distinct layers with dual release of growth factors in a rabbit carotid artery interposition model	A relatively faster release of VEGF on the luminal side of the graft and a slower release of PDGF-BB on the inner layer lead to patency and specifically located endothelialization of the lumen and ingrowth of vascular smooth muscle cells after 8 weeks	Temporal and spacial control over release of factors is feasible and can influence cellular development in specific locations within a synthetic graft
	Tsai et al PMID 22613026	Implantation of a mouse carotid artery interposition graft based of decellularized descending aorta with VEGF applied to the adventitial side through gel	Cells were isolated from the neointima of decellurized grafts without VEGF and shown to be capable of differentiation to endothelial and smooth muscle cell types. Application of VEGF increased endotheliazation and reduced hyperplasia.	the plastic cell types that play a role in neointima formation can be influenced by growth factors applied to cell-free grafts in vivo
Valvular				
	De Visscher et al PMID 19775751	Fibronectin and SDF1α coated onto photooxidized bovine pericardium used to make and implant pulmonary heart valve grafts in sheep	matrix deposition comparable to native valves, endothelial lining, and complete re-cellularization after 5 months with increased numbers of CD34+ and CD117+ positive cells	attraction of progenitor cells to the material by a combination of fibronectin and SDF1α
	Flameng et al PMID 23896322	decellularized ovine aortic valves coated with FN and SDF1a grafted into the right ventricular outflow tract	coated valves were calcification free, reduced immune response was found, collagen density and orientation improved, as well as endotheliazation	Coating of decellularized allografts with FN/SDF-1a prevents cryopreserved heart valve– mediated immune response, conduit calcification, and pannus formation and stimulates re-endotheliazation.

material (Figure 2). Synthetic short peptide sequences such as RGD, which represents a cellular binding molecule based on fibronectin, have been anchored directly to the surface of synthetic materials and enhance cellular adhesion[49]. The molecular presentation of chemokines is crucial to maximizing their potency, illustrated by the enhanced recruitment of muscle progenitor cells to SDF1a immobilized on hyaluronan poly(L-lysine) films[50]. Fibers composed of self-degrading implantable materials [39,51-53] with the added advantage of tunable mechanical properties, can be used to engineer load-bearing vascular structures. The main difference with non-covalent approaches is the minimal leakage of the incorporated bioactive molecules from the material, making it an attractive method to incorporate cellular adhesion molecules. The fibers may be loaded internally with bioactive compounds or even expression constructs which are released as the fibers break down[54] (Figure 2).

II. Supramolecular Materials and Timing

In a supramolecular approach, bioactive molecules are incorporated in or on the scaffold and, depending on the association constant, can be released or presented on the surface. Bioactive peptide sequences can be mixed in and linked to polymers via 2-ureido-4-pyrimidinone (UPy) units in the polymer chain, which dimerize due to their self-complementary quadruple hydrogen bonding[55]. An advantage of such material is the relative ease of mixing the bioactive segments into the polymer, combined with the possibility of tuning mechanical properties [56-58]. The timing of release of bioactive factors is of major influence to cellular development[59], and can be controlled by methods such as direct incorporation inside the degrading fibers[60,61], direct coating[42,60,62,63], or smart release systems through designed MMP cleavage sites for release of peptides[36,63]. The speed of breakdown of the scaffold material also influences graft development and function. A fast degrading scaffold may enable fast remodeling by the host [64], though vascular and valvular grafts need to stay intact long enough for neotissue to take over their mechanical function.The systems described above can control the release and degradation of bioactive factors. This is highly relevant in a complex inflammatory environment, where the effects of factors such as SDF1α are limited by local proteolytic breakdown by factors such as MMPs and dipeptidylpeptidase IV (DPPIV)[63,65]. Agents that inhibit the cleavage of SDF1α by DPPIV have been shown to increase the migration of peripheral blood mononuclear cells (PBMCs) to SDF1α[66,67] and improve vascular tissue repair [65,66,68-71].

III. Molecular Design

Redesigning a biologically active molecule itself can enhance its function. By fusing a strongly matrix-binding molecular domain directly onto several growth factors Martino et al. where able to enhance wound repair at lower topical concentrations[72]. Hiesinger et al have developed a fully synthetic analog of SDF1a, replacing a central domain in the protein with two proline residues resulting in a smaller and more easily produced molecule[73], which enhanced progenitor cell attraction and limited infarct expansion in an ovine myocardial infarction model[74].

Molecular breakdown can be prevented by altering the amino acid sequence, mutating specific cleavage sites while retaining function. The N-terminal receptor-activating domain of SDF1α has previously been redesigned to resist degradation and incorporated into implantable slow release systems [27,63,68-70]. Baumann et al. showed that a modified SDF1α protein capable of withstanding proteolytic degradation induced more progenitor cell migration than wild-type SDF1α[71,75]. Molecular design represents an interesting strategy, where short peptide sequences based on active domains of chemokines can be used to emulate or even enhance bioactivity. Short peptides containing only the first 8 residues on the N terminus of SDF1α are sufficient to activate CXCR4 and induce migration[27,52,63,70,76]. Segers et al. used local delivery of self-assembling nanofibers containing a peptide sequence based on SDF1α, which was made resistant to degradation through targeted amino-acid substitution but still retained its activity[35,75]. These results point the way for advanced, fully synthetic production methods that

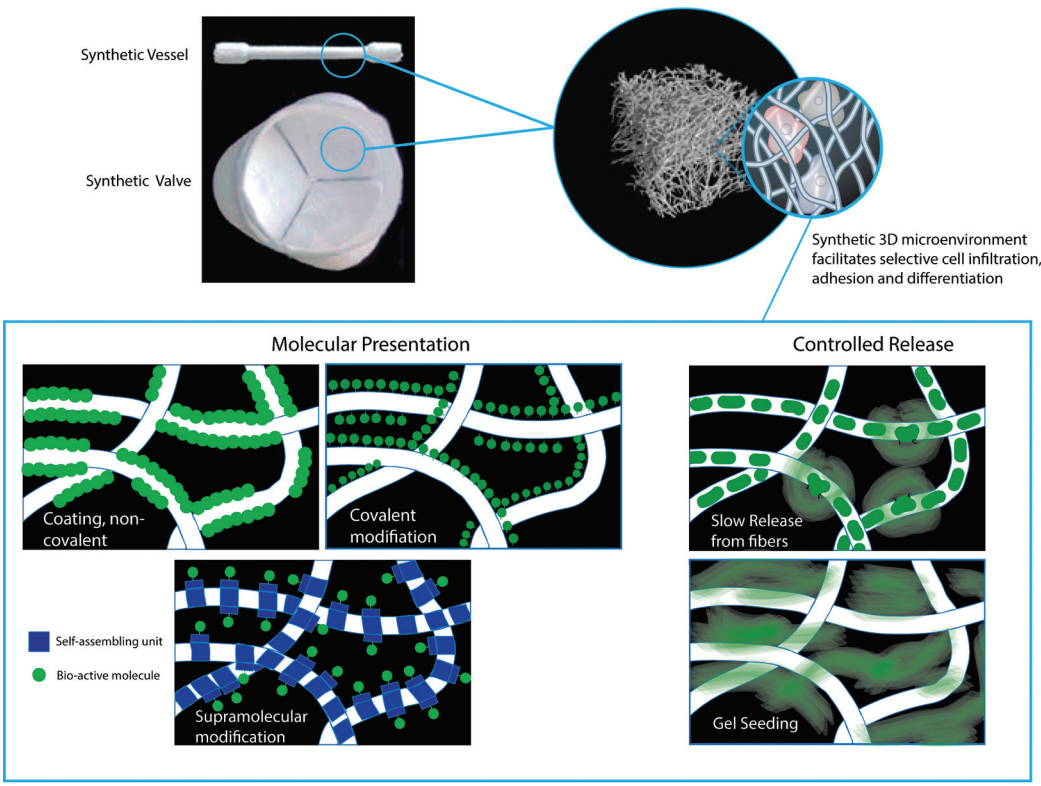

Figure 2. Representation of synthetic scaffold material for vascular and valvular replacement grafts. Synthetic fibres resembling a 3D extracellular matrix environment can be acquired using techniques like electrospinning, and facilitate cell infiltration and adhesion. Within the fibres, local release or presentation of specific factors can guide cell differentiation. The timing and presentation of incorporated factors depends on how they are incorporated into the fibres, varying from strongly bound, minimally leaking dynamics to loosely associated, burst release dynamics. The various approaches can be combined to mimic elements of the in vivo damage response, affording elaborate control over the subsequent cellular response and tissue regeneration. Additional artwork courtesy of Marc Simonet and Rogier Trompert.

offer off-the-shelf availability, limited batch-to-batch variation, and reduced perishability of the bioactive peptides. These approaches (Figure 2) allow the approximation of the dynamics of release and presentation of molecules found in a damage response environment (Figure 1), with increased control over timing and type of bioactive stimuli.

Future Challenges and Conclusion

In humans, there is evidence that local delivery of SDF1α enhances tissue repair. Penn et al. have recently described one of the first in-man studies using non-viral over-expression of SDF1α constructs[52,76]. In this phase 1 trial a dose of non-viral SDF1α DNA plasmid was injected into the peri-infarct region of the myocardium. At 4 and 12 months quality of life, 6-minute walking distance, maintenance of perfusion, heart size and ventricular function were improved, underlining the potential of SDF1a in repair. However, in addition to bioactivity within a graft, the crucial relevance of a systemic response is illustrated by Abbott et al. who introduced SDF1α to the heart via adenoviral delivery [35] and induced a myocardial infarct in mice transplanted with GFP-labeled bone marrow. They found an increase of bone marrow-derived cell engraftment in response to SDF1α after myocardial infarction, but none in the absence of ischemic damage. Following ischemic events factors are released that systemically increase the number of circulating progenitor cells to engage in repair [77,78]. This observation is highly relevant to tissue engineering, as the success of an a-cellular graft is entirely dependent on the response of the recipient. Agents that increase the number of circulating progenitor cells[79] have already been approved for humans in other clinical areas but could also be used to boost the number of circulating progenitor cells prior to implantation.

Fully synthetic bioactive scaffold materials hold promise for the treatment of vascular disease, and knowledge of repair processes may inspire increasingly efficient strategies. Advances in bioactive materials allow for more complex approximations of in vivo repair dynamics. There are important hurdles to overcome before we can ensure the safety and efficacy of such grafts. Following further research into which biological factors will yield the best results, it is important to investigate the long-term performance of implanted grafts. Neo-intima hyperplasia, re-stenosis, early degradation of materials and calcifications are potential complications, and the graft must function in the same environment as the original, malfunctioning, structure. The patient's underlying pathologies must be treated as much as possible. A great challenge lies in controlling the mechanical properties of graft material following implantation. Further development of in vitro models is crucial to predict in vivo responses to novel materials.

Combining the advanced capabilities of synthetic materials with knowledge of in vivo cardiac repair processes can lead to replacement grafts that manipulate cellular responses, are available off the shelf, have minimal batch-to-batch variation, and, most importantly, result in fully autologous, living cardiac tissues.

Acknowledgements and Declarations

This research forms part of the Project P1.01 iValve of the research program of the BioMedical Materials institute, co-funded by the Dutch Ministry of Economic Affairs.
The financial contribution of the Nederlandse Hartstichting is gratefully acknowledged.

References

1. Shirozu M, Nakano T, Inazawa J, et al. Structure and chromosomal localization of the human stromal cell-derived factor 1 (SDF1) gene. Genomics 1995;28:495–500. doi:10.1006/geno.1995.1180
2. van Oostrom O, Fledderus J, de Kleijn D, et al. Smooth muscle progenitor cells: friend or foe in vascular disease. Curr Stem Cell Res Ther 2009;4:131–40.
3. Xu X, Zhu F, Zhang M, et al. Stromal cell-derived factor-1 enhances wound healing through recruiting bone marrow-derived mesenchymal stem cells to the wound area and promoting neovascularization. Cells Tissues Organs (Print) 2013;197:103–13. doi:10.1159/000342921
4. Chavakis E, Urbich C, Dimmeler S. Homing and engraftment of progenitor cells: A prerequisite for cell therapy. J Mol Cell Cardiol 2008;45:514–22. doi:10.1016/j.yjmcc.2008.01.004
5. Chavakis E, Dimmeler S. Homing of progenitor cells to ischemic tissues. Antioxidants & Redox Signaling 2011;15:967–80. doi:10.1089/ars.2010.3582
6. Heissig B, Hattori K, Dias S, et al. Recruitment of stem and progenitor cells from the bone marrow niche requires MMP-9 mediated release of kit-ligand. Cell 2002;109:625–37.
7. Morris LM, Klanke CA, Lang SA, et al. Characterization of endothelial progenitor cells mobilization following cutaneous wounding. Wound Repair Regen 2010;18:383–90. doi:10.1111/j.1524-475X.2010.00596.x
8. Yu S, Crawford D, Tsuchihashi T, et al. The chemokine receptor CXCR7 functions to regulate cardiac valve remodeling. Dev Dyn 2011;240:384–93. doi:10.1002/dvdy.22549
9. Semenza GL. Hypoxia-inducible factors in physiology and medicine. Cell 2012;148:399–408. doi:10.1016/j.cell.2012.01.021
10. Vanden Berg-Foels WS. In SituTissue Regeneration: Chemoattractants for Endogenous Stem Cell Recruitment. Tissue Engineering Part B: Reviews 2014;20:28–39. doi:10.1089/ten.teb.2013.0100
11. Zaruba M-M, Franz W-M. Role of the SDF-1-CXCR4 axis in stem cell-based therapies for ischemic cardiomyopathy. wwwexpertopincom/ebt 2010;10:321–35.

doi:10.1517/14712590903460286
12. Zamilpa R, Lindsey ML. Extracellular matrix turnover and signaling during cardiac remodeling following MI: causes and consequences. J Mol Cell Cardiol 2010;48:558–63. doi:10.1016/j.yjmcc.2009.06.012
13. Artlett CM. Inflammasomes in wound healing and fibrosis. J Pathol 2013;229:157–67. doi:10.1002/path.4116
14. Baay-Guzman GJ, Bebenek IG, Zeidler M, et al. HIF-1 expression is associated with CCL2 chemokine expression in airway inflammatory cells: implications in allergic airway inflammation. Respir Res 2012;13:60. doi:10.1186/1465-9921-13-60
15. Koenig GC, Rowe RG, Day SM, et al. MT1-MMP–Dependent Remodeling of Cardiac Extracellular Matrix Structure and Function Following Myocardial Infarction. Am J Pathol 2012;180:1863–78. doi:10.1016/j.ajpath.2012.01.022
16. Sharma M, Afrin F, Satija N, et al. Stromal-derived factor-1/CXCR4 signaling: indispensable role in homing and engraftment of hematopoietic stem cells in bone marrow. Stem Cells Dev 2011;20:933–46. doi:10.1089/scd.2010.0263
17. Arthur A, Shi S, Zannettino ACW, et al. Implanted Adult Human Dental Pulp Stem Cells Induce Endogenous Axon Guidance. Stem Cells 2009;27:2229–37. doi:10.1002/stem.138
18. Ghadge SK, Mühlstedt S, Özcelik C, et al. SDF-1α as a therapeutic stem cell homing factor in myocardial infarction. Pharmacol Ther 2011;129:97–108. doi:10.1016/j.pharmthera.2010.09.011
19. Sica A, Mantovani A. Macrophage plasticity and polarization: in vivo veritas. J Clin Invest 2012;122:787–95. doi:10.1172/JCI59643
20. Peled A, Petit I, Kollet O, et al. Dependence of human stem cell engraftment and repopulation of NOD/SCID mice on CXCR4. Science 1999;283:845–8.
21. Murray P. Obstacles and opportunities for understanding macrophage polarization. J Leukoc Biol 2011.
22. Galli SJ, Borregaard N, Wynn TA. Phenotypic and functional plasticity of cells of innate immunity: macrophages, mast cells and neutrophils. Nat Immunol 2011;12:1035–44. doi:10.1038/ni.2109
23. Ploeger DT, Hosper NA, Schipper M, et al. Cell plasticity in wound healing: paracrine factors of M1/ M2 polarized macrophages influence the phenotypical state of dermal fibroblasts. Cell Commun Signal 2013;11:29. doi:10.1186/1478-811X-11-29
24. Chen C-W, Okada M, Proto JD, et al. Human pericytes for ischemic heart repair. Stem Cells 2013;31:305–16. doi:10.1002/stem.1285
25. Sánchez-Martín L, Estecha A, Samaniego R, et al. The chemokine CXCL12 regulates monocyte-macrophage differentiation and RUNX3 expression. Blood 2011;117:88–97. doi:10.1182/blood-2009-12-258186
26. Sheng J, Cai W-W, Fang N-Y, et al. Role of stromal-derived factor-1/CXCR4 in neo-intimal repair. Cardiovasc J Afr 2011;22:313–8. doi:10.5830/CVJA-2010-075
27. Kurobe H, Maxfield MW, Breuer CK, et al. Concise review: tissue-engineered vascular grafts for cardiac surgery: past, present, and future. Stem Cells Transl Med 2012;1:566–71.

doi:10.5966/sctm.2012-0044
28. Min B-J, Kim YJ, Choi J-W, et al. Histologic Characteristics and Mechanical Properties of Bovine Pericardium Treated with Decellularization and α-Galactosidase: A Comparative Study. Korean J Thorac Cardiovasc Surg 2012;45:368–79. doi:10.5090/kjtcs.2012.45.6.368
29. Kanie K, Narita Y, Zhao Y, et al. Collagen type IV-specific tripeptides for selective adhesion of endothelial and smooth muscle cells. Biotechnol Bioeng 2012;109:1808–16. doi:10.1002/bit.24459
30. Tsai T-N, Kirton JP, Campagnolo P, et al. Contribution of stem cells to neointimal formation of decellularized vessel grafts in a novel mouse model. Am J Pathol 2012;181:362–73. doi:10.1016/j.ajpath.2012.03.021
31. Doshi J, Reneker DH. Electrospinning process and applications of electrospun fibers. Journal of Electrostatics 1995;35:151–60. doi:10.1016/0304-3886(95)00041-8
32. Persano L, Camposeo A, Tekmen C, et al. Industrial Upscaling of Electrospinning and Applications of Polymer Nanofibers: A Review. Macromol Mater Eng 2013;298:n/a–n/a. doi:10.1002/mame.201200290
33. Wheeldon I, Farhadi A, Bick AG, et al. Nanoscale tissue engineering: spatial control over cell-materials interactions. Nanotechnology 2011;22:212001. doi:10.1088/0957-4484/22/21/212001
34. Ye X, Wang H, Zhou J, et al. The Effect of Heparin-VEGF Multilayer on the Biocompatibility of Decellularized Aortic Valve with Platelet and Endothelial Progenitor Cells. PLoS ONE 2013;8:e54622. doi:10.1371/journal.pone.0054622
35. Abbott JD, Huang Y, Liu D, et al. Stromal cell-derived factor-1alpha plays a critical role in stem cell recruitment to the heart after myocardial infarction but is not sufficient to induce homing in the absence of injury. Circulation 2004;110:3300–5. doi:10.1161/01.CIR.0000147780.30124.CF
36. Patel DD, Koopmann W, Imai T, et al. Chemokines have diverse abilities to form solid phase gradients. Clin Immunol 2001;99:43–52. doi:10.1006/clim.2000.4997
37. Assmann A, Delfs C, Munakata H, et al. Acceleration of autologous in vivo recellularization of decellularized aortic conduits by fibronectin surface coating. Biomaterials 2013;34:6015–26. doi:10.1016/j.biomaterials.2013.04.037
38. De Visscher G, Mesure L, Meuris B, et al. Improved endothelialization and reduced thrombosis by coating a synthetic vascular graft with fibronectin and stem cell homing factor SDF-1α. Acta Biomaterialia 2012;8:1330–8. doi:10.1016/j.actbio.2011.09.016
39. Thevenot PT, Nair AM, Shen J, et al. The effect of incorporation of SDF-1alpha into PLGA scaffolds on stem cell recruitment and the inflammatory response. Biomaterials 2010;31:3997–4008. doi:10.1016/j.biomaterials.2010.01.144
40. Zhang H, Jia X, Han F, et al. Dual-delivery of VEGF and PDGF by double-layered electrospun membranes for blood vessel regeneration. Biomaterials 2013;34:2202–12. doi:10.1016/j.biomaterials.2012.12.005
41. Han F, Jia X, Dai D, et al. Performance of a multilayered small-diameter vascular scaffold dual-loaded with VEGF and PDGF. Biomaterials 2013;34:7302–13. doi:10.1016/j.biomate-

rials.2013.06.006
42. De Visscher G, Lebacq A, Mesure L, et al. The remodeling of cardiovascular bioprostheses under influence of stem cell homing signal pathways. Biomaterials 2010;31:20–8. doi:10.1016/j.biomaterials.2009.09.016
43. Flameng W, De Visscher G, Mesure L, et al. Coating with fibronectin and stromal cell-derived factor-1α of decellularized homografts used for right ventricular outflow tract reconstruction eliminates immune response-related degeneration. The Journal of Thoracic and Cardiovascular Surgery 2014;147:1398–1404.e2. doi:10.1016/j.jtcvs.2013.06.022
44. Hirano Y, Mooney DJ. Peptide and Protein Presenting Materials for Tissue Engineering. Adv Mater 2004;16:17–25. doi:10.1002/adma.200300383
45. Simon P, Kasimir M, Seebacher G, et al. Early failure of the tissue engineered porcine heart valve SYNERGRAFTTM in pediatric patients. European Journal of Cardio-thoracic Surgery 2003;23:1002.
46. Ravi S, Qu Z, Chaikof EL. Polymeric materials for tissue engineering of arterial substitutes. Vascular 2009;17 Suppl 1:S45–54.
47. Prokoph S, Chavakis E, Levental KR, et al. Sustained delivery of SDF-1α from heparin-based hydrogels to attract circulating pro-angiogenic cells. Biomaterials 2012;33:4792–800. doi:10.1016/j.biomaterials.2012.03.039
48. Wang Y, Irvine DJ. Engineering chemoattractant gradients using chemokine-releasing polysaccharide microspheres. Biomaterials 2011;32:4903–13. doi:10.1016/j.biomaterials.2011.03.027
49. Hersel U, Dahmen C, Kessler H. RGD modified polymers: biomaterials for stimulated cell adhesion and beyond. Biomaterials 2003;24:4385–415.
50. Dalonneau F, Liu XQ, Sadir R, et al. The effect of delivering the chemokine SDF-1α in a matrix-bound manner on myogenesis. Biomaterials 2014.
51. Penn MS, Pastore J, Miller T, et al. SDF-1 in myocardial repair. Gene Ther 2012;19:583–7. doi:10.1038/gt.2012.32
52. Penn MS, Mendelsohn FO, Schaer GL, et al. An Open Label Dose Escalation Study to Evaluate the Safety of Administration of Non-Viral SDF-1 Plasmid to Treat Symptomatic Ischemic Heart Failure. Circ Res 2013;112:816–25. doi:10.1161/CIRCRESAHA.111.300440
53. Lee K-W, Johnson NR, Gao J, et al. Human progenitor cell recruitment via SDF-1α coacervate-laden PGS vascular grafts. Biomaterials 2013;34:9877–85. doi:10.1016/j.biomaterials.2013.08.082
54. He S, Xia T, Wang H, et al. Multiple release of polyplexes of plasmids VEGF and bFGF from electrospun fibrous scaffolds towards regeneration of mature blood vessels. Acta Biomaterialia 2012;8:2659–69. doi:10.1016/j.actbio.2012.03.044
55. Dankers P, Harmsen M, Brouwer L, et al. A modular and supramolecular approach to bioactive scaffolds for tissue engineering. 2005;4:568–74.
56. Wisse E, Spiering A, Dankers P, et al. Multicomponent supramolecular thermoplastic elastomer with peptide-modified nanofibers. Journal of Polymer … 2011.
57. Maartje MC, Almen GÁ, Erwin WL. Modular synthesis of supramolecular ureidopy-

rimidinone – peptide conjugates using an oxime ligation strategy - Chemical Communications (RSC Publishing) DOI:10.1039/C1CC14728E. Chemical … 2012.
58. Mollet BB, Comellas-Aragones M, Spiering AJH, et al. A modular approach to easily processable supramolecular bilayered scaffolds with tailorable properties. J Mater Chem B 2014;2:2483–93. doi:10.1039/c3tb21516d
59. de Jonge N, Muylaert DEP, Fioretta ES, et al. Matrix production and organization by endothelial colony forming cells in mechanically strained engineered tissue constructs. PLoS ONE 2013;8:e73161. doi:10.1371/journal.pone.0073161
60. Montero RB, Vial X, Nguyen DT, et al. bFGF-containing electrospun gelatin scaffolds with controlled nano-architectural features for directed angiogenesis. Acta Biomaterialia 2012;8:1778–91. doi:10.1016/j.actbio.2011.12.008
61. Seyednejad H, Ji W, Yang F, et al. Coaxially Electrospun Scaffolds Based on Hydroxyl-Functionalized Poly(ε-caprolactone) and Loaded with VEGF for Tissue Engineering Applications. Biomacromolecules 2012;13:3650–60. doi:10.1021/bm301101r
62. Jordan JE, Williams JK, Lee S-J, et al. Bioengineered self-seeding heart valves. The Journal of Thoracic and Cardiovascular Surgery 2012;143:201–8. doi:10.1016/j.jtcvs.2011.10.005
63. Segers VFM, Tokunou T, Higgins LJ, et al. Local delivery of protease-resistant stromal cell derived factor-1 for stem cell recruitment after myocardial infarction. Circulation 2007;116:1683–92. doi:10.1161/CIRCULATIONAHA.107.718718
64. Wu W, Allen RA, Wang Y. Fast-degrading elastomer enables rapid remodeling of a cell-free synthetic graft into a neoartery. Nature medicine 2012;18:1148–53. doi:10.1038/nm.2821
65. Jungraithmayr W, De Meester I, Matheeussen V, et al. CD26/DPP-4 inhibition recruits regenerative stem cells via stromal cell-derived factor-1 and beneficially influences ischaemia-reperfusion injury in mouse lung transplantation. Eur J Cardiothorac Surg 2012;41:1166–73. doi:10.1093/ejcts/ezr180
66. Fadini GP, Avogaro A. Cardiovascular effects of DPP-4 inhibition: Beyond GLP-1. Vascular Pharmacology 2011;55:10–6. doi:10.1016/j.vph.2011.05.001
67. Post S, van den Broek AJ, Rensing BJ, et al. Reduced CD26 expression is associated with improved cardiac function after acute myocardial infarction: insights from the REPERATOR study. J Mol Cell Cardiol 2012;53:899–905. doi:10.1016/j.yjmcc.2012.08.026
68. Tudan C, Willick GE, Chahal S, et al. C-terminal cyclization of an SDF-1 small peptide analogue dramatically increases receptor affinity and activation of the CXCR4 receptor. J Med Chem 2002;45:2024–31.
69. Chevigné A, Fievez V, Schmit J-C, et al. Engineering and screening the N-terminus of chemokines for drug discovery. 2011;82:1438–56. doi:10.1016/j.bcp.2011.07.091
70. Pelus LM, Bian H, Fukuda S, et al. The CXCR4 agonist peptide, CTCE-0021, rapidly mobilizes polymorphonuclear neutrophils and hematopoietic progenitor cells into peripheral blood and synergizes with granulocyte colony-stimulating factor. 2005;33:295–307. doi:10.1016/j.exphem.2004.11.008
71. Baumann L, Prokoph S, Gabriel C, et al. A novel, biased-like SDF-1 derivative acts

synergistically with starPEG-based heparin hydrogels and improves eEPC migration in vitro. J Control Release 2012;162:68–75. doi:10.1016/j.jconrel.2012.04.049
72. Martino MM, Briquez PS, Guc E, et al. Growth Factors Engineered for Super-Affinity to the Extracellular Matrix Enhance Tissue Healing. Science 2014;343:885–8. doi:10.1126/science.1247663
73. Hiesinger W, Perez-Aguilar JM, Atluri P, et al. Computational protein design to reengineer stromal cell-derived factor-1α generates an effective and translatable angiogenic polypeptide analog. Circulation 2011;124:S18–26. doi:10.1161/CIRCULATIONAHA.110.009431
74. MacArthur JW, Cohen JE, McGarvey J, et al. Preclinical Evaluation of the Engineered Stem Cell Chemokine Stromal Cell-Derived Factor 1-alpha Analogue in a Translational Ovine Myocardial Infarction Model. Circ Res 2013;:CIRCRESAHA.113.302884.
75. Segers VFM, Revin V, Wu W, et al. Protease-resistant stromal cell-derived factor-1 for the treatment of experimental peripheral artery disease. Circulation 2011;123:1306–15. doi:10.1161/CIRCULATIONAHA.110.991786
76. Sundararaman S, Miller TJ, Pastore JM, et al. Plasmid-based transient human stromal cell-derived factor-1 gene transfer improves cardiac function in chronic heart failure. Gene Ther 2011;18:867–73. doi:10.1038/gt.2011.18
77. Xia W-H, Li J, Su C, et al. Physical exercise attenuates age-associated reduction in endothelium-reparative capacity of endothelial progenitor cells by increasing CXCR4/JAK-2 signaling in healthy men. Aging Cell 2012;11:111–9. doi:10.1111/j.1474-9726.2011.00758.x
78. Jung K-H, Chu K, Lee S-T, et al. Multipotent PDGFRβ-expressing cells in the circulation of stroke patients. Neurobiol Dis 2011;41:489–97. doi:10.1016/j.nbd.2010.10.020
79. Nervi B, Link DC, DiPersio JF. Cytokines and hematopoietic stem cell mobilization. Journal of cellular biochemistry 2006;99:690–705. doi:10.1002/jcb.21043

VI

In Situ Tissue Engineering of Functional Small-Diameter Blood Vessels by Host Circulating Cells Only

(Published in Tissue Engineering part A)

Hanna Talacua*

Anthal I.P.M Smits*

Dimitri E.P. Muylaert

Jan Willem van Rijswijk

Aryan Vink

Marianne C. Verhaar

Anita Driessen-Mol

Lex A. van Herwerden

Carlijn V.C. Bouten

Jolanda Kluin*

and Frank P.T. Baaijens*

* these authors contributed equally

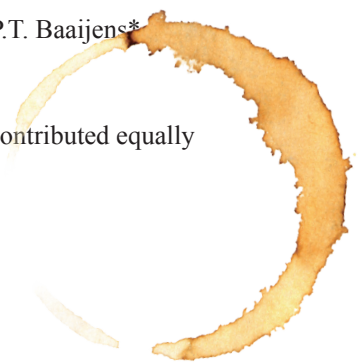

Abstract

Inflammation is a natural phase of the wound healing response, which can be harnessed for the in situ tissue engineering of small-diameter blood vessels using instructive, bioresorbable synthetic grafts. This process is dependent on colonization of the graft by host circulating cells and subsequent matrix formation. Typically, vascular regeneration in small animals is governed by transanastomotic cell ingrowth. However, this process is very rare in humans and hence less relevant for clinical translation. Therefore, a novel rat model was developed, in which cell ingrowth from the adjacent tissue is inhibited using Gore-Tex sheathing. Using this model, our aim here was to prove that functional blood vessels can be formed in situ via the host inflammatory response, specifically by blood-borne cells. The model was validated by implanting sex-mismatched aortic segments on either anastomoses of an electrospun poly(ε-caprolactone) (PCL) graft, filled with fibrin gel, into the rat abdominal aorta. Fluorescent in situ hybridization analysis revealed that after 1 and 3 months in vivo, over 90% of infiltrating cells originated from the bloodstream, confirming the effective shielding of transanastomotic cell ingrowth. Using the validated model, PCL/fibrin grafts were implanted, either or not loaded with Monocyte Chemotactic Protein-1 (MCP-1), and cell infiltration and tissue development was investigated at various key time points in the healing cascade. A phased healing response was observed, initiated by a rapid influx of inflammatory cells, mediated by the local release of MCP-1. After 3 months in vivo, the grafts consisted of a medial layer with smooth muscle cells in an oriented collagen matrix, an intimal layer with elastin fibers, and confluent endothelium. This study proves the regenerative potential of cells in the circulatory system in the setting of in situ vascular tissue engineering.

Introduction

There is a clear clinical demand for suitable artificial small-diameter (Ø < 6 mm) blood vessels, in particular for lower-limb peripheral artery disease with an overall prevalence estimated to be in the range of 3-10% (1,2). Current artificial small-caliber vessels have poor patency rates compared to their living counterparts, which is inherently due to their non-adaptive constitution. Tissue engineering has been proposed to overcome these shortcomings by delivering living small-diameter grafts (3,4). However, traditional tissue engineering approaches comprise lengthy and costly in vitro procedures. In situ tissue engineering is emerging as a promising alternative, in which an acellular bioresorbable synthetic graft is implanted, allowing the body to populate the scaffold with host cells and develop extracellular matrix while the scaffold is degraded (5). This approach is built on the notion that inflammation is not merely a detrimental response to biomaterials, but when harnessed properly, can be exploited to induce a natural regenerative response (6–8). By omitting time-consuming cell-expansion and bioreactor phases, this method can deliver cost-effective, off-the-shelf available grafts (6). Recent studies following the in situ tissue engineering principle have demonstrated colonization and subsequent remodeling of a biodegradable synthetic graft into functional neoarteries in various animal models (9–13). However, the cellular and molecular mechanisms underlying this functional regeneration remain elusive (4,14). An inflammation-mediated response has been suggested, comprising an initial rapid recruitment of immune cells to the scaffold, followed by an influx of tissue cells that remodel the graft into a native-like artery (15). Monocyte Chemotactic Protein-1 (MCP-1) has been identified as one of the key mediators in this process, and local release of exogenous MCP-1 from a biodegradable scaffolds was shown to enhance de novo tissue formation (15).

To translate preclinical results to human application, it is essential to recognize and predict regenerative processes (cell colonization and tissue development) representative for the human situation. From previous small-animal studies employing degradable and non-degradable grafts, it is clear that transmural migration is a predominant source of macrophages as well as a-smooth mucle actin (α-SMA)-expressing cells in rodents (16–18). Furthermore, transanastomotic ingrowth of mature endothelial cells (EC) and smooth muscle cells (SMC) was identified as the predominant source of tissue cells in the rodent model (19). However, given the fact that transanastomotic endothelialization in humans is restricted to the immediate perianastomotic region, the question arises how predictive these model-dependent processes are for the clinical situation, especially considering that vascular prostheses for humans often require extensive anatomic lengths (20,21). Moreover, this suggests that physiological remodeling of a graft in human is heavily dependent on the contribution of circulating cells. Therefore, our aim was to prove that functional blood vessels can be formed in situ via the host inflammatory response solely by circulating cells. To isolate the role of blood-borne cells in the regenerative process, we employed a more predictive rat model, in which the graft is isolated from surrounding tissues, both transmurally and transanastomotically. To preclude cell ingrowth from the adjacent tissue,

highly porous electrospun poly(ε-caprolactone) (PCL) tubes were shielded by impenetrable Gore-Tex sheet material on both anastomoses as well as enclosing the adventitial side of the PCL scaffold over the entire length. To enhance rapid cell recruitment from the circulation, we incorporated fast-releasing MCP-1 into our scaffold using fibrin gel. Grafts were implanted as abdominal aortic interposition grafts in rats and were explanted at different time points in the remodeling cascade. We hypothesized that (i) extracellular matrix-producing cells can be recruited from the circulation, and that (ii) increased early monocyte recruitment to the graft by MCP-1 has a positive effect on long-term tissue remodeling and regeneration.

Materials And Methods

I. Experimental Animals

Seventy-six healthy Sprague Dawley rats, 250-300 g, were used, purchased from Harlan Laboratories. Each animal was fed ad libitum and was housed in groups in an environment maintained at room temperature for 24 h a day and with a 12h-light and 12h-dark cycle. Two studies were performed; Study 1 was dedicated to validate the model, and Study 2 was dedicated to investigate the effect of MCP-1 in the scaffold. In Study 1, Gore-Tex shielded grafts (n=12) were compared to grafts without shielding (n=12) (Figure 1A-C). To study general cell infiltration in both groups over time, grafts were explanted at 1 day (n=2), 3 days (n=2), 1 week (n=2), 2 weeks (n=2) and 3 months (n=4). To specifically study the efficacy of the model in transanastomotic shielding, a sex-mismatch experiment was performed, in which sections of male rat aorta were interpositioned proximally and distally to the graft in female rats, either shielded or unshielded with Gore-Tex (n=12 per group). These grafts were explanted after 1 or 3 months (n=3 per group, per time point) for fluorescent in situ hybridization (FISH) analysis.

Study 2 was dedicated to study the effect of MCP-1, comparing fibrin-seeded grafts with incorporated MCP-1 (n=20) versus fibrin-seeded controls (n=20). All grafts in this study group were shielded with Gore-Tex. Grafts were explanted at 1 day, 3 days, 1 week, 2 weeks and 3 months (n=4 per time point). All procedures were performed in accordance with and approved by the Institutional Animal Care and Use Committee of the University of Utrecht, the Netherlands.

II. Scaffold Fabrication

Electrospun poly(ε-caprolactone) (PCL) tubular scaffolds were manufactured and provided by Xeltis BV. In brief, PCL (Purasorb; Purac Biochem) was dissolved in chloroform at 20% (w/w), and driven through a horizontally fixed nozzle at high voltage (15 kV) toward a grounded rotating cylindrical copper target (Ø 2 mm) at 15 cm distance. The resulting tube diameter, wall thickness and average fiber diameter were determined with scanning electron microscopy (SEM; Quanta 600F, Fei). The materials were sterilized by gamma irradiation. Before implantation, the

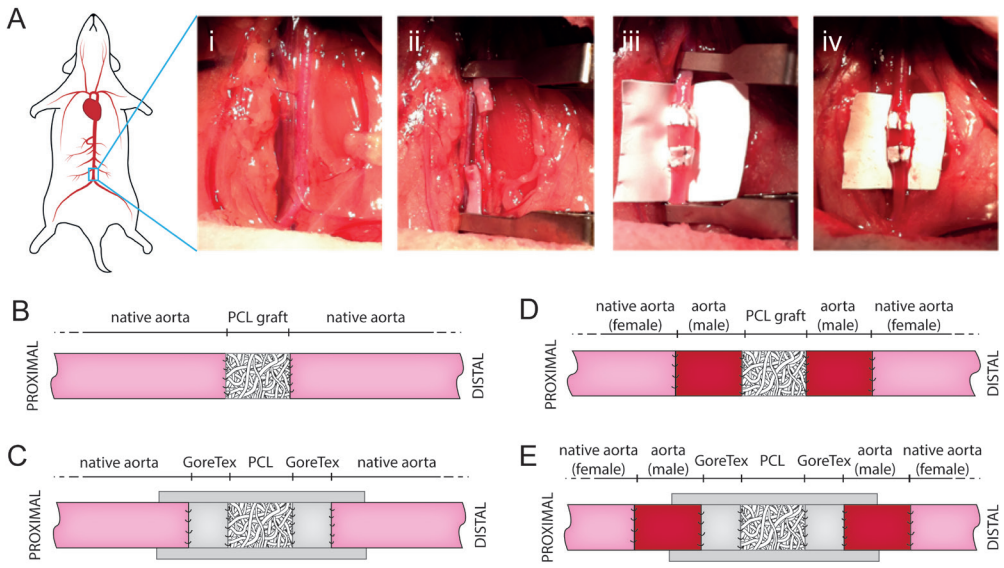

FIG. 1. Implantation procedure and experimental groups. (A) Camera microscopy images of the graft implantation with, in bright white, the Gore-Tex sheet. The aorta before (i), after transection (ii), after implantation of the graft (iii), and directly after removing the vascular clamps (iv). (B–E) Schematic representation of the experimental groups in Study 1, with the shielded grafts (C) versus unshielded control (B) and the sex-mismatched shielded graft (E) versus the unshielded control (D).

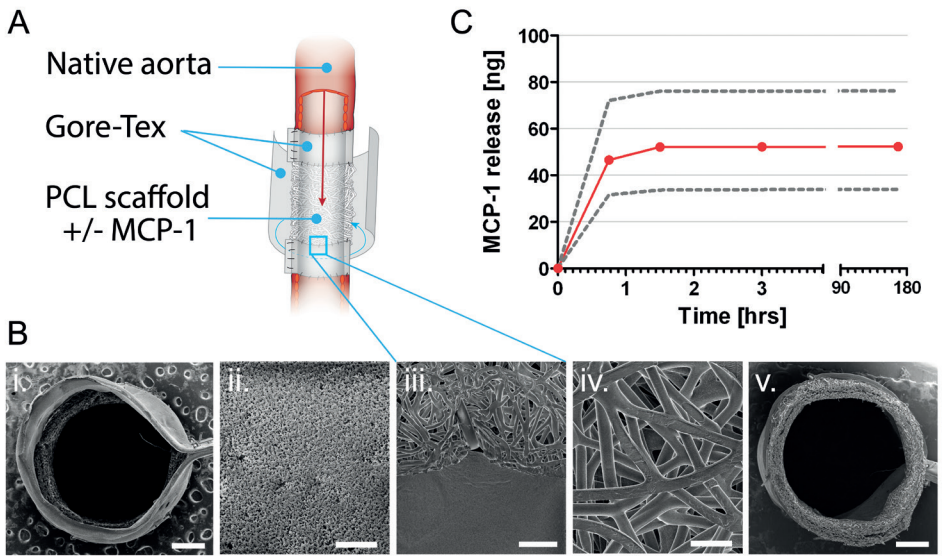

FIG. 2. Graft composition. Schematic representation of the monocyte chemotactic protein-1 (MCP-1)-loaded graft (A) with scanning electron microscopy images (B) showing a transection (i), the luminal surface of the Gore-Tex (ii), the Gore-Tex anastomosed to the poly(e-caprolactone) (PCL) (iii), and the luminal surface (iv) and transection of the porous PCL scaffold (v). (C) MCP-1 release curve as determined in vitro. Scale bars represent 500 mm (i and v), 40 mm (ii and iv), and 100 mm (iii).

PCL tube was cut to size and the vessel wall was impregnated with fibrin gel (5 U/ml thrombin + 5 mg/ml fibrinogen (Sigma)). Depending on the test group, MCP-1 (4 µg/ml; Chemicon) was added to the fibrin solution. To measure the release rate of the MCP-1 from the graft, a cumulative leakage experiment was performed in vitro. For this, MCP-1-loaded scaffold samples were incubated in culture medium (RPMI-1640, Sigma), supplemented with 10% (v/v) fetal bovine serum (FBS Gold, PAA Laboratories) over a period of 7 days. At each time point (0, 0.75, 1.5, 3, 8, 24, 48, 72, 120, 168 h), all supernatant was collected, replaced with fresh medium, and samples were stored at -80 °C until further analysis. MCP-1 content was determined cumulatively using a human ELISA kit, according to manufacturer's protocol (RayBiotech) (n=3).

III. Surgical Procedure

Prior to implantation, graft composites were prepared depending on study group. To shield the electrospun grafts, an end-to-end anastomosis was made to a 4 x 10 mm^2 impenetrable Gore-Tex strip (Preclude Pericardial Membrane; Gore Medical) using 10-0 interrupted sutures, distally and proximally of the electrospun tube. Additionally, Gore-Tex was wrapped around the PCL in samples creating an impenetrable outer layer (Figure 1A-C). For the FISH experiments, sex-mismatched segments of aorta were interpositioned on the proximal and distal anastomosis between the native aorta and the graft (Control group, n=3 per time point; Figure 1D) or Gore-Tex (Test group, n=3 per time point; Figure 1E). Animals were anesthetized using Isoflurane gas. Once adequate anesthesia was achieved, a midline laparotomy was performed and the abdominal viscera were lateralized for exposure of the abdominal aorta and the inferior vena cava. After separation of the aorta from the inferior vena cava and surrounding tissue, the segment of the abdominal aorta between the renal arteries and the aortic bifurcation was occluded with microvascular clamps. The aorta was transected and the graft composite was introduced with end-to-end anastomosis performed at both the proximal and distal ends using interrupted sutures. After removing the vascular clamps, the pulsatile flow was confirmed in the aorta distal to the graft (Figure 1A). The abdomen was closed in two layers. Immediately after implantation, all scaffolds were exposed to arterial hemodynamic conditions. There was no heparin administration during or after surgery. Animals recovered on warmed pads to promote blood flow through the grafts. Before rats were returned to their cages, they were assessed for evidence of hind limb paralysis or acute graft thrombosis. Post-operative Buprenorphine was given intraperitoneal. At termination, animals were anaesthetized using Isoflurane. Tubes were dissected free from surrounding tissue. The Gore-tex on the outer layer was opened the PCL graft was carefully explanted. All explants were examined with immunohistochemistry. In Study 2, two explants per time point were additionally analyzed with qPCR to determine the expression of genes involved in the inflammatory response. Furthermore, blood samples were collected and analyzed with ELISA to determine systemic protein levels of MCP-1 in the blood serum (Supplementary Data).

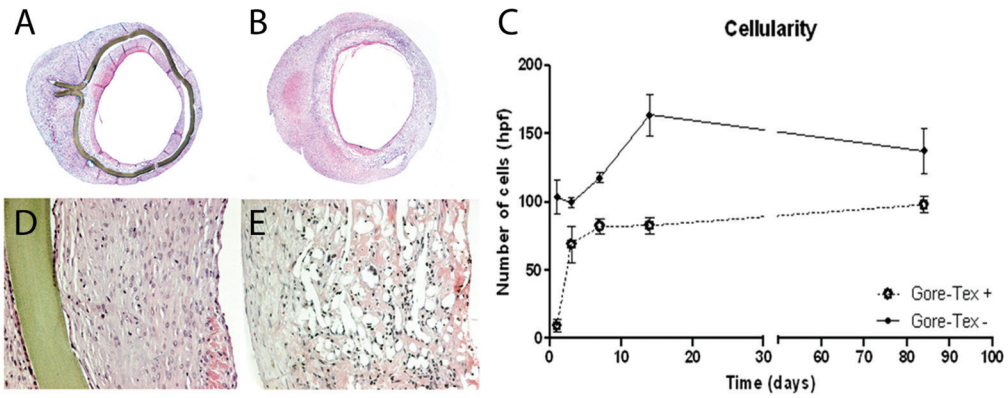

FIG. 3. Efficacy of transmural isolation. Scaffold cellularity of the shielded (A, D) versus nonshielded grafts (B, E). Cellularity decreased significantly in the grafts shielded with Gore-Tex when compared with the control group (98 – 6 cells per high-power field [hpf] vs. 137 – 17 cells per hpf, p = 0.03 at 84 days), with the largest differences at day 1 (9 – 4 cells per hpf vs. 103 – 12 cells per hpf) and day 14 (82 – 6 cells per hpf vs. 163 – 15 cells per hpf) (C).

IV. Immunohistochemistry

Explants were fixed in formalin 10% before pre-embedding in 1% (w/v) agar (Eurogentec), followed by embedding in paraffin. Consecutive 4 µm sections were stained with Mayer's hematoxylin and eosin (H&E), Verhoeff van Gieson and 0.1% (w/v) Sirius red F3B (Gurr BDH) in saturated picric acid solution, respectively. Immunohistochemical stainings were performed on 4 µm sections after deparaffinization and dehydration. Sections were stained for myeloperoxidase (MPO; Dako, A398, 1:2000), CD68 (Serotec, MCA341GA, 1:400) CD163 (Serotec, MCA342GA, 1:75), CCR7 (Cell Applications, CG1678, 1:15000), CD34 (R&D Systems, AF4117, 1:100), alpha-smooth muscle actin (α-SMA; Sigma, A2547, 1:32000), and Von Willebrand Factor (vWF; Dako, A0082, 1:1600). All antibodies were diluted in PBS/BSA/Azide. Following deparaffinization, antigen retrieval was performed in citrate (For CD68, CCR7, and MPO), pepsin (CD163), or EDTA (vWF), before blocking with 10% normal goat serum (α-SMA and CCR7) or Ultra V block (MPO; Thermo Scientific). Sections were blocked for endogenous peroxidase when a HRP-conjugated secondary antibody was used. Appropriate BrightVision signal amplification was used for labeling of primary antibody binding sites: Poly AP anti-mouse for α-SMA, poly HRP anti-mouse (CD68 and CD163), and poly HRP anti-rabbit (CCR7, MPO, and vWF) (Immunologic). Slides were subsequently incubated with liquid permanent red substrate-chromogen (Dako) or diaminobenzidine substrate-chromogen (Sigma) and counterstained with Mayer's hematoxylin. Slides were dehydrated in alcohol

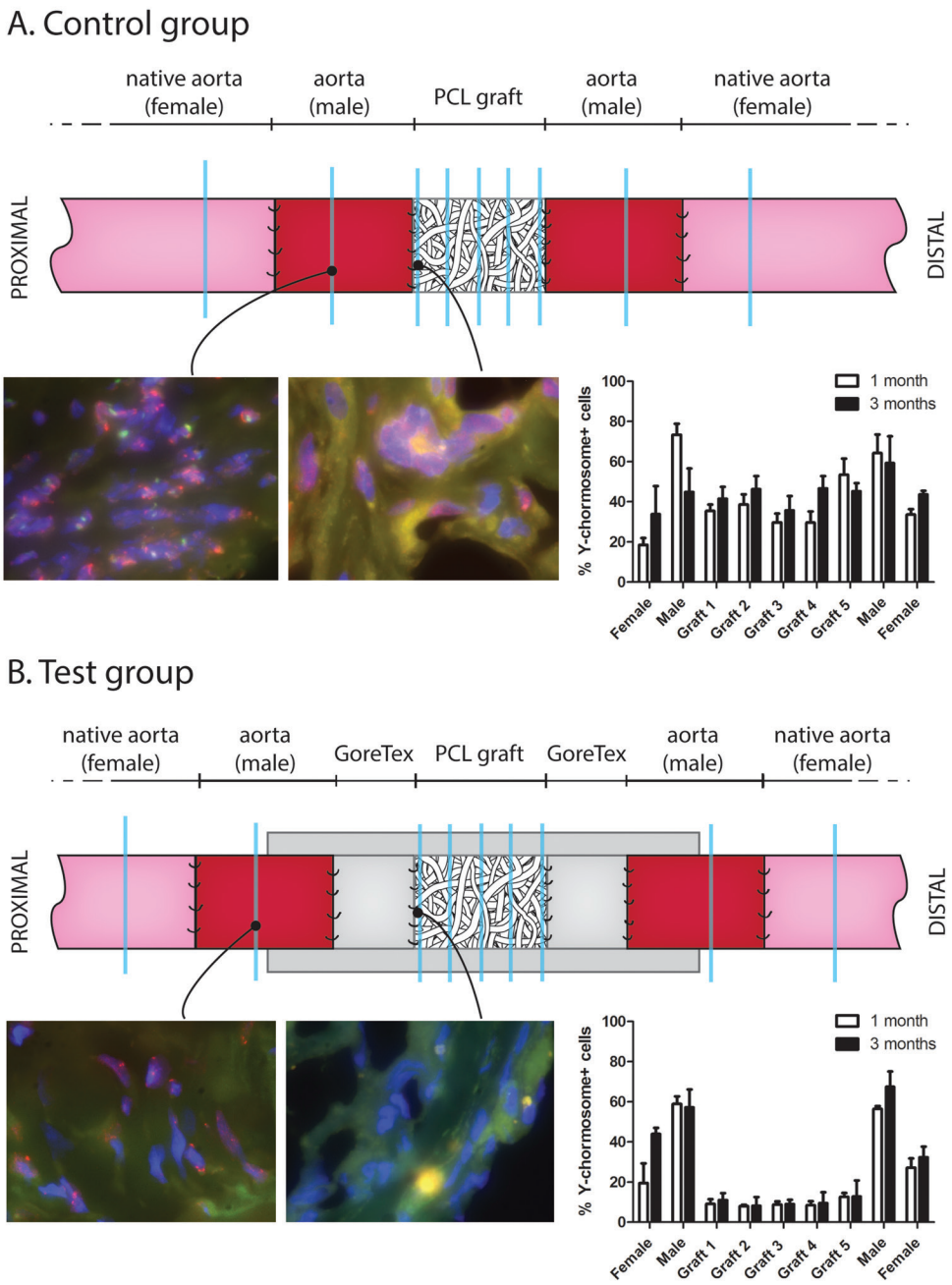

FIG. 4. Efficacy of transanastomotic isolation. Schematic representation of the graft composition and the results of the fluorescent in situ hybridization analysis for the unshielded Control (A) and shielded Test (B) group. Blue lines indicate the approximate locations of the analyzed sections. Red staining indicates the pres- ence of Y-chromosome; cell nuclei are in blue (DAPI). Quantification of the staining reveals that transanastomotic cell ingrowth of male cells into the graft is effectively blocked in the Test group, while male cells are homogeneously distributed in the Control group.

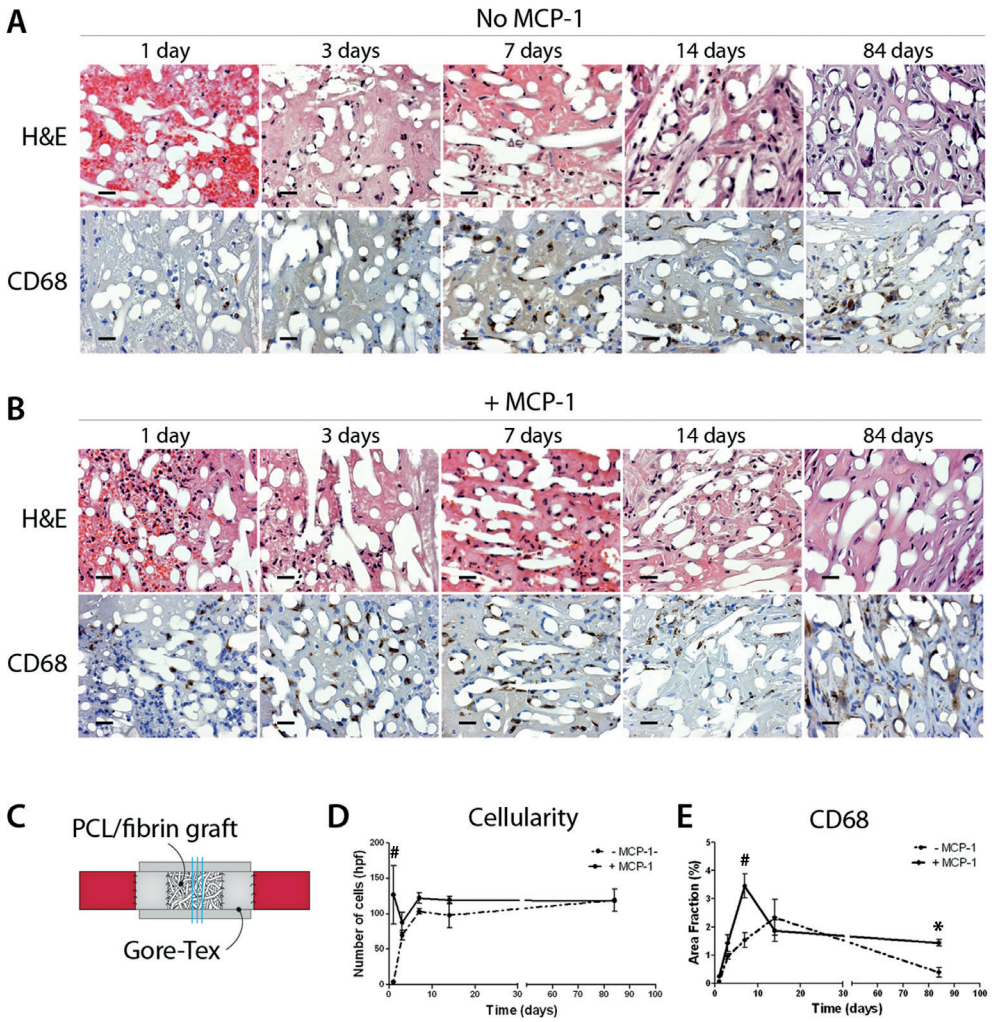

FIG. 5. Infiltration of immune cells. Histological evaluation on transverse sections of the center part of the PCL grafts (C), without and with MCP-1, explanted at days 1, 3, 7, 14, and 84 (A, B). The MCP-1 group displayed an immediate peak in overall graft cellularity at day 1 with significantly more cells compared with the control group (127 – 40 vs. 4 – 2 per hpf) (D). The percentage of CD68+ macrophages rapidly increased in the first 2 weeks, with a significantly higher concentration in the MCP-1 group compared with the control group at day 7 (33.2 – 4.7 vs. 15.3 – 2.7 per hpf) and day 84 (14.9 – 0.2 vs. 5.6–4.1 per hpf) (E). PCL fibers are visible in white. Scale bars represent 20mm. #p<0.001, *p<0.05.

changes and coverslipped using pertex. Double-label immunohistochemistry for a-SMA and vWF was performed after EDTA-antigen retrieval by incubating sections for 1 hour at room temperature with a mix of 1:32,000 mouse anti- α-SMA and 1:1600 rabbit anti-vWF antibodies. The sections were then incubated with anti-mouse Alexa Fluor 488 and anti-rabbit Alexa Fluor 555 conjugated secondary antibodies (Invitrogen, 1:200) for 30 minutes. Cell nuclei were counterstained with DAPI.

V. Quantitative Histologic and Immunohistological Analysis

Two investigators, who were blinded to the investigated groups and the time point of explantation, independently conducted analysis. Sections were photographed using a Nikon E800 microscope with ACT-1 software. Wall thickness and lumen diameter were measured manually under 2x objective lens. Wall thickness was measured in 2 sections of each graft and in 4 locations per section. The lumen diameter was measured in 2 sections of each graft and in 2 directions per section. Cellularity was studied under high-power magnification (high-power field (hpf), 40x objective lens; area comprising 0.034 mm^2), with cell sizes being comparable between groups. The total number of cells in 4 random hpf areas per PCL tube was manually counted using ImageJ software. Quantification of aligned collagen was performed with picrosirius red stains and circularly polarized light. Stained sections were digitally photographed and converted into gray-value images and regions of interest (ROI) were drawn lining the graft. The average gray value per ROI was calculated using ImageJ software. A quantitative analysis of the immunopositive cells of each stained slide was performed at 4 random hpfs. The portion of area staining positively for the marker within the 4 hpfs was counted and summed for each image. The mean of the sums for 4 high power images was then calculated for each sample. Area of positive staining was measured as a percentage of the total from binarised images.

VI. Fluorescent In Situ Hybridization (FISH)

To identify X- and Y-chromosomes, FISH was performed on fresh sectioned paraffin sections using Rat idetect Chr X FISH Probe Green and Chr Y FISH Paint Probe Red (ID Labs, IDRF1067 and IDRR1070, respectively). Following deparaffinization, slides were pretreated with 0.2N HCl for 20 min at room temperature, citrate buffer (pH 6.0) for 20 min at 100°C, and digested with 0.1% proteinase K for 10 min at 37°C. After dehydration in graded ethanol, 7.5 µl of probe mixture was added. Sections were then denatured for 5 min at 69°C, cooled on ice for 5 min, and hybridized overnight at 37°C in a ThermoBrite. The next day, slides were washed in 0.4x SSC/0.3% NP-40 at 73°C, 2x SSC/0.1% NP-40 at room temperature, and 2x SSC for 2, 1, and 5 min, respectively. After washing, the sections were counterstained with DAPI, dehydrated and mounted in Vectashield (Vectorlabs, H-1000). To quantification the FISH results, at least 30 images per sample were analyzed by two investigators, blinded to the experimental group, sample location and time of implantation.

VII. Statistical Analysis

Statistical differences were determined using two-way ANOVA with time and test factor as the variables, with Bonferroni post-tests to compare the means per time point using GraphPad Prism software. $P < 0.05$ was considered statistically significant.

Results

I. Grafts Are Constructed From Porous Electrospun PCL and Dense Gore-Tex

SEM analysis showed the dense microstructure of the Gore-Tex, with an internodal distance < 1μm. In contrast, the PCL graft was highly porous with interconnected pores and an average fiber diameter of 9 μm (range 8.4 to 9.7 μm) (Figure 2A, B). The inner diameter of the graft was approximately 2 mm with an average wall thickness of 275 μm (range 210 to 340 μm). Grafts were seeded with a fibrin gel with or without MCP-1. In vitro leakage experiments revealed a burst-release of MCP-1 within the first three hours, after which the release gradually leveled off (Figure 2C).

II. Gore-Tex shielding led to a significant reduction of cell ingrowth from neighbouring tissues

All grafts remained patent and there were no signs of stenosis or thrombosis in all groups studied. Lumen diameter and wall thickness remained constant throughout the whole study (1.8 mm ± 0.1 and 385 μm ± 108 respectively), with no signs of intimal hyperplasia or aneurysms. Macroscopically, granulation tissue was seen on the adventitial side of Gore-Tex sleeves (Figure 3A, B, D, E). No cell infiltration into the dense adventitial sleeve was detected at any time point. Adventitial Gore-Tex shielding led to a significant reduction in total cellularity at all intervals compared to unshielded controls, with the largest difference at day 1 and day 14 (Figure 3C). For the FISH experiments, sections were taken from five different locations in the graft as well as the native (female) aorta and the implanted male segment (as indicated in Figure 4) and analyzed for the presence of Y-chromosome using FISH. In the Control group, the average fraction of male cells detected in the graft was 37.4 ± 12.1% and 43.1 ± 9.8% after 1 and 3 months, respectively. Moreover, after 3 months of implantation, the distribution of male cells was homogenous throughout all sections of the control group, with an average of 44.1 ± 14.5% (Figure 4A). In contrast, in the Test group, the fraction of male cells detected in the graft was severely limited, with an average of 9.4 ± 3.2% and 10.1 ± 7.7% after 1 and 3 months, respectively. There were no marked differences between the different locations in the graft (Figure 4B). After 3 months, the native (female) aorta contained on average 38.1 ± 9.3% male cells in this group, indicating a comparable migration of male cells to unshielded tissues as compared to the control group.

These results demonstrate effective isolation of the graft using Gore-Tex sheathing in this rat model, both transmurally and transanastomotically.

III. MCP-1 Recruits Immune Cells in Early Inflammatory Phase

Cells penetrated immediately after implantation through the entire thickness of the PCL in all grafts (Figure 5A-C). Directly after implantation, mainly neutrophilic granulocytes infiltrated all grafts, with a significant increase in overall cell infiltration in the MCP-1 group compared to the control group at day 1 (Figure 5D). There was a marked increase in CD68+ macrophage infiltrates in the MCP-1 and control group up to day 7 and day 14, respectively, with an even distribution throughout the graft. At day 7, the concentration of macrophages was significantly higher in the MCP-1 group compared to the control group. After the first 2 weeks, macrophage numbers gradually decreased in both groups with a significantly higher macrophage concentration in the MCP-1 group after 3 months (Figure 5E). In both groups macrophage giant cells were seen. Macrophage subtypes were characterized by CCR7 (M1) and CD163 (M2) expression. Surprisingly, CD163+ cells were detected very sparsely (< 1%). CCR7 expression was detected, but only a small fraction of the CCR7 staining double stained positive for the pan-macrophage marker CD68.

IV. Initial MCP-1 Release Results in Enhanced Tissue Formation in Healing Phase

A progressive increase in CD34+ cells was observed in both groups, with no significant differences between groups up to day 14 (Figure 6A, B). At day 84, the expression of CD34 was significantly higher in the MCP-1 group compared to the control group. For α-SMA expression, no significant differences were detected between groups for all time points (Figure 6C, D). In both groups, the first α-SMA+ cells were detected at day 7. After 3 months, the myofibroblast population formed a circumferentially oriented neointima layer of SMC under an endothelium in both groups (Figure 6C). vWF staining revealed no significant differences between groups, with first evidence of EC in the grafts at day 7 in both groups. Small patches of vWF-expressing cells lined the lumen, growing more confluent through week 2, before reaching a fully confluent monolayer at 3 months (Figure 6J-L). This was similar in both the MCP-1 and the control group. At day 14, the first signs of collagen fibers were detected in both groups. After 3 months, circumferentially orientated bundles of collagen fibers were found lining the endothelial and outer layers of the graft, with more loose fibers towards the center of the wall (Figure 7A-F). Aligned collagen was markedly increased after 3 months in both groups, with a significantly higher expression of aligned collagen in the MCP-1 group compared to the control group (Figure 7M). In the MCP-1 group, first signs of elastin were seen in the Verhoeff van Giesson-stained slides in 3 out of 4 rats after 84 days. In the control group only 1 out of 4 rats stained positive (Figure 7G-I).

V. Myofibroblasts Do Not Originate From Endothelial-To-Mesenchymal Transdifferentiation

All explants were analyzed for occurrence of endothelial-to-mesenchymal transdifferentiation

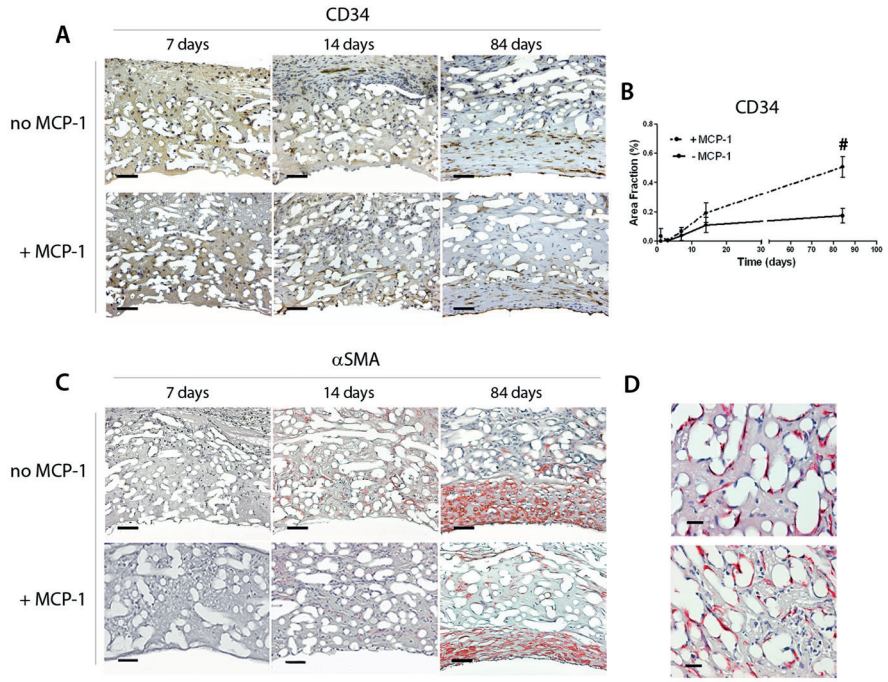

FIG. 6. Infiltration of tissue cells. Histological evaluation of transections of the center part of the grafts demonstrates an increase in CD34+ cells over time in both groups, with a significantly elevated CD34 expression in the MCP-1 group at day 84 (0.5 – 0.1 vs. 0.2 – 0.01 per hpf) (A, B). First α-SMA expression was detected at day 7 in both groups, forming an organized medial layer at 3 months follow-up (C). (D) High-magnification images of α-SMA expression at day 14, revealing α-SMA+ cells aligned with the PCL fibers, visible in white. Scale bars represent 50 mm (A, C) and 20 mm (D). #p < 0.001.

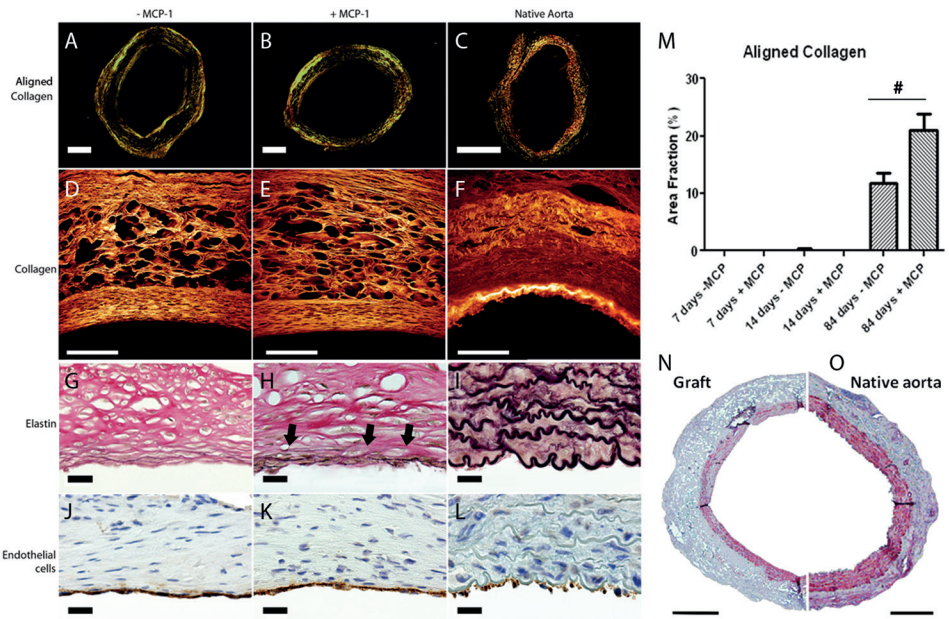

FIG. 7. Tissue organization. Implanted grafts show similarities to the native rat aorta after 84 days. Collagen (PSR staining, polarized light) content in grafts without MCP-1 (A), grafts with MCP-1 (B), and in a native rat aorta (C). Collagen (PSR staining, confocal microscopy) in grafts without MCP-1 (D), grafts with MCP-1 (E), and in a native rat aorta (F). Elastin in grafts without MCP-1 (G), grafts with MCP-1 (H), and in a native rat aorta (I). Endothelial cell (EC) lining (von Willebrand factor) in grafts without MCP-1 (J), grafts with MCP-1 (K), and native rat aorta (L). Collagen alignment was significantly higher in the +MCP-1 group after 84 days (21 – 2.9 vs. 11.9 – 1.7 area fraction per hpf) (M). Smooth muscle cell lining in the graft (N) and native aorta (O). Scale bars represent 500 mm (A–C), 100 mm (D–F), 500 mm (N), 200 mm (O), and 20 mm (G–L). Arrows indicate elastin fibers (H). #p < 0.001.

(endoMT) using immunofluorescent double-staining of vWF and α-SMA. No co-localization of vWF and α-SMA was detected in any of the explants of all time points, apart from a single cell showing co-localization of vWF and α-SMA at the 14-days time point, indicating possible endoMT (Figure 8).

Discussion

In situ tissue engineering of vascular grafts using synthetic scaffolds could deliver an off-the-shelve alternative to current vascular prostheses. In the context of clinical translation, we aimed to achieve an early attraction of circulating cells into a graft releasing MCP-1, using a novel rat model that prevents transanastomotic pannus overgrowth, as well as periadventitial ingrowth. Our results demonstrate that (i) extracellular matrix-producing cells can be recruited from the circulation, and that (ii) increased early monocyte recruitment to the graft by MCP-1 has a positive effect on long-term tissue remodeling and regeneration. Grafts underwent extensive cellularization by blood-derived cells followed by tissue formation throughout the entire PCL graft, with all grafts remaining patent up to 3 months follow-up, without signs of aneurysms or intimal hyperplasia. Driven by early MCP-1 release, our remodeled synthetic graft showed several similarities to the native aorta after 3 months in vivo; the intimal layer with EC lining the lumen, with early signs of a developing elastic lamina, and a medial layer consisting of SMC in an aligned collagen matrix.

Ingrowth of host cells into vascular implants in rodent models is typically dominated by two mechanisms: transmural (mainly macrophages and α-SMA-expressing cells) and transanastomotic infiltration (EC and SMC) (16–19). The infiltration of cells via these routes is typically rapid and progressive and may obscure any contribution of fallout healing when using these animal models. However, the consistent observation that transanastomotic cell ingrowth,

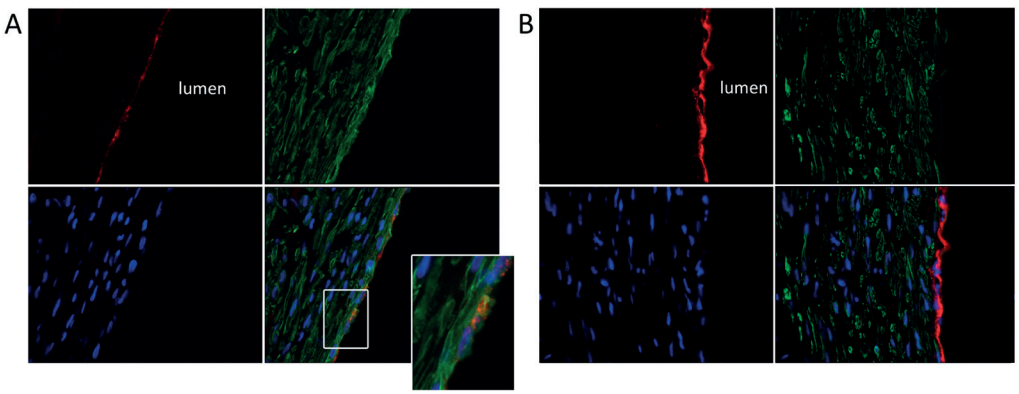

FIG. 8. Endothelial-to-mesenchymal transdifferentiation (EndoMT) analysis. Recruited ECs did not undergo EndoMT. Representative images at 14 (A) and 84 days (B) of immunofluorescent double staining of vWF (red) and α-SMA (green) with cell nuclei in blue (DAPI). Rare colocalization of vWF and α-SMA was detected (A).

in particular, is limited in humans, makes that such rodent models may have limited predictive value for the clinical outcome, and the importance of a transanastomotic isolation model has been advocated previously (20,21). Moreover, since recruitment of blood-derived cells represents a valuable target for colonization of a-cellular grafts, this study was specifically aimed at isolating the role of circulating cells in the regenerative process (fallout healing) of a degradable vascular graft from transmural and transanastomotic events. The impermeable circumferential Gore-Tex sheathing as applied in the current study effectively isolated the periadventitial foreign body response from the porous PCL graft, preventing the excessive infiltration of α-SMA+ cells. In addition, we constrained progressive transanastomotic overgrowth using dense anastomotic Gore-Tex patches. Gore-Tex is a type of expanded polytetrafluoroethylene (ePTFE), which has been used extensively in vivo for several decades. When employed as vascular grafts, varying endothelial outgrowth rates have been reported, ranging from virtually absent up to as high as 0.2 mm/day, dependent on the model and materials used (22,23). Recently, a vascular loop-graft model was proposed to overcome the limited space in the infra-renal rat aorta, employing lengthy ePTFE segments to shield transanastomotic ingrowth (21). However, cell overgrowth on Gore-Tex substrates is known to be highly dependent on the microstructure of the material used. Golden et al. demonstrated pore size-dependent healing of ePTFE grafts in a baboon model, and they suggest a sharp threshold of pore size (intermodal distance between 30 and 60 μm) below which healing is abrogated in this animal model (24). Based on these reports, we opted for a type of Gore-Tex with extremely low porosity (internodal distance < 1μm), which has shown to hamper tissue integration as it does not facilitate cell adhesion on its surface (25). Consequently, this would provide a sufficient barrier to isolate the porous PCL graft from the native artery, even over a small distance. The FISH analysis of sex-mismatched implants confirms that the Gore-Tex shielding effectively hampered transanastomotic ingrowth in our model, despite the limited width of the barriers. To the best of our knowledge, this is the first small-animal model to effectively hamper both transmural and transanastomotic cell ingrowth in order to study purely the role of circulating cells, which is important for clinical translation and personalized application, for example via pre-operative boosting of specific cell populations in the circulatory system.

The most obvious contribution of circulatory cells to the regenerative process is attributed to peripheral immune cells. It is well-recognized that monocytes and macrophages are the predominant effector cells mediating wound healing and repair in response to injury or infection (8,26,27). Monocyte and macrophage trafficking was shown to be dependent on MCP-1 and its primary receptor CCR2 (28,29). Exogenous MCP-1 delivery has been shown to increase monocyte/macrophage recruitment and induce angiogenesis (30). Moreover, the use of MCP-1 in our scaffolds was motivated by previous findings demonstrating an enhanced secretion of MCP-1 by bone marrow-derived mononuclear cells when in interaction with immune cells (15,31). MCP-1 is a potent chemoattractant of various types of immune cells and, consequently, the burst-release of MCP-1 in the present study resulted in an increased early influx of leukocytes. This was also reflected in gene expression data (Supplementary Figure S2), leading to improved

tissue formation in the later stage. Prolonged upregulation of MCP-1 has been related to systemic complications, such as fibrosis and atherosclerosis (32). Therefore, we opted for a rapid release of MCP-1 from our scaffold to induce a favorable initial cellular response. The MCP-1 dose was determined from previous in vitro experiments (33). No systemic upregulation of MCP-1 was detected in the peripheral blood of the rats despite peak measurements at day 1 (Supplementary Figure S1).

Macrophage function during inflammation and healing is governed by polarization state (33). Unexpectedly, we detected only very sparse expression of CD163, a typical surface marker for the M2 macrophage type that was reported in previous findings (9,14). However, on gene level, we did observe indications which suggest a shift in macrophage polarization in response to MCP-1 (Supplementary Figure S2). Additionally, peripheral-derived macrophages have been shown to acquire myofibroblast-like characteristics during the foreign body response in rodents (34,35). The observed absence of coexpression of vWF and α-SMA, suggests that the process of endoMT was virtually absent during the in vivo timeframe of the current study, implicating that the vast majority of α-SMA+ myofibroblasts did not originate from recruited EC via endoMT. Taking into account that transmural and transanastomotic infiltration of mature SMC was hampered, combined with the apparent absence of endoMT, it is plausible that the infiltrating blood-derived α-SMA+ cells descent directly from transdifferentiated macrophages.

In addition to peripheral leukocytes, circulating progenitor cells may contribute to vascular regeneration in terms of endothelialization as well as extracellular matrix production. Blood stream-derived cellularization of vascular grafts was proven in dogs, represented by patchy endothelial coverage with underlying α-SMA+ SMC (36,37). Immunohistochemical characterization of infiltrated cells in our grafts demonstrates an increasing presence of CD34+ cells over time, with a significant upregulation in the MCP-1 group. CD34 is expressed by various circulating progenitor populations, including fibrocytes, which can differentiate into mature myofibroblasts upon activation by transforming growth factor-β and via cross-talk with macrophages (38,39). On gene level, this coincided with a trend in upregulation of Stromal cell-Derived Factor-1α (SDF-1α), which is a known attractant for CD34+ progenitor cells (40) (Supplementary Figure S2). MCP-1 has been shown to mobilize angiogenic monocytes (41,42), which may be responsible for the increased SDF-1α expression and secondary recruitment of progenitors. The burst-release of exogenous MCP-1 in the present study led to a remarkable effect on downstream events up to 3 months later, ignited by an increased early influx of leukocytes. Although the exact chain-of-events between the early and late-term observations in this study remains to be clarified, our results suggest that MCP-1-recruited monocytes/macrophages have a dual role; indirectly by creating a biochemical milieu favorable for attraction of secondary progenitor cells, and directly via possible contribution of macrophage-to-myofibroblast transdifferentiation.

The rat model used in this study enables us to study the colonization of grafts by circulating

cells, which is particularly relevant for the human situation. However, for clinical translation, it should be considered that the populations of specific cell types in the blood stream (e.g. monocyte subsets, progenitor cells) is highly variable between patients. Normal biological patient-to-patient variability, as well as age and comorbidities will result in dissimilarities in the immunological and regenerative competence between patients (44–46). The use of the current methodology in a diseased animal model, in combination with mechanistic studies in human in vitro models will be a valuable contribution to the understanding of the regenerative potential of circulating cells in various clinical settings.

In conclusion, the results of the current study prove the in situ regenerative potential of circulating cells in rats. In these conditions, relevant for the human situation, a short local burst of exogenous MCP-1 led to improved, or at least accelerated neotissue formation and organization, with a layered structure of intimal endothelium and a medial layer of SMC in an oriented collagen matrix with elastin fibers. These findings represent a valuable contribution in the clinical translation towards the development of safe and effective synthetic grafts for in situ tissue engineering.

Acknowledgements

The authors would like to thank Marc Simonet and Dr. Anand Nandakumar (Xeltis B.V.) for their contribution to the electrospinning of the tubular scaffolds. This research forms part of the iValve project of the research program of the BioMedical Materials institute, co-funded by the Dutch Ministry of Economic Affairs. The financial contribution of the Nederlandse Hartstichting is gratefully acknowledged.

Author Disclosure Statement

No competing financial interests exist.

References

1. Nichols, M., Townsend, N., Scarborough, P., Luengo-Fernandez, R., Leal, J., Gray, A., et al. European Cardiovascular Disease Statistics 2012. Brussels:, 2012.
2. Norgren, L., Hiatt, W., Dormandy, J., Nehler, M., Harris, K., and Fowkes, F. Inter-Society Consensus for the Management of Peripheral Arterial Disease (TASC II). J Vasc Surg. 45 Suppl S, S5, 2007.
3. Peck, M., Gebhart, D., Dusserre, N., McAllister, T.N., and L'Heureux, N. The evolution of vascular tissue engineering and current state of the art. Cells Tissues Organs. 195, 144, 2012.
4. Cleary, M., Geiger, E., Grady, C., Best, C., Naito, Y., and Breuer, C. Vascular tissue engineering: the next generation. Trends Mol Med. 18, 394, 2012.

5. Mol, A., Smits, A.I.P.M., Bouten, C.V.C., and Baaijens, F.P.T. Tissue engineering of heart valves: advances and current challenges. Expert Rev. Med. Devices. 6, 259, 2009.
6. Bouten, C.V.C., Dankers, P.Y.W., Driessen-Mol, A., Pedron, S., Brizard, A.M., and Baaijens, F.P.T. Substrates for cardiovascular tissue engineering. Adv Drug Deliv Rev. 63, 221, 2011.
7. Mahler, G.J., and Butcher, J.T. Inflammatory regulation of valvular remodeling: the good(?), the bad, and the ugly. Int. J. Inflam. 2011, 721419, 2011.
8. Van Loon, S.L.M., Smits, A.I.P.M., Driessen-Mol, A., Baaijens, F.P.T., and Bouten, C.V.C. The immune response in in situ tissue engineering of aortic heart valves. In: Aikawa, E., editor. Calcif. Aortic Valve Dis. Rijeka: InTech, pp. 207–45, 2013.
9. Wu, W., Allen, R., and Wang, Y. Fast-degrading elastomer enables rapid remodeling of a cell-free synthetic graft into a neoartery. Nat Med. 18, 1148, 2012.
10. Yokota, T., Ichikawa, H., Matsumiya, G., Kuratani, T., Sakaguchi, T., Iwai, S., et al. In situ tissue regeneration using a novel tissue-engineered, small-caliber vascular graft without cell seeding. J. Thorac. Cardiovasc. Surg. 136, 900, 2008.
11. Brennan, M.P., Dardik, A., Hibino, N., Roh, J.D., Nelson, G.N., Papademitris, X., et al. Tissue-engineered vascular grafts demonstrate evidence of growth and development when implanted in a juvenile animal model. Ann. Surg. 248, 370, 2008.
12. Mrówczyński, W., Mugnai, D., De Valence, S., Tille, J.C., Khabiri, E., Cikirikcioglu, M., et al. Porcine carotid artery replacement with biodegradable electrospun poly-e-caprolactone vascular prosthesis. J. Vasc. Surg. 59, 210, 2014.
13. De Valence, S., Tille, J.-C., Mugnai, D., Mrowczynski, W., Gurny, R., Möller, M., et al. Long term performance of polycaprolactone vascular grafts in a rat abdominal aorta replacement model. Biomaterials. 33, 38, 2012.
14. Hibino, N., Yi, T., Duncan, D.R., Rathore, A., Dean, E., Naito, Y., et al. A critical role for macrophages in neovessel formation and the development of stenosis in tissue-engineered vascular grafts. FASEB J. 25, 4253, 2011.
15. Roh, J.D., Sawh-Martinez, R., Brennan, M.P., Jay, S.M., Devine, L., Rao, D., et al. Tissue-engineered vascular grafts transform into mature blood vessels via an inflammation-mediated process of vascular remodeling. Proc. Natl. Acad. Sci. U. S. A. 107, 4669, 2010.
16. Van der Lei, B., Wildevuur, C.R., Nieuwenhuis, P., Blaauw, E.H., Dijk, F., Hulstaert, C.E., et al. Regeneration of the arterial wall in microporous, compliant, biodegradable vascular grafts after implantation into the rat abdominal aorta. Ultrastructural observations. Cell Tissue Res. 242, 569, 1985.
17. Zhang, Z., Wang, Z., Liu, S., and Kodama, M. Pore size, tissue ingrowth, and endothelialization of small-diameter microporous polyurethane vascular prostheses. Biomaterials. 25, 177, 2004.
18. Martakos, P., and Karwoski, T. Healing characteristics of hybrid and conventional polytetrafluoroethylene vascular grafts. ASAIO J. 41, M735, 1995.
19. Hibino, N., Villalona, G., Pietris, N., Duncan, D.R., Schoffner, A., Roh, J.D., et al. Tissue-engineered vascular grafts form neovessels that arise from regeneration of the adjacent

blood vessel. FASEB J. 25, 2731, 2011.
20. Zilla, P., Bezuidenhout, D., and Human, P. Prosthetic vascular grafts: wrong models, wrong questions and no healing. Biomaterials. 28, 5009, 2007.
21. Pennel, T., Zilla, P., and Bezuidenhout, D. Differentiating transmural from transanastomotic prosthetic graft endothelialization through an isolation loop-graft model. J. Vasc. Surg. 58, 1053, 2013.
22. Robinson, P.H., Bartels, H.L., and van der Lei, B. Patency and healing of 10-cm long microarterial polytetrafluoroethylene prostheses in the rat abdominal aorta. J. Reconstr. Microsurg. 5, 331, 1989.
23. Clowes, A.W., Kirkman, T.R., and Reidy, M. Mechanisms of arterial graft healing. Rapid transmural capillary ingrowth provides a source of intimal endothelium and smooth muscle in porous PTFE prostheses. Am. J. Pathol. 123, 220, 1986.
24. Golden, M.A., Hanson, S.R., Kirkman, T.R., Schneider, P.A., and Clowes, A.W. Healing of polytetrafluoroethylene arterial grafts is influenced by graft porosity. J Vasc Surg. 11, 838, 1990.
25. Leprince, P., Rahmati, M., Bonnet, N., Bors, V., Rama, A., Léger, P., et al. Expanded polytetrafluoroethylene membranes to wrap surfaces of circulatory support devices in patients undergoing bridge to heart transplantation. Eur. J. Cardiothorac. Surg. 19, 302, 2001.
26. Wong, K.L., Yeap, W.H., Tai, J.J.Y., Ong, S.M., Dang, T.M., and Wong, S.C. The three human monocyte subsets: implications for health and disease. Immunol. Res. 53, 41, 2012.
27. Brancato, S.K., and Albina, J.E. Wound macrophages as key regulators of repair: origin, phenotype, and function. Am J Pathol. 178, 19, 2011.
28. Willenborg, S., Lucas, T., van Loo, G., Knipper, J., Krieg, T., Haase, I., et al. CCR2 recruits an inflammatory macrophage subpopulation critical for angiogenesis in tissue repair. Blood. 120, 613, 2012.
29. Shi, C., and Pamer, E.G. Monocyte recruitment during infection and inflammation. Nat Rev Immunol. 11, 762, 2011.
30. Voskuil, M., van Royen, N., Hoefer, I.E., Seidler, R., Guth, B.D., Bode, C., et al. Modulation of collateral artery growth in a porcine hindlimb ligation model using MCP-1. Am. J. Physiol. Heart Circ. Physiol. 284, H1422, 2003.
31. Ballotta, V., Smits, A.I.P.M., Driessen-Mol, A., Bouten, C.V.C., and Baaijens, F.P.T. Synergistic protein secretion by mesenchymal stromal cells seeded in 3D scaffolds and circulating leukocytes in physiological flow. Biomaterials. 35, 9100, 2014.
32. Niu, J., and Kolattukudy, P.E. Role of MCP-1 in cardiovascular disease: molecular mechanisms and clinical implications. Clin. Sci. (Lond). 117, 95, 2009.
33. Smits, A.I.P.M., Ballotta, V., Driessen-Mol, A., Bouten, C.V.C., and Baaijens, F.P.T. Shear flow affects selective monocyte recruitment into MCP-1-loaded scaffolds. J. Cell. Mol. Med. 18, 2176, 2014.
34. Brown, B.N., Ratner, B.D., Goodman, S.B., Amar, S., and Badylak, S.F. Macrophage polarization: an opportunity for improved outcomes in biomaterials and regenerative medicine. Biomaterials. 33, 3792, 2012.

35. Mooney, J.E., Rolfe, B.E., Osborne, G.W., Sester, D.P., van Rooijen, N., Campbell, G.R., et al. Cellular plasticity of inflammatory myeloid cells in the peritoneal foreign body response. Am. J. Pathol. 176, 369, 2010.
36. Jabs, A., Moncada, G., Nichols, C.E., Waller, E.K., and Wilcox, J.N. Peripheral blood mononuclear cells acquire myofibroblast characteristics in granulation tissue. J. Vasc. Res. 42, 174, 2005.
37. Shi, Q., Wu, M.H., Hayashida, N., Wechezak, A.R., Clowes, A.W., and Sauvage, L.R. Proof of fallout endothelialization of impervious Dacron grafts in the aorta and inferior vena cava of the dog. J Vasc Surg. 20, 546, 1994.
38. Kouchi, Y., Onuki, Y., Wu, M.H., Shi, Q., Ghali, R., Wechezak, A.R., et al. Apparent blood stream origin of endothelial and smooth muscle cells in the neointima of long, impervious carotid-femoral grafts in the dog. Ann. Vasc. Surg. 12, 46, 1998.
39. Mesure, L., De Visscher, G., Vranken, I., Lebacq, A., and Flameng, W. Gene expression study of monocytes/macrophages during early foreign body reaction and identification of potential precursors of myofibroblasts. PLoS One. 5, e12949, 2010.
40. Reilkoff, R., Bucala, R., and Herzog, E.L. Fibrocytes: emerging effector cells in chronic inflammation. Nat Rev Immunol. 11, 427, 2011.
41. Chavakis, E., Urbich, C., and Dimmeler, S. Homing and engraftment of progenitor cells: a prerequisite for cell therapy. J Mol Cell Cardiol. 45, 514, 2008.
42. Rehman, J., Li, J., Orschell, C.M., and March, K.L. Peripheral blood "endothelial progenitor cells" are derived from monocyte/macrophages and secrete angiogenic growth factors. Circulation. 107, 1164, 2003.
43. Fujiyama, S., Amano, K., Uehira, K., Yoshida, M., Nishiwaki, Y., Nozawa, Y., et al. Bone marrow monocyte lineage cells adhere on injured endothelium in a monocyte chemoattractant protein-1-dependent manner and accelerate reendothelialization as endothelial progenitor cells. Circ. Res. 93, 980, 2003.
44. Seidler, S., Zimmermann, H.W., Bartneck, M., Trautwein, C., and Tacke, F. Age-dependent alterations of monocyte subsets and monocyte-related chemokine pathways in healthy adults. BMC Immunol. 11, 30, 2010.
45. Jie, K.E., Goossens, M.H.J., van Oostrom, O., Lilien, M.R., and Verhaar, M.C. Circulating endothelial progenitor cell levels are higher during childhood than in adult life. Atherosclerosis. 202, 345, 2009.
46. Shantsila, E., Wrigley, B.J., Shantsila, a, Tapp, L.D., Gill, P.S., and Lip, G.Y.H. Monocyte-derived and CD34+/KDR+ endothelial progenitor cells in heart failure. J. Thromb. Haemost. 10, 1252, 2012.

Supplemental Material

Detailed Methods

Experimental animals

Seventy-six healthy Sprague Dawley rats, 250-300 gram were used, purchased from Harlan Laboratories. Each animal was fed ad libitum and was housed in groups in an environment maintained at room temperature for 24 hours a day and with a light: dark cycle of 12:12 hours. Rats were divided in two study groups. Study group 1 was dedicated to validate the model, comparing Gore-Tex shielded grafts (n=12) to grafts without shielding (n=12). To study general cell infiltration in both groups over time, grafts were explanted at 1 day (n=2), 3 days (n=2), 1 week (n=2), 2 weeks (n=2) and 3 months (n=4). To specifically study the efficacy of the model in transanastomotic shielding, a sex-mismatch experiment was performed, in which sections of male rat aorta were interpositioned proximally and distally to the graft in female rats, either shielded or unshielded with Gore-Tex (n=12). These grafts were explanted after 1 or 3 months (n=3 per group, per time point) for fluorescent in situ hybridization (FISH) analysis. Study group 2 was dedicated to study the effect of MCP-1, comparing fibrin-seeded grafts with incorporated MCP-1 (n=20) versus fibrin-seeded controls (n=20). All grafts in this study group were shielded with Gore-Tex. Grafts were explanted at 1 day, 3 days, 1 week, 2 weeks and 3 months (n=4 per time point). All procedures were performed in accordance with and approved by the Institutional Animal Care and Use Committee of the University of Utrecht, the Netherlands.

Scaffold Fabrication

Electrospun poly(ε-caprolactone) (PCL) tubular scaffolds were manufactured and provided by Xeltis BV. In brief, PCL (Purasorb; Purac Biochem) was dissolved in chloroform at 20% (w/w), and driven through a horizontally fixed nozzle at high voltage (15 kV) toward a grounded rotating cylindrical copper target (Ø 2 mm) at 15 cm distance. The resulting tube diameter, wall thickness and average fiber diameter were determined with scanning electron microscopy (SEM; Quanta 600F, Fei). The materials were sterilized by gamma irradiation. Before implantation, the PCL tube was cut to size and filled with fibrin gel (5 U/ml thrombin + 5 mg/ml fibrinogen (Sigma)). Depending on the test group, MCP-1 (4 µg/ml; Chemicon) was added to the fibrin solution. To measure the release rate of the MCP-1 from the graft, a cumulative leakage experiment was performed in vitro. For this, MCP-1-loaded scaffold samples were incubated in culture medium (RPMI-1640, Sigma), supplemented with 10% (v/v) fetal bovine serum (FBS Gold, PAA Laboratories) over a period of 7 days. At each time point (0, 0.75, 1.5, 3, 8, 24, 48, 72, 120, 168 hours), all supernatant was collected, replaced with fresh medium, and samples were stored at -80 °C until further analysis. MCP-1 content was determined cumulatively using a human ELISA kit, according to manufacturer's protocol (RayBiotech) (n=3).

Surgical Procedure

Prior to implantation, graft composites were prepared depending on study group. To shield the electrospun grafts, an end-to-end anastomosis was made to a 4x10 mm^2 impenetrable Gore-Tex strip (Preclude Pericardial Membrane; Gore Medical) using 10-0 interrupted sutures, distally and proximally of the electrospun tube. Additionally, Gore-Tex was wrapped around the PCL in samples creating an impenetrable outer layer (Figure 1B). For the FISH experiments, an additional end-to-end anastomosis was made to a segment of male aorta, distally and proximally of the Gore-Tex (for shielded samples) or directly anastomosed to the graft (for unshielded controls). Animals were anesthetized using Isoflurane gas. Once adequate anesthesia was achieved, a midline laparotomy was performed and the abdominal viscera were lateralized for exposure of the abdominal aorta and the inferior vena cava. After separation of the aorta from the inferior vena cava and surrounding tissue, the segment of the abdominal aorta between the renal arteries and the aortic bifurcation was occluded with microvascular clamps. The aorta was transected and the graft composite was introduced with end-to-end anastomosis performed at both the proximal and distal ends using interrupted sutures. After removing the vascular clamps, the pulsatile flow was confirmed in the aorta distal to the graft (Figure 1A, D). The abdomen was closed in two layers. Immediately after implantation, all scaffolds were exposed to arterial hemodynamic conditions. There was no heparin administration during or after surgery. Animals recovered on warmed pads to promote blood flow through the grafts. Before rats returned to their cages, they were assessed for evidence of hind limb paralysis or acute graft thrombosis. Post-operative Buprenorphine was given intraperitoneal.

At termination, animals were anaesthetized using Isoflurane. Tubes were prepared free from surrounding tissue. The Gore-tex on the outer layer was opened the PCL graft was carefully explanted. All explants were examined with immunohistochemistry. In study group 2, two explants per time point were additionally analyzed with qPCR and ELISA to determine systemic protein levels in the blood serum.

MCP-1 Blood Serum Levels

Blood samples were collected at time of explantation to determine MCP-1 protein levels in the blood serum. The MCP-1 concentrations were measured using a rat MCP-1 ELISA kit (RayBiotech), according to the manufacturer's protocol (n=2 for each time point).

Gene Expression Analysis

Explanted tissue grafts were collected in Trizol (TRIzol, Invitrogen) (n=2 for each time point). Samples where homogenized using shakebeads in a Precellys 24 tissue homogenizer (Bertin Technologies). Total RNA was isolated using TRIzol isolation according to the manufacturer's protocol. cDNA was synthesized using iScript (Bio-Rad), according to the manufacturers

protocol. qPCR was performed for the genes interleukin-23, -12, -10, -2 (IL23, IL12, IL10, IL2, respectively), inducible nitric oxide synthase (iNOS), arginase-I (ArgI), MCP-1, and stromal cell-derived factor 1α (SDF-1α), using primers listed in Table S1. Data was analyzed using the delta-delta CT method, corrected for GAPDH expression. Data was normalized per group on the first time point to assess changes in gene expression over time for individual groups. To compare gene expression levels between the different groups, the +MCP-1 data was normalized on the control group per time point.

Immunohistochemistry

Explants were fixed in formalin 10% before pre-embedding in 1% (w/v) agar (Eurogentec), followed by embedding in paraffin. Consecutive 4 μm sections were stained with Mayer's hematoxylin and eosin (H&E), Elastin van Gieson and 0.1% (w/v) Sirius red F3B (Gurr BDH) in saturated picric acid solution, respectively. Immunohistochemical stainings were performed on 4 μm sections after deparaffinization and dehydration. Sections were stained for myeloperoxidase (MPO; Dako, A398, 1:2000), CD68 (Serotec, MCA341GA, 1:400) CD163 (Serotec, MCA-342GA, 1:75), CCR7 (Cell Applications, CG1678, 1:15000), CD34 (R&D Systems, AF4117, 1:100), alpha- smooth muscle actin (α-SMA; Sigma, A2547, 1:32000), and Von Willebrand Factor (vWF; Dako, A0082, 1:1600). All antibodies were diluted in PBS/BSA/Azide. Following deparaffinization, antigen retrieval was performed in citrate (For CD68, CCR7, and MPO), pepsin (CD163), or EDTA (vWF), before blocking with 10% normal goat serum (α-SMA and CCR7) or Ultra V block (MPO; Thermo Scientific). Sections were blocked for endogenous peroxidase when a HRP-conjugated secondary antibody was used. Appropriate BrightVision signal amplification was used for labeling of primary antibody binding sites: Poly AP anti-mouse for α-SMA, poly HRP anti-mouse (CD68 and CD163), and poly HRP anti-rabbit (CCR7, MPO, and vWF) (Immunologic). Slides were subsequently incubated with liquid permanent red substrate-chromogen (Dako) or diaminobenzidine substrate-chromogen (Sigma) and counterstained with Mayer's hematoxylin. Slides were dehydrated in alcohol changes and coverslipped using pertex. Double-label immunohistochemistry for α SMA and vWF was performed after EDTA-antigen retrieval by incubating sections for 1 hour at room temperature with a mix of 1:32,000 mouse anti- α-SMA and 1:1600 rabbit anti-vWF antibodies. The sections were then incubated with anti-mouse Alexa Fluor 488 and anti-rabbit Alexa Fluor 555 conjugated secondary antibodies (Invitrogen, 1:200) for 30 minutes. Cell nuclei were counterstained with DAPI.

Quantitative Histologic and Immunohistological Analysis

Two investigators, who were blinded to the investigated groups and the time point of explantation, independently conducted analysis. Sections were photographed using a Nikon E800 microscope with ACT-1 software. For the quantification of wall thickness and lumen diameter, each slide was studied under 2x objective lens. Cellularity was studied under high-power magnification (high- power field (hpf), 40x objective lens; area comprising 0.034 mm2). The total number

of cells in 4 random hpf areas per PCL tube was manually counted using ImageJ software. Quantification of aligned collagen was performed with picrosirius red stains and circularly polarized light. Stained sections were digitally photographed and converted into gray-value images and regions of interest (ROI) were drawn lining the graft. The average gray value per ROI was calculated using ImageJ software. A quantitative analysis of the immunopositive cells of each stained slide was performed at 4 random hpfs. The portion of area staining positively for the marker within the 4 hpfs was counted and summed for each image. The mean of the sums for 4 high power images was then calculated for each sample. Area of positive staining was measured as a percentage of the total from binarised images.

Fluorescent In situ Hybridization (FISH)

To identify X- and Y-chromosomes, FISH was performed on fresh sectioned paraffin sections using Rat idetect Chr X FISH Probe Green and Chr Y FISH Paint Probe Red (ID Labs, IDRF1067 and IDRR1070, respectively). Following deparaffinization, slides were pretreated with 0.2N HCl for 20 min at room temperature, citrate buffer (pH 6.0) for 20 min at 100 °C, and digested with 0.1% proteinase K for 10 min at 37 °C. After dehydration in graded ethanol, 7.5 µl of probe mixture was added. Sections were then denatured for 5 min at 69 °C, cooled on ice for 5 min, and hybridized overnight at 37 °C in a ThermoBrite. The next day, slides were washed in 0.4x SSC/0.3% NP-40 at 73 °C, 2x SSC/0.1% NP-40 at room temperature, and 2x SSC for 2, 1, and 5 min, respectively. After washing, the sections were counterstained with DAPI, dehydrated and mounted in Vectashield (Vectorlabs, H-1000). To quantification the FISH results, at least 30 images per sample were analyzed by two investigators, blinded to the experimental group, sample location and time of implantation.

Statistical Analysis

Statistical differences were determined using a student's T test or a Mann-Whitney test for non- parametric data using GraphPad Prism software. $P < 0.05$ was considered statistically significant.

Table S1. Genes analyzed by qPCR.

Gene	function	expressed by	Forward Primer Sequence	Reverse Primer Sequence
MCP1	attraction of monocytes	monocytes, macrophages, dendritic cells	aagtgaccagtatgacagagaac	tctacatcttgcatttaaggatt
SDF1α	attraction of progenitor cells	expressed in response to tissue damage	atttttgtgcacttttatgttt	acactactatggcttctcttcaa
iNOS	inducible production of nitrous oxide	Endothelium	cagaagcacaaagtcacaga	gtccttttcctctttcaggt
Arg2	regulation of vasodilatation	smooth muscle, macrophages	cgtgtatcctcgctcagtgg	ctgtagccacctgacacagc
IL 23	inflammatory response	macrophages, dendritic cells	gctcctccagccagaggatcacc	gccactgctggctgggactc
IL12	inflammatory response	macrophages, dendritic cells	gcagcagcagttcccctgagt	cctcggcagttgggcaggtg
IL2	development of T Cells	T cells	taaaactaaagggctctgaaaac	ttactgagtcattgttgagatga
IL10	anti-inflammatory response	monocytes	ttttaataagctccaagacaaag	gttcaatttttcattttgagtgt

Figure S1. Systemic MCP-1 concentrations. No apparent differences in serum levels of MCP- 1 were detected between groups.

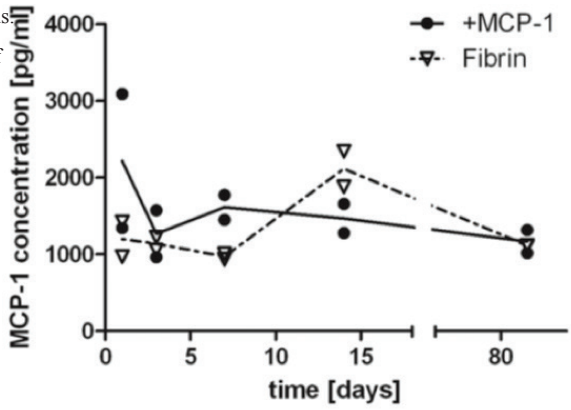

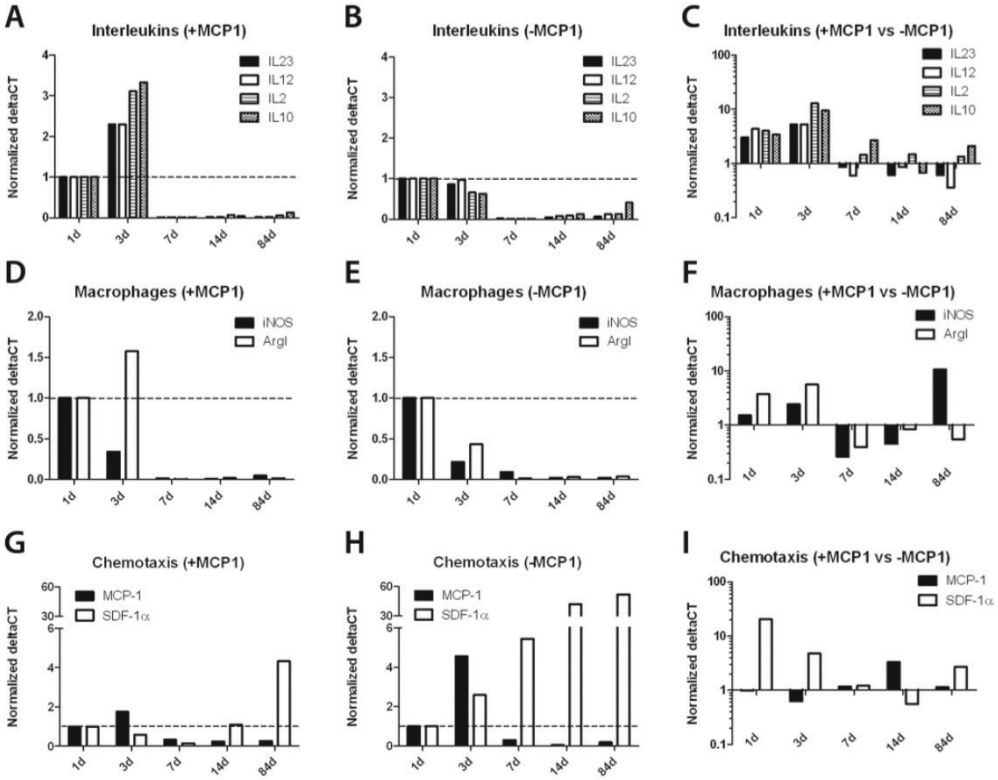

Figure S2. Gene expression as determined with qPCR. (A-C) Expression of pro- inflammatory (IL23 and IL12) and anti-inflammatory (IL2 and IL10) interleukins in the MCP-1 group (A), control group (B), and in direct comparison of the MCP-1 versus control (C). (D-F) Expression of macrophage subset markers iNOS (M1 type) and ArgI (M2 type) in the MCP-1 group (D), control group (E), and in direct comparison of the MCP-1 versus control (F). (G-I) Expression of chemotactic cytokines MCP-1 and SDF-1α in the MCP-1 group (G), control group (H), and in direct comparison of the MCP-1 versus control (I). To analyze variations in gene expression levels over time, data was normalized on the day 1 data per group. Data represent mean value of 2 data points (A-B, D-E and G-H). To compare gene expression levels of the MCP-1 group versus the control group, the MCP-1 data was normalized on the control group per individual time point. Data was plotted on a logarithmic scale with a value of 1 representing the control sample (C, F, I).

VII

Early in-situ cellularization of a supramolecular vascular graft is modified by synthetic stromal cell-derived factor-1a derived peptides

(Published in Biomaterials)

Dimitri E.P. Muylaert

Geert C. van Almen

Hanna Talacua

Joost O. Fledderus

Jolanda Kluin

Simone I.S. Hendrikse

Joost L.J. van Dongen

Eline Sijbesma

Anton W. Bosman

Tristan Mes

Shraddha H. Thakkar

Anthal I.P.M. Smits

Carlijn V.C. Bouten

Patricia Y.W. Dankers

and Marianne C. Verhaar

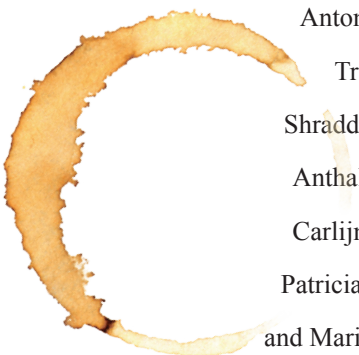

Abstract

In an in-situ approach towards tissue engineered cardiovascular replacement grafts, cell-free scaffolds are implanted that engage in endogenous tissue formation. Bioactive molecules can be incorporated into such grafts to facilitate cellular recruitment. Stromal cell derived factor 1α (SDF1α) is a powerful chemoattractant of lymphocytes, monocytes and progenitor cells and plays an important role in cellular signaling and tissue repair. Short SDF1α-peptides derived from its receptor-activating domain are capable of activating the SDF1α–specific receptor CXCR4. Here, we show that SDF1α-derived peptides can be chemically modified with a supramolecular four-fold hydrogen bonding ureido-pyrimidinone (UPy) moiety, that allows for the convenient incorporation of the UPy- SDF1α-derived peptides into a UPy-modified polymer scaffold. We hypothesized that a UPy-modified material bioactivated with these UPy-SDF1α-derived peptides can retain and stimulate circulating cells in an anti-inflammatory, pro-tissue formation signaling environment. First, the early recruitment of human peripheral blood mononuclear cells to the scaffolds was analyzed in vitro in a custom-made mesofluidic device applying physiological pulsatile fluid flow. Preferential adhesion of lymphocytes with reduced expression of inflammatory factors TNFα, MCP1 and lymphocyte activation marker CD25 was found in the bioactivated scaffolds, indicating a reduction in inflammatory signaling. As a proof of concept, in-vivo implantation of the bioactivated scaffolds as rat abdominal aorta interposition grafts showed increased cellularity by CD68+ cells after 7 days. These results indicate that a completely synthetic, cell-free biomaterial can attract and stimulate specific leukocyte populations through supramolecular incorporation of short bioactive SDF1α derived peptides.

Introduction

Replacement of small diameter blood vessels relies mainly on autologous tissue, which is often limited by availability and requires invasive harvesting. Common non-living prostheses for vascular structures have considerable drawbacks such as high risk of occlusion, lack of growth potential, the consequent need for re-operation in pediatric patients, and life-long anti-coagulation therapy[1]. In an in situ tissue engineering approach, synthetic scaffolds are implanted that provide the necessary mechanical support. Ideally, scaffold material will contain bioactive molecules capable of instructing cells of the recipient to migrate into the graft and stimulate the development of living, growing tissue[2]. Molecules involved in cellular adhesion have largely been the focus to be introduced in synthetic materials[3]. Chemokines play a considerable role in the process of tissue repair by attracting progenitor cells but also by modulating the inflammatory environment. Therefore, immobilization of chemokines on synthetic grafts may simultaneously allow for both specific cell retention and subsequent stimulation of cellular development[2]. Stromal cell derived factor 1α (SDF1α) is a potent chemoattractant of lymphocytes[4], monocytes and progenitor cells but not neutrophils[5]. It is important for the homing of bone-marrow resident stem cells[6], and plays a central role in tissue repair signaling[5]. Importantly, following implantation the systemic response to a cell-free vascular graft material involves the influx of immune cells. The nature and amount of these cells can be influenced by SDF1α[7]. Short SDF1α-peptides that are homologous to the receptor-activating domain of the full protein, have been shown to improve damage repair after local delivery in ischemic tissue[8]. This indicates that short peptide sequences, which are synthetically more accessible compared to full-length proteins, are capable of retaining specific SDF1α activity. Maintaining a stable local gradient of SDF1α and avoiding a burst release of bioactive molecules after implantation has been shown to further improve the retention of progenitor cells under fluid flow conditions[9]. In addition to inducing cellular mobilization as a soluble factor, SDF1α is an important anchoring molecule for progenitor cells in bone marrow stroma [10] as well as a homing beacon bound to the ECM in the vicinity of tissue damage, guiding the migration of cells towards the site of repair[11]. Therefore an approach to anchor the SDF1α protein to a scaffold material may be advantageous for biological signaling at the site of graft implantation.

In this study we apply a synthetic cell-free scaffold based on the supramolecular modification of poly(L-lactic acid caprolactone) (PLLCL) functionalized with quadruple hydrogen bonding ureido-pyrimidinone (UPy) units[12], with SDF1α-derived peptide sequences also modified with these UPy-moieties, in order to facilitate the early cellularization of a vascular graft [2]. The base material consists of PLLCL prepolymers modified with UPy-moieties in the main chain yielding a chain-extended UPy-PLLCL (or CE-UPy-PLLCL) polymer (Figure 1)[13]. To prevent rapid proteolytic degradation of the SDF1α-derived peptides, we abolished the cleavage sites for the enzymes MMP2 and CD26, which are capable of abrogating the SDF1α signal and are abundant in an inflammatory environment[8,14]. The second valine in the natural sequence was substitut-

ed with a serine residue, leading to two peptide sequences: SKPVSLSYR and SKPVVLSYR, i.e. the proteolytically resistant and non-resistant peptides, respectively (after UPy-modification UPy-SDF1α(R) and UPy-SDF1α(NR), respectively). The material was processed into fibrous scaffolds by electrospinning. Using a previously developed mesofluidic device[15] applying a physiological pulsatile fluid flow of medium-suspended human peripheral blood mononuclear cells (PBMCs) the homing of cells into the scaffolds functionalized with short SDF1α peptides was analyzed. As a proof-of-concept to investigate the in vivo specific recruitment of circulating cells, we implanted electrospun tubular scaffolds in a abdominal aorta interposition graft rat model and analyzed the cellular influx after 24 hours and 7 days.

Materials and Methods

I. Synthesis of UPy-Peptide Materials

Synthesis of the SDF1α peptides

The synthesis of the investigated peptides is described in the supplemental files (See supplemental Materials & Methods).

Synthesis of CE-UPy-PLLCLa

The CE-UPy-PLLCL polymer was obtained using the same procedure as described for polymer 2 described in [13] (chain-extended UPy-poly[2-methyl–1,3-propylene adipate) in which the poly[2-methyl–1,3-propylene adipate diol is replaced with poly(L-lactic acid caprolactone) diol (purchased from SyMO-Chem BV) with a Mn of 1 kDa. The CE-UPy-PLLCL polymer was obtained as an elastic solid after two-times precipitation in methanol from chloroform. GPC (in

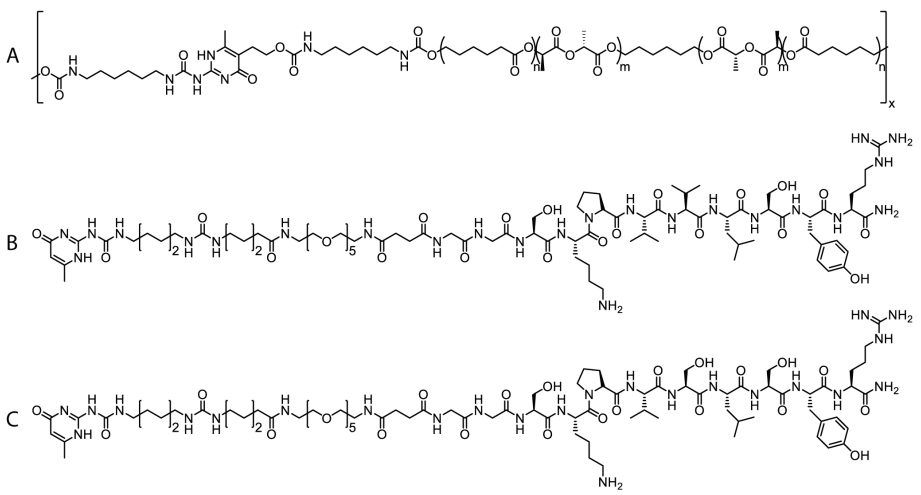

Figure 1. Chemical structures of used peptides and polymers. A: Chain-extended UPy-poly[L- lactide-co-caprolactone] (CE-UPy-PLLCL) prepolymer (Mn,PLLCL = 1 kDa)) B: UPy-SDF1α(NR) (MW = 1918 Da); C: UPy-SDF1α(R) (MW = 1930 Da).

chloroform based on polystyrene standards): Mn = 10.5 kg/mol, Mw = 15.2 kg/mol. DSC (1st heating run at 20 °C/min): Tg = -3 °C, Tm = 97 °C J/g with a corresponding enthalpy change of ΔHm= 0.78 J/g.

Electrospinning

Electrospinning was used to produce fibrous tubular grafts. Three different conditions were investigated; i.e. I) CE-UPy-PLLCL + UPy-SDFα(R), II) CE-UPy-PLLCL + UPy-SDF1α(NR), and III) CE-UPy-PLLCL without peptides (control) (Figure 1). CE-UPy-PLLCL and either the UPy-SDF1α(R) peptide or the UPy-SDF1α(NR) peptide, were dissolved in a mixture of chloroform (CHCl3): hexafluoroisopropanol (HFIP) (85:15 v/v) at a final concentration of 1.1 mol% UPy-peptide and a 15% w/v polymer solution Prior to electrospinning, 5 mL of this solution was prepared on the same day. The polymer solution was stirred for 2 hours on a magnetic stirrer at 200-250 rpm at room temperature.

Fibrous meshes and vascular grafts were electrospun using a climate controlled electrospinning apparatus (IME Technology, Geldrop, NL). The polymer solution was delivered to a metallic needle with a syringe pump connected with 19G capillary. One end of the power supply was connected to the metallic needle and other end to the target. Meshes were spun at 12 kV, using a feed rate of 0.050 mL per minute and a tip-to-target distance of 18 cm. Micrometer thick fibers were deposited on a grounded needle (10 cm in length) with an internal diameter of 18 mm that rotated at 100 rpm. Vascular grafts were spun in a similar manner to the meshes with the exception of the following parameters; a voltage of 20 kV with a feed rate of 0.025 mL per minute, at a tip-to-target distance of 20 cm and collection on a rotating target with an internal diameter of 2.1 mm, yielding a tube-like scaffold. All grafts were spun under controlled temperature of 23 °C and relative humidity of 25%. After complete removal of residual solvent by overnight drying in vacuo, the scaffolds were removed from the collector needle by wetting the scaffold in milliQ water for 1 minute, gently loosening the scaffold from the target, followed by an additional 2 minutes in milliQ water before completely removing the graft. Subsequently, the excess of solvent and water was removed by drying in vacuo at 21°C for 24 hours.

SEM analysis

In order to study the fibrous morphology and the exact fiber dimensions of the scaffolds scanning electron microscopy imaging using FEI Quanta 600 and Xt Microscope Control software was performed. Samples of comparable size and thickness were fixed on a metal stub using adhesive conductive carbon tape, and imaged under high vacuum (<1.3 0-4 mbar) conditions. Secondary electrons were detected with an accelerating voltage of 1-2 kV and a working distance of 10 mm.

Samples (containing cells) from the pulsatile flow bioreactor experiments were fixed in 1.5% glutaraldehyde for 24 hours before being washed with PBS and dehydrated in a graded alcohol series, and imaged with SEM as described above.

II. Cell Culture, Migration and Adhesion Assays

PBMC isolation

The study conforms to the principles outlined in the Declaration of Helsinki [28]. For migration assays, adhesion assays and culture experiments peripheral blood was collected via a specific department for blood donation for scientific purposes (minidonordienst, University Medical Center Utrecht, the Netherlands). For analyses performed in the pulsatile-flow bioreactor buffy coats were obtained from Sanquin Blood Supply (Sanquin, Amsterdam, the Netherlands). PBMCs were isolated using Ficol Paque PLUS (Cat. #17-1440-02, GE healthcare Life Sciences, Diegem, Belgium) density gradient centrifugation according to the manufacturer's protocol and resuspended in DMEM for the adhesion and migration assays or RPMI for the bioreactor. Culture media were supplemented with 10% fetal calf serum (FCS) and 1% penicillin/streptomycin except for the migration experiments, which were performed without FCS.

Migration assay

Migration assays were performed in a Boyden transwell chamber with 5 μm pores (Cat# 3421, Corning, Lowell, Massachusetts, USA). One million PBMCs were applied to the upper chamber in serum-free medium and allowed to migrate to the bottom compartment, which contained either full-length SDF1α (cat#167300-28A-B, Peprotech), or one of the following peptide sequences: SKPVVLSYR, GGSKPVVLSYR, SKPVSLSYR or GGSKPVSLSYR. The assay was performed for 4 hours at 37 °C. Results were compared to the migration of PBMCs in the absence of the SDF1α-derived peptides in serum free medium. A specific CXCR4 (the SDF1α receptor) inhibitor AMD3100 (50 μM) was incubated with the PBMCs in serum free medium for 30 minutes before the cells were transferred to the migration chamber. After migration the cells in the lower compartment were collected, including cells adhering to the bottom of the membrane, which were rinsed off, and re-suspended and counted after 1:1 dilution in trypan blue (cat# 15250-061, Life Technologies) using a hematocytometer.

Adhesion assay

Adhesion assays were performed on dropcast films of CE-UPy-PLLCL containing 1.1 mol% of UPy-SDF1α(R) peptide or UPy-SDF1α(NR) peptide, and compared to pristine UPy-PLLCL substrates. The dropcast films were by casting 5 w/v% polymer/peptide solution in HFIP onto 15 mm round glass coverslips and left to dry for 24 hours followed by additional incubation at 40 °C in vacuo to remove residual solvent. One million PBMCs were seeded on the polymer films in DMEM supplemented with 10% FCS and 1% penicillin/streptomycin for 30 minutes before being rinsed with phosphate buffered saline (PBS). Cells were fixed using 4% paraformaldehyde/PBS and stained using 4',6-diamidino-2-phenylindole (DAPI). Cell numbers were quantified per 400x magnified field.

Cell recruitment in a mesofluidic device by electrospun scaffolds

Cell recruitment under pulsatile flow conditions was analyzed using a mesofluidic device connected to an Ibidi flow system[15]. Electrospun sheets were prepared from CE-UPy-PLLCL with UPy-SDF1α(R) peptide or UPy-SDF1α(NR) peptide, and compared to pristine CE-UPy-PLLCL. In order to achieve a physiologically relevant cell concentration, 5 07 PBMCs were resuspended in 10 mL medium for each flow-chamber. A dual syringe-pump created a unidirectional flow by applying continuous pressure at 120 mmHg. A pulsatile flow was created by intermittent mechanical pinching of the inlet tube. Electrospun meshes (10x15 mm) where placed in a custom designed chamber, allowing flow to pass underneath the material. After 2 or 14 hours the circulation was stopped and the electrospun material was collected along with the non-adhering cells in the medium.

In vivo evaluation of peptide-containing electrospun grafts

All procedures were approved by the institutional Animal Care and Use Committee of the University of Utrecht, the Netherlands. Eighteen healthy male Sprague Dawley rats (350-450 gram), purchased from Charles River Laboratories received an electrospun aortic interposition graft. Rats were divided in three groups: the first group received a graft composed from CE-UPy-PLLCL material with UPy-SDF1α(R) peptide, the second group received the same graft but with UPy-SDF1α(NR) peptide, and the third group served as a control group receiving scaffolds of pristine CE-UPy-PLLCL (n=6 per group). Grafts were explanted at day 1 (n=9) or day 7 (n=9). To inhibit transmural and transanastomotic ingrowth of cells within the first week, all grafts were shielded with Gore-Tex®: Distally and proximally of each electrospun graft an end-to-end anastomosis was made to a 4x10 mm^2 impenetrable Gore-Tex strip (Preclude Pericardial Membrane; Gore Medical). In addition to shielding the anastomoses, Gore-Tex was also wrapped around the grafts creating a barrier for cells migrating from the adjacent tissue. Animals were anaesthetized using isoflurane gas. Explants were cut in half and fixed in 10% formalin for immunohistochemistry and Trizol for qPCR.

III. Immunohistochemistry

In vitro samples were fixed in 3.7% formaldehyde/PBS and blocked in PBS/BSA 2% for 1 hour, after which primary antibodies against CD3 and CD14 (Serotec) were incubated for 1 hour at room temperature. Secondary antibodies (goat anti rabbit-cy5, goat anti mouse AF568) were incubated for 1 hour at room temperature shielded from the light. Nuclei were stained with DAPI for 10 minutes in the dark. Confocal microscopy (Zeiss LSM700) was used to image the cells. Cell numbers were quantified per 40x magnification. For in vivo samples, before pre-embedding in 1% (w/v) agar (Eurogentec), explants were fixed in 10% formalin followed by embedding in paraffin. Consecutive 4 μm sections were stained with Mayer's hematoxylin and eosin (H&E). Immunohistochemical stainings were performed after deparaffinization and dehydration. Sections were stained for CD3, CD68, CD34 and αSMA. Investigators were blinded to the experimental groups and the time point of explantation. Photographs were taken using a Nikon

E800 microscope with ACT-1 software. Cellularity was studied under high-power magnification (high-power field, 40x objective lens; area comprising 0.034 mm2). Using ImageJ software, the total number of cells in 4 random hpf areas per graft was manually counted. Area of positive staining was measured as a percentage of the total from binarised images.

IV. qPCR

Total RNA was extracted using Trizol according to the manufacturer's protocol (TRIzol, cat#10296-010, Invitrogen, Life Technologies Europe BV, Bleiswijk, the Netherlands). The electrospun mesh was homogenized in Trizol using a Precellys 24 tissue homogenizer (Precellys, Bertin Technologies, Aix-en Provence, France). cDNA was synthesized using iScript according to the manufacturer's protocol (iScript, Cat#170-8891, Bio-Rad, Hercules, California, United States). qPCR was analyzed using the delta-delta CT method, normalized to P0 expression

V. Statistics

Data are presented as mean ± standard deviation. Statistical analysis was performed using one-way analysis of variance (ANOVA) with post-hoc Tukey or post-hoc Dunnett test, student's T test and Mann-Whitney test where appropriate. P value <0.05 was considered statistically significant.

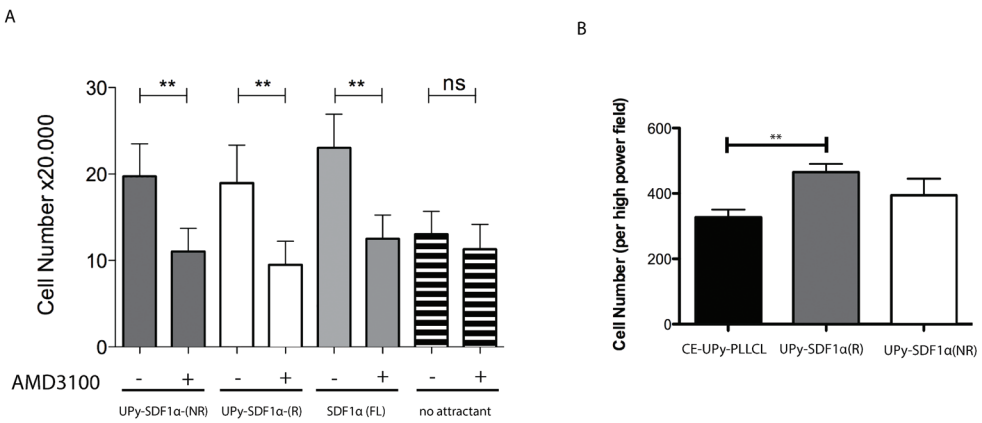

Figure 2. A: Migration assay. Specific CXCR4 inhibition by incubating cells with the specific receptor antagonist AMD3100 abrogates migration to UPy-SDF1α(NR) and UPy-SDF1α(R) peptides similarly to full length (FL) SDF1α. N=3. B: Adhesion assay. Cells were allowed to adhere to UPy-PLLCL surfaces modified with UPy-SDF1α(NR), UPy-SDF1α(R), or to the pristine polymer surface (CE-UPy-PLLCL). Nuclei were counted per high-power field. CE-UPy-PLLCL with UPy-SDF1α(R) adhered significantly more PBMCs. P=0.007, N=6.

Results

I. Synthetic SDF1α-Derived Peptides are Biologically Active Through CXCR4 and are Resistant To Proteolytic Degradation by MMP2

The ability of the SDF1α-derived peptides to induce receptor-mediated migration was analyzed to confirm biological activity though the SDF1α-CXCR4 axis. In a Boyden chamber migration assay both SDF1α(R) and SDF1α(NR) peptides induced significant migration of PBMCs compared to the non-peptide control condition and to a similar degree to full-length SDF1α. Pre-incubation of PBMCs with the CXCR4-specific antagonist AMD-3100 significantly reduced the number of migrating cells (Figure 2A). This indicates that the short peptides retain their receptor-mediated SDF1α activity.

Sensitivity to proteolytic degradation by matrix metalloproteinases was studied via incubation of GGSKPVSLSYR and GGSKPVVLSYR peptides in the presence of MMP-2. MMP-2 is known to selectively hydrolyze the peptide bond between the serine and valine residues within the SDF peptide, yielding a LSYR-peptide fragment with a typical molecular weight of 537.3 Da. LC-MS analysis of the GGSKPVSLSYR-peptide revealed a distinct peak in the chromatogram after proteolytic degradation, corresponding to the LSYR-fragment at 537.3 Da, which was not observed prior to incubation with MMP-2. The LSYR-fragment was also found after expo-

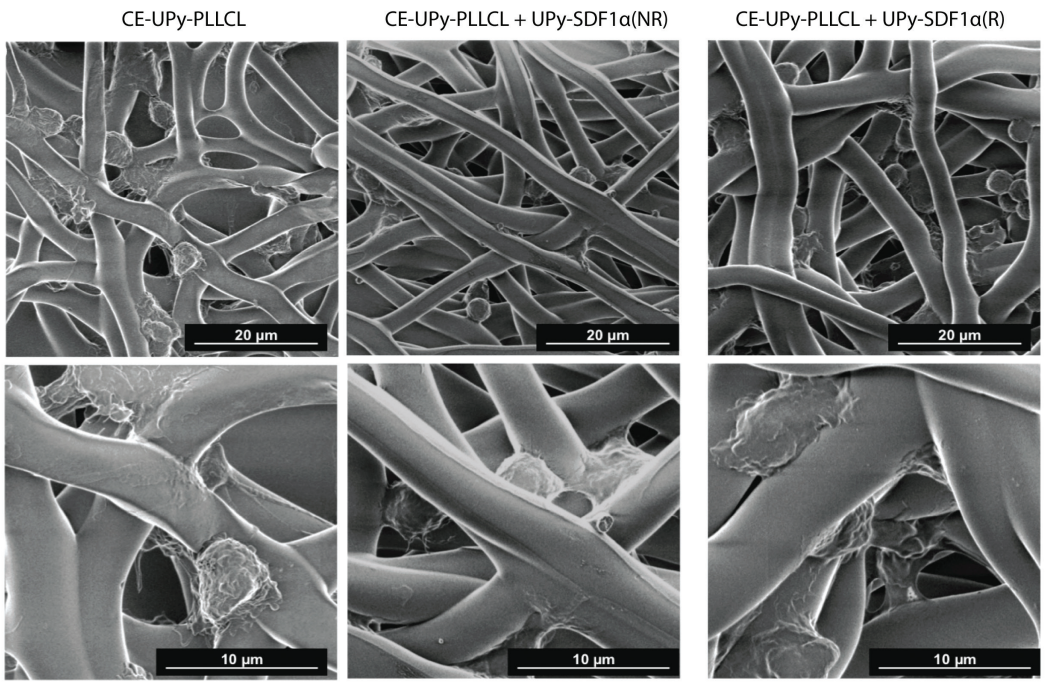

Figure 3. SEM of electrospun meshes after 14 hours of exposure to PBMCs under pulsatile flow in vitro. Cells adhere to the fibers.

sure of the GGSKPVVLSYR to MMP-2, but at levels close to the detection limit of the LC-MS apparatus, and therefore considered non-significant (Supplemental Figure 1).
The adhesion of PBMCs to films modified with the UPy-SDF1α-derived peptides was studied by culturing the cells for 30 minutes on these materials. On films containing the UPy-SDF1α(R) peptides significantly more PBMCs were adhered (Figure 2B) compared to pristine CE-UPy-PLLCL.The UPy-SDF1α(NR) peptides showed a similar trend for more adhered PBMCs though no statistical significance was found (Figure 2B). Together these results demonstrate that substitution of the serine residue with a valine indeed abolished rapid proteolytic degradation of the SDF1α-derived peptides, and that the peptides retained their activity after incorporation into UPy-PLLCL.

II. Electrospun Fibers Functionalized With UPy-SDF1α(R) Peptides or UPy-SDF1α(NR) Peptides Retain Lymphocytes Under Pulsatile Flow Conditions In Vitro and Reduce Inflammatory Protein Expression.

SEM analysis of the electrospun meshed showed a fiber diameter of 2.3 μm (± 0.3μm) for both peptide materials and 3.2 μm (±0.4 μm) for control CE-UPy-PLLCL (Supplemental Figure 2), which enables cells to migrate into the mesh[16]. Electrospun meshes were exposed to a physiological concentration of $5x10^6$ cells/mL of PBMCs in a custom-designed bioreactor under an unidirectional pulsatile flow [15]. Both the CE-UPy-PLLCL/UPy-SDF1α(R) peptide scaffold and pristine material, analyzed by SEM, showed cellular adhesion throughout the fibers (Figure 3). The cells appeared flattened and well-adhered with some cells showing a round morphology. Confocal microscopy on the lymphocyte marker CD3 and the monocyte marker CD14 shows that the adhering cells after 2 hours of flow were predominantly lymphocytes and monocytes with no significant differences between materials (supplemental Figure 3). After 14 hours of flow, however, markedly more CD3+ lymphocytes and less CD14+ monocytes were found in both UPy-SDF1α(R) peptide and UPy-SDF1α(NR) peptide materials (Figure 4), indicating a specific retention of lymphocytes by the peptides after 14 hours.
After 2 hours of flow, analysis by qPCR showed a significantly higher expression of CD3 (a lymphocyte marker) and CD8 (a cytotoxic t-cell marker) in the UPy-SDF1α(R) modified material indicating an initial predominance of cytotoxic t-cells (Supplemental Figure 3). This pattern changed after 14 hours when there was a significantly higher expression of CD4 (a t-helper cell marker) while the expression of CD8 was lower. At this time point a trend for higher expression of CD3 in peptide materials was found, consistent with the immunohistological stainings. This implies an enhanced recruitment of t-helper cells (Figure 4) in peptide-functionalized scaffolds. In addition, we found significantly lower expression of the inflammatory proteins MCP1 and TNFα in peptide material after 14 hours but not after 2 hours. Concordantly the expression of the lymphocyte activation marker CD25 was significantly lowered at this time point. ELISA performed on the circulating medium showed no significant differences between protein concentrations of anti-inflammatory protein IL10 and pro-inflammatory protein TNFa after 14 hours (supplemental Figure 4).

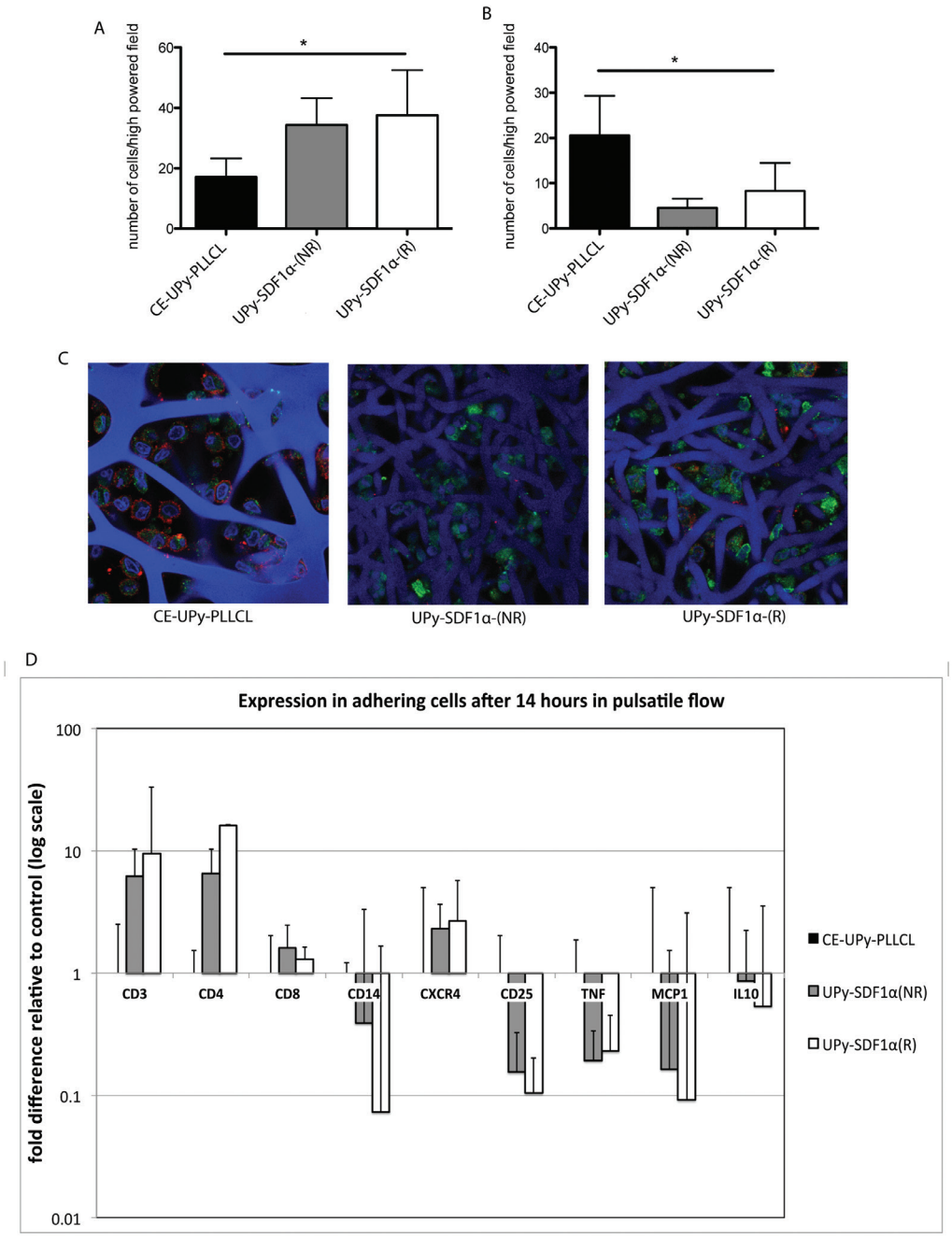

Figure 4. A: Significantly more CD3+ cells were found in electrospun meshes after 14 hours of exposure to human PB-MCs under pulsatile flow in vitro and B: Significantly less CD14+ cells were found in both peptide containing materials. N=4 C: Representative images from confocal microscopy. Red: CD14 Green: CD3 and Blue: nuclei/fibers (background). D: Gene expression in adhering cells after 14 hours in pulsatile flow. qPCR of cells adhered to electrospun meshes after 14 hours in pulsatile flow conditions. There was a significantly higher expression of CD4+ and and a trend for more CXCR4 in peptide-functionalized materials, and significantly lower expression of CD25, MCP1 and TNF. No expression of CD68 was detected.

III. UPy-SDF1α Peptides Increase Cellularization in Electrospun Vascular Grafts In Vivo

Electrospun tubular scaffolds were implanted into interposition grafts in rat abdominal aortas and explanted for histological analysis after 24 hours and 7 days. After 24 hours, predominantly granulocytes and macrophages had infiltrated the scaffold, based on cell morphology. After 7 days cellularity had increased to 89 ± 15 cells per (high power field) hpf in material with UPy-SDF1α(NR) and 88 ± 6 cells per hpf in material with UPy-SDF1α(R) while the control group showed 51 ± 12 cells per hpf. This increased cellularity was significant at day 7 in material with UPy-SDF1α(NR) ($p = 0.03$) and material with UPy-SDF1α(R) ($p = 0.02$) compared to the control group (Figure 5). At this time point the cells were predominantly present in deeper layers of both peptide materials while control material showed most cells near the luminal side indicating that the peptides influenced cell migration (Figure 5). For this in vivo analysis CD68 was used as a macrophage marker. The amount of CD68+ cells was also significantly higher at day 7 in UPy-SDF1α(NR) material compared to the control group ($p = 0.02$) (Figure 5), having

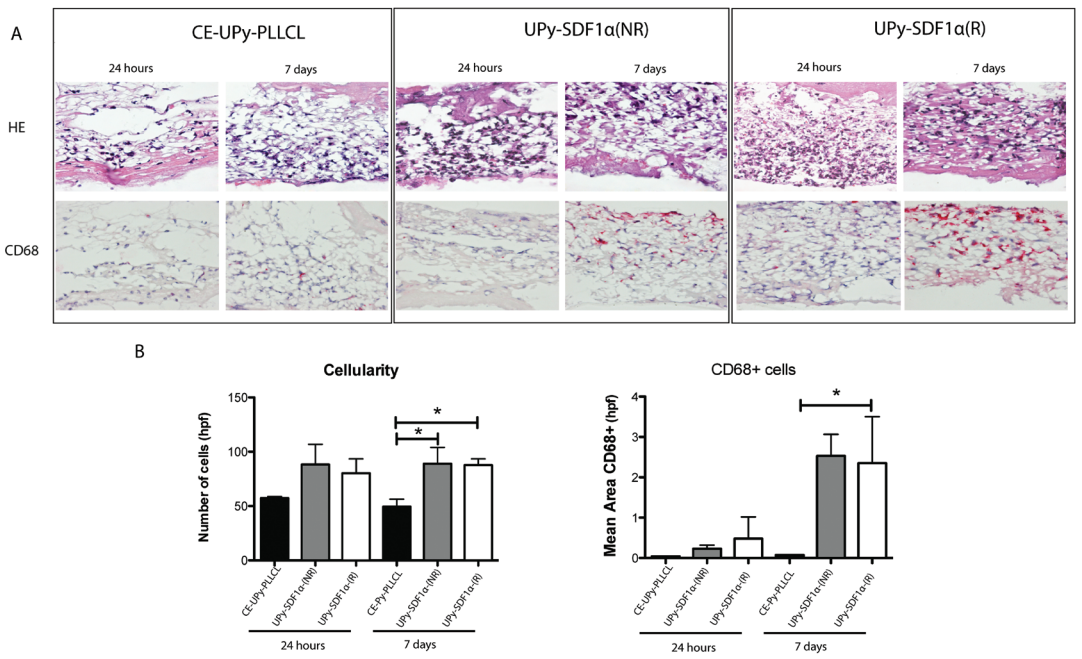

Figure 5. A; In vivo cellularization. Peptide-functionalized materials show deeper cellular penetration through the graft after 7 days while control material shows cellularization remains close to the lumen (bottom of picture). Cellularity and CD68+ cells in graft material after 1 and 7 days of implantation into rat abdominal aorta interposition grafts. Cellularity and CD68+ cell count is significantly raised in both peptide-functionalized materials after 7 days.

increased to 2.53% ± 0.53% in material with UPy-SDF1α(NR) and 2.35 % ± 1.15% in material with UPy-SDF1α(R) compared to 0.07% ± 0.01 % in the control group. No CD3+ cells were detected by immunohistochemistry. There was a trend for higher number of CD34 and αSMA positive cells in both peptide-containing materials after 7 days, though no significant differences were found (supplemental Figure 5).

Discussion

Previous efforts to use biofunctionalized synthetic materials for vascular grafting have mostly focused on ECM derived peptides such as RGD to enhance cellular adhesion [17]. Considering their ability to simultaneously attract and stimulate targeted cell populations chemokines may provide more specific biological activity. We report, for the first time, that the supramolecular bioactivation of a fully synthetic material using short peptides based on the chemokine SDF1α can attract and stimulate cells into a cell-free vascular replacement graft scaffold. The supramolecular mix-and-match approach combined with electrospinning enables control over the structural and biochemical properties of the graft, which can greatly influence cellular influx and behavior[18-20]. Electrospinning yields fibrous mesh scaffolds that form a 3-dimensional microenvironment of microfibers that allow cellular infiltration throughout the graft[16]. We used a supramolecular approach to modify these electrospun fibers with bioactive molecules using UPy-moieties[12]. This surface presentation of the peptides facilitated the binding to the receptor CXCR4 and mimics the in vivo interaction of matrix-bound chemokines with cells in tissue damage repair[2]. In our in vitro analyses, specific retention of human PBMCs due to the peptides becomes apparent after 14 hours. In addition, expression was significantly lowered for the inflammatory proteins MCP1 and TNFα after 14 hours, which indicates that the presence of the peptides reduces inflammatory signaling by the adhering cells in an early stage of cellular influx. Consistent with the chemoattractive function of SDF1α in vivo, after 7 days of implantation of scaffolds in an abdominal aorta interposition graft, the distribution of the infiltrating cells within the graft material was more homogenous with deeper penetration in scaffolds containing UPy-SDF1α(R) peptides or UPy-SDF1α(NR) peptides compared to control material. The additional penetration of cells seen in the peptide-containing materials may be due to the production of signaling proteins by the adhering cells induced by interaction through the CXCR4-SDF1a axis. In contrast, cell retention due to a generic immune response and hemodynamic pressure was restricted to the luminal side of the graft in material without peptides. Furthermore, the higher number of CD68+ cells and reduced number of lymphocytes found in-vivo differs from the higher number of lymphocytes found early timepoints in-vitro. It is likely that the early retention of lymphocytes found in vitro influenced the subsequent attraction of additional monocytes in our in vivo model, which contains a replenishing immune system in contrast with the in vitro model.

Flameng et al. recently showed that pre-existing, decellularized heart valves coated with fibronectin and full length SDF1α protein developed fully recellularized vascular tissue in vivo

after 5 months in sheep, due to the presentation of the full length SDF1α protein by fibronectin[7]. This further illustrates that mimicking the molecular dynamics of chemokines is of great potential in tissue engineering strategies. Molecular re-design of the SDF1α protein has previously improved applicability in tissue damage repair applications, but not yet tissue engineering. Enhancing the interaction between cells and chemokines by influencing molecular presentation is a promising approach to bio-activating materials. By fusing SDF1α to a glycoprotein VI (GPVI)-domain, which binds to collagen, Ziegler et al. were able to increase the localization of intravenously injected recombinant protein to the site of myocardial infarction[21]. Schesny et al. exploited the resulting enhanced matrix-binding to incorporate it into poly(ethylene glycol) based hydrogels as a delivery tool to treat ischemic cardiovascular disease[22]. While the above-mentioned research focuses on damage repair in pre-existing living tissues, our data shows, for the first time, that SDF1α-derived peptides are also of great potential in enhancing developing new tissue in fully synthetic cell-free grafts.

In cell-free grafts, early cellularization is pivotal for neotissue formation[23]. A systemic response to implanted foreign material involves early invasion by monocytes, lymphocytes and progenitor cells from the circulation. In vivo, these cells dictate the inflammatory signaling environment of tissue regeneration[24,25], among others influencing the polarization of macrophage subtypes[26,27], which is an important step in the progression to a pro-tissue repair phase. There is evidence that one of the mechanisms in which SDF1α induces tissue repair is through influencing the development of CD68 monocytes towards a pro-tissue formation phenotype[7]. The differentiation of monocytes into macrophages is an important step in the regulation of tissue development and remodeling, and is greatly influenced by signaling factors produced by cells in the microenvironment. In particular, alternatively activated macrophages, or M2 macrophages, have been associated with improved tissue formation in tissue engineered implanted constructs[28,29]. There is evidence that SDF1a can induce the polarization of monocytes towards an M2 phenotype [30,31]. Our in vivo data show that short-term implantation of UPy-SDF1α(R) peptide or UPy-SDF1α(NR) peptide materials in an abdominal aorta interposition graft in rat increased cellularity by CD68+ monocytes after 7 days, indicating that the early signaling environment triggered by the peptides directly influences subsequent cellularization.

In an inflammatory environment the presence of the enzymes MMP2 and CD26 are an important limiting factor of the longevity of the wild-type SDF1α protein[8,14,32,33]. For this reason resistance to enzymatic degradation is highly desirable to promote cellular infiltration and ultimately neotissue formation over a longer period of time. Longer implantation time points will help to investigate the potentially prolonged activity of UPy-SDF1α(R) peptides in vivo. Though we found no significant advantage of resistant peptides over non-resistant peptides in our early in vivo time point analyses, our in vitro data consistently shows a stronger effect of UPy-SDF1α(R) over UPy-SDF1α(NR).

Our results provide a first step towards in situ cardiovascular tissue engineering by combining

electrospinning with the advantages of supramolecular chemistry, through non-covalent functionalization of scaffold material with short peptides based on SDF1α. Our data show that we have achieved bio-instructive scaffold materials that can enhance the cellularization of implanted vascular replacement grafts. Due to the fully synthetic approach and the versatility of the supramolecular introduction of bioactive molecules, we propose that our approach is highly translatable to diverse cardiovascular clinical applications.

Acknowledgements

This research forms part of the Project P1.01 iValve of the research program of the BioMedical Materials institute, co-funded by the Dutch Ministry of Economic Affairs.
The financial contribution of the Nederlandse Hartstichting is gratefully acknowledged.
Part of this research is funded by the Ministry of Education, Culture and Science (Gravity program 024.001.035), the Netherlands Organisation for Scientific Research (NWO), the European Research Council (FP7/2007-2013), ERC Grant Agreement 308045 and the Netherlands Institute for Regenerative Medicine (NIRM).

References

[1] Kurobe H, Maxfield MW, Breuer CK, Shinoka T. Concise review: tissue-engineered vascular grafts for cardiac surgery: past, present, and future. Stem Cells Transl Med 2012;1:566–71. doi:10.5966/sctm.2012-0044.

[2] Muylaert DEP, Fledderus JO, Bouten CVC, Dankers PYW, Verhaar MC. Combining tissue repair and tissue engineering; bioactivating implantable cell-free vascular scaffolds. Heart 2014;100:1825–30. doi:10.1136/heartjnl-2014-306092.

[3] Chong DST, Lindsey B, Dalby MJ, Gadegaard N, Seifalian AM, Hamilton G. Luminal surface engineering, “micro and nanopatterning”: potential for self endothelialising vascular grafts? Eur J Vasc Endovasc Surg 2014;47:566–76. doi:10.1016/j.ejvs.2014.02.007.

[4] Dürr C, Pfeifer D, Claus R, Schmitt-Graeff A, Gerlach UV, Graeser R, et al. CXCL12 mediates immunosuppression in the lymphoma microenvironment after allogeneic transplantation of hematopoietic cells. Cancer Research 2010;70:10170–81. doi:10.1158/0008-5472.CAN-10-1943.

[5] Bleul CC, Fuhlbrigge RC, Casasnovas JM, Aiuti A, Springer TA. A highly efficacious lymphocyte chemoattractant, stromal cell-derived factor 1 (SDF-1). J Exp Med 1996;184:1101–9.

[6] Hidalgo A, Sanz-Rodríguez F, Rodríguez-Fernández JL, Albella B, Blaya C, Wright N, et al. Chemokine stromal cell-derived factor-1alpha modulates VLA-4 integrin-dependent adhesion to fibronectin and VCAM-1 on bone marrow hematopoietic progenitor cells. Exp Hematol 2001;29:345–55.

[7] Flameng W, De Visscher G, Mesure L, Hermans H, Jashari R, Meuris B. Coating with fibronectin and stromal cell-derived factor-1α of decellularized homografts used for right ventricular outflow tract reconstruction eliminates immune response-related degeneration. The Journal of Thoracic and Cardiovascular Surgery 2014;147:1398–1404.e2. doi:10.1016/j.jtcvs.2013.06.022.

[8] Segers VFM, Tokunou T, Higgins LJ, MacGillivray C, Gannon J, Lee RT. Local delivery of pro-

tease-resistant stromal cell derived factor-1 for stem cell recruitment after myocardial infarction. Circulation 2007;116:1683–92. doi:10.1161/CIRCULATIONAHA.107.718718.
[9] Yu J, Wang A, Tang Z, Henry J, Li-Ping Lee B, Zhu Y, et al. The effect of stromal cell-derived factor-1α/heparin coating of biodegradable vascular grafts on the recruitment of both endothelial and smooth muscle progenitor cells for accelerated regeneration. Biomaterials 2012;33:8062–74. doi:10.1016/j.biomaterials.2012.07.042.
[10] Sugiyama T, Kohara H, Noda M, Nagasawa T. Maintenance of the hematopoietic stem cell pool by CXCL12-CXCR4 chemokine signaling in bone marrow stromal cell niches. Immunity 2006;25:977–88. doi:10.1016/j.immuni.2006.10.016.
[11] Muylaert DEP, Muylaert DE, Fledderus JO, Fledderus JO, Bouten CVC, Bouten CV, et al. Combining tissue repair and tissue engineering; bioactivating implantable cell-free vascular scaffolds. Heart 2014;100:1825–30. doi:10.1136/heartjnl-2014-306092.
[12] Sijbesma RP, Beijer FH, Brunsveld L, Folmer BJ, Hirschberg JH, Lange RF, et al. Reversible polymers formed from self-complementary monomers using quadruple hydrogen bonding. Science 1997;278:1601–4.
[13] Söntjens SHM, Renken RAE, van Gemert GML, Engels TAP, Bosman AW, Janssen HM, et al. Thermoplastic Elastomers Based on Strong and Well-Defined Hydrogen-Bonding Interactions. Macromolecules 2008;41:5703–8. doi:10.1021/ma800744c.
[14] Segers VFM, Revin V, Wu W, Qiu H, Yan Z, Lee RT, et al. Protease-resistant stromal cell-derived factor-1 for the treatment of experimental peripheral artery disease. Circulation 2011;123:1306–15. doi:10.1161/CIRCULATIONAHA.110.991786.
[15] Smits AIPM, Driessen-Mol A, Bouten CVC, Baaijens FPT. A Mesofluidics-Based Test Platform for Systematic Development of Scaffolds for In Situ Cardiovascular Tissue Engineering. Tissue Engineering Part C: Methods 2012;18:475–85. doi:10.1089/ten.TEC.2011.0458.
[16] Balguid A, Mol A, van Marion MH, Bank RA, Bouten CVC, Baaijens FPT. Tailoring fiber diameter in electrospun poly(epsilon-caprolactone) scaffolds for optimal cellular infiltration in cardiovascular tissue engineering. Tissue Eng Part A 2009;15:437–44. doi:10.1089/ten.tea.2007.0294.
[17] Dankers PYW, Harmsen MC, Brouwer LA, van Luyn MJA, Meijer EW. A modular and supramolecular approach to bioactive scaffolds for tissue engineering. Nature Materials 2005;4:568–74. doi:10.1038/nmat1418.
[18] Huang NF, Li S. Regulation of the matrix microenvironment for stem cell engineering and regenerative medicine. Ann Biomed Eng 2011;39:1201–14. doi:10.1007/s10439-011-0297-2.
[19] Pu J, Yuan F, Li S, Komvopoulos K. Electrospun bilayer fibrous scaffolds for enhanced cell infiltration and vascularization in vivo. Acta Biomaterialia 2015;13:131–41. doi:10.1016/j.actbio.2014.11.014.
[20] Sengupta D, Waldman SD, Li S. From in vitro to in situ tissue engineering. Ann Biomed Eng 2014;42:1537–45. doi:10.1007/s10439-014-1022-8.
[21] Ziegler M, Elvers M, Baumer Y, Leder C, Ochmann C, Schönberger T, et al. The bispecific SDF1-GPVI fusion protein preserves myocardial function after transient ischemia in mice. Circulation 2012;125:685–96. doi:10.1161/CIRCULATIONAHA.111.070508.
[22] Schesny MK, Monaghan M, Bindermann AH, Freund D, Seifert M, Eble JA, et al. Preserved bioactivity and tunable release of a SDF1-GPVI bi-specific protein using photo-crosslinked PEGda hydrogels. Biomaterials 2014;35:7180–7. doi:10.1016/j.biomaterials.2014.04.116.
[23] Franz S, Rammelt S, Scharnweber D, Simon JC. Immune responses to implants - a review of the implications for the design of immunomodulatory biomaterials. Biomaterials 2011;32:6692–709. doi:10.1016/j.biomaterials.2011.05.078.

[24] Netelenbos T, Zuijderduijn S, Van Den Born J, Kessler FL, Zweegman S, Huijgens PC, et al. Proteoglycans guide SDF-1-induced migration of hematopoietic progenitor cells. J Leukoc Biol 2002;72:353–62.

[25] Chen L, Mehta ND, Zhao Y, DiPietro LA. Absence of CD4 or CD8 lymphocytes changes infiltration of inflammatory cells and profiles of cytokine expression in skin wounds, but does not impair healing. Exp Dermatol 2014;23:189–94. doi:10.1111/exd.12346.

[26] Weidenbusch M, Anders H-J. Tissue microenvironments define and get reinforced by macrophage phenotypes in homeostasis or during inflammation, repair and fibrosis. J Innate Immun 2012;4:463–77. doi:10.1159/000336717.

[27] Sica A, Mantovani A. Macrophage plasticity and polarization: in vivo veritas. J Clin Invest 2012;122:787–95. doi:10.1172/JCI59643.

[28] Brown BN, Londono R, Tottey S, Zhang L, Kukla KA, Wolf MT, et al. Macrophage phenotype as a predictor of constructive remodeling following the implantation of biologically derived surgical mesh materials. Acta Biomaterialia 2012;8:978–87. doi:10.1016/j.actbio.2011.11.031.

[29] Wang Z, Cui Y, Wang J, Yang X, Wu Y, Wang K, et al. The effect of thick fibers and large pores of electrospun poly(ε-caprolactone) vascular grafts on macrophage polarization and arterial regeneration. Biomaterials 2014;35:5700–10. doi:10.1016/j.biomaterials.2014.03.078.

[30] Sanchez-Martin L, Estecha A, Samaniego R, Sanchez-Ramon S, Vega MA, Sanchez-Mateos P. The chemokine CXCL12 regulates monocyte-macrophage differentiation and RUNX3 expression. Blood 2011;117:88–97. doi:10.1182/blood-2009-12-258186.

[31] Brenner C, Franz WM, Kühlenthal S, Kuschnerus K, Remm F, Gross L, et al. DPP-4 inhibition ameliorates atherosclerosis by priming monocytes into M2 macrophages. International Journal of Cardiology 2015;199:163–9. doi:10.1016/j.ijcard.2015.07.044.

[32] Zaruba M-M, Theiss HD, Vallaster M, Mehl U, Brunner S, David R, et al. Synergy between CD26/DPP-IV Inhibition and G-CSF Improves Cardiac Function after Acute Myocardial Infarction. Cell Stem Cell 2009;4:313–23. doi:10.1016/j.stem.2009.02.013.

[33] McQuibban GA, Butler GS, Gong JH, Bendall L, Power C, Clark-Lewis I, et al. Matrix metalloproteinase activity inactivates the CXC chemokine stromal cell-derived factor-1. J Biol Chem 2001;276:43503–8. doi:10.1074/jbc.M107736200.

Supplemental Materials & Methods

Synthesis of the SDF1α Peptides

SDF1α-derived peptide sequences SKPVVLSYR, GGSKPVVLSYR, SKPVSLSYR and GGSKPVSLSYR were synthesized by manual solid phase peptide synthesis (SPPS) using Fmoc chemistry. Batches of Rink Amide MBHA resin were set to swell in N-methyl-2-pyrrolidone (NMP) for an hour, after which the resins were deprotected twice for 5 minutes with 20% (v/v) piperidine in NMP to remove the Fmoc protection. Subsequently, the resins were washed with NMP, and a coupling cocktail was added containing the respective amino acid, 2-(1H-benzotriazol-1-yl)-1,1,3,3-tetramethyluronium hexafluorophosphate (HBTU) as an activator and N,N-diisopropylethylamine (DIPEA) as a base (0.4, 1.6 and 0.4 mmole, respectively) and was agitated for 20 minutes to allow full coupling. The resins were washed again with NMP and this cycle of deprotection-washing-coupling-washing was repeated for every amino acid in the peptide sequences. In the last step, all peptide resins were deprotected to remove remaining the N-terminal Fmoc groups. Then,a cleavage cocktail containing trifluoroacetic acid (TFA), triisopropylsilane (TIS), 1,2-ethanedithiol (EDT) and water (94:2:2:2 v/v) was added and agitated for 4 hours to allow cleavage of the resin and protecting groups of the amino acids. The cleaved peptides were precipitated in cold diethyl ether, incubated at -20 oC for 15 minutes and centrifuged for 10 minutes at 20k RPM. Subsequently, the supernatant was removed and the pellet was dissolved in water and lyophilized. The peptides were purified using preparative RP-HPLC with a gradient of 10-30% acetonitrile in water over 10 minutes, resulting in pure peptides with a yield of 55.1% (SKPVVLSYR, 28.9 mg), 37.2% (GGSKPVVLSYR, 21.6 mg), 52.7% (SKPVSLSYR, 27.3 mg) and 37.6% (GGSKPVSLSYR, 21.6 mg).
RPLC-MS: SKPVVLSYR: MWcalc = 1047.2 g/mol, m/zobs = 1047.9 [M+H]+, 524.6 [M+2H]2+, 350.1 [M+3H]3+. GGSKPVVLSYR: MWcalc = 1161.4 g/mol, m/zobs = 1162.0 [M+H]+, 581.7 [M+2H]2+ and 388.2 g/mol [M+3H]3+. SKPVSLSYR: MWcalc = 1035.2 g/mol, m/zobs = 1035.8 [M+H]+, 518.6 [M+2H]2+ and 346.1 g/mol [M+3H]3+. GGSKPVSLSYR: MWcalc = 1149.3 g/mol, m/zobs = 1149.9 [M+H]+, 575.7 [M+2H]2+ and 384.1 g/mol [M+3H]3+. Both peptides without the two N-terminal glycines were included only in the subsequent cell migration assays.

Coupling of succinic anhydride to peptides GGSKPVVLSYR and GGSKPVSLSYR on the resin

The Fmoc-GGSKPVVLSYR-resin and Fmoc-GGSKPVSLSYR-resin (200 μmole each) were set to swell in NMP for 1 hour, followed by deprotection (twice, 5 minutes) with 20% (v/v) piperidine. The resins were washed with NMP and dimethylformamide (DMF), and subsequently, a succinic anhydride (sa) (400 mg, 4 mmole) in pyridine (2 mL, 25 mmole) was added to the resin. The reaction mixture was agitated overnight, followed by washing with DMF and dichloromethane (DCM). Test cleavage revealed successful coupling of the succinic anhydride. RPLC-MS:

sa-GGSKPVVLSYR: MWcalc = 1261.5 g/mol, m/zobs = 1262.0 [M+H]+ and 631.8 g/mol [M+2H]2+. sa-GGSKPVSLSYR: MWcalc = 1249.4 g/mol, m/zobs = 1250.0 [M+H]+ and 625.8 g/mol [M+H]2+ .

Coupling of UPy-U-C6-U-C5-OEG5-NH2 to sa-GGSKPVVLSYR and sa-GGSKPVSLSYR on the resin

UPy-U-C6-U-C5-OEG5-NH2 was synthesized as previously described[1] and coupled (240 mg, 300 µmole) to the acid functionalized peptides on the resins (200 µmole) using the coupling reagent PyBOP (208 mg, 400 µmole) and the base DIPEA (3 mL, 2 mmole) in DMF (4 mL). The mixture was agitated overnight. Then the resin was washed with DMF and DCM, and dried. The UPy-peptides were cleaved from the resin and the protecting groups were removed, using a cleavage cocktail containing TFA, TIS and water (94:2.5:2.5 v/v) for 4 hours. The UPy-peptides were purified using preparative RP-HPLC with a gradient of 20-40 % acetonitrile over 10 minutes, resulting in pure UPy-GGSKPVVLSYR and UPy-GGSKPVSLSYR with a yield of 20.0 (77.4 mg) and 16.3 % (62.5 mg), respectively. RPLC-MS: UPy-sa-GGSKPVVLSYR: MWcalc = 1931.3 g/mol, m/zobs = 1931.3 [M+H]+, 966.2 [M+2H]2+ and 644.5 g/mol [M+3H]3+. UPy-sa-GGSKPVSLSYR: MWcalc = 1919.2 g/mol, m/zobs = 1919.1 [M+H]+, 960.2 [M+2H]2+ and 640.5 g/mol [M+3H]3+.

Synthesis of CE-UPy-PLLCL

The CE-UPy-PLLCL polymer was obtained using the same procedure as described for polymer 2 described in [2] (chain-extended UPy-poly[2-methyl–1,3-propylene adipate) in which the poly[2-methyl–1,3-propylene adipate diol is replaced with poly(L-lactic acid caprolactone) diol (purchased from SyMO-Chem BV) with a Mn of 1 kDa. The CE-UPy-PLLCL polymer was obtained as an elastic solid after two times precipitation in methanol from chloroform. GPC (in chloroform based on polystyrene standards): Mn = 10.5 kg/mol, Mw = 15.2 kg/mol. DSC (1st heating run at 20 °C/min): Tg = -3 °C, Tm = 97 °C J/g with a corresponding enthalpy change of ΔHm= 0.78 J/g.

Material & Methods belonging to Supplemental Figure 1

Enzymatic degradation of SDF-1a peptides

In order to study proteolytic degradation of both SDF1α –derived peptides by MMP-2, 26 nmol of GGSKPVVLSYR (SDF1α(R)), and GGSKPVSLSYR (SDF1α(NR)) were incubated with 0.1 mg/mL MMP2 (Calbiochem, #PF025) in a buffer containing 50 mM Tris 200 mM sodium chloride, 10 mM calcium chloride, and 10 mM zinc chloride at pH 7.4, at 37 °C for two hours. Intact peptides and the cleaved peptide LSYR-fragment were detected by LCMS on a C18 column (Acquity UPLC BEH C18, 1.7 µm, 2.1 $_x$ 50 mm).

LCMS: GGSKPVVLSYR: m/z (calc.) = 1161.67 Da, m/z (obs) = 1161.68 Da. GGSKPVSLSYR:

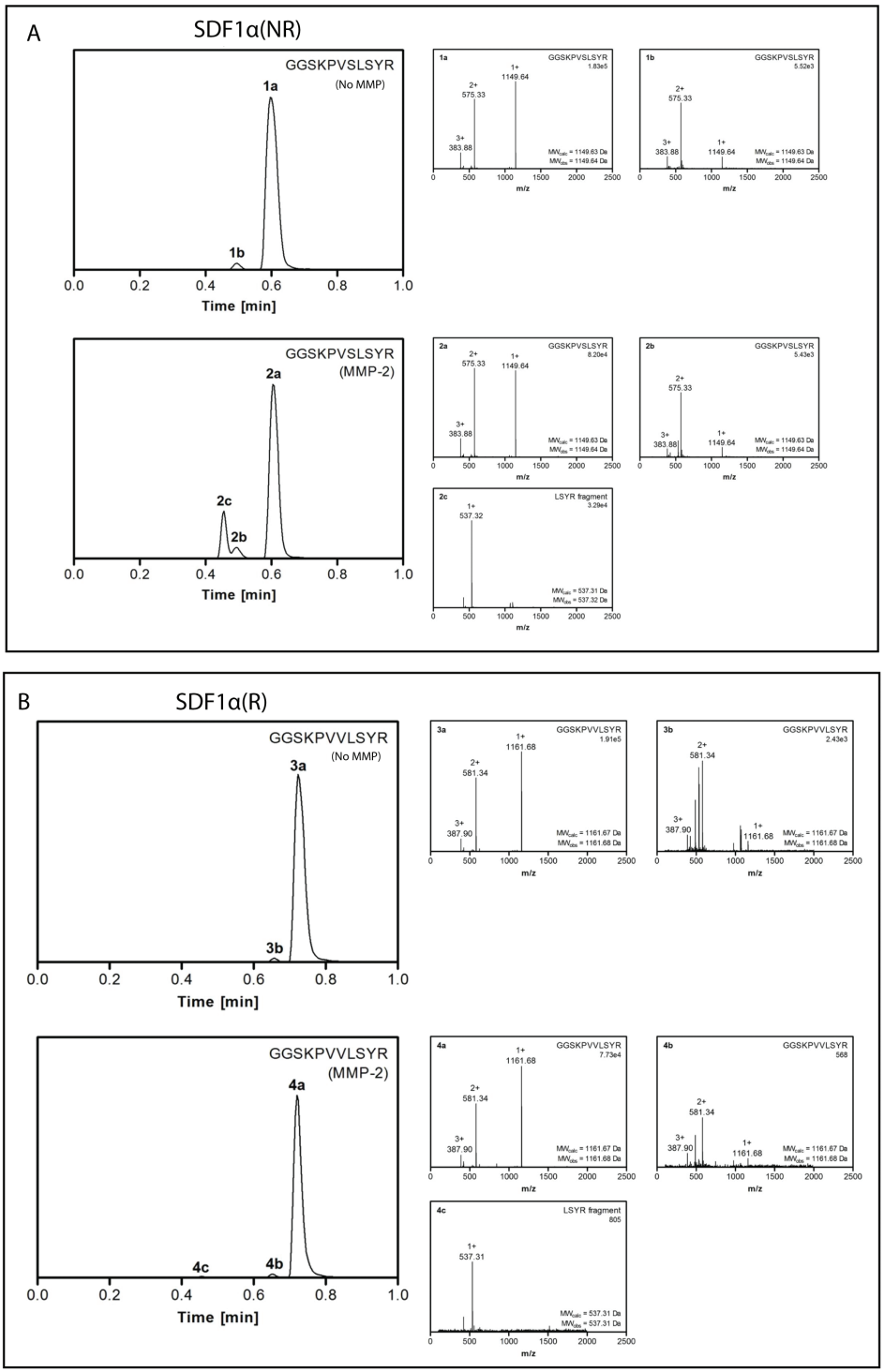

Supplemental Figure 1. Proteolytic cleavage of SDF-derived peptides by MMP2 was followed by mass spectrometry. (A) The non-resistant SDF-derived peptide was identified by mass spectrometry with a mass of 1149.64 Da (peak 1a-b and 2a-b). After incubation with MMP-2 a second fragment (peak 2c) was identified with a mass of 537.32 Da, corresponding to the cleaved LSYR-fragment. (B) The resistant SDF-derived peptide was identified with a mass of 1161.68 Da (peak 3a-b and 4a-b). The LSYR-fragment (peak 4c) was detected at a mass of 537.31 Da.

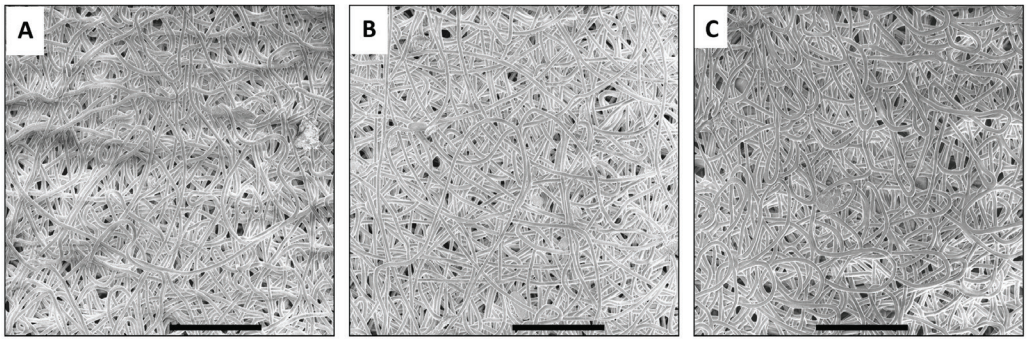

Supplemental Figure 2. SEM images after electrospinning. CE-UPy-PLLCL grafts with peptide SDF1α : A: UPy-SDF1α(R), B: UPy-SDF1α(NR) and C: Control, CE-UPy-PLLCL without the peptide. Scale bar represents 100 μm.

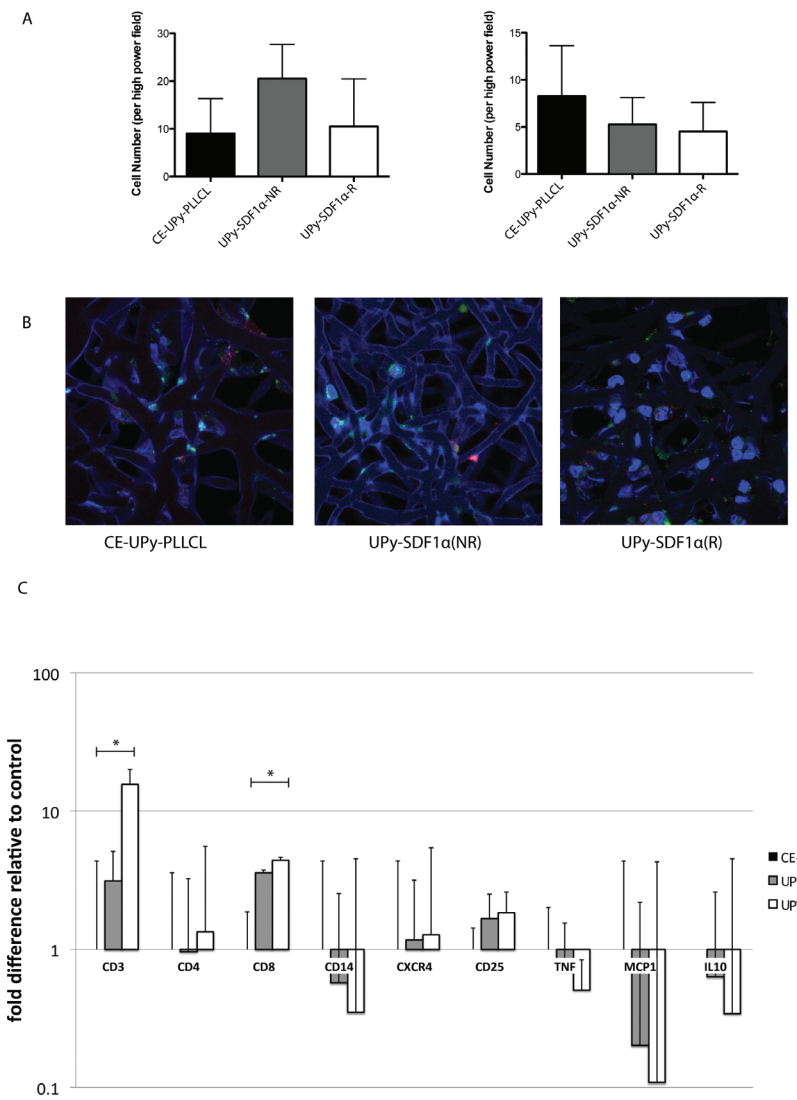

Supplemental Figure 3. A and B: Confocal microscopy of electrospun meshes after 2 hours of exposure to PBMCs in pulsatile flow. Red: CD14 Green: CD3 Blue: nuclei/fibers (background). No significant differences were found. N=4. C: qPCR of cells adhering to electrospun meshes after 2 hours in pulsatile flow conditions. A significantly higher level of CD3 and CD8 was found. No expression of CD68 was detected.

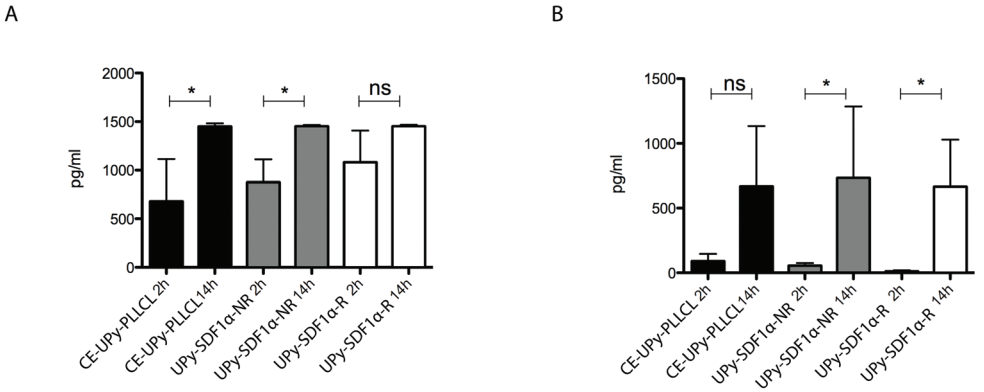

Supplemental Figure 4. A: ELISA for TNF on circulating media from bioreactor after 2 and 14 hours of pulsatile flow. N=4. B: ELISA for IL10 on circulating media from bioreactor after 2 and 14 hours of pulsatile flow. Increases were found for both TNF and IL10 after 14 hours with no significant differences between materials. N=4.

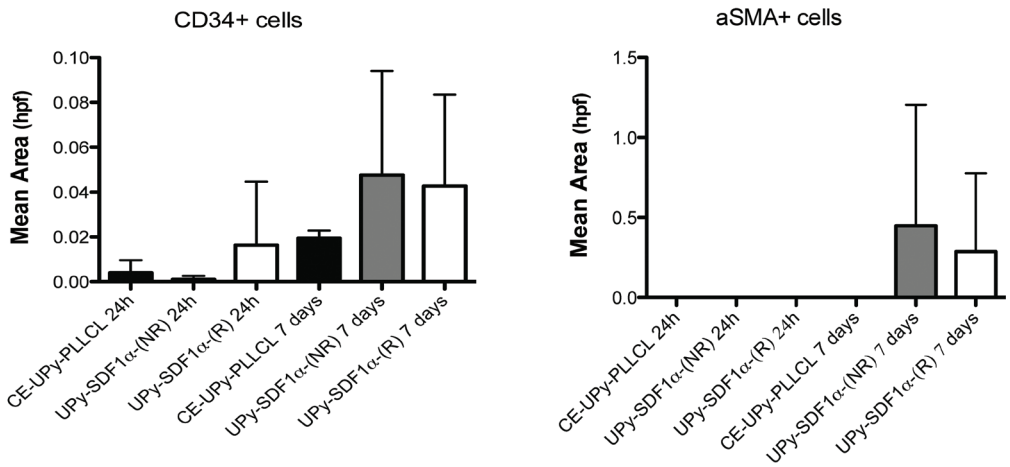

Supplemental Figure 5. CD34 and aSMA positive cells in material after 24 hours or 7 days of implantation in rat abdominal aorta interpostition graft.

m/z (calc.) = 1149.63 Da, m/z (obs) = 1149.64 Da. LSYR: m/z (calc.) = 537.31 Da, m/z (obs) = 537 Da.

References

[1] Mollet BB, Comellas-Aragones M, Spiering AJH, Söntjens SHM, Meijer EW, Dankers PYW. A modular approach to easily processable supramolecular bilayered scaffolds with tailorable properties. J Mater Chem B 2014;2:2483–93. doi:10.1039/c3tb21516d.

[2] Söntjens SHM, Renken RAE, van Gemert GML, Engels TAP, Bosman AW, Janssen HM, et al. Thermoplastic Elastomers Based on Strong and Well-Defined Hydrogen-Bonding Interactions. Macromolecules 2008;41:5703–8. doi:10.1021/ma800744c.

VIII

Tricking the body into building new heart valves and blood vessels

(a layman's summary)

(Published in the Atlas of Science)

Dimitri E.P. Muylaert

Tricking the body into building new heart valves and blood vessels

When heart valves or small blood vessels fail, surgically implanting a replacement can be a life-saving operation. Right now, replacement blood vessels are harvested from the patient's leg or chest, which is an additional invasive procedure. Heart valves can be replaced with a number of non-living materials, but none of these will grow along with the patient. This is a particular disadvantage for children receiving new heart valves, since their hearts will grow in size while the new heart valve will have to be replaced to keep up. Ideally, an implanted graft will be a living, growing structure that adapts itself during the patient's life. After implanting a blood vessel or a heart valve the new structures will be directly exposed to blood as it flows through. Blood is filled with a number of cell types that are capable of repairing and rebuilding damaged tissues. It would be beneficial if the material of a replacement graft could attract those same cells and could 'trick' the body into a repair process that will lead to the development of a new, living tissue. In order to achieve this we looked at the way damaged areas in the body, such as an infarcted heart muscle, give off a signal to blood cells to attract and stimulate them. Such a signal is usually a protein that is expelled by damaged cells which then attaches itself to the surroundings of the cells, creating a field of proteins that are attractive for blood cells. One of the most potent proteins that is capable of this is called stromal cell derived factor 1α (SDF1α). This protein works by attaching itself, on one end, to fibers such as collagens surrounding the cells. The other end of the protein sticks up into the space where blood cells flow and roll by. Receptors on the surface of the cells can easily roll over the presented SDF1α protein and, in response, will anchor themselves firmly. They will then crawl along the presented SDF1α proteins towards the highest concentration and start the process of repair.

We took the part of the SDF1α protein that binds and activates the cells and incorporated that part into the fibers of a completely synthetic material. This material was built by shooting a liquid fiber of a bioplastic towards a collector plate, which is a technique that resembles a cotton-candy machine. This technique is called electrospinning. The result is a meshwork that looks like a network of fibers under the microscope (Figure 1). Coated all along these fibers are our SDF1α fragments. We made tubes out of this material and tested its ability to attract and stimulate blood cells. We tested human blood cells in a bioreactor, a machine that simulated a pulsatile blood flow, and by implanting tubes in rats to see how a living circulatory system would influence the development of the material. We found that cells invaded and spread all through the tube material, and showed signs of reducing their inflammatory response. Materials with SDF1α fragments contained more cells than materials without them. The advantage of our material is that it is fully synthetic, meaning it is easily produced in larger quantities and easier for a surgeon to take out of a package and implant. Grafts like these will develop into living tissues made of the patient's own cells and will never be rejected. However, before we can use these materials in humans, more research is needed to see how the grafts do in longer implantation times and in larger animal models such as pigs or sheep.

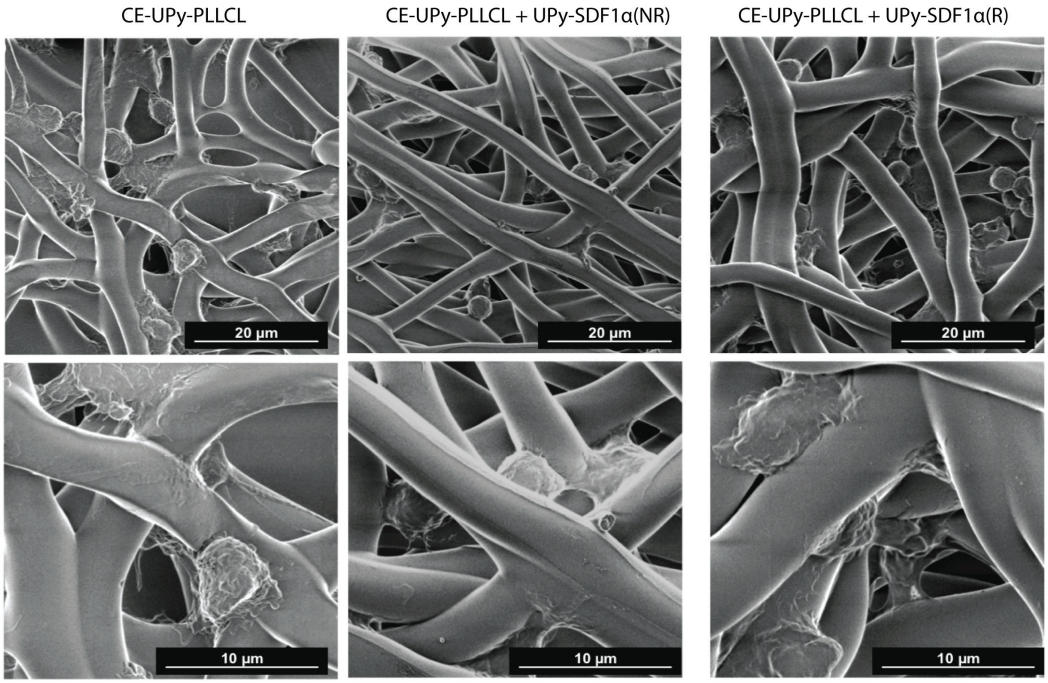

Figure 1. Scanning electron microscopy of fibers after blood cells were allowed to flow along the material. Cells adhere to the fibers. CE-UPy-PLLCLmaterial has no SDF1α fragments, CE-UPy-PLLCL + UP-SDF1a(NR) and CE-UPy-PLL-CL + UP-SDF1a(R) do contain fragments of SDF1α.

References

[1] D.E.P. Muylaert, G.C. van Almen, H. Talacua, J.O. Fledderus, J. Kluin, S.I.S. Hendrikse, et al., Early in-situ cellularization of a supramolecular vascular graft is modified by synthetic stromal cell-derived factor-1α derived peptides, Biomaterials. 76 (2015) 187–195. doi:10.1016/j.biomaterials.2015.10.052.

IX

General Discussion

General Discussion

The ideal replacement graft for cardiovascular applications would be capable of recruiting host cells and stimulating the development of tissue in situ. This concept poses many challenges such as how to design a scaffold material that functions immediately upon implantation, how to attract and stimulate the appropriate population of cells, how to modulate the foreign body response, how to maintain functionality throughout the patient's lifespan and, importantly, how to avoid adverse development of the neotissue, for instance by hyperplasia, fibrosis or stenosis.

I. The Environment of an Implanted Cardiovascular Graft

When designing a replacement graft for cardiovascular application it is important to consider the environment that the graft will function in. The stimuli in this environment are of particular importance to a cellularized graft that needs to develop into a functional living tissue. In chapter II we give an overview of the biochemical and mechanical stimuli in the environment of an implanted cardiovascular graft, with particular emphasis on their effects on endothelial to mesenchymal transition (EndMT)[1]. While heart valves and blood vessels require different approaches to tissue engineering, both can benefit from EndMT. The endothelium is capable of contributing to the formation and maintenance of extracellular matrix (ECM) through EndMT. The process is marked by a gain of alpha smooth muscle actin (αSMA) and increased expression of ECM production as well as loss of endothelium-specific cell-cell adhesion molecules such as CD31[1]. Master regulators of EndMT can be targeted by members of the transforming growth factor beta (TGFβ) family, which are released into an inflammatory environment[2]. TGFβ signaling is complicated and elaborate, involving co-factors, microRNAs, dose-dependency, fine-tuned regulation through expression of co-receptors such as endoglin and β-glycan, and the influence of mechanical stimuli. The implantation of a graft will provoke a foreign body immune response. The combination of factors released into this environment is likely to stimulate EndMT. EndMT highlights the plasticity of cells and is of immense potential for tissue engineering, however EndMT must be carefully controlled as it has also been implicated in fibrotic disease[3,4]. Modulating the immunological environment to guide or limit EndMT by incorporating factors such as interleukins or chemokines may allow for such control. In addition to chemical stimuli the mechanical environment of the graft will influence both endothelial cell alignment, signaling and ECM development. Fluid shear stress exercised by blood flow is dependent on viscosity of the blood, fluid flow and the radius of blood vessels[5]. It can either stimulate or inhibit EndMT depending on its force and direction[6]. In the case of a heart valve the properties of hemodynamic flow are different between the inlet and outlet side. With each systole blood is forced along the ventricular face in a single direction. The aortic or pulmonary face of the valve, however, sees very little flow at this stage. During diastole the blood is forced back down onto these surfaces in a turbulent pattern, which is an altogether different stimulus to the endothelium[7]. Considering that in a newly implanted graft both the endothelium and underlying mesenchyme need to undergo ho-

mogenous tissue development it is important to understand how the hemodynamic flow patterns influence EndMT. In addition to hemodynamic shear stress both valves and vessels will experience mechanical strain[8,9]. Strain is known to influence both the production and the orientation of ECM, and plays a part in EndMT[10]. Manipulating how mechanical strain is guided along the fibers of a synthetic graft may help guide ECM orientation by adhering cells[11]. Bioreactors capable of controlling the environment of cultured cells allow for the study of the combination of the mechanical stimuli and the biochemical stimuli found in situ. Improved understanding of these mechanical stimuli and how to use or influence them will lead to the optimized design of endothelialized tissue engineered cardiovascular grafts.

II. Straining Candidate Cells

Methods to study combinations of biochemical and mechanical stimuli are evolving and allowing more complex scenarios to be investigated. In chapter III we show that endothelial colony forming cells (ECFCs), endogenous candidate cells for in vivo application, are capable of producing extracellular matrix in a mechanically active environment[10]. ECM fiber alignment directly influences the load bearing properties of a tissue. Human Vena Saphena Magna cells(HVSC) align the ECM they produce in response to cyclic strain[12]. ECFCs are a candidate cell source for tissue engineered cardiovascular constructs because they can be harvested from the blood of recipients, are capable of constituting large monolayers of endothelium and can undergo EndMT[13]. By varying combinations of growth factors in the culture medium of a bioreactor capable of applying cyclic strain to 3-dimensional fibrin gels loaded with ECFCs we tested the response of ECFCs to a combination of stimuli. While cyclic strain induces EndMT in valvular endothelial cells (VECs), we found an inhibitory effect of cyclic strain on matrix expression in ECFCs, even in the presence of TGFβ1. This indicates that cyclic strain may impede EndMT in tissue engineered constructs incorporating ECFCs. The behavior of ECFCs in these conditions was opposite to the response of HVSCs. However, priming the ECFCs with TGFβ1 prior to exposure to cyclic strain reversed the response to mechanical strain and led to increased matrix production. Interestingly, ECFCs produce organized elastin, a protein that is responsible for elastic properties in vascular structures. Elastin is not properly produced and deposited by HVSCs, the current golden standard for ECM-based tissue engineering[10]. The data presented in chapter III indicates that the timing of exposure to stimuli influences how cells respond to a mechanical environment, and that cells may be ‘prepared’ for this exposure before implantation.

III. A MIR-aculous Flow

In addition to cyclic strain, another inevitable mechanical stimulus to implanted cardiovascular tissue engineered grafts will be hemodynamic shear stress caused by fluid flow[1]. Endothelial cells sense fluid flow through cilia[14], activation by integrins following tension transferred through cell-cell adhesion molecules[15], or nuclear displacement due to hemodynamic drag[16]. In response, endothelial cells align in the direction of flow and alter their cross-talk to

adjacent cell types such as myofibroblasts, which results in changes to ECM composition and subsequently the mechanical properties of blood vessels[17]. Through this mechanism endothelium regulates a homeostasis between force sensing and force generation. Shear stresses between 10 and 20dyn/cm^2 are typical of vasculature, and weaker flow is associated with pathological conditions such as atherosclerosis[18] and aneurysmata[19]. Fluid flow regulates TGFβ signaling in the developing heart[20,21]. The TGFβ family regulates the expression of microRNAs[22]. The microRNA29 family (mir29a, mir29b, mir29c) targets the mRNA of elastin and collagen type 1, repressing their expression[23]. TGFβ1, which we investigated in chapter III, mostly lowers the expression of mir29b. Considering the redundancy between the mir29 subtypes it is likely that some repression of the targets still occurs. TGFβ2, however, is capable of lowering the expression of all three mir29s[22]. Chapter IV reports preliminary findings that indicate that lowering the expression of the mir29 family by knockdown using locked nucleic acid (LNA) transfection indeed increases the expression of elastin in ECFCs. Static culturing of ECFCs with TGFβ2, however, did not appear to lower the expression of the microRNAs. In shear conditions ECFCs showed a trend for lower expression of TGFβ2 and a trend for increased expression of the mir29 family. In addition, endothelial markers were increased in fluid flow, particularly VE cadherin, PECAM and VEGFR2, which together form an essential endothelial mechanosensory complex. Taken together these pilot experiments may indicate that physiological flow on ECFCs confers some protection to the endothelial phenotype and may inhibit EndMT. Coupled to the results of chapter III, a picture emerges where physiological mechanical stimuli, namely cyclic strain and hemodynamic shear stress, may constitute a pro-endothelium and anti-EndMT stimulus. The relevance of these findings pertains to EndMT: If EndMT is desired in tissue engineered constructs these potential anti-EndMT conditions must be anticipated, for instance by delivery of bioactive molecules through the scaffold materials themselves.

IV. Tissue Regeneration: Learning From the Best

To identify bioactive factors for application in tissue engineering, much can be learned from in vivo repair processes. Neotissue formation, for instance in the context of wound healing, is guided by chemokine signaling in vivo[24]. In chapter V we give an overview of the events that guide tissue repair and highlight processes that may be exploited in tissue engineering approaches. Tissue damage creates a complex environment of inflammatory factors released by damaged cells such as vascular endothelial growth factor (VEGF), stromal cell derived factor 1a (SDF1α), platelet derived growth factor b (PDGFbb) and macrophage chemoattractant protein 1 (MCP1) [24]. These factors stimulate the expression of adhesion molecules such as integrins and bind to the ECM in the damaged area, creating a field of chemoattractive molecules[25]. Circulating cells home towards the highest concentration of the chemokines but are also activated along the way. In response to this activation the cells produce and secrete additional signaling factors that further contribute to the ‘orchestra’ of signaling factors that ultimately guides neotissue formation[24]. Considering that the attraction of cells and the subsequent stimulation of a pro-tissue forming signaling environment would be of great benefit to implanted graft materials, mimicking

these in vivo repair processes is an attractive approach to tissue engineering. One of the most important factors in tissue repair is SDF1α. It is highly expressed in hypoxic tissues such as the bone marrow where it regulates the homing and mobilization of progenitor cells in the stroma[26], where it causes progenitor cells to mobilize into circulation and home to the site of damage[27]. SDF1α is involved in repair signaling in heart, kidney, lung, brain and vascular tissues. It is a strong attractant of lymphocytes and capable of influencing the polarization of t-helper cells and t-regulatory cells[28]. It also plays a role in the development of neointimal hyperplasia, indicating that while SDF1α is capable of regulating tissue repair, it may also cause pathological tissue development[29].

Cell-free biological grafts for cardiovascular application are already being applied in clinical practice in the form of decellularized extracellular matrix, often derived from animal tissue such as pericardium treated to remove immunogenic epitopes[30]. Biologically active molecules such as VEGF can be added to these materials and have been shown to reduce neointimal hyperplasia[31]. There are various ways to incorporate these molecules, and the manner in which the molecules are presented to the cellular environment can influence their potency. The molecular structure of SDF1α, for instance, contains an ECM binding domain that is coupled to a receptor-activating domain via a stabilizing middle section[32]. This allows the receptor-activating domain to be presented to cells facilitating interaction with the receptor CXCR4. Exploiting this property of the molecule, combining an ECM coating with SDF1α on biological graft material results in improved cellularization and tissue formation[33]. Decellularization of pre-existing tissues, however, has limited scalability and there is an inherent risk of incomplete decellularization which has been documented to have fatal consequences[34]. Fully synthetic materials may avoid these adverse effects. Fabrication methods such as electrospinning can yield a 3-dimensional environment that resembles ECM fibers with tunable mechanical properties[35]. In addition, the materials used in the process are easily accessible for modification with bioactive molecules and have good reproducibility and scalability[36].

In a non-covalent approach factors may be mixed directly into scaffold meshwork, for instance through gels. Depending on the characteristics of the gel the factors may be released with a measure of control over the timing. Multiple factors may be incorporated into a single scaffold[37]. In a covalent approach factors are directly anchored to the surface of the graft material [38], offering more direct control over the presentation of the molecules. The graft material itself may be loaded with bioactive factors that are released as the material breaks down. In a supramolecular approach factors are mixed in with the polymers used to produce graft material, which allows for a greater manufacturing ease[38]. Enhanced design of the molecules themselves may be a powerful way to influence the cellular response in addition to the presentation or delivery of bioactive molecules. An example is smart release of the factors by incorporating cleavage sites for enzymes known to be released in the environment of the graft[39]. Accurate in vivo models are required to investigate the in situ dynamics of the cellular response.

V. A Burst of Blood Cells

An inflammatory response to implanted material is traditionally considered an adverse event and much effort and research is aimed towards minimizing the interaction of the immune system with graft materials. However, the phase of neotissue formation and inflammation reduction, which is a part of this response, may be exploited to induce a natural regenerative response. MCP1 is a major attractor of immune cells involved in tissue resolution following damage in vivo[40]. In chapter VI we used a fast-releasing gel to bioactivate electrospun PCL vascular grafts with MCP1 and implanted these in the abdominal aorta of rats in an interposition graft. While this rodent model is accessible and allows for reproducible results with a high number of test subjects there are inherent differences between human and rodent tissue repair that complicate the extrapolation of results. One of the most important differences is that in rodent vascular repair transmural ingrowth and transanastomosal ingrowth in the interposition graft contributes greatly to the cellular influx[41,42]. In human vasculature such transanastomosal ingrowth is much more limited[43]. In order to investigate the contribution of cells out of circulation and restrict the lateral ingrowth across the anastomosis we shielded the implanted tubes on their ends with a section of gore-tex tube material, connecting the rat aorta to the graft material. Another gore-tex sheet wrapped around the graft prevented transmural ingrowth, ensuring that only cells derived out of circulation could respond to the eluting MCP1 and contribute to the developing implant. The release of MCP1 from the graft was highest in the first three hours indicating that we achieved a burst release, which likely also induced systemic mobilization of immune cells in the host. Importantly, all implanted grafts were highly cellularized. The contribution of MCP1 to the long-term development of the implants became most pronounced after 3 months, when the neotissue contained more CD34+ progenitor cells and showed a confluent monolayer of endothelium. In addition, there was a trend for higher expression of SDF1α, potentially accounting for the higher number of progenitor cells. Combined these data indicate that influencing the immune response even in the first few hours of implantation can influence the graft outcome as much as three months later. A possible explanation for this observation is that the initial, 'first responder' population of cells dictates the environment for the subsequent cellular events.

VI. Fully Synthetic Biology

The use of a full-length protein presents challenges to the scalability and clinical translatability of the approach. As described in chapter V, SDF1α is one of the most potent factors in homing and mobilization of progenitor cells[24] and a modulator of the expression of signaling factors by immune cells. Short peptide sequences based on SDF1α retain specific activity through CXCR4[44]. Such short peptide sequences are accessible for synthetic production methods that are reproducible, cheap, easy to scale up and comply with Good Manufacturing Practices (GMP). Direct peptide synthesis allows for the tweaking of the molecular properties on an amino-acid level. For instance, the wild-type protein contains cleavage sites for matrix metalloproteinases (MMPs) that inhibit SDF1α and are expressed in inflammatory environments[45].

Removing this cleavage site improves the longevity of the SDF1α molecule in the presence of MMPs[46]. In chapter VII we modified peptide sequences based on the receptor activating domain of SDF1α with supramolecular four-fold hydrogen bonding ureido-pyrimidinone (UPy) moiety, which allows for the incorporation of the UPy- SDF1α-derived peptides into a UPy-modified polymer scaffold. We used poly(L-lactic acid caprolactone) (PLLCL) functionalized with UPy-moieties to anchor the peptides to polymeric material suitable for processing through electrospinning. Considering the nature of the molecular bonding to the material there was minimal leakage and therefore no burst release as was investigated in chapter VI. The local presentation of the molecules resulted in docking sites for circulating cells specifically stimulating them to produce a pro-tissue formation signaling environment. We used human blood cells in a bioreactor applying pulsatile unidirectional flow to investigate the specific retention and stimulation of peripheral blood mononuclear cells. We found specific retention of lymphocytes and a downregulation of inflammatory markers, consistent with the known function of full-length SDF1α in vivo. We further confirmed that the peptide sequences indeed function through activating the specific SDF1α receptor CXCR4 by specifically blocking cellular migration towards the peptides with specific CXCR4 inhibitors. Short implantation in vivo in rat abdominal aorta interposition grafts showed enhanced, homogenous and deep cellular penetration into the grafts by cells derived out of circulation. The cell population found in the grafts after 7 days showed reduced expression of inflammatory factors MCP1 and TNFα while the cellularity was higher. In chapter VI a burst release of MCP1 induced enhanced cellularization of a graft. Subsequent higher expression of SDF1α in those grafts coincided with a higher number of progenitor cells and better tissue development in long-term implantations. Immediately incorporating a stable SDF1α signal into graft material may correspond to a step in the inflammatory process closer to tissue regeneration. The control we achieved over presentation of bioactive factors in synthetic materials is a first step towards tailoring an ideal signaling environment and 'trick' the immune system into rebuilding living functional tissue into a fully synthetic graft.

VII. Clinical considerations

The approach to in situ tissue engineering described in chapter VII focusses on a synthetic scaffold that is meant to be temporary and which will break down over time. This approach allows the incorporation of bioactive factors within the fibers, leading to a slow release mechanism built into the structure of the graft. However, it is difficult to assess the degradation dynamics of the material in vivo, and future research will need to focus on finding the ideal balance between breakdown of the synthetic material and build-up of the autologous neo-tissue to avoid sudden graft failure. This balance is in no small part dependent on the health of the recipient. It is therefore highly likely that, in future clinical practice, patients should be screened for their ability to repopulate and regenerate a vascular graft prior to undergoing the procedure. Similar methods are currently employed to screen patients prior to autologous bone marrow transplants. Before this practical clinical screening process can be designed more basic scientific research is needed to identify which cells and what sources dictate or predict the success of a cell-free

vascular graft. In addition to screening, boosting the number of circulating progenitor cells prior to implantation may be a feasible approach to maximizing the success rate of cell-free implanted grafts. Lastly, it may not be necessary for graft material to disintegrate if surface-adhering bioactive molecules such as we describe in chapter VII are sufficient to induce tissue development and endothelialization that leads to a quiescent, cellularized and functional graft, avoiding the considerable risk of graft failure due to loss of structural integrity.

The Language of Tissue Engineering

The strategies employed in future studies should investigate conditions based on the in vivo situation of a graft. 'Reverse engineering' is the process of taking apart and studying an object in order to duplicate or enhance it. When applied to biological mechanisms (and with a little creativity) 'Reverse Tissue Engineering' may lead to faster development of clinically feasible applications. To move the field forward, however, we need to overcome not only scientific challenges. The intricacies of biomedical and in vivo work are numerous and require great expertise. Likewise, the science behind synthetic molecular technology is elaborate and dauntingly complicated. It is crucial to the future of tissue engineering that experts working on clinical translation and experts working on basic molecular science can speak the same language.

References

[1] D.E.P. Muylaert, O.G. de Jong, G.G.G. Slaats, F.E. Nieuweboer, J.O. Fledderus, M.-J. Goumans, et al., Environmental Influences on Endothelial to Mesenchymal Transition in Developing Implanted Cardiovascular Tissue-Engineered Grafts, (2015) ten.teb.2015.0167–10. doi:10.1089/ten.teb.2015.0167.

[2] M.-J. Goumans, F. Lebrin, G. Valdimarsdottir, Controlling the angiogenic switch: a balance between two distinct TGF-b receptor signaling pathways, Trends in Cardiovascular Medicine. 13 (2003) 301–307.

[3] R.B. Hinton Jr, J. Lincoln, G.H. Deutsch, H. Osinska, P.B. Manning, D.W. Benson, et al., Extracellular matrix remodeling and organization in developing and diseased aortic valves, Circ Res. 98 (2006) 1431.

[4] L.A. van Meeteren, P. ten Dijke, Regulation of endothelial cell plasticity by TGF-β, Cell Tissue Res. 347 (2011) 177–186. doi:10.1007/s00441-011-1222-6.

[5] J.D. Humphrey, S.L. Delange, An Introduction to Biomechanics: Solids and Fluids, Analysis and Design - Jay D. Humphrey, Sherry L. Delange - Google Books, (2004).

[6] A.D. Egorova, P.P.S.J. Khedoe, M.-J.T.H. Goumans, B.K. Yoder, S.M. Nauli, P. ten Dijke, et al., Lack of primary cilia primes shear-induced endothelial-to-mesenchymal transition, Circ Res. 108 (2011) 1093–1101. doi:10.1161/CIRCRESAHA.110.231860.

[7] K. Van der Heiden, B.P. Hierck, R. Krams, R. de Crom, C. Cheng, M. Baiker, et al., Endothelial primary cilia in areas of disturbed flow are at the base of atherosclerosis, Atherosclerosis. 196 (2008) 542–550. doi:10.1016/j.atherosclerosis.2007.05.030.

[8] N.J.B. Driessen, A. Mol, C.V.C. Bouten, F.P.T. Baaijens, Modeling the mechanics of tissue-engineered human heart valve leaflets, J Biomech. 40 (2007) 325–334. doi:10.1016/j.jbiomech.2006.01.009.

[9] M.A.J. Cox, J. Kortsmit, N. Driessen, C.V.C. Bouten, F.P.T. Baaijens, Tissue-Engineered Heart Valves Develop Native-like Collagen Fiber Architecture, Tissue Eng Part A. 16 (2010) 1527–1537. doi:10.1089/ten.tea.2009.0263.

[10] N. de Jonge, D.E.P. Muylaert, E.S. Fioretta, F.P.T. Baaijens, J.O. Fledderus, M.C. Verhaar, et al., Matrix production and organization by endothelial colony forming cells in mechanically strained engineered tissue constructs, PLoS ONE. 8 (2013) e73161. doi:10.1371/journal.pone.0073161.

[11] E.S. Fioretta, M. Simonet, A.I.P.M. Smits, F.P.T. Baaijens, C.V.C. Bouten, Differential Response of Endothelial and Endothelial Colony Forming Cells on Electrospun Scaffolds with Distinct Microfiber Diameters, Biomacromolecules. 15 (2014) 821–829. doi:10.1021/bm4016418.

[12] L.V. Thomas, Lekshmi V, P.D. Nair, Tissue engineered vascular grafts — Preclinical aspects, International Journal of Cardiology. 167 (2013) 1091–1100. doi:10.1016/j.ijcard.2012.09.069.

[13] I. Vranken, G. De Visscher, A. Lebacq, E. Verbeken, ScienceDirect.com - Biomaterials - The recruitment of primitive Lin− Sca-1+, CD34+, c-kit+ and CD271+ cells during the early intraperitoneal foreign body reaction, Biomaterials. (2008).
[14] S. Kallakuri, J.A. Yu, J. Li, Y. Li, B.M. Weinstein, S. Nicoli, et al., Endothelial Cilia Are Essential for Developmental Vascular Integrity in Zebrafish, Journal of the American Society of Nephrology. 26 (2014) 864–875. doi:10.1681/ASN.2013121314.
[15] E. Tzima, M. Irani-Tehrani, W.B. Kiosses, E. Dejana, D.A. Schultz, B. Engelhardt, et al., A mechanosensory complex that mediates the endothelial cell response to fluid shear stress, Nature. 437 (2005) 426–431. doi:10.1038/nature03952.
[16] E. Tkachenko, E. Gutierrez, S.K. Saikin, P. Fogelstrand, C. Kim, A. Groisman, et al., The nucleus of endothelial cell as a sensor of blood flow direction, Biol Open. 2 (2013) 1007–1012. doi:10.1242/bio.20134622.
[17] M. Coen, G. Gabbiani, M.-L. Bochaton-Piallat, Myofibroblast-mediated adventitial remodeling: an underestimated player in arterial pathology, Arteriosclerosis, Thrombosis, and Vascular Biology. 31 (2011) 2391–2396. doi:10.1161/ATVBAHA.111.231548.
[18] A.M. Malek, S.L. Alper, S. Izumo, Hemodynamic shear stress and its role in atherosclerosis, Jama. 282 (1999) 2035–2042.
[19] H. Meng, V.M. Tutino, J. Xiang, A. Siddiqui, High WSS or low WSS? Complex interactions of hemodynamics with intracranial aneurysm initiation, growth, and rupture: toward a unifying hypothesis, AJNR Am J Neuroradiol. 35 (2014) 1254–1262. doi:10.3174/ajnr.A3558.
[20] M. Azhar, K. Brown, C. Gard, H. Chen, S. Rajan, D.A. Elliott, et al., Transforming growth factor Beta2 is required for valve remodeling during heart development, Dev. Dyn. 240 (2011) 2127–2141. doi:10.1002/dvdy.22702.
[21] P.W. Riem Vis, J. Kluin, J.P.G. Sluijter, L.A. van Herwerden, C.V.C. Bouten, Environmental regulation of valvulogenesis: implications for tissue engineering, Eur J Cardiothorac Surg. 39 (2011) 8–17. doi:10.1016/j.ejcts.2010.05.032.
[22] C. Luna, G. Li, J. Qiu, D.L. Epstein, P. Gonzalez, Cross-talk between miR-29 and Transforming Growth Factor-Betas in Trabecular Meshwork Cells, Invest. Ophthalmol. Vis. Sci. 52 (2011) 3567–3572. doi:10.1167/iovs.10-6448.
[23] E. van Rooij, L.B. Sutherland, J.E. Thatcher, J.M. DiMaio, R.H. Naseem, W.S. Marshall, et al., Dysregulation of microRNAs after myocardial infarction reveals a role of miR-29 in cardiac fibrosis, Proceedings of the National Academy of Sciences. 105 (2008) 13027–13032. doi:10.1073/pnas.0805038105.
[24] D.E.P. Muylaert, J.O. Fledderus, C.V.C. Bouten, P.Y.W. Dankers, M.C. Verhaar, Combining tissue repair and tissue engineering; bioactivating implantable cell-free vascular scaffolds, Heart. 100 (2014) 1825–1830. doi:10.1136/heartjnl-2014-306092.
[25] D.D. Patel, W. Koopmann, T. Imai, L.P. Whichard, O. Yoshie, M.S. Krangel, Chemokines have diverse abilities to form solid phase gradients, Clin. Immunol. 99 (2001) 43–52. doi:10.1006/clim.2000.4997.
[26] M. Shirozu, T. Nakano, J. Inazawa, K. Tashiro, H. Tada, T. Shinohara, et al., Structure and Chromosomal Localization of the Human Stromal Cell-Derived Factor 1 (SDF1) Gene, Ge-

nomics. 28 (1995) 495–500. doi:10.1006/geno.1995.1180.
[27] X. Xu, F. Zhu, M. Zhang, D. Zeng, D. Luo, G. Liu, et al., Stromal cell-derived factor-1 enhances wound healing through recruiting bone marrow-derived mesenchymal stem cells to the wound area and promoting neovascularization, Cells Tissues Organs (Print). 197 (2013) 103–113. doi:10.1159/000342921.
[28] N. Karin, The multiple faces of CXCL12 (SDF-1) in the regulation of immunity during health and disease, J. Leukoc. Biol. 88 (2010) 463–473. doi:10.1189/jlb.0909602.
[29] J. Sheng, W.-W. Cai, N.-Y. Fang, S.-Q. Wang, J.-J. Wu, Role of stromal-derived factor-1<alpha>/CXCR4 in neo-intimal repair, Cardiovasc J Afr. 22 (2011) 313–318. doi:10.5830/CVJA-2010-075.
[30] H. Kurobe, M.W. Maxfield, C.K. Breuer, T. Shinoka, Concise review: tissue-engineered vascular grafts for cardiac surgery: past, present, and future, Stem Cells Transl Med. 1 (2012) 566–571. doi:10.5966/sctm.2012-0044.
[31] X. Ye, H. Wang, J. Zhou, H. Li, J. Liu, Z. Wang, et al., The Effect of Heparin-VEGF Multilayer on the Biocompatibility of Decellularized Aortic Valve with Platelet and Endothelial Progenitor Cells, PLoS ONE. 8 (2013) e54622. doi:10.1371/journal.pone.0054622.
[32] W. Hiesinger, J.M. Perez-Aguilar, P. Atluri, N.A. Marotta, J.R. Frederick, J.R. Fitzpatrick, et al., Computational Protein Design to Reengineer Stromal Cell-Derived Factor-1 Generates an Effective and Translatable Angiogenic Polypeptide Analog, Circulation. 124 (2011) S18–S26. doi:10.1161/CIRCULATIONAHA.110.009431.
[33] W. Flameng, G. De Visscher, L. Mesure, H. Hermans, R. Jashari, B. Meuris, Coating with fibronectin and stromal cell-derived factor-1α of decellularized homografts used for right ventricular outflow tract reconstruction eliminates immune response-related degeneration, The Journal of Thoracic and Cardiovascular Surgery. 147 (2014) 1398–1404.e2. doi:10.1016/j.jtcvs.2013.06.022.
[34] P. Simon, M.T. Kasimir, G. Seebacher, G. Weigel, R. Ullrich, U. Salzer-Muhar, et al., Early failure of the tissue engineered porcine heart valve SYNERGRAFTTM in pediatric patients, European Journal of Cardio-Thoracic Surgery. 23 (2003) 1002.
[35] J. Doshi, J. Doshi, D.H. Reneker, D.H. Reneker, Electrospinning process and applications of electrospun fibers, Journal of Electrostatics. 35 (1995) 151–160. doi:10.1016/0304-3886(95)00041-8.
[36] L. Persano, A. Camposeo, C. Tekmen, D. Pisignano, Industrial Upscaling of Electrospinning and Applications of Polymer Nanofibers: A Review, Macromol. Mater. Eng. 298 (2013) 504–520. doi:10.1002/mame.201200290.
[37] H. Zhang, X. Jia, F. Han, J. Zhao, Y. Zhao, Y. Fan, et al., Dual-delivery of VEGF and PDGF by double-layered electrospun membranes for blood vessel regeneration, Biomaterials. 34 (2013) 2202–2212. doi:10.1016/j.biomaterials.2012.12.005.
[38] P. Dankers, M. Harmsen, L. Brouwer, M. van Luyn, E. Meijer, A modular and supramolecular approach to bioactive scaffolds for tissue engineering, 4 (2005) 568–574.
[39] V.F.M. Segers, T. Tokunou, L.J. Higgins, C. MacGillivray, J. Gannon, R.T. Lee, Local Delivery of Protease-Resistant Stromal Cell Derived Factor-1 for Stem Cell Recruitment After

Myocardial Infarction, Circulation. 116 (2007) 1683–1692. doi:10.1161/CIRCULATIONAHA.107.718718.
[40] J.D. Roh, R. Sawh-Martinez, M.P. Brennan, S.M. Jay, L. Devine, D.A. Rao, et al., Tissue-engineered vascular grafts transform into mature blood vessels via an inflammation-mediated process of vascular remodeling, Proceedings of the National Academy of Sciences. 107 (2010) 4669–4674. doi:10.1073/pnas.0911465107.
[41] B. van der Lei, C.R. Wildevuur, P. Nieuwenhuis, E.H. Blaauw, F. Dijk, C.E. Hulstaert, et al., Regeneration of the arterial wall in microporous, compliant, biodegradable vascular grafts after implantation into the rat abdominal aorta. Ultrastructural observations, Cell Tissue Res. 242 (1985) 569–578.
[42] Z. Zhang, Z. Wang, S. Liu, M. Kodama, Pore size, tissue ingrowth, and endothelialization of small-diameter microporous polyurethane vascular prostheses, Biomaterials. 25 (2004) 177–187.
[43] P. Zilla, D. Bezuidenhout, P. Human, Prosthetic vascular grafts: wrong models, wrong questions and no healing, Biomaterials. 28 (2007) 5009–5027. doi:10.1016/j.biomaterials.2007.07.017.
[44] W. Hiesinger, J.M. Perez-Aguilar, P. Atluri, N.A. Marotta, J.R. Frederick, J.R. Fitzpatrick, et al., Computational protein design to reengineer stromal cell-derived factor-1α generates an effective and translatable angiogenic polypeptide analog, Circulation. 124 (2011) S18–26. doi:10.1161/CIRCULATIONAHA.110.009431.
[45] G.A. McQuibban, G.S. Butler, J.H. Gong, L. Bendall, C. Power, I. Clark-Lewis, et al., Matrix Metalloproteinase Activity Inactivates the CXC Chemokine Stromal Cell-derived Factor-1, J. Biol. Chem. 276 (2001) 43503–43508. doi:10.1074/jbc.M107736200.
[46] V.F.M. Segers, T. Tokunou, L.J. Higgins, C. MacGillivray, J. Gannon, R.T. Lee, Local delivery of protease-resistant stromal cell derived factor-1 for stem cell recruitment after myocardial infarction, Circulation. 116 (2007) 1683–1692. doi:10.1161/CIRCULATIONAHA.107.718718.

Appendix

X

Nederlandstalige Samenvatting

Algemene Discussie

Het ideale cardiovasculaire implantaat zou het vermogen hebben om cellen van de gastheer aan te trekken en de ontwikkeling van weefsel in situ te stimuleren. Materiaal dat ontworpen is om uiteindelijk af te breken kan als tijdelijke structuur functioneren dat langzaam opgevuld en vervangen wordt door autoloog weefsel, waarna uiteindelijk een volledig functionele en levende structuur achterblijft. Dit concept kent veel uitdagingen en onbeantwoorde vragen zoals: hoe maken we een materiaal dat direct functioneert na implantatie, hoe trekken we de juiste cellen aan en hoe stimuleren we deze, hoe moduleren we de afweerreactie, hoe zorgen we ervoor dat de nieuwe structuur een leven lang functioneel blijft en, ten slotte, hoe voorkomen we dat het implantaat zich pathologisch ontaard, bijvoorbeeld door de ontwikkeling van hyperplasie, fibrose of stenose.

I. De Omgeving van een Geïmplanteerd Cardiovasculair Construct

Bij het ontwerpen van een vervangende structuur voor cardiovasculaire toepassing is het belangrijk om de omgeving van het implantaat in het oog te houden. De stimuli die in deze omgeving ervaren worden zijn van groot belang voor de ontwikkeling van een gecellulariseerd construct. In hoofdstuk II geven we een overzicht van de biochemische en mechanische prikkels die in de omgeving van een geïmplanteerd construct een rol spelen met speciale nadruk op de effecten op endotheel-naar-mesenchymale transitie (EndMT) [1]. Hoewel hartkleppen en bloedvaten uiteindelijk een aparte aanpak behoeven kunnen ze beiden gebruik maken van dit proces. Het endotheel kan bijdragen aan de productie en het onderhoud van extracellulaire matrix (ECM) door EndMT. Het proces wordt gekenmerkt door het tot expressie brengen van alpha smooth muscle actin (αSMA) en verhoogde expressie van ECM eiwitten gepaard met een verlies aan expressie van endotheel-specifieke cell-cell adhesie moleculen zoals CD31[1]. ‘Master-regulators’ van EndMT kunnen worden aangegrepen door leden van de transforming growth factor 1 beta familie (TGFβ), welke een grote rol spelen in de inflammatoire micro omgeving[2]. TGFβ signalering is complex en uitgebreid, onder andere beïnvloed door co-factoren, microRNAs, dosis-afhankelijkheid, regulatie door co-receptoren zoals endoglin en β-glycan, en de invloed van mechanische prikkels. Het implanteren van een ontworpen cardiovasculair construct zal een afweer response veroorzaken. De combinatie van factoren die in deze omgeving wordt losgelaten zal waarschijnlijk pro-EndMT zijn. EndMT onderstreept de plasticiteit van cellen en is van immens potentieel nut voor Tissue Engineering, maar het proces moet voorzichtig onder controle gehouden worden aangezien het ook geïmpliceerd is bij fibrotische ziekten[3,4]. Het moduleren van de immunologische omgeving om EndMT te besturen of beperken kan mogelijk gemaakt worden door het inbouwen van factoren zoals interleukines of chemokines. Ook de mechanische omgeving zal een grote invloed hebben op endotheel cell uitlijning, signalering en ECM productie. Schuifkracht door vloeistofstroming van langsstromend bloed is afhankelijk van de viscositeit, de stroomsnelheid en de radius van het bloedvat[5]. Deze stress kan een stimuleren of remmend

effect hebben op EndMT afhankelijk van de kracht en richting van de stroming[6]. In het geval van een hartklep verschillen de eigenschappen van hemodynamische flow tussen de instroom- en uitstroomzijde van de klep. Bij elke systole wordt bloed langs de ventriculaire zijde van de klep geforceerd in een enkele richting. De aorta of pulmonaire zijde van de klep ziet in dit stadium weinig tot geen flow, wat op zichzelf al een prikkel is voor endotheelcellen. Tijdens diastole wordt bloed terug geforceerd op de sluitende klep in een turbulent patroon, wat een volledig andere prikkel geeft aan het endotheel van de klep[7]. Aangezien een nieuw geïmplanteerde structuur zich uniform en homogeen zal moeten ontwikkelen aan beide zijden is het belangrijk om te begrijpen hoe de hemodynamische flow de weefselontwikkeling zal beïnvloeden. Bovenop de vloeistofstroming zullen hartkleppen en bloedvaten ook mechanische rek ervaren[8,9]. Rek beïnvloedt zowel de productie als oriëntatie van ECM strengen en speelt een rol in de regulatie van EndMT[10]. Mogelijk kan het begeleiden van de mechanische rek langs de strengen van synthetisch materiaal helpen met de depositie van ECM door adherende cellen[11]. Bioreactoren die in staat zijn om zowel de mechanische als biochemische omgeving van materialen te manipuleren staan gelijktijdig onderzoek toe van deze prikkels. Verbeterd inzicht in hoe de omgeving van een implantaat de ontwikkeling zal beïnvloeden zal leiden tot verbeterd ontwerp van tissue engineered cardiovasculaire constructen.

II. De Kandidaat Oprekken

De methoden om combinaties van biochemisch en mechanische prikkels gelijktijdig te bestuderen evolueren en staan telkens complexere scenarios toe. In hoofdstuk III laten we zien dat endotheel kolonie vormende cellen (ECFCs), kandidaat cellen voor in vivo applicatie, in staat zijn om ECM te produceren in een mechanisch actieve omgeving[10]. ECM streng depositie en organisatie heeft direct invloed op de verdeling van krachten in een weefsel. Menselijke vena saphena magna cellen (HVSCs) zijn in staat om hun geproduceerde ECM uit te lijnen in de richting van cyclische rek[12]. ECFCs zijn een kandidaat cel type voor tissue engineering omdat ze direct uit het bloed kunnen worden geïsoleerd, in staat zijn om grote hoeveelheden monolaag endotheel te produceren en het vermogen hebben om EndMT te ondergaan[13]. Ze worden gezien als een model cel type voor single-step tissue engineering, in welke cel-vrije constructen worden geïmplanteerd. Door het variëren van groeifactoren in het kweek medium van een bioreactor die cyclische rek geeft op 3-dimensionele fibrine gelen met ECFCs hebben we de reactie van ECFCs op verschillende stimuli getest. Hoewel cyclische rek EndMT kan veroorzaken in valvulaire endotheel cellen (VECs) vonden we een remmend effect van cyclische rek op ECM productie door ECFCs. Deze reactie geeft aan dat cyclische rek mogelijk een remmend effect heeft op EndMT in ECFCs. Het gedrag van ECFCs staat haaks op dat van HVSCs. Echter, het voorbehandelen van ECFCs met TGFβ1, vooraf aan blootstelling aan mechanische rek, keerde de reactie om en gaf een cel type dat in staat was meer ECM te produceren. Opvallend was dat ECFCs elastine kunnen produceren, het eiwit dat verantwoordelijk is voor de elastische eigenschappen van vasculaire structuren. HVSCs produceren geen functioneel elastine[10]. De data van hoofdstuk III geven aan dat de timing van blootstelling aan stimuli beïnvloedt hoe cellen reageren op een

mechanische omgeving, en dat cellen kunnen worden 'voorbereid' op deze omgeving vooraf aan implantatie.

III. Een MIR-aculeuze Stroming

Een andere onontkomelijke mechanische prikkel, naast cyclische rek, is hemodynamische vloeistofstroming[1]. Endotheelcellen voelen stroming door cilia[14], activatie door integrines na tensie die doorgegeven wordt door cel-cel adhesie moleculen[15], of door verplaatsing van de nucleus door hemodynamische sleepkracht[16]. In response veranderen endotheelcellen hun cross-talk met naastliggende cel types zoals myofibroblasten, wat uiteindelijk leidt tot veranderingen in ECM samenstelling en daarmee de mechanische eigenschappen van bloedvaten[17]. Door dit mechanisme reguleert endotheel een homeostase tussen het voelen van mechanische krachten en het beïnvloeden ervan. Schuifkrachten tussen 10 en 20 dyn/cm^2 zijn typisch voor bloedvaten en zwakkere krachten zijn geassocieerd met pathologische condities zoals atherosclerose[18] en aneurysmata[19]. Stroming reguleert TGFβ signalering in het ontwikkelende hart[20,21]. De TGFβ familie kan de expressie van microRNAs reguleren[22]. De microRNA 29 familie (mir29a, mir29b, mir29c) bindt aan het mRNA van elastine en collageen type 1 en onderdrukt hun expressie[23]. TGFβ reguleert de expressie van mir29. TGFβ1, welke we hebben onderzocht in hoofdstuk III, verlaagt vooral de expressie van mir29b. Aangezien er overlap is in de targets van de drie mir29s is het waarschijnlijk dat enige onderdrukking van de targets overblijft. TGFβ2, echter, is in staat om alle drie de mir29s te verlagen[22]. In hoofdstuk IV laat pilot data zien dat het verlagen van de expressie van de mir29 familie door knockdown met locked nucleic acid (LNA) transfectie inderdaad een stijging van elastine veroorzaakt in ECFCs. Statische kweek van ECFCs met TGFβ2, echter, verlaagde niet de expressie van mir29. Onder vloeistofstroming verlaagden ECFCs de expressie van TGFβ2 en lieten een trend zien voor verhoogde expressie van de mir29 familie. Daarbij waren endotheel markers verhoogd onder vloeistof stroming, met name VE cadherine, PECAM1 en VEGFR2, welke samen een essentieel endotheel mechanosensing complex vormen. Samengenomen wijzen deze pilot-data er op dat fysiologische flow op ECFCs enige bescherming bied aan een endotheel fenotype in ECFCs en mogelijk EndMT tegen gaat. Gekoppeld aan de resultaten van hoofdstuk III ontstaat een beeld waarin fysiologische mechanische stress, namelijk cyclische rek en hemodynamische schuifkracht een pro-endotheel en anti-EndMT stimulus vormen. De relevantie hiervan ligt in de potentiële rol voor EndMT in tissue engineering; als EndMT ingezet wordt om een functioneel weefsel op te bouwen zullen de directe omstandigheden van een implantaat in acht genomen moeten worden. Daarbij kan, bijvoorbeeld, het afleveren van biologisch actieve stoffen via het implantaat materiaal zelf een mate van controle geven.

IV. Weefsel Regeneratie: Leren van de Beste

Om bioactieve stoffen te vinden die kandidaat zijn voor toepassing in tissue engineering kan veel geleerd worden van in vivo herstel processen. De aanmaak van nieuw weefsel of neo-weef-

sel, bijvoorbeeld in de context van wondgenezing, wordt gereguleerd door chemokines[24]. In hoofdstuk V geven we een overzicht van de gebeurtenissen die weefselherstel aansturen en onderstrepen processen die mogelijk nuttig kunnen zijn voor tissue engineering strategieën. Weefselschade creëert een complexe omgeving van inflammatoire factoren die worden losgelaten uit beschadigde cellen zoals vascular endothelial growth factor (VEGF), stromal cell-derived factor 1a (SDF1a), platelet growth factor 1b (PDGFbb) en macrophage chemoattractive protein 1 (MCP1) [24]. Deze factoren stimuleren de expressie van adhesie moleculen zoals integrines en binden aan de omliggende ECM in het beschadigde gebied, waarbij een veld ontstaat van chemoattractieve moleculen[25]. Circulerende cellen migreren naar de hoogste concentratie chemokines maar raken onderweg ook geactiveerd. Als reactie hierop produceren de cellen extra signaleringstoffen die verder bijdragen aan het 'orkest' van factoren die uiteindelijk de vorming van neo-weefsel bepaalt[24]. Aangezien het aantrekken en stimuleren van circulerende cellen om een pro-weefselformatie milieu te creëren een enorm voordeel zou zijn voor geïmplanteerde cardiovasculaire structuren is het nabootsen van in vivo herstel processen een aantrekkelijke strategie. Een van de meest belangrijke factoren in weefselherstel is SDF1a. Het komt sterk tot expressie in hypoxische weefsels zoals beenmerg waar het verantwoordelijk is voor het vasthouden en mobiliseren van progenitor cellen in het stroma[26]. Het wordt ook losgelaten in de omgeving van weefselschade en in de circulatie, waarna het mobilisatie van progenitor cellen veroorzaakt die vervolgens naar het beschadigde gebied migreren[27]. SDF1a speelt een rol in het herstel van hart-, nier-, long-, hersen- en vasculair weefsel. Het is een sterke attractant van lymfocyten en beïnvloedt de polarisatie van t-helper cellen richting een pro-weefsel formatie subtype[28]. Het speelt ook een rol in het onstaan van neo-intima hyperplasie, wat aangeeft dat SDF1a ook een rol kan spelen in pathologische ontwikkelingen[29].

Cel-vrije biologische implantaten voor cardiovasculaire implantaten worden al in de kliniek toegepast in de vorm van gedecellularizeerde ECM, vaak afgeleid van dierlijk pericardium dat behandeld is om epitopen af te dekken[30]. Biologisch actieve stoffen zoals VEGF kunnen aan deze constructen worden toegevoegd en kunnen neointima hyperplasie verminderen[31]. Er zijn verschillende manieren om deze moleculen toe te voegen, en de manier waarop de moleculen gepresenteerd worden aan de cellulaire omgeving beïnvloedt hun efficiëntie. De moleculaire structuur van SDF1a bevat een ECM-bindend domein dat gekoppeld is aan een receptor-activerend domein via een tussenliggend linker gebied[32]. Dit zorgt ervoor dat het receptor-activerend domein gepresenteerd wordt aan cellen wat interactie met de oppervlakte receptor CXCR4 vergemakkelijkt. Inhakend op deze eigenschap leidde het combineren van een fibronectine coating met SDF1a tot verbeterde cellularisatie en weefselvorming[33]. Gedecellularizeerde constructen hebben echter een beperkte schaalbaarheid en er is een inherent risico op incomplete decellularizatie, hetgeen in enkele gevallen fatale gevolgen heeft gehad[34]. Volledig synthetische materialen kunnen deze problemen voorkomen. Fabricatie methoden zoals electrospinning kunnen 3 dimensionale micro-omgevingen maken die overeenkomen met ECM strengen en geven controle over de mechanische aspecten van het construct[35]. Daarbij zijn de materialen toegankelijk voor chemische modificatie met biologisch actieve moleculen en zijn

gemakkelijk reproduceerbaar[36]. Er zijn een aantal manieren om biologisch actieve moleculen in synthetische materialen te verwerken. In een non-covalente aanpak worden factoren direct een construct ingemengd, bijvoorbeeld via een gel. Afhankelijk van de eigenschappen van de gel worden de factoren losgelaten met enige mate van controle over de timing. Op deze manier kunnen gemakkelijk meerdere factoren tegelijk worden toegevoegd in een enkel construct[37]. In een covalente aanpak worden factoren direct aan het oppervlakte van een construct gekoppeld met minimale loslating[38]. Deze aanpak geeft meer controle over de wijze waarop moleculen worden aangeboden aan cellen. Het materiaal zelf kan gevuld worden met extra factoren die los worden gelaten naar mate het materiaal afbreekt. In een supramoleculaire aanpak worden factoren ingemengd met de polymeren wat productie aanzienlijk makkelijker maakt[38]. Ook het ontwerp van bioactieve moleculen, in aanvulling op de wijze waarop ze gepresenteerd worden, geeft mogelijkheden voor manipulatie. Een voorbeeld hiervan is geavanceerde loslating door het inbouwen van klievinglocaties voor enzymen die een rol spelen in de omgeving van een implantaat[39]. De dynamiek van de moleculen reageert zo automatisch mee met de cellulaire processen. Om de in situ dynamiek van implantaten te kunnen onderzoeken is het van groot belang om accurate in vitro modellen te ontwikkelen.

V. Een Uitbarsting van Bloedcellen

Een inflammatoire reactie op geïmplanteerd materiaal wordt doorgaans gezien als een negatieve situatie en veel moeite en onderzoek wordt besteed aan het voorkomen ervan. Echter, de fase van neo-weefsel formatie en remming van inflammatie die ook onderdeel is van deze reactie kan uitgebaat worden om een natuurlijke regeneratieve response op te wekken. MCP1 is een belangrijke attractant van immuun cellen die betrokken zijn bij de resolutie van schade herstel in vivo[40]. In hoofdstuk VI hebben we met een gel met snel-loslatende dynamiek buisvormige electro-gesponnen PCL constructen gebioactiveerd met MCP1 en deze geïmplanteerd in de abdominale aorta van ratten. Hoewel dit knaagdiermodel toegankelijk is en reproduceerbare resultaten geeft met een hoog aantal proefdieren zijn er inherent verschillen tussen menselijk en knaagdier weefselherstel. Een van de belangrijkste verschillen is dat bij knaagdieren in vasculair herstel een groot deel van de cellulaire influx afkomstig is van transanastomale ingroei[41,42]. In humaan vasculair herstel is deze laterale ingroei sterk beperkt[43]. Om de bijdrage van cellen uit de circulatie te bestuderen en de laterale ingroei zo veel mogelijk te beperken hebben we de vasculaire constructen afgeschermd aan de uiteinden met gore-tex buisjes tussen de aorta en het construct. Een gore-tex blad werd om het construct gevouwen om transmurale ingroei te voorkomen, waardoor uiteindelijk de enige bijdrage van cellen uit circulatie kon komen. Het loslaten van MCP1 uit de gel was het hoogst in de eerste drie uur na implantatie wat aangeeft dat we een plotse loslating hebben bereikt welke waarschijnlijk sterk bij heeft gedragen aan de vroege mobilisatie van immuun cellen in de gastheer. Alle implantaten werden sterk gecellulariseerd. De bijdrage van MCP1 aan de lange termijn-weefselontwikkeling werd het duidelijkst na 3 maanden, toen het neo-weefsel meer CD34 progenitor cellen bevatte en een confluente monolaag endotheel liet zien. Er was een trend voor hogere expressie van SDF1a, wat mogelijk samenhangt

met het hogere aantal progenitor cellen. Gecombineerd geven deze data aan dat het beïnvloeden van de imuunreactie zelfs in de eerste paar uur na implantatie de ontwikkeling van het implantaat tot maanden later kan beïnvloeden. Een mogelijke verklaring voor deze observatie is dat de oorspronkelijke 'eerste responder' populatie van cellen het milieu dicteert voor verdere cellulaire gebeurtenissen.

VI. Volledig Synthetische Biologie

Het gebruik van een volledig eiwit maakt schaalbaarheid en reproduceerbaarheid van een synthetische aanpak uitdagender. Zoals omschreven in hoofdstuk V is SDF1α een van de meest krachtige factoren in het aantrekken en mobiliseren van progenitor cellen[24]. Het is ook in staat om de expressie van signaleringseiwitten door immuuncellen te beïnvloeden. Korte peptide sequenties gebaseerd op SDF1α behouden specifieke activiteit door CXCR4[44]. Dergelijke korte peptides zijn toegankelijk voor synthetische productie methoden die goedkoop, reproduceerbaar, gemakkelijk schaalbaar en binnen Good Manufacturing Procedure (GMP) vallen. Directe synthese van peptides staat manipulatie van de moleculare eigenschappen toe op een aminozuur niveau. Bij voorbeeld; het wild-type eiwit SDF1α bevat een klievingslocatie voor matrix metalloproteinases (MMPs) welke SDF1α kunnen klieven in inflammatoire omgevingen[45]. Het verwijderen van deze klievingslocatie verlengt de levensduur van SDF1α in aanwezigheid van MMPs[46]. In hoofdstuk VII hebben we peptide sequenties, gebaseerd op het receptor activerend domein van SDF1α aangepast met een supramoleculair vier-maal waterstof bindend ureido-pyrimidinone (UPy) moieteit. We gebruikten poly(L-lactic acid caprolactone) (PLLCL) gefunctionalizeerd met UPy linkers om de peptiden te verankeren aan een polmeer materiaal dat toegankelijk was voor electrospinning. Gezien de aard van de moleculaire binding van de peptiden aan het materiaal was er sprake van minimale lekkage en geen plotse loslating zoals onderzocht in hoofdstuk VI. De lokale presentatie van de peptides resulteerden in koppel-plaatsen voor circulerende cellen en het specifiek activeren van de cellen om een pro-weefselproductie milieu te creëren. We gebruikten humane bloed cellen in een bioreactor die een pulsatiele unidirectionele vloeistofstroom geeft om de retentie en stimulatie van perifere mononucleare bloed cellen (PBMCs) te bestuderen in een model dat de in vivo toepassing benaderd. We vonden een specifieke retentie van lymfocyten en een daling in expressie van inflammatoire markers, consistent met de bekende rol van SDF1α in vivo. We bevestigden dat de peptide sequentie specifiek via de receptor CXCR4 signaleerde door deze te blokkeren met een specieke receptorblokker. Korte implantatie in vivo in een rat adbominaal aorta interpositiemodel liet een versterkte cellularizatie zien door cellen afkomstig uit de circulatie. De cel populatie die gevonden werd na 7 dagen liet verminderde expressie zien van inflammatoire factoren MCP1 en TNFα terwijl er een hoger cel aantal gevonden werd. In hoofdstuk VI leidde MCP1 tot een hogere celluarizatie van implantaten. In deze implantaten werd een hogere expressie van SDF1α gevonden, een hoger aantal progenitor cellen en een verbeterde weefselvorming in lange termijn implantatie experimenten. Het direct inbouwen van een stabiel SDF1α signaal in het implantaat materiaal kan overeenkomen met een verder stap in het proces naar weefsel regeneratie. De controle die we hiermee bereikt hebben over het presenteren

van bioactieve moleculen in synthetische materialen is een eerste stap naar het ontwerpen van een ideale signaleringsomgeving en het verleiden van het immuun systeem om een nieuw levend weefsel in te bouwen in een synthethische structuur.

VII. Klinische Overwegingen

De aanpak die omschreven wordt in hoofdstuk VII richt zich op een volledig synthetisch materiaal dat zich gedurende de tijd zal afbreken na implantatie. Deze aanpak staat het opvullen van het materiaal toe zodat factoren uit kunnen lekken terwijl het materiaal afbreekt. Het is echter erg moeilijk om de dynamiek van afbraak te beoordelen na implantatie en toekomstig onderzoek zal zich moeten richten op het vinden van een ideale balans tussen afbraak en opbouw van nieuw weefsel om de mechanische integriteit van het implantaat niet in het geding te brengen. Deze balans is voor een enorm deel afhankelijk van de gezondheid van de ontvanger. Het is daarom zeer waarschijnlijk dat, in toekomstige klinische praktijk, patiënten gescreend zullen moeten worden op het vermogen op een cel-vrij construct te cellularizeren en regenereren tot een functioneel weefsel vooraf aan implantatie. Vergelijkbare methoden worden al toegepast op patiënten vooraf aan autologe beenmergtransplantaties. Voordat een dergelijk screeningsproces kan worden ontworpen is meer basale wetenschap nodig om in kaart te brengen welke cellen en welke bronnen de ontwikkeling van een cel-vrij construct bepalen en voorspellen. Naast screening zou er een rol kunnen zijn voor het boosten van de hoeveelheid circulerende progenitor cellen vooraf aan implantatie. Deze aanpak zou de ontwikkeling kunnen bespoedigen en de kans op succes kunnen vergroten. Ten laatste is het misschien niet noodzakelijk dat het materiaal van een implantaat zichzelf afbreekt wanneer oppervlakte gebonden moleculen zoals omschreven in hoofdstuk VII voldoende bioactiviteit geven om de ontwikkeling van een rustig, levend en functioneel weefsel te leiden zonder de risico's van verlies van structurele integriteit.

De Taal van Tissue Engineering

De strategieën die in toekomstige studies zullen worden toegepast moeten omstandigheden onderzoeken die gebaseerd zijn op de in vivo situatie van een implantaat. 'Reversed Engineering' is het proces van het uit elkaar halen en bestuderen van een voorwerp om het te dupliceren of verbeteren. Toegepast op biologische mechanismen (en met een beetje creativiteit) zal 'Reversed Tissue Engineering' sneller leiden tot de ontwikkeling van klinisch toepasbare applicaties. Om het veld vooruit te blijven helpen moeten echter niet alleen wetenschappelijke uitdagingen overwonnen worden. Het uitvoeren van biomedisch, in vivo werk is gedetailleerd en afhankelijk van aanzienlijke expertise. Vergelijkbaar is de wetenschap van synthetische moleculaire technologie uitgebreid en overdonderend complex. Het is cruciaal voor de toekomst van tissue engineering dat experts die werken aan klinische translatie en experts die werken aan basale moleculaire wetenschap dezelfde taal spreken.

Referenties

[1] D.E.P. Muylaert, O.G. de Jong, G.G.G. Slaats, F.E. Nieuweboer, J.O. Fledderus, M.-J. Goumans, et al., Environmental Influences on Endothelial to Mesenchymal Transition in Developing Implanted Cardiovascular Tissue-Engineered Grafts, (2015) ten.teb.2015.0167–10. doi:10.1089/ten.teb.2015.0167.

[2] M.-J. Goumans, F. Lebrin, G. Valdimarsdottir, Controlling the angiogenic switch: a balance between two distinct TGF-b receptor signaling pathways, Trends in Cardiovascular Medicine. 13 (2003) 301–307.

[3] R.B. Hinton Jr, J. Lincoln, G.H. Deutsch, H. Osinska, P.B. Manning, D.W. Benson, et al., Extracellular matrix remodeling and organization in developing and diseased aortic valves, Circ Res. 98 (2006) 1431.

[4] L.A. van Meeteren, P. ten Dijke, Regulation of endothelial cell plasticity by TGF-β, Cell Tissue Res. 347 (2011) 177–186. doi:10.1007/s00441-011-1222-6.

[5] J.D. Humphrey, S.L. Delange, An Introduction to Biomechanics: Solids and Fluids, Analysis and Design - Jay D. Humphrey, Sherry L. Delange - Google Books, (2004).

[6] A.D. Egorova, P.P.S.J. Khedoe, M.-J.T.H. Goumans, B.K. Yoder, S.M. Nauli, P. ten Dijke, et al., Lack of primary cilia primes shear-induced endothelial-to-mesenchymal transition, Circ Res. 108 (2011) 1093–1101. doi:10.1161/CIRCRESAHA.110.231860.

[7] K. Van der Heiden, B.P. Hierck, R. Krams, R. de Crom, C. Cheng, M. Baiker, et al., Endothelial primary cilia in areas of disturbed flow are at the base of atherosclerosis, Atherosclerosis. 196 (2008) 542–550. doi:10.1016/j.atherosclerosis.2007.05.030.

[8] N.J.B. Driessen, A. Mol, C.V.C. Bouten, F.P.T. Baaijens, Modeling the mechanics of tissue-engineered human heart valve leaflets, J Biomech. 40 (2007) 325–334. doi:10.1016/j.jbiomech.2006.01.009.

[9] M.A.J. Cox, J. Kortsmit, N. Driessen, C.V.C. Bouten, F.P.T. Baaijens, Tissue-Engineered Heart Valves Develop Native-like Collagen Fiber Architecture, Tissue Eng Part A. 16 (2010) 1527–1537. doi:10.1089/ten.tea.2009.0263.

[10] N. de Jonge, D.E.P. Muylaert, E.S. Fioretta, F.P.T. Baaijens, J.O. Fledderus, M.C. Verhaar, et al., Matrix production and organization by endothelial colony forming cells in mechanically strained engineered tissue constructs, PLoS ONE. 8 (2013) e73161. doi:10.1371/journal.pone.0073161.

[11] E.S. Fioretta, M. Simonet, A.I.P.M. Smits, F.P.T. Baaijens, C.V.C. Bouten, Differential Response of Endothelial and Endothelial Colony Forming Cells on Electrospun Scaffolds with Distinct Microfiber Diameters, Biomacromolecules. 15 (2014) 821–829. doi:10.1021/bm4016418.

[12] L.V. Thomas, Lekshmi V, P.D. Nair, Tissue engineered vascular grafts — Preclinical aspects, International Journal of Cardiology. 167 (2013) 1091–1100. doi:10.1016/j.ijcard.2012.09.069.

[13] I. Vranken, G. De Visscher, A. Lebacq, E. Verbeken, ScienceDirect.com - Biomaterials - The recruitment of primitive Lin− Sca-1+, CD34+, c-kit+ and CD271+ cells during the early intraperitoneal foreign body reaction, Biomaterials. (2008).
[14] S. Kallakuri, J.A. Yu, J. Li, Y. Li, B.M. Weinstein, S. Nicoli, et al., Endothelial Cilia Are Essential for Developmental Vascular Integrity in Zebrafish, Journal of the American Society of Nephrology. 26 (2014) 864–875. doi:10.1681/ASN.2013121314.
[15] E. Tzima, M. Irani-Tehrani, W.B. Kiosses, E. Dejana, D.A. Schultz, B. Engelhardt, et al., A mechanosensory complex that mediates the endothelial cell response to fluid shear stress, Nature. 437 (2005) 426–431. doi:10.1038/nature03952.
[16] E. Tkachenko, E. Gutierrez, S.K. Saikin, P. Fogelstrand, C. Kim, A. Groisman, et al., The nucleus of endothelial cell as a sensor of blood flow direction, Biol Open. 2 (2013) 1007–1012. doi:10.1242/bio.20134622.
[17] M. Coen, G. Gabbiani, M.-L. Bochaton-Piallat, Myofibroblast-mediated adventitial remodeling: an underestimated player in arterial pathology, Arteriosclerosis, Thrombosis, and Vascular Biology. 31 (2011) 2391–2396. doi:10.1161/ATVBAHA.111.231548.
[18] A.M. Malek, S.L. Alper, S. Izumo, Hemodynamic shear stress and its role in atherosclerosis, Jama. 282 (1999) 2035–2042.
[19] H. Meng, V.M. Tutino, J. Xiang, A. Siddiqui, High WSS or low WSS? Complex interactions of hemodynamics with intracranial aneurysm initiation, growth, and rupture: toward a unifying hypothesis, AJNR Am J Neuroradiol. 35 (2014) 1254–1262. doi:10.3174/ajnr.A3558.
[20] M. Azhar, K. Brown, C. Gard, H. Chen, S. Rajan, D.A. Elliott, et al., Transforming growth factor Beta2 is required for valve remodeling during heart development, Dev. Dyn. 240 (2011) 2127–2141. doi:10.1002/dvdy.22702.
[21] P.W. Riem Vis, J. Kluin, J.P.G. Sluijter, L.A. van Herwerden, C.V.C. Bouten, Environmental regulation of valvulogenesis: implications for tissue engineering, Eur J Cardiothorac Surg. 39 (2011) 8–17. doi:10.1016/j.ejcts.2010.05.032.
[22] C. Luna, G. Li, J. Qiu, D.L. Epstein, P. Gonzalez, Cross-talk between miR-29 and Transforming Growth Factor-Betas in Trabecular Meshwork Cells, Invest. Ophthalmol. Vis. Sci. 52 (2011) 3567–3572. doi:10.1167/iovs.10-6448.
[23] E. van Rooij, L.B. Sutherland, J.E. Thatcher, J.M. DiMaio, R.H. Naseem, W.S. Marshall, et al., Dysregulation of microRNAs after myocardial infarction reveals a role of miR-29 in cardiac fibrosis, Proceedings of the National Academy of Sciences. 105 (2008) 13027–13032. doi:10.1073/pnas.0805038105.
[24] D.E.P. Muylaert, J.O. Fledderus, C.V.C. Bouten, P.Y.W. Dankers, M.C. Verhaar, Combining tissue repair and tissue engineering; bioactivating implantable cell-free vascular scaffolds, Heart. 100 (2014) 1825–1830. doi:10.1136/heartjnl-2014-306092.
[25] D.D. Patel, W. Koopmann, T. Imai, L.P. Whichard, O. Yoshie, M.S. Krangel, Chemokines have diverse abilities to form solid phase gradients, Clin. Immunol. 99 (2001) 43–52. doi:10.1006/clim.2000.4997.
[26] M. Shirozu, T. Nakano, J. Inazawa, K. Tashiro, H. Tada, T. Shinohara, et al., Structure and Chromosomal Localization of the Human Stromal Cell-Derived Factor 1 (SDF1) Gene, Ge-

nomics. 28 (1995) 495–500. doi:10.1006/geno.1995.1180.
[27] X. Xu, F. Zhu, M. Zhang, D. Zeng, D. Luo, G. Liu, et al., Stromal cell-derived factor-1 enhances wound healing through recruiting bone marrow-derived mesenchymal stem cells to the wound area and promoting neovascularization, Cells Tissues Organs (Print). 197 (2013) 103–113. doi:10.1159/000342921.
[28] N. Karin, The multiple faces of CXCL12 (SDF-1) in the regulation of immunity during health and disease, J. Leukoc. Biol. 88 (2010) 463–473. doi:10.1189/jlb.0909602.
[29] J. Sheng, W.-W. Cai, N.-Y. Fang, S.-Q. Wang, J.-J. Wu, Role of stromal-derived factor-1<alpha>/CXCR4 in neo-intimal repair, Cardiovasc J Afr. 22 (2011) 313–318. doi:10.5830/CVJA-2010-075.
[30] H. Kurobe, M.W. Maxfield, C.K. Breuer, T. Shinoka, Concise review: tissue-engineered vascular grafts for cardiac surgery: past, present, and future, Stem Cells Transl Med. 1 (2012) 566–571. doi:10.5966/sctm.2012-0044.
[31] X. Ye, H. Wang, J. Zhou, H. Li, J. Liu, Z. Wang, et al., The Effect of Heparin-VEGF Multilayer on the Biocompatibility of Decellularized Aortic Valve with Platelet and Endothelial Progenitor Cells, PLoS ONE. 8 (2013) e54622. doi:10.1371/journal.pone.0054622.
[32] W. Hiesinger, J.M. Perez-Aguilar, P. Atluri, N.A. Marotta, J.R. Frederick, J.R. Fitzpatrick, et al., Computational Protein Design to Reengineer Stromal Cell-Derived Factor-1 Generates an Effective and Translatable Angiogenic Polypeptide Analog, Circulation. 124 (2011) S18–S26. doi:10.1161/CIRCULATIONAHA.110.009431.
[33] W. Flameng, G. De Visscher, L. Mesure, H. Hermans, R. Jashari, B. Meuris, Coating with fibronectin and stromal cell-derived factor-1α of decellularized homografts used for right ventricular outflow tract reconstruction eliminates immune response-related degeneration, The Journal of Thoracic and Cardiovascular Surgery. 147 (2014) 1398–1404.e2. doi:10.1016/j.jtcvs.2013.06.022.
[34] P. Simon, M.T. Kasimir, G. Seebacher, G. Weigel, R. Ullrich, U. Salzer-Muhar, et al., Early failure of the tissue engineered porcine heart valve SYNERGRAFTTM in pediatric patients, European Journal of Cardio-Thoracic Surgery. 23 (2003) 1002.
[35] J. Doshi, J. Doshi, D.H. Reneker, D.H. Reneker, Electrospinning process and applications of electrospun fibers, Journal of Electrostatics. 35 (1995) 151–160. doi:10.1016/0304-3886(95)00041-8.
[36] L. Persano, A. Camposeo, C. Tekmen, D. Pisignano, Industrial Upscaling of Electrospinning and Applications of Polymer Nanofibers: A Review, Macromol. Mater. Eng. 298 (2013) 504–520. doi:10.1002/mame.201200290.
[37] H. Zhang, X. Jia, F. Han, J. Zhao, Y. Zhao, Y. Fan, et al., Dual-delivery of VEGF and PDGF by double-layered electrospun membranes for blood vessel regeneration, Biomaterials. 34 (2013) 2202–2212. doi:10.1016/j.biomaterials.2012.12.005.
[38] P. Dankers, M. Harmsen, L. Brouwer, M. van Luyn, E. Meijer, A modular and supramolecular approach to bioactive scaffolds for tissue engineering, 4 (2005) 568–574.
[39] V.F.M. Segers, T. Tokunou, L.J. Higgins, C. MacGillivray, J. Gannon, R.T. Lee, Local Delivery of Protease-Resistant Stromal Cell Derived Factor-1 for Stem Cell Recruitment After

Myocardial Infarction, Circulation. 116 (2007) 1683–1692. doi:10.1161/CIRCULATIONAHA.107.718718.
[40] J.D. Roh, R. Sawh-Martinez, M.P. Brennan, S.M. Jay, L. Devine, D.A. Rao, et al., Tissue-engineered vascular grafts transform into mature blood vessels via an inflammation-mediated process of vascular remodeling, Proceedings of the National Academy of Sciences. 107 (2010) 4669–4674. doi:10.1073/pnas.0911465107.
[41] B. van der Lei, C.R. Wildevuur, P. Nieuwenhuis, E.H. Blaauw, F. Dijk, C.E. Hulstaert, et al., Regeneration of the arterial wall in microporous, compliant, biodegradable vascular grafts after implantation into the rat abdominal aorta. Ultrastructural observations, Cell Tissue Res. 242 (1985) 569–578.
[42] Z. Zhang, Z. Wang, S. Liu, M. Kodama, Pore size, tissue ingrowth, and endothelialization of small-diameter microporous polyurethane vascular prostheses, Biomaterials. 25 (2004) 177–187.
[43] P. Zilla, D. Bezuidenhout, P. Human, Prosthetic vascular grafts: wrong models, wrong questions and no healing, Biomaterials. 28 (2007) 5009–5027. doi:10.1016/j.biomaterials.2007.07.017.
[44] W. Hiesinger, J.M. Perez-Aguilar, P. Atluri, N.A. Marotta, J.R. Frederick, J.R. Fitzpatrick, et al., Computational protein design to reengineer stromal cell-derived factor-1α generates an effective and translatable angiogenic polypeptide analog, Circulation. 124 (2011) S18–26. doi:10.1161/CIRCULATIONAHA.110.009431.
[45] G.A. McQuibban, G.S. Butler, J.H. Gong, L. Bendall, C. Power, I. Clark-Lewis, et al., Matrix Metalloproteinase Activity Inactivates the CXC Chemokine Stromal Cell-derived Factor-1, J. Biol. Chem. 276 (2001) 43503–43508. doi:10.1074/jbc.M107736200.
[46] V.F.M. Segers, T. Tokunou, L.J. Higgins, C. MacGillivray, J. Gannon, R.T. Lee, Local delivery of protease-resistant stromal cell derived factor-1 for stem cell recruitment after myocardial infarction, Circulation. 116 (2007) 1683–1692. doi:10.1161/CIRCULATIONAHA.107.718718.

XI

Dankwoord / Acknowledgements

Acknowledgements / Dankwoord

Dit proefschrift is niet alleen van mij, en daar ben ik trots op. Ik heb het voorrecht gehad om telkens te werken met gemotiveerde en talentvolle mensen, maar bovenal mensen die het dagelijks leven als promovendus stukken leuker hebben gemaakt. Een deel van het werk is vertegenwoordigd in de figuren en tekst van dit boekje, maar er zit veel meer achter de schermen van dit soort wetenschap; talloze samenwerkingen, besprekingen, vergaderingen, treinreizen, werklunches, praatjes, posters, telefoongesprekken, lab-bezoekjes, e-mails, presentaties, urenlang naar de muur staren en veel, veel, veel, oh, zo ontzettend veel **koffie**.

#

Professor dr. Verhaar, beste **Marianne**, toen ik om vijf uur 's ochtends in San Francisco (in pak, voor het gevoel) dat eerste telco gesprek voerde met jou en Joost had ik geen idee waar ik aan begonnen was. Ik was nog aan het afstuderen van een biomedische Master of Science, nog lang niet klaar met Geneeskunde; ik was vlees noch vis. Ik durfde amper te hopen dat ik de kans zou krijgen om te promoveren op zo een ambitieus project. Je hebt sinds het begin ontzettend veel interesse getoond voor mijn persoonlijke vooruitgang. Ik ben niet alleen onmetelijk dankbaar voor het feit dat je me zo veel verder hebt geholpen, maar ook voor de manier waarop.

Dr. Fledderus, beste **Joost**, toen je belde om te zeggen dat ik was aangenomen wist ik niet waar ik in terecht was gekomen. In de jaren daarna wist ik soms nog steeds niet volledig wat ik aan het doen was. Jij bent telkens het rotsvaste punt geweest waar ik op kon terugvallen, en je wist me telkens weer wat zelfvertrouwen te geven. Ontzettend bedankt daarvoor.

Professor dr. Bouten, beste **Carlijn**, de TUE is een soort speeltuin vol met technisch speelgoed. Ik kwam elke keer terug uit Eindhoven vol van frisse motivatie, mede dankzij jouw toewijding en enthousiasme. Het is ongelofelijk wat bereikt kan worden als je verschillende velden bij elkaar brengt, en jij maakt dat mogelijk.

Professor dr. Dankers, beste **Patricia**, door de moleculaire magie die jij voor elkaar krijgt heb ik altijd het gevoel gehad dat alles mogelijk was. Het is ontzettend fijn samenwerken als iedereen zo nieuwsgierig en gemotiveerd is als jij.

Professor dr Giles, dear **Rachel**, your enthusiasm and drive are unbelievably powerful, and I admire how intensely you love what you do. Thank you for always being available to brainstorm and to point me in the right direction.

Professor dr. Goumans, beste **Marie-Jose**, ik heb ontzettend veel aan je advies gehad, tijdens mijn onderzoek in Utrecht maar ook op de gezellige BMM annual meetings!

Dr. Kluin, beste **Jolanda**, het is in een lab makkelijk om te vergeten waar je uiteindelijk voor aan het werken bent. Dankzij jou was de klinische toepassing van ons onderzoek nooit ver van mijn gedachten. Ik kijk enorm vooruit naar mijn klinische toekomst!

Mijn **collega's in Eindhoven** hebben een enorm deel van dit proefschrift mogelijk gemaakt. **Anthal**, de ervaren iValve veteraan. Je hebt het tegen de stroom inzwemmen, dat nodig was bij iValve, tot een kunst verheven. **Geert**, ik heb met veel plezier samen gewerkt, je spreekt vloeiend TUE en UMC. Heel erg verfrissend! **Nicky**, we hebben ons er goed doorheen geworsteld! **Tina, Emanuela**, **Ginny**, **Tonny, Marc,** this whole BMM adventure has been fantastic, it felt like we were changing the world a little bit.

Mijn lieve collega's uit het **Verre Oosten**; wat een team! Jammer dat die patiënten de kamer harder nodig hadden. **Ollie**, we zijn samen een beetje opgegroeid in het PhD-en. Ik heb zo ontzettend veel gehad aan het brainstormen en idee-stuiteren, ik heb enorme bewondering voor je, als briljante wetenschapper maar ook als briljante dude. **Gies**, wat ben je toch een f*cking rockstar! Je bent eigenlijk overal goed in, maar als collega ben je al helemaal een topper. **Nynk**, het is een wonder dat je computer nog leeft. Zonder serieuze psychologische schade. Je bent een force of nature!

Hendrik, jij uitzonderlijke man. Je bent het hart en ziel van het lab, en het lab heeft een gouden hart en ziel. Ik heb ein Biest van een paranifm! **Arianne**, het is zo leuk geweest om je af en toe even gek te maken in onze kamer. Er is een roze toeter die je vast nooit meer gaat vergeten. **Diana**, Здравствуйте! Je brengt altijd wat extra vrolijkheid naar het lab. Superveel succes in je vernieuwde klinische carrière! **Martin**, ik bewonder je toewijding en discipline, en ik blijf erbij dat ik je kan verslaan met lasergamen! **Petra**, lieve Pee-de-Bree, je bent gewoon m'n maatje. Tsss. Met je ge-whatsapp ;). **Bas**, de kleppenboys hielpen enorm om het overzicht te houden en om scherp te blijven, bedankt! **Tim**, you've really grown in your research, I envy your dedication and drive, and your ability to make fish sit up straight. **Maarten**, jonge vader en md/phd! je bent een inspirerend voorbeeld. **Christa**, bedankt voor de ondersteuning en wat maak je toch mooie foto's. **Ive**, je was mijn redder in nood, ik ben blij dat je bij het lab bent gekomen! **Merle**, ik kan niemand bedenken die de uitdagingen van het onderzoek beter aan zou kunnen. Je bent een heldin, blijf knokken, we gaan hopelijk samen nog veel mooie dingen maken! **Chris**, ook door jouw bijdrage is het uiteindelijk toch gelukt. Je bent een topper en ik ben je heel erg dankbaar voor je hulp.

Hanna, het is gelukt! Ik ben zo ontzettend blij dat ik jou had om af en toe heerlijk mee te kunnen klagen! We zijn een topteam. En nu weer de kliniek in! **Jan-Willem**, je hebt veel bijgedragen en je wordt gewaardeerd. Succes gewenst! **Sailay**, ik denk dat de cardiothoracale een mooie toekomst heeft! Thanks for the good times. **Marcelle,** er staat je nog veel spannends te wachten. Ik blijf in de buurt voor brainstorms, succes! **Jesper,** je bent een motiverend voorbeeld, ik kijk met

spanning uit naar de toekomst.

Frederieke, jeetje wat ben jij vervelend, en ik ben helemaal dol op je! **Janine**, superveel succes met al je spannende avonturen en je opleiding! **Zhiyong**, the very best of luck to you and your beautiful family. **Alain**, het was telkens weer gezellig in de kweek. **Judith**, je hoorde er meteen bij. Ik ga de borrels missen! **Krijn**, stiekem was het erg fijn om even jou te mogen zijn, hoe kort ook. **Paul**, ik heb erg veel aan je adviezen gehad aan het begin, bedankt! **Dries**, we had so much fun at those BMM annual meetings! Grote wasjes, kleine wasjes, I'll never forget it. **Peter-Paul,** superveel succes nog, man! **Esther**, **Corine, Arjan, Sander,** bedankt voor alles!

Mijn lieve **Jaarclub**, volgens mij ben ik de laatste die *Het Horloge* ontvangt. Het was pittig, maar een Sequoia wankelt niet. **T4b-ers**, na al die jaren zijn we nog zo hecht, en het is een heerlijk gevoel dat ik altijd op jullie terug kan vallen. **Olaf en Sjoerd,** jullie hebben me dat laatste jaar (soms letterlijk) door gesleept met onwaarschijnlijke energie en motivatie. Dankzij jullie en mijn geweldige **mede-kaputters** had ik nooit een tekort aan energie (of spierpijn). **Jennifer en Claire**, Penny en Bear, my fellow kids, het is bijna oneerlijk dat ik voor een tweede keer zo een leuk studentenleven krijg. Mijn lieve **nieuwe studiegenootjes en mede Caput M-ers**, mijn aanstaande collegae, door jullie voel ik me tegelijk vijf jaar jonger en vijf jaar ouder.

Barthold, **Alexander**, **Jasper**, **Laura**, **Renée**, **Tristan**, zonder mijn Utrechtse familie zou ik niet weten wat ik zou doen. Jullie zijn er altijd voor me en dat is me alles waard. **Han**, je bent nu al een geweldige onderzoeker en ik weet zeker dat je bij de wereldtop gaat horen. Je eindeloze energie is aanstekelijk, ik wens je het allerbeste tijdens je postdoc in Californië! **Lucas**, kaas, je bent niet alleen mijn paranimf, je bent gewoon mijn broer. Ik ben zo blij dat ik dit allemaal niet alleen doe. En het mooiste is dat we eigenlijk nog maar net beginnen. **Sophie**, **Caroline**, **Barbara**, het is zo goed dat we elkaar altijd hebben, en het lijkt elk jaar leuker te worden, zeker nu met **de mannen** erbij, het **neefje** dat er aan komt, en alle spannende ontwikkelingen van de komende jaren! **Nonkel Pierre**, nu ben ik wel eindelijk echt dr. Dimi! We zullen een goede steak gaan eten om het te vieren.

Mama en **Papa**, nu kunnen jullie eindelijk eens goed doorlezen wat ik die hele tijd aan het doen was. Dankzij jullie voelt het alsof alles in de wereld mogelijk is. Er bestaan geen meer motiverende ouders dan jullie. Ik ben onbeschrijfelijk dankbaar voor alles dat jullie mij hebben gegeven. Mijn lieve grootouders, **Mamie** en **Papie,** jullie zijn en blijven mijn grootste inspiratie en voorbeeld.

List of Publications and Curriculum Vitae

List Of Publications

Tricking the Body into Building New Heart Valves and Blood Vessels. **Dimitri EP Muylaert**. Atlas of Science 2015 Dec 16. http://atlasofscience.org/tricking-the-body-into/

Early in-situ cellularization of a supramolecular vascular graft is modified by synthetic stromal cell-derived factor-1α derived peptides. **Muylaert DE**, van Almen GC, Talacua H, Fledderus JO, Kluin J, Hendrikse SI, van Dongen JL, Sijbesma E, Bosman AW, Mes T, Thakkar SH, Smits AI, Bouten CV, Dankers PY, Verhaar MC.Biomaterials. 2016 Jan;76:187-95. doi: 10.1016/j.biomaterials.2015.10.052. Epub 2015 Oct 23. PMID:26524538

Environmental Influences on Endothelial to Mesenchymal Transition in Developing Implanted Cardiovascular Tissue-Engineered Grafts. **Muylaert DE**, de Jong OG, Slaats GG, Nieuweboer FE, Fledderus JO, Goumans MJ, Hierck BP, Verhaar MC. Tissue Eng Part B Rev. 2015 Oct 8. [Epub ahead of print] PMID:26414174

In Situ Tissue Engineering of Functional Small-Diameter Blood Vessels by Host Circulating Cells Only. Talacua H, Smits AI, **Muylaert DE**, van Rijswijk JW, Vink A, Verhaar MC, Driessen-Mol A, van Herwerden LA, Bouten CV, Kluin J, Baaijens FP. Tissue Eng Part A. 2015 Oct;21(19-20):2583-94. doi: 10.1089/ten.TEA.2015.0066. Epub 2015 Aug 25. PMID:26200255

Combining tissue repair and tissue engineering; bioactivating implantable cell-free vascular scaffolds. **Muylaert DE**, Fledderus JO, Bouten CV, Dankers PY, Verhaar MC.Heart. 2014 Dec;100(23):1825-30. doi: 10.1136/heartjnl-2014-306092. Epub 2014 Jul 22. Review. PMID:25053725

Matrix production and organization by endothelial colony forming cells in mechanically strained engineered tissue constructs. de Jonge N, **Muylaert DE**, Fioretta ES, Baaijens FP, Fledderus JO, Verhaar MC, Bouten CV. PLoS One. 2013 Sep 2;8(9):e73161. doi: 10.1371/journal.pone.0073161. eCollection 2013. PMID:24023827

Curriculum Vitae

Dimitri Elke Paul Muylaert was born in Amsterdam on January 22, 1986. He completed bilingual (English/Dutch) university entrance level secondary school at the Rijnlands Lyceum in Oegstgeest in 2004. After one year of the bachelor program of Biomedical Sciences at the University of Utrecht he enrolled in Medical School at the Erasmus University of Rotterdam via de-central selection (entrance exams) in 2005. In 2006 he began an additional Master of Science program, Molecular Medicine, alongside the Medical School curriculum at the Erasmus University of Rotterdam, for which he spent one year of full-time research under prof. dr. Chris Lau at the University of California, San Francisco between 2009 and 2010. During his studies he was involved in a number of theatrical productions as writer, director, actor and organizer for which he won several awards. In addition, he worked as part of the medical student's team for the department of Cardiothoracic Surgery at the University Medical Center of Utrecht. In 2010 he began his PhD research under prof. dr. Marianne C. Verhaar at the University of Utrecht in 2010, resulting in this dissertation and PhD in 2016. Having transferred from the Erasmus University of Rotterdam and finishing the final internships of Medical School at the University of Utrecht, he will also complete his MD in 2016.